ICM VPE XXI

2024 Las Vegas, NV

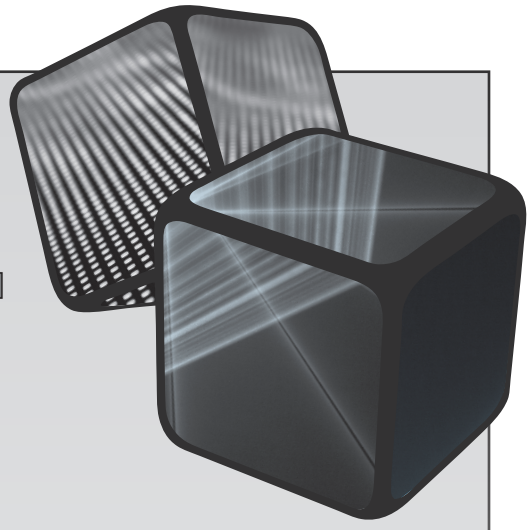

MONDAY

Oral Presentations

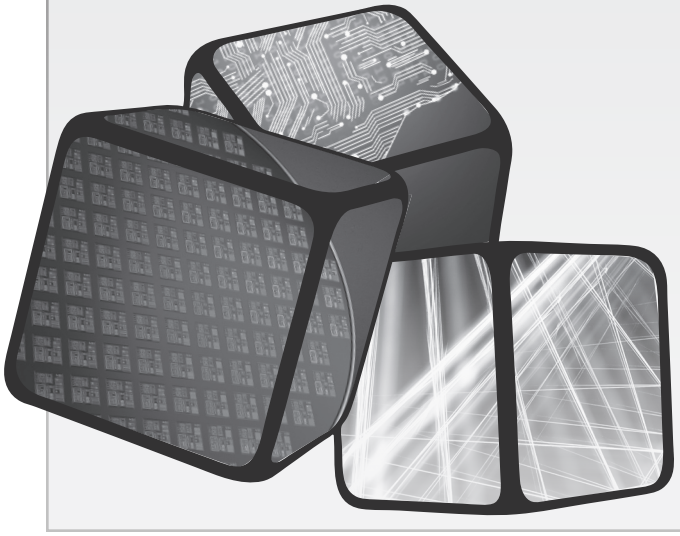

Program current as of May 7, 2024

21st International Conference on Metal Organic Vapor Phase Epitaxy

SESSION 1A: Plenary Session I
Session Chairs: Xiuling Li and Luke Mawst
Monday Morning, May 13, 2024
Resort Tower, Ground Level, Silver Room

8:15 AM OPENING REMARKS

8:30 AM *1A.1
AlN—Dopant Incorporation and Activation by MOVPE
Zlatko Sitar; NCSU, United States

Single crystal aluminum nitride with a direct bandgap of 6.1 eV brings about technological opportunities to realize deep UV optoelectronics, extreme RF and power devices, in addition to being a possible host for quantum interaction. With the dislocations practically absent in AlN substrates, surface morphology in homoepitaxy by MOVPE can be controlled from 2D-nucleation to step-flow-growth and even to layer-by-layer growth. The growth process is quantitatively described by an all-inclusive surface kinetic framework that connects the input vapor supersaturation, surface supersaturation, surface diffusion length, and substrate misorientation angle. Management of surface features is crucially important for the growth of ternary alloys and uniform doping.
Historically, the conductivity in AlN has been very limited, presumably due to a DX^- transition forming an acceptor state and subsequent self-compensation, which imposed a severe upper limit on the achievable free carrier concentration. However, recent results show that the transition represents an equilibrium thermodynamic transition from a shallow to a deep donor state, which can be kinetically controlled. These developments resulted not only in robust UV optoelectronic devices but also in near-ideal, AlN-based Schottky diodes supporting currents as high as 3 kA/cm^2 and stable operation up to 700°C, demonstrating the potential of AlN as a platform for power devices for extreme environments.

9:15 AM *1A.2
A New Paradigm for Integration of III-V Active Devices on SOI—Lateral Selective MOVPE
Kei May Lau; Hong Kong University of Science and Technology, Hong Kong

High-performance high-frequency and photonic devices have been dominated by compound semiconductors, which have an innate wavelength-tuning flexibility and can facilitate extremely high-speed transport of electrons, with incorporation of heterostructures. III-V compound semiconductors now widely used in optical fiber networks for both tele- and data-communications are being integrated with Si-based electronics by various means to extend the performance and functionalities of integrated systems. In addition to the speed and bandwidth advantages, sending data via photons instead of electrons can be much more energy efficient. Silicon photonics is being developed to extend integrated photonics adopting the highly successful Si IC infrastructure for high-speed and wide bandwidth switching and sensing. The eventual goal is to integrate photonics with electronics on the same silicon platform, so that data communication and signal processing can be performed on a single small formfactor chip with energy-efficiency, high speed, and minimal delay.
Conventional heteroepitaxy involves the growth of thick buffer layers to minimize and block defects generated at the mismatched III-V/Si interface to propagate to the active device region. Lasers grown with such techniques with long lifetimes have been reported. In our laboratory, we have taken various approaches and developed high-quality III-V on silicon for transistors and lasers by direct hetero-epitaxy, including blanket and selective growth. The crystalline quality of these epitaxies is gauged by various material characterizations as well as active device performance benchmarked against those grown on native substrates. For monolithic integration of Si photonics, efficient coupling of light between active and passive components is essential. We developed a novel lateral aspect ratio trapping (LART) technique to grow lasers and high-speed photodetectors on patterned commercial SOI substrates for integrated Si photonics. Multimode and single-mode lasing from lateral quantum wells (QWs) as the gain media using LART have been achieved in the 1433 -1630 nm band with varying dimensions of lasers. High-performance PDs coupled to Si tapers were also constructed on the monolithic InP/SOI platform with laterally grown PIN structures. This talk will describe these technologies in our toolbox.
References
Y. Xue, J. Li, Y. Wang, K. Xu, Z. Xing, K. S. Wong, H. K. Tsang, and K. M. Lau, “In-Plane 1.5um Distributed Feedback Lasers Selectively Grown on (001) SOI”, Laser & Photonics Reviews, 2300549, 2023.
J. Li, Y. Xue, Z. Yan, Y. Han and K. M. Lau, “III-V selective regrowth on SOI for telecom lasers in silicon photonics”, Journal of Applied Physics, Vol.133, Issue 13, 133103, 2023.
Y. Xue, Y. Han, Y. Wang, J. Li, J. Wang, Z. Zhang, X. Cai, H. K. Tsang, and K. M. Lau, “High-speed and low dark current silicon-waveguide-coupled III-V photodetectors selectively grown on SOI”, Optica, Vol. 9, no. 11, 1219-1228, 2022.
Y. Han, H. Park, J. E. Bowers, and K. M. Lau (invited), “Recent Advances in Light Sources on Silicon,” to appear, Advances in Optics and Photonics, Vol. 14, Iss. 3 pp: 291-570, 2022.
J. Li, Y. Xue, L. Lin, Z. Xing, K. S. Wong, and K. M. Lau, “Telecom InGaAs/InP quantum well lasers laterally grown on silicon-on-insulator,” J. Lightwave Technology, Vol. 40-16, 5631, 2022.
Z. Yan, Y. Han, L. Lin, Y. Xue, C. Ma, W. K. Ng, K. S. Wong, and K. M. Lau, “A monolithic InP/SOI platform for integrated photonics”, Light: Science & Applications, Vol. 10, no. 200, 2021.

10:00 AM BREAK

SESSION 1B-1: Visible LED
Session Chair: Tomoyuki Tanikawa
Monday Morning, May 13, 2024
Resort Tower, Ground Level, Bronze Room 1

10:30 AM *1B-1.1
Challenges of MOCVD in Mass Production of MicroLEDs
Yun-Li Li, Yen-Lin Lai, Hsin-Chiao Fang, Kuang-Yuan Hsu, Jyun-De Wu and Ying-Tsang Liu; PlayNitride Inc., Taiwan

MicroLED displays excel in large TVs, autos, wearables, and AR. Samsung sells MicroLED TVs, highlighting its benefits in brightness, contrast, color, reliability, flexibility, and transparency. The chip, thinner than 10 microns, serves as the source for each sub-pixel, containing red, green, and blue chips for full-color generation. Key advantages include lower energy use, heightened reliability compared to LCDs/OLEDs. MicroLED's inorganic LED chips enhance efficiency and save energy. The display matrix, with millions of subpixels, demands impeccable uniformity and defect-free production, requiring a fresh approach from development to large-scale production.

Reducing MicroLED size to the micron scale poses initial efficiency challenges, stemming from complications in epitaxy, chip processing, and packaging. Epitaxy, a critical process, may introduce defects impacting quantum efficiency. Focused on enhancing epitaxy control, we achieved a 3~6% improvement in external quantum efficiency (EQE) for red/green/blue chips from 2021 to 2023, with plans for an additional 6% improvement over the next two years.

Ensuring consistent performance across millions of MicroLED chips is vital for high display uniformity. Initial efforts centered on within-wafer wavelength uniformity improvements. Innovative solutions, including a unique pattern sapphire substrate (PSS), disc compensation design, and recipe tuning, resulted in a remarkable accomplishment: halving the standard deviation of domain wavelength (Wd) over four years.

As we transition to mass production, maintaining wafer-to-wafer and run-to-run performance uniformity is crucial. Precise temperature control in epitaxy and in-situ chamber cleaning ensure consistent performance. Achieving over 50% reduction in wavelength variation and run-to-run differences below 1.5nm underscores our commitment to unparalleled uniformity and performance reliability.

Stable production control established, focus shifts to enhancing yield for cost reduction. Particle contamination, identified as a major yield obstacle, is mitigated through in-situ cleaning, resulting in a 40% reduction in defects larger than 3μm. This intervention not only reduces costs but also facilitates efficient mass production of MicroLEDs.

Larger wafers have been considered a cost-effective solution for MicroLEDs in semiconductor history. While the idea of using larger sapphire and GaAs substrates has been discussed, the high production cost makes it impractical. In contrast, silicon wafers, with their mature ecosystem, appear more feasible. However, transitioning to larger wafers presents challenges such as significant lattice mismatch, differences in the coefficient of thermal expansion, and increased wafer bow. Extensive research and development efforts are addressing these challenges.

Although the possibility of moving to 8-inch and 12-inch wafers is on the horizon, the current focus on 6-inch wafers is crucial for achieving mass production readiness. This strategic emphasis aligns with the industry's current state and paves the way for a smoother transition to larger wafer sizes in the future.

MicroLED is progressing towards mass production, emphasizing epitaxy as a crucial process for optimal display performance. Challenges and achievements in improving external quantum efficiency, ensuring wavelength uniformity, and enhancing yield through effective particle control have been addressed. The use of 8/12-inch wafers is expected to play a pivotal role in cost reduction, though ongoing research tackles existing challenges. MicroLED TVs are now available in the market, with smartwatches soon to follow. Automotive manufacturers are also keen on MicroLED due to its high brightness and exceptional reliability, positioning it as a dominant solution for various display applications.

11:00 AM *1B-1.2
MOVPE Growth of Stacked RGB Monolithic GaInN-Based μLED Arrays Connected via Tunnel Junctions and Challenges for VR/AR Display Applications
Motoaki Iwaya[1], Tatsunari Saito[1], Yoshinobu Suehiro[1], Tetsuya Takeuchi[1], Satoshi Kamiyama[1], Daisuke Iida[2] and Kazuhiro Ohkawa[2]; [1]Meijo University, Japan; [2]King Abdullah University of Science and Technology (KAUST), Saudi Arabia

Technological advances have led to the emergence of various virtual space services, and the keyword "metaverse" has become a trending term encompassing these new services. Among them, developments are attention in various directions, including head-mounted displays, smart glasses, and devices that enable VR. These displays are used very close to the human eye and must provide a realistic and immersive visual experience. Thus, high resolution, high definition, high brightness, high efficiency and a wide color gamut are required. The viewing angle of the human eye's limiting resolution is said to be about 0.02°. Assuming that the distance from the eye to the device is several cm, it is necessary to develop a display with a pixel size of several to several tens of μm to obtain a display with extremely high realism. To achieve this high performance, the application of various technologies such as LCD, organic EL, and QD has been studied, and some of them have been put into practical use. However, there are still strong demands for improvement in efficiency, resolution, color gamut, and brightness.
One promising approach is the use of μLEDs. GaInN-based

LEDs, in particular, have excellent performance with high luminance and high efficiency in the blue and green regions, and it has been reported that even when miniaturized as in μLEDs, the efficiency reduction due to increased non-luminescent recombination caused by leakage current in the side walls and surface recombination is kept low. In addition, nitride-based LEDs are now becoming possible to achieve high-efficiency red light emission even using nitride semiconductor materials, thanks to innovations in crystal growth technologies such as GaInN and Eu-doped GaN. Thus, the application of μLEDs to self-illuminated displays is attracting attention in a wide range of fields.
Considering the realization of head-mounted displays with extremely small pixel size, it is ideal to form a monolithic display by stacking RGB LEDs on a single wafer using a crystal growth process or semiconductor process. The application of RGB pn-junction LEDs stacked in sequence to a monolithic structure has already been reported. Monolithic structures in which carrier injection into the RGB active layers is controlled using selective growth have also been verified and reported. However, both methods have their challenges. In the former, to drive the device, the p-type and n-type layers of each LED must be exposed by etching, and electrodes must be formed on their respective surfaces. However, dry etching, which is common for nitride semiconductors, causes donor defects, and although good low contact resistance electrodes can be obtained in the n-type layer, no method has been established to form low contact resistance electrodes in the etched p-type layer. For the latter, there are also issues such as the need for complex selective growth and the difficulty of fabricating fine devices after selective growth.
Therefore, we have reported a method to form stacked monolithic μLED arrays by forming tunnel junction layers between each RGB element by crystal growth using the MOVPE method and forming electrodes on the etched n-type layer. In this report, GaInN-based blue, green, and red LED structures were stacked on the same wafer, and tunnel junctions were formed between each element. A monolithic RGB μLED array with 330ppi integration was formed by semiconductor process, and each device was driven to obtain blue, green, and red emission. Although there are issues to be solved, such as the lower light output of blue and red LEDs compared to green LEDs and the matching of emission wavelengths, the devices are expected to be used for head-mounted displays. In this presentation, we report the results of crystal growth of RGB μLEDs by tunnel junction using the MOVPE method and their arraying as well as their crystallographic and detailed device characteristics.

11:30 AM 1B-1.3
Large Area Blue Cascaded LEDs with GaN:Ge/GaN:Mg Tunnel Junctions Grown by MOVPE Christoph Berger, Armin Dadgar and André Strittmatter; Otto von Guericke Universität Magdeburg, Germany

The implementation of tunnel-junctions (TJs) on the p-side of blue light emitting diodes (LEDs) offers an exciting way to realize transparent, highly conductive electrodes for enhanced hole injection, better current spreading and higher efficiency. We realized TJ-LEDs by growth of a 100 nm thick GaN:Ge layer with an electron concentration of $1x10^{20}$ cm^{-3} on top of the GaN:Mg layer of a standard LED structure in a continuous growth process by MOVPE. TJ-LEDs grown by MOVPE often suffer from poor light emission and high resistivity, since sufficient activation of the buried p-GaN layer by thermal annealing is challenging. Therefore, demonstration of MOVPE-grown TJ-LEDs is limited to micrometer-sized LEDs in most cases, whereby p-activation is achieved by lateral hydrogen out-diffusion through etched mesa sidewalls. We present TJ-LEDs with sizes up to 1 mm^2 that show homogeneous light emission with more than 60 % higher output power than standard reference LEDs with ITO or Ni/Au semitransparent contact while having comparable turn-on voltage and virtually the same series resistance of $1.1x10^{-2}$ Ωcm^{-2} at a current density of 100 A/cm^2. Remarkably, no in-situ or ex-situ activation schemes had to be carried out for the TJ-LEDs to achieve these properties. We propose that p-GaN activation happens during overgrowth with the highly doped GaN:Ge when using nitrogen as carrier gas. Although n-doped GaN is known to block hydrogen diffusion, we assume an out-diffusion of H_2 promoted by V-pits that are formed during GaN:Ge growth in N_2 ambient. Cascaded double LED structures hold promise two-fold light intensity per chip area if the buried LED maintains the same performance as single LED devices. We successfully realized cascaded double LED devices showing light output and IV characteristics exactly corresponding to the sum of the individual LEDs. Since growth of the top LED structure by MOVPE requires some steps under hydrogen atmosphere re-passivation of the buried GaN:Mg or deterioration of the active region might occur. However, the buried LED section exhibits only moderate increase in voltage penalty by about 0.6 V but strongly reduced light output by about a factor of 8. From IV- and PL-measurements, re-passivation of GaN:Mg or deterioration of InGaN/GaN active region by diffusion effects is not supported by annealing experiments in H_2 and N_2 atmospheres. However, a spotty emission pattern from the buried LED shows severe alteration of the current injection mechanism which is currently under investigation.

11:50 AM 1B-1.4
Full Visible Range Emission with Ultra-High Density InGaN/GaN QDs Achieved by Selective Area Growth Cheng Liu, Nikhil Pokharel, Miguel B. Ponce, Qinchen Lin, Shining Xu, Padma Gopalan, Chirag Gupta, Shubhra Pasayat and Luke Mawst; University of Wisconsin-Madison, United States

III-nitride quantum dots (QDs) have attracted considerable attentions in (μ)LED/laser applications due to their exceptional characteristics such as high quantum confinement, low threshold current density, high differential gain, better carrier confinement and less sensitivity to dislocations [1]. Among all the approaches to create III-nitride QDs, lithography-defined QDs have shown great potential to realize narrow emission linewidth but compromise in QD density. Our previous study developed a technique using the diblock co-polymer lithography, followed by selective area metal

organic vapor phase epitaxy (MOVPE) growth, which successfully improves the InGaN/GaN QD density up to 8 x 10^{10} cm^{-2} with uniform QD size of 23.48 nm. Blue and Cyan emissions with wavelengths of 483nm and 517nm have been observed from such QDs [3].

In this work, we extend the study of SAG InGaN/GaN nano-pyramid QDs to full visible spectrum range, including the challenging red emission. Besides, the QD cap growth is also developed, which enables the realization of electrically driven QD based optoelectronic devices. All the QDs achieved in this study were grown by MOVPE in the temperature range of 695°C - 724°C, with consistent QD density of 7 - 9 × 10^{10} cm^{-2}. The baseline structure of the QDs in this study consists of 10nm GaN, 1.5nm InGaN and 3.5nm GaN, all of which are calibrated on a planar template.

Different growth conditions, such as V/III ratio, TMIn flow rate, growth temperature, growth rate, as well as different InGaN layer thickness has been investigated in this work. Clear QDs emission were observed from all QDs ranging from 460 nm to 680 nm with increased full width at half maximum (FWHM) as emission wavelength becomes longer. The QDs also show enhanced internal quantum efficiency (IQE) collected by temperature-dependent photoluminescence (PL) measurement, as compared to the epitaxial layers grown on co-loaded planar template. For example, up to 63% IQE was observed for the baseline QD structure emitting at 488nm, which is much higher than the 20% IQE from coloaded planar structure, showing the potential of such QDs for full visible optoelectronic applications.

In order to realize electrically driven devices, the QDs should be capped with (p-type) GaN layer with minimum defects at regrowth interface. Nonoptimized cap growth condition will degrade QD emission and strongly limit carrier injection [4]. The typical process prior to the cap regrowth includes both HF clean, and fluorine based dry etching processes to effectively remove the dielectric mask. Theoretically, low NH3 flow rate, low pressure, as well as high temperature are typical preferred growth conditions to promote lateral growth for micron level or larger features. However, those conditions might not be suitable to transfer to nanometer QD cap growth. From our findings, QDs capped under high growth rate will end up with hazy surface and increased dislocation density of > 1 x 10^{11} cm^{-2} measured by electron channeling contrast image (ECCI). For the QDs capped with higher temperature, the QD peak will disappear due to indium desorption during temperature ramp up. Carrier gas is also critical for QD cap growth, N_2 only growth condition will result in hexagonal pits formation while H_2 only will lead to large dislocation density although the surface is smooth. After optimization, we developed a two-step cap growth procedure, including a 40-nm low-temperature, low-pressure, low-growth rate deposition and a 100 - 200 nm high temperature standard p-GaN growth. The dislocation density of 5 x 10^{8} cm^{-2} and surface roughness of < 1nm was achieved for the QD samples with no PL intensity reduction and wavelength shift after the cap growth, indicating the good regrowth interface under such growth condition.

Reference:
[1] G. T. Liu, *et. al.*, IEEE J. Quantum Electron. 36, 1272 (2000).
[2] C. Liu *et. al.,* J. Vac. Sci. Technol. A 41,062705 (2023).
[3] G. T. Wang *et. al.*, No. SAND2017-7539C. (2017).

12:10 PM 1B-1.5
Dislocation Half-Loop Control for Optimal V-Defect Density in MOCVD-Grown GaN-Based Light Emitting Diodes Alejandro Quevedo, Feng Wu, Jacob Ewing, Tanay Tak, Shuji Nakamura, Steven P. DenBaars and James Speck; University of California, Santa Barbara, United States

V-defects are morphological defects that typically form at threading dislocations during epitaxial growth of (0001) oriented GaN layers. A V-defect is a hexagonal pyramid depression with six (10-11)-oriented sidewalls. These semipolar sidewalls have a lower polarization barrier than the polar c-plane and provide an efficient avenue for lateral carrier injection into quantum wells in GaN-based light emitting diodes (LEDs). This is especially important, as the high polarization fields in c-plane GaN is a significant driver for the high forward voltage of GaN LEDs. The optimal V-defect density for efficient lateral carrier injection in a GaN LED is typically one order of magnitude higher than the threading dislocation density for GaN grown on patterned sapphire substrates. Recently it has been found that dislocation half-loops can be formed in GaN via low temperature growth with high Si-doping to intentionally generate threading dislocations and large V-defects. Here we develop a method for half-loop formation and density control via disilane flow, growth temperature, and thickness of a half-loop generation layer. We also develop a method of forming these small V-defects resulting from half-loops into V-defects of comparable size to those originating from substrate threading dislocations using low temperature growth and V/III ratio control.

SESSION 1B-2: Heterogeneous Integration/Wafer Bonding
Session Chair: Bernardette Kunert
Monday Morning, May 13, 2024
Resort Tower, Ground Level, Bronze Room 2

10:30 AM 1B-2.1
Development of AlGaInAs Multi-Quantum Well Laser on Silicon via Direct-Bonding and MOVPE Semi-Insulating Buried Heterostructure Regrowth Nicolas Vaissiere[1], Claire Besançon[1], Delphine Neel[1], Célia Cruz[1], Giancarlo Cerulo[1], Dalila Make[1], Valentin Ramez[2], Franck Fournel[2], Frederic Pommereau[1] and Jean Decobert[1]; [1]III-V Lab, a joint lab of Nokia Bell Labs, Thales Research and Technology and CEA LETI, France; [2]Univ. Grenoble Alpes, CEA/LETI, France

The III-V-on-SOI heterogeneous integration is an established photonics platform for creating scalable and compact active devices, such as lasers, modulators, or photodetectors on large

Si wafers [1]. However, effective thermal management is crucial to enhance the performance of photonic integrated circuits (PICs) on the silicon photonics platform. At the component level, the poor thermal properties of the oxide isolation layer on SOI wafers and the ridge-like geometry of waveguides (WGs) contribute to increased thermal spreading resistance [2], leading to self-heating effects during operation and a subsequent reduction in gain.

To address these challenges, a Semi-Insulating Buried Heterostructure (SIBH) technology is developed. This involves regrowing a InP:Fe layer to bury the III-V gain material, utilizing its thermal conductivity, efficient current injection scheme, and circular mode transmission [3]. The paper introduces a thick vertical p-i-n AlGaInAs Multiple Quantum Wells (MQWs) buried laser performance, achieved through direct bonding on silicon wafers and SIBH regrowth.

The fabrication process involves growing an inverted III-V laser stack by MOVPE on an InP substrate. In this study, our emphasis was on laser test prototypes, ensuring that the optical mode remains unaffected by interactions with passive WGs on the SOI wafer. Consequently, we bonded the III-V wafer to an oxidized silicon wafer, which included a 200 nm-thick silica layer, using a conventional hydrophilic direct bonding process [4]. The InP substrate as well as the sacrificial layers were then selectively removed. Afterwards, WGs are etched down to two-thirds of the MQWs stack, and a semi-insulating InP:Fe cladding layer is regrown laterally. Vias were etched down and, metallic pads were defined to obtain p-/n- contacts. Finally, bars of 1 mm-long FP lasers, with different WG widths, were cleaved and soldered on thermally conductive sub-mounts. In parallel, a sample clone underwent annealing at 620°C to mimic SIBH regrowth conditions after the bonding step. The X-ray diffraction profiles and AFM measurements confirm the stability and quality of the MQWs material.

The resulting structure exhibits successful laser operation, with a low threshold current (45 mA) and an output power of 9.4 mW at 150 mA for a WG width of 2.5 µm. The slope efficiency at threshold indicates similar injection efficiency for different waveguide widths (0.103 W/A). The series resistance values are comparable to standard shallow-ridge lasers on the same SOI platform [5]. Thanks to optical confinement induced by SIBH regrowth, far-field measurements demonstrate a quasi-circular mode profile with specific horizontal and vertical divergence angles of 26.3° and 27.8°.

In conclusion, this work presents a novel approach to address thermal challenges in III-V-on-SOI integration through the development of SIBH technology, showcasing promising results in the fabrication and performance of thick vertical p-i-n AlGaInAs MQWs buried lasers on silicon wafers.

[1] R. Jones, "Overview and Future Challenges on III-V Integration Technologies in Silicon Photonics Platform," in *2021 OFC*, 2021, pp. 1–3.
[2] J. M. Ramirez *et al.*, "III-V-on-Silicon Integration: From Hybrid Devices to Heterogeneous Photonic Integrated Circuits," *IEEE J. Sel. Top. Quantum Electron.*, vol. 26, no. 2, 2020.
[3] V. Rustichelli *et al.*, "Monolithic integration of buried-heterostructures in a generic integrated photonic foundry process," *IEEE J. Sel. Top. Quantum Electron.*, vol. 25, no. 5, Sep. 2019.
[4] F. Fournel, C. Morales, L. Libralesso, H. Moriceau, F. Rieutord, and C. Ventosa, "Hydrophilic low-temperature direct wafer bonding," *J. Appl. Phys.*, vol. 104, no. 12, p. 123524, 2008.
[5] C. Besancon *et al.*, "AlGaInAs Multi-Quantum Well Lasers on Silicon-on-Insulator Photonic Integrated Circuits Based on InP-Seed-Bonding and Epitaxial Regrowth," *Appl. Sci.*, vol. 12, no. 1, p. 263, Dec. 2021, doi: 10.3390/app12010263.

10:50 AM 1B-2.2
van der Waals Epitaxy on 2D Hexagonal Boron Nitride for Flexible MicroLEDs Jean Paul Salvestrini and Simon Gautier; Georgia Tech Europe, France

Micro-LED fabrication traditionally involves top-down or bottom-up methods, each with drawbacks [1-6]. Top-down methods, using dry-etch after epitaxy, induce crystallographic defects, and trap states, reducing performance and viability tiny microLEDs. Bottom-up approaches overcome sidewall damage but entail complex processing and multiple epi-growth steps in different reactors. Successful commercialization faces challenges in lifting-off and transferring LEDs from native substrates and diminished performance in tiny micro-LEDs due to chemical etching.

This work integrates selective area growth with van der Waals epitaxy on 2D hexagonal Boron Nitride (h-BN) to address aforementioned challenges. Initial steps include van der Waals epitaxy of 2D h-BN on silica masks defining micro-LED regions, followed by selective area growth of MQWs LED heterostructures. The process is applied to micro-LEDs ranging from 32 µm to 1.4 µm in diameter, using square, hexagonal, and triangular mask openings. Challenges addressed in this work include (a) selectivity and quality of micro-LED heterostructures in small openings, ensuring smooth sidewalls even for 1.4 µm structures, (b) demonstrating SiO2 mask widths of 2 to 5 µm for optimal separation and cost reduction, (c) fabricating ultra-small micro-LEDs down to 1.4 µm, and (d) achieving liftoff and transfer of various shapes and sizes down to 8 µm.

The process yields ultra-smooth crystalline sidewalls, enabling straightforward mechanical lift-off and transfer of LED heterostructures, even as small as 1.4 µm. Beyond device fabrication, lift-off control and a self-lift-off and transfer (SLOT) technique to copper supports are explored. MicroLEDs on flexible copper substrates with a bend radius as small as 3mm are demonstrated, showcasing the versatility and potential of the proposed approach.

References

[1 K. R. Son, V. Murugadoss, K. H. Kim, T. G. Kim, Appl. Surf. Sci. 2022, 584, 152612.
[2] J.M.Smith,R.Ley,M.S.Wong,Y.H.Baek,J.H.Kang,C.H.Kim,M. J. Gordon, S. Nakamura, J. S. Speck, S. P. DenBaars, Appl. Phys. Lett. 2020, 116, 071102.
[3] M. Sheen, Y. Ko, D. Kim, J. Kim, J. Byun, Y. Choi, J. Ha, K. Y. Yeon, D. Kim, J. Jung, J. Choi, R. Kim, J. Yoo, I. Kim, C. Joo, N. Hong, J. Lee, S. H. Jeon, S. H. Oh, J. Lee, N. Ahn, C. Lee, Nature 2022, 608, 56.
[4] Y. Cai, J. I. H. Haggar, C. Zhu, P. Feng, J. Bai, T. Wang, ACS Appl. Electron. Mater. 2021, 3, 445.
[5] J. Oh, J. Ryu, D. Yang, S. Lee, J. Kim, K. Hwang, J. Hwang, D. Kim, Y. Park, E. Yoon, H. W. Jang, Cryst. Growth Des. 2022, 22, 1770.
[6] Y. Peng, M. Que, H. E. Lee, R. Bao, X. Wang, J. Lu, Z. Yuan, X. Li, J. Tao, J. Sun, J. Zhai, K. J. Lee, C. Pan, Nano Energy 2019, 58, 633.

11:10 AM 1B-2.3
van der Waals Epitaxy and Lift-Off of GaN for Bonded Heterostructures Michael Snure, Eric Blanton and Stefan Nikodemski; Air Force Research Laboratory, United States

Semiconducting heterostructures are essential to modern electronics; however, to meet demands for higher frequency, higher power, and more efficient operation, new material combinations, thicknesses, and geometries will be required. High quality heterostructures suitable for such devices are traditionally limited to material combinations that are lattice, chemically, and thermally matched due to the formation of defects during growth. As an alternative to epitaxial growth, bonding can be used to create heterostructures between highly mismatch materials. Wafer bonding has been explored for decades to produce such heterostructures but can result in mechanical and chemical defects due to the pressure and temperatures required to bond thick wafers. Alternatively, using thin flexible membranes, heterostructures can be improved by alleviating much of the mechanical issues present in the bonding process, which can reduce bonding temperature and pressure requirements making processing simpler and reducing some of the interface defects. Here, we present work on bonded heterostructures fabricated by epitaxial lift-off and bonding of GaN membranes. Freestanding GaN membranes were produced by metal organic chemical vapor deposition of GaN on BN/sapphire van der Waals (vdW) templates. Due to the weak interplanar bonding between layers in vdW BN layer, GaN can be mechanically separated from the substrate and transferred. We will discuss vdW epitaxy of GaN on 2D BN emphasizing key challenges to achieving high quality films that can be easily lifted-off and transferred. The mechanical lift-off approach will also be discussed and its impact on GaN membrane quality. Finally, pn and Schottky diodes fabricated using isolated GaN membranes bonded to 3D and 2D material substrates including p-Si, p-GaN, and graphene/SiO2 will be discussed. Temperature dependent IV and CV characterization will be presented, which indicates good rectification and low defect density interfaces. On/off ratios of 107, 109, and 105 were measured for the GaN/Si, GaN/GaN, and GaN/graphene diodes, respectively. This work demonstrates that diodes between high mismatched materials can be fabricated using high quality membrane films produced by vdw epitaxy and lift-off.

11:30 AM 1B-2.4
Selective GaN Growth on Patterned hBN for Transferring MEMS onto Flexible Substrates Jean Paul Salvestrini and Simon Gautier; Georgia Tech Europe, France

Gallium Nitride (GaN) has garnered significant attention in the field of MEMS due to its various characteristics [1,2]. The quality of epitaxial layers grown on a substrate is a critical parameter that significantly influences device performance, especially in microelectromechanical systems (MEMS), where mechanical functionality, depends on crystal quality. Two key parameters shape this quality: the lattice parameter mismatch, as well as the difference in thermal expansion coefficients between the desired epilayers and the substrate. Despite the option of using the same desired growth layer as a substrate to achieve the best crystal quality of the epitaxial layer, the high cost of these substrates restricts their usage in high-volume production. Moreover, specific applications require substrates with distinct characterizations, such as high-temperature dispersion substrates, transparent, or even flexible substrates. However, these substrates often fail to meet the lattice parameter and thermal expansion coefficient requirements and are unable to endure the high temperatures associated with MOCVD growth.
Recently, we have demonstrated the possibility of growing III-nitride layers on two-dimensional materials using van der Waals epitaxy [3-5]. 2D materials, including graphene or hexagonal Boron Nitride, serve as a release layer. This approach consists of a mechanical peeling-off of epilayers from the substrate, allowing a dry and instantaneous release [6]. The structures can be transferred to any desired substrate using various methods, such as elastomer stamps, commercial adhesive tapes for retraction, and thermocompression, or capillary forces for placement. In this work, a new h-BN-enabled approach is reported. This process is facilitated by the use of a thick layer of electroplated copper deposited on top of III-N MEMS device, adding rigidity to the structure to prevent crack generation. Furthermore, when combined with moderate thermal treatment, it enables the self-lift-off and transfer (SLOT) of MEMS structures from the sapphire initial wafer [6]. Importantly, the separated surface is atomically flat, and the native substrate can be reused repeatedly as a growth substrate.
We aim to create high-quality III-Nitride MEMS with integrated transduction schemes that can be transferred onto pre-patterned flexible substrates, using Van der Waals epitaxy. The process involves localized Selective Area Growth (SAG) at the micron scale of MEMS structures on a rigid patterned initial sapphire substrate. SAG eliminates the need for subsequent etching procedures to generate MEMS geometry. Our results could pave the way for the development of more advanced and sophisticated flexible electronics applicable in a

wide range of applications.

References :
1. Mina Rais-Zadeh et al., J. Microelectr. Syst. 23. 1252-1271 (2014)
2. Brueckner, K. et al. Two-dimensional electron gas based actuation of piezoelectric AlGaN/GaN microelectromechanical resonators. Appl. Phys. Lett. 93, 173504 (2008).
3. Ayari, T. et al. Wafer-scale controlled exfoliation of metal organic vapor phase epitaxy grown InGaN/GaN multi quantum well structures using low-tack two-dimensional layered h-BN. Appl. Phys. Lett. 108, 171106 (2016).
4. Ayari, T. et al. Gas sensors boosted by two-dimensional h-BN enabled transfer on thin substrate foils: towards wearable and portable applications. Sci. Rep. 7, (2017).
5. S. Karrakchou et al., Monolithic Free-Standing Large-Area Vertical III-N Light-Emitting Diode Arrays by One-Step h-BN-Based Thermomechanical Self-Lift-Off and Transfer, ACS Appl. Electronic Mat. 2021 3 (6), 2614-2621
6. Y. Kobayashi et al., Layered boron nitride as a release layer for mechanical transfer of GaN-based devices. Nature 484, 223–227 (2012).

11:50 AM *1B-2.5
Epitaxy Innovation for Future of 3D Electronic System
Jeehwan Kim; Massachusetts Institute of Technology, United States

Reduction in the size of devices is no longer an option for enhancing the performance of next-generation electronic products. Vertical stacking of wafers containing electronic devices, known as 3D heterogeneous integration, is being considered as the most promising strategy for further performance enhancement. However, this technique requires the following complex processes: i) drilling holes through the wafer (TSV), filling the holes with Cu, and bonding the wafers through bumps. Omitting wafers during such a complicated 3D stacking process would greatly simplify the process and minimize device loss. However, there are almost no options available to transfer active devices detached from the wafer and restack them together. The direct growth of device layers on top of finished circuitry is even more challenging. For the past decade, we have developed ways to transfer and stack single-crystalline semiconductor device membranes to revolutionize 3D heterogeneous integration [1-8]. More recently, we have successfully discovered a way to directly grow perfect single-crystalline semiconductors on amorphous insulators to even more advance monolithic 3D heterointegration [9]. In this talk, I will discuss about our epitaxial solutions to advance the 3D monolithic integration technology and their applications for advanced electronics [9, 10], optoelectronics [11], and bioelectronics [12-13].

References: [1] *Nature* 544, 340 (2017), [2] *Nature Materials* 17, 999 (2018), [3] *Nature Materials* 18, 550 (2019), [4] *Nature Nanotechnology* 15, 272-276 (2020), [5] *Nature Electronics*, 2, 439 (2019), [6] *Nature*, 578, 75 (2020), [7] *Nature Nanotechnology* 15, 574 (2020), [8] *Nature Nanotechnology*, 17, 1054 (2022), [9] *Nature*, 614, 88 (2023), [10] *Nature Electronics*, 5, 386 (2022), [11] *Nature*, 614, 81 (2023), [12] *Science Advances*, 7, 27 (2021) [13] *Science* 377, 859 (2022)

SESSION 1C-1: Doping in Nitrides
Session Chair: Jeehwan Kim
Monday Afternoon, May 13, 2024
Resort Tower, Ground Level, Bronze Room 1

2:00 PM 1C-1.1
Conductivity Analysis of Si-Doped AlN on Sapphire with Varied Growth Conditions
Haicheng Cao[1], Mingtao Nong[1], Xiao Tang[1], Chehao Liao[2], Vishal Khandelwal[1], Ying Wu[1], Xiaohang Li[1] and Tingang Liu[1]; [1]King Abdullah University of Science and Technology, Saudi Arabia; [2]National Yunlin University of Science and Technology, Taiwan

Semiconductors with larger bandgaps are increasingly crucial due to rapid advancements in power device technology [1]. Among them, Aluminum nitride (AlN), with its ultra-wide bandgap (6-6.2eV), high breakdown field, thermal conductivity, and its seamless integration with nitride-based devices has attracted extensive interest. To date, the epitaxial growth of high-quality Si-doped AlN via MOCVD has predominantly been conducted on native AlN substrates to mitigate dislocation densities. However, the limited size and prohibitive cost of native AlN substrates necessitate exploring the growth of high-quality doped AlN on alternative substrates for commercial viability. Therefore, our study focuses on MOCVD growth of Si-doped AlN epitaxy on sapphire substrate, and aims to examine the relation between epitaxial conditions, surface morphology, defects, and AlN film conductivity on sapphire substrate.
In this research, we grew a 636nm undoped AlN layer and a 500nm Si-doped layer (Si: 4.6×10^{18} cm^{-3}) on AlN template on sapphire. We primarily investigated two critical growth conditions: temperature (1100°C to 1300°C) and V/III ratio (1000 to 5000), using a single quarter of a substrate for each individual condition to eliminate substrate differences. Cathodoluminescence (CL) spectra and Circular Transmission Line Measurement (CTLM) method were used to characterize the defect and conductivity of the Si-doped AlN, respectively. During CL characterization, the acceleration voltage was precisely maintained at 4 keV to ensure all the signals are from the Si-doped layer.
The full width at half maximum (FWHM) of the rocking curves on AlN (002) and (102) orientations showed crystallization and dislocation density to be largely unaffected by varying growth conditions. However, atomic force microscopy (AFM) images revealed that increased growth temperature led to a morphological shift from bilayer to macro-step flow due to a reduced aluminum surface supersaturation [2]. Higher temperatures also resulted in decreased conductivity, rendering Si-doped AlN non-conductive at 1300°C. CL spectra showed the emergence of

Al vacancy-Si (V_{Al}-Si) complex peaks at higher temperatures, indicating the formation of V_{Al}-Si complexes that lead to Si compensation and reduced conductivity. At 1300°C, the V_{Al}-Si peak shifted to higher energies, suggesting the creation of high-order V_{Al}-nSi complexes [3] and further increased resistivity. Temperature-dependent conductivity measurements indicated no significant change in Si ionization energy in AlN, implying a dominant role for Si deep state (DX) centers [4].
Surface morphology comparisons showed 3D growth features with increased roughness and enhanced nAlN conductivity with increasing V/III ratio. CL spectra variations revealed a strong relationship between conductivity and reduced carbon defect (C_N) peak intensity, as evidenced by the decrease of C_N (an acceptor center). Moreover, the ionization energy of Si remained consistent across different V/III ratios, with Si DX centers still predominant.
Overall, this study is crucial in demonstrating the interdependence between Si-doped AlN epitaxial conditions on sapphire and factors like conductivity, surface morphology, and defects, providing essential insights for the cost-effective heteroepitaxial growth of AlN-based power devices.

References

[1] J. Y. Tsao et al. Adv. Electron. Mater, 4, 1600501 (2018).
[2] I. Bryan et al. Journal of Crystal Growth 438, 81 (2016).
[3] R. Matthew et al. APL Mater. 8, 091110 (2020).
[4] W. Alan Doolittle et al. Appl. Phys. Lett. 123, 070501 (2023)

2:20 PM 1C-1.2

Diffusion of Magnesium and Silicon in AlGaInN Layers Grown by MOVPE Layers Ewa A. Grzanka[1], Mikolaj Grabowski[1], Pawel Michalowski[2], Rafal Jakiela[3], Robert Czernecki[1], Andrzej Turos[2] and Michal Leszczynski[1]; [1]Institute of High Pressure Physics PAS, Poland; [2]Lukasiewicz Research Network - Institute of Microelectronics and Photonics, Poland; [3]Institute of Physics PAS, Poland

The aim of this presentation is to show an easy diffusion of magnesium atoms which are the only acceptors in nitrides. This topic has been discussed in a number of papers. However, most of the results have been obtained for rather high temperatures (1100-1300ºC) and are in –c direction (from Ga-face towards N-face). In this work, we grew Mg-doped layers buried in the epi-structure what enabled us to compare the diffusion in +c and –c directions. Moreover, we examined Mg-diffusion not only for GaN, but also for InGaN and AlGaN layers. Mg diffusion is compared with Si diffusion. The samples were grown using AIXTRON Close Coupled Showerhead 3x2". The epi structures were grown on GaN/sapphire templates and consisted of the following layers: 200 nm of Mg doped, 400 nm undoped, 200 nm Si doped, 400 nm undoped. 1st sample consisted of only GaN layers, the 2nd sample had undoped layers of InGaN, the 3rd sample had doped layers of InGaN (1.5% In), the 4th sample had undoped layers of AlGaN and the 5th sample had doped layers of AlGaN (6% Al). GaN and AlGaN layers were grown at 980ºC, InGaN at 820ºC.Growth rate was 1.9 mm/h in sample with GaN layers only, and 0.6 mm/h in case of the rest of samples. After growth part of the samples were annealed at 1030ºC for 1 hour. All the samples (before and after annealing) were examined using SIMS.
From the SIMS measurement of 1st sample following conclusions can be drawn: Si-dopant is almost exactly as it had been planned; no significant diffusion has been observed for the as-grown sample; after annealing Si diffused out in +c and –c direction, but only slightly; Mg diffused out during the growth very significantly: almost 300 nm in +c direction and about 150 nm in –c direction; annealing caused further Mg diffusion: additional 200 nm in +c direction and about 50 nm in –c. From measurement of 2nd sample, the additional following conclusion can be drawn: diffusion of Mg is smaller in InGaN compared to GaN. The results for 3rd sample are very similar to the results given for 2nd sample. Surprizing is the smaller Mg-diffusion in GaN than it was observed for the 1st sample. Also in case of sample 4th, Mg diffusion is smaller than in the case of GaN, but in case of the 5th sample, diffusion into GaN is again similar to the 1st sample.
From the experimental results, we may conclude the following: (i) Mg diffuses much easier as compared to silicon, (ii) Mg diffusion is easier in +c than in –c direction, (iii) AlGaN and InGaN may reduce Mg diffusion. At present, we are not able to give convincing explanations of these results. The first question which deserves further experiments is the following: Is the Mg diffusion via dislocations, via gallium vacancies or via nitrogen vacancies? The big difference between Si-doping and Mg-doping in MOVPE is that the latter is always incorporated with hydrogen atoms. However, how it could influence Mg diffusion is not clear, but one should be aware of the experimental fact, that H diffuses much easier in GaN:Mg, than in GaN undoped or Si-doped. Concerning the direction of Mg diffusion, one can speculate that MOVPE reactor has an Mg- memory. This could explain the asymmetry of Mg concentration for the as-grown samples, but not for the annealed ones. The origin of the easier diffusion into +c direction has to be explained. Concerning the results for InGaN/GaN samples, it is not clear why Mg diffusion rate from InGaN to GaN is smaller than for the situation when Mg diffuses from GaN or AlGaN to GaN. This can be related to the lower growth temperature of InGaN and smaller vacancy concentration. Moreover, during annealing indium atoms easily move what may influence the Mg diffusion. Smaller diffusion rate in AlGaN as compared to GaN may have an origin in smaller point defect concentration, but, again, this has to be checked in the experiments we are planning.

2:40 PM 1C-1.3

MOCVD Growth of Diluted AlGaN and Study of Defects Related to Carbon and Iron Pawel Prystawko[1], Piotr Kruszewski[1], Ewa Grzanka[1] and Vladimir P. Markevich[2]; [1]Institute of High Pressure Physics, PAS, Poland; [2]University of Manchester Manchester, United Kingdom

Understanding and identification of point defects in GaN layers are important for the improvement of breakdown voltage of electronic devices as well as efficiency of III-nitride-based light emmitting devices. In case of the thernary AlGaN layers this subject is at the less mature stage.

In this work we present results of a deep-level transient spectroscopy (DLTS) and high-resolution Laplace DLTS measurements study of traping states in Schottky diodes fabricated on silicon-doped GaN and AlGaN grown by metal-organic-vapor-phase epitaxy (MOVPE) on highly conductive n-type Ammono-GaN substrates. The selected growth conditions promoted low compensation by reduction of carbon residual acceptor concentration in GaN layers. Similar attempt was done in low aluminium composition ternary layers. Results of net donor concentration obtained from CV-measurements of n-type layers under study were compared with concentrations of impurities (C, Si, O and Fe) determined by secondary ion massspectrometry (SIMS). We also obtained activation energies of respective point defects from the extrapolated Arrhenius plots and calculated point defect concentrations. An excellent agreement with carbon-related deep level signatures can be noticed. In case of AlGaN layers there is significant influence of iron impurity on charge trapping in addition to residual carbon. It leads to increased serial resistance of Schottky diodes as compared to GaN diodes. The reported results are of the utmost importance for the improvement in performance of high-voltage avalanche-capable AlGaN diodes.
We also proposed and discussed model explaining electron emission rate dependence of point defect of the Fe_{Ga}(0/-) acceptor level on numer of aluminium atoms surrounding this site in the second-nearest neighbor (2NN). Our finding shows that in dilute AlGaN layers grown by MOVPE, aluminum and iron atoms are randomly distributed in the material up to about 6% of AlN content .

3:00 PM 1C-1.5
Ohmic Contact Improvement of AlNAl0.8Ga0.2N Heterostructure by Atomic Layer Etching (ALE) Tingang Liu, Haicheng Cao, Mingtao Nong, Zhiyuan Liu and Xiaohang Li; King Abdullah University of Science and Technology, Saudi Arabia

AlGaN/GaN heterostructures are extensively used in applications such as radio frequency (RF) and power devices. For higher power applications, there is a growing trend to shift from conventional AlGaN/GaN to AlN/AlGaN structures, due to the higher electric breakdown field of AlGaN compared to GaN as the channel layer. However, a significant challenge with AlN/AlGaN heterostructures is the formation of effective ohmic contacts, impeded by difficult electron tunneling through the AlN cap layer between the contact and the AlGaN layer. The typical approach involves etching down this cap layer to bring the contacts closer to the AlGaN channel layer, thereby improving electron tunneling. However, the common reactive ion etching (RIE) method can cause significant plasma-induced damage, negatively impacting the contact quality. Atomic Layer Etching (ALE) offers a solution, being a self-limiting process that removes layers atomically with minimal damage, thereby enhancing the surface quality for contacts. This study employs ALE to etch recessed ohmic contacts in AlN/$Al_{0.8}Ga_{0.2}N$ heterostructures, achieving a reduced contact resistivity of 4.59×10^{-3} Ωcm^2. This demonstrates ALE's effectiveness in advancing ohmic contact, potentially for HEMT applications.
In this study, an AlN (26 nm)/$Al_{0.8}Ga_{0.2}N$ (200 nm)/AlN (600 nm) heterostructure was synthesized using Metal-Organic Chemical Vapor Deposition (MOCVD) on a 1 µm AlN commercial template. The 80% aluminum composition in the AlGaN layer was confirmed by UV-Vis and X-ray diffraction analysis. The Full Width at Half Maximum (FWHM) values for the (002) and (102) rocking curves of the AlGaN layer were determined to be 179 and 256 arcsec, respectively. Root Mean Square (RMS) of the roughness of the surface is 493 pm measured by Atomic Force Microscope (AFM). The AlN/$Al_{0.8}Ga_{0.2}N$ heterostructure has a sheet concentration of 3.994×10^{13} /cm^2, measured via the Hall effect, and sheet resistance of 2.061×10^{3} Ω/square extracted from CTLM.
To investigate the ALE effect, Ti/Al/Ti metal stack (20 nm/120 nm/80 nm) was deposited on the heterostructure etched by RIE (25 nm), etched by RIE (18 nm) and ALE (7 nm), and without etching, and are named as S1, S2, and S3, respectively. The samples S1, S2, and S3 show onset voltage of 2V, 0.5V, and 5V, respectively; and contact resistivity of 1.96×10^{-2}, 4.59×10^{-3}, and 3.02×10^{-2} Ωcm^2, respectively. The results reveal a positive effect of ALE by inducing a significant decrease in current and contact resistivity.

3:20 PM BREAK

SESSION 1C-2: Optical Device
Session Chair: Yun-Li Li
Monday Afternoon, May 13, 2024
Resort Tower, Ground Level, Bronze Room 2

2:20 PM 1C-2.2
Low-Leakage GaN-Based *p-i-n* Avalanche Photodiodes by Edge-Termination Engineering with Shallow-Bevel Mesas Zhiyu Xu, Theeradetch Detchprohm, Shyh-Chiang Shen, Nepomuk Otte and Russell Dupuis; Georgia Institute of Technology, United States

III-N compound semiconductors, having a wide and direct bandgap and bandgap engineering flexibility, are promising materials for UV detection applications. GaN-based avalanche photodiodes (APDs) inherently possess a high visible-to-UV rejection ratio, low dark currents, high-efficiency UV spectral response, and high-temperature operation. With the advancement in high-quality bulk GaN substrates having a low threading dislocation density, vertical GaN devices grown on GaN substrates can exhibit a robust avalanching capability under reverse bias. As is normally observed for APDs with thin multiplication layers, the performance of GaN-based APDs can suffer from leakage currents arising from insufficient edge electric-field termination. Under high fields when reverse biased, local premature breakdown may occur due to field crowding at the junction interface near the edge of the device mesa structure. Various methods have been developed to control the electric-field profile at the edges of the device. In this report, low-leakage GaN *p-i-n* (PIN)

homojunction APDs with a device mesa side-wall termination employing a shallow-bevel mesa of ~1-2° will be described. The APD structures were grown by metalorganic chemical vapor deposition (MOCVD) in an AIXTRON 6x2 CSS reactor and consisted of a 1 μm *n*-GaN:Si ([*n*] = 7×10^{18} cm^{-3}), a 350 nm GaN:uid (UID) drift layer, a 300 nm *p*-GaN:Mg ([*p*] ~ 1×10^{18} cm^{-3}), and a 20 nm p^+-GaN:Mg ([Mg] = 1×10^{20} cm^{-3}) on the Ga-face of an ammonothermal (0001) *n*-type bulk GaN substrate. Photoresist masks employed for shallow-bevel-mesa etching were created by multi-step lithography followed by thermal reflow above 200°C. The bevel-edged device mesas of ~90 μm diameter were then formed by Cl_2/BCl_3 inductively coupled plasma (ICP) etching to the UID-GaN layer. The top-illuminated APDs were further processed to reduce optical absorption losses in the thick *p*-GaN:Mg layer by forming a 150 nm-deep recessed window region by ICP etching in the center of the device to partially remove a portion of the *p*-GaN layer. The *p*-contact metal stack of Ni/Ag/Pt was formed by electron-beam evaporation followed by annealing in compressed dry air, and the backside *n*-contact was deposited by e-beam evaporation to form a metal stack of Ti/Al/Ti/Au. The APDs were then passivated with a layer of spin-on glass (SOG). No anti-reflection coatings were applied.
The 300K *J-V* and spectral response characteristics were measured for 90-μm-diameter GaN PIN APDs with a shallow-bevel-mesa edge termination and an etched recessed window under dark and UV-illuminated conditions. Under dark condition, the leakage current density is fairly constant at < 10^{-9} A/cm^2 up to a reverse bias of -70 V. The breakdown voltage (V_{BR}) is -106.9 V, and the leakage current density at the onset of breakdown is ~3.4×10^{-5} A/cm^2. Under λ = 360 nm UV illumination, the avalanche gain increased to 4.7×10^6 which is limited by a current compliance of 1 mA. The spectral response of the GaN UV APDs with a 150 nm-deep recessed window was measured under various reverse bias conditions. At zero bias, the peak of the photoresponse was at λ = 350 nm with a responsivity of 121 mA/W, corresponding to an external quantum efficiency (EQE) of 42%. At reverse bias of -110 V, just beyond avalanche breakdown, the responsivity was increased across the UV wavelengths with a peak responsivity of 772 mA/W and the peak absorption shifted to λ = 360 nm, corresponding to an EQE of 264% due to the avalanche current gain. The true avalanche capability of the UV GaN APDs was confirmed by temperature-dependent measurements of the reverse-bias breakdown voltage, V_{BR}, vs. T , with derived positive temperature coefficient of 0.02V/K, which indicates that impact ionization and avalanche processes are the dominant mechanisms at breakdown. Further descriptions of the device and UV performance will be given.

2:40 PM 1C-2.3
Growth and Characterization of GaN-Based Avalanche Photodetectors with AlGaN Windows Davide Balzerani, Alexandra Dolgashev, Zhiyu Xu, Nepomuk Otte, Shyh-Chiang Shen, Theeradetch Detchprohm and Russell Dupuis; Georgia Institute of Technology, United States

GaN-based avalanche photodiodes (APDs) operating in the ultraviolet (UV) spectrum have many potential applications. We report on GaN-based UV APDs with AlGaN windows grown on low-dislocation-density Free-Standing (FS) GaN substrates by metalorganic chemical vapor deposition (MOCVD) to improve the responsivity for a top-illuminated III-N UV APD design. The studied devices employed *p-i-n* (PIN) GaN based device structures with various *p*-type windows: (1) a uniformly doped *p*-GaN:Mg layer, (2) a graded-composition *p*-AlGaN:Mg window, and (3) a *p*-AlGaN:Mg short-period superlattice (SPSL) window.

The APD epitaxial structures were grown on (0001) FS GaN:Si ([*n*]~1E18 cm^{-3}) substrates in an AIXTRON close-coupling-showerhead 6x2 reactor. Trimethylgallium, trimethylaluminum, ammonia, biscyclopentadienyl magnesium (Cp_2Mg) and SiH_4 were used as sources. The growth of the device structures started with a 800 nm-thick GaN:Si ([*n*]~1E18 cm^{-3}) layer followed by a 1 μm-thick GaN:Si ([*n*]=6E18 cm^{-3}) layer. A 200 nm-thick unintentionally doped GaN:*uid* ([*n*]~2E16 cm^{-3}) multiplication layer was grown on the top of the *n*-type layer. A 100 nm-thick *p*-GaN:Mg layer was grown on top of the GaN:*uid* layer of the all-GaN PIN structure. In addition, an APD with a graded-composition *p*-AlGaN:Mg "window" was grown with a 200 nm-thick $Al_xGa_{1-x}N$:Mg layer (*x* was linearly graded from 0.25 to 0.00) on top of the GaN:*uid* multiplication layer. A third structure was grown with a 200 nm-thick *p*-doped AlGaN (average *x*=0.13) SPSL window with a period of 5 nm. The device structures were completed with a 20 nm contact layer of heavily doped ([Mg]~1E20 cm^{-3}) GaN.

In the device fabrication process, the *p*-type layers in regions around the intended mesa areas were implanted with nitrogen to create an insulating region for suppressing sidewall current leakage [1]. Then mesas with implanted sidewall regions were formed using inductively coupled plasma $BCl_3/Cl_2/Ar$ etching. *n*-type and *p*-type ohmic contact metals were deposited with an e-beam evaporator. The device surface was passivated by depositing a ~600 nm-thick SiO_2 layer via plasma-enhanced chemical vapor deposition.

The *J-V* characteristics of 96 μm diameter APDs were measured under both forward and reverse bias. The all-GaN APDs, the APDs with graded composition AlGaN window, and the APDs with a *p*-AlGaN SPSL window exhibited breakdown voltages of about -85, -102 and -99 V at 0.1 A/cm^2, respectively. These values were equivalent to a breakdown electric field of 4MV/cm and higher. The estimated optical gains extracted from their *J-V* characteristics at the compliance current density of 1 A/cm^2 were in the range of 4-7E5. The responsivity of the different structures were also evaluated at different reverse biases. The devices with the graded-composition AlGaN window and the AlGaN SPSL window showed a significant improvement with an about 36% higher responsivity at a bias of about 80% of their respective breakdown voltages with respect to all-GaN devices. More details on device characteristics will be presented.

[1] M. Cho et al. IEEE Tran. Electron Devices 68, 2760 (2021).

3:00 PM 1C-2.4
Epitaxial Growth of AlGaN/AlN Multiple Quantum Wells (MQWs) by Metalorganic Vapor Phase Epitaxy for Far-UV Second Harmonic Generation Shahzeb Malik[1,2], Masaaki Ito[1], Hiroto Honda[1], Ryosuke Noro[1], Kanako Shojiki[3], Hideto Miyake[2], Masahiro Uemukai[1], Tomoyuki Tanikawa[1] and Ryuji Katayama[1]; [1]Osaka University, Japan; [2]Mie University, Japan; [3]Kyoto University, Japan

Far-ultraviolet (UV) light has a plethora of diverse global applications, including virus inactivation, bacterial disinfection, human body sterilization, communication, and sensing. Due to their higher optical nonlinearity and transparency in the far-UV region, AlN and AlGaN materials have been particularly useful for wavelength conversion device applications based on their large bandgap energy up to ~6 eV, which corresponds to ~210 nm. AlN has a high value of 4 to 7 pm/V for the second-order nonlinear susceptibility coefficient along the *c-axis, making it* particularly useful for high-performance far-UV second harmonic generation (SHG) device applications. Wavelength conversion efficiency can be enhanced using transverse quasi-phase matching (QPM) based on spatial modulation of the nonlinear optical constants d_{33} and modal dispersion. We have demonstrated 229-nm far-UV SHG using a polarity-inverted AlN bilayer channel waveguide [1]. In this study, we introduced a novel method of modulating d_{33} by a strong piezoelectric field and third-order nonlinear optical effects using AlGaN/AlN heterostructure instead of polarity inversion. Metalorganic vapor phase epitaxy (MOVPE) of AlGaN multiple quantum wells (MQWs) was demonstrated on a <100 nm thin AlN layer that has been grown over sapphire by sputtering and subsequent face-to-face annealing (SP-FFA) for a 230 nm SHG device application. An 84-nm-thick AlN layer was prepared by SP-FFA on sapphire substrate, and 14-fold AlGaN/AlN MQWs and a 115 nm-thick AlN layer were grown by MOVPE on it. Thanks to the strain-relaxed state for the SP-FFA-grown AlN layer, the MOVPE initiated in a two-dimensional growth mode in the early stage, and we have successfully grown ultrathin AlN/AlGaN MQWs over 84 nm thin AlN. X-ray diffraction (XRD) pattern showed a sharp zeroth-order diffraction peak from the MQWs with high-order satellite fringes, which are attributed to high structural quality and smooth interfaces. The XRD analysis revealed the thicknesses of AlGaN well and AlN barrier layers to be 2.15 nm and 4 nm, respectively, and the AlN molar fraction in AlGaN to be 88%. Atomic force microscopy (AFM) was performed to visualize the surface roughness value of 0.27nm. Further, the channel fabrication process and SHG demonstration will be reported.

References:
H. Honda *et al*., Appl. Phys. Express 16, 062006 (2023).

3:20 PM BREAK

SESSION 1D-1: Nanostructure Epitaxy
Session Chair: Ryan France
Monday Afternoon, May 13, 2024
Resort Tower, Ground Level, Bronze Room 1

4:00 PM 1D-1.1
Formation of InP Crystal Phase Heterojunction by Selective-Area MOVPE and New Junction Transistor Yu Katsumi, Hironori Gamo, Junichi Motohisa and Katsuhiro Tomioka; Hokkaido University, Japan

Crystal phase transition can form hetero phase junction with the different atomic arrangement in the same material, the so-called crystal phase heterojunction (CPHJ) [1], which is an ideal heterojunction regardless of misfit dislocation with critical thickness. Recently, the CPHJ was demonstrated in two-dimensional (2D) transition-metal dichalcogenide (TMD) [2] and perovskite materials [1]. The use of a CPHJ-based perovskite material was demonstrated in a photovoltaic device. The 2D TMD-based CPHJs were utilized for 2D TMD FETs with reducing the contact resistance and Shottky barrier height of the CPHJ. However, the demonstrations of the 2D TMD-based CPHJ were limited in in-plane transistor structure and traditional thermionic emission and lacked the scalability of multi-gate structure and miniaturization. The CPHJ in conventional semiconductors can avoid any concerning for misfit dislocation with the critical thickness that occurs in conventional heteroepitaxial systems and forms unique potential barrier without extrinsic doping or use of Schottky metal contacts. Furthermore, the CPHJ forms two-dimensional electron gas (2DEG) across the CPHJ which is advantage point as compared to the other TMD-based CPHJ and perovskite CPHJ [3]. However, the semiconductor CPHJ was focused on the unique optical properties and the electrical properties and functionalities of III-V-based CPHJs remained unexplored because of the difficulties in fabrication of the complex device structure that can apply the required electric field normal to the CPHJ plane. Therefore, we clarified the crystallographic and electrical properties of the InP CPHJ and demonstrated a CPHJ transistor with a VGAA structure.
The InP NWs were grown in a horizontal low-pressure MOVPE system. Trimethylindium (TMIn), tertiarybuthylphosphine (TBP) and diethylzinc were used as the compensated intrinsic and p-type dopants. Mono-silane (SiH_4) gas was used as the n-type dopant. After thermal cleaning at 600°C in a H_2 and TBP flow, the InP NWs were grown for 15 min at 650°C. The partial pressures of TMIn and TBP were 3.7×10^{-7} and 9.7×10^{-7} atm, respectively. Vertical NW diode and VGAA structure were fabricated by using 3D device processes in previous reports [4].
Growth results showed the vertical InP NW array was uniformly formed and the vertical side facets of the grown InP NWs were rotated by 30° with respect to the {–110} cleavage planes, which means that the crystal structure of the grown InP NWs was the WZ structure. TEM and micro-photoluminescence measurements evidenced that the WZ crystal phase transition occurred in the NWs. And the TEM analysis exhibited the InP CPHJ had atomically flat junction

with lamellar strain. A vertical NW-diode structure was fabricated to characterize the electrical properties of the InP CPHJ. The current density – voltage curves exhibited rectifying properties indicating a formation of Schottky-like band structure due to type-II band discontinuity. The Schottky barrier height of the InP CPHJ was estimated to 0.34 eV. Next, the VGAA structure was fabricated to modulate current transport through the CPHJ and the associated potentials via the gate bias. The device properties indicated that the CPHJ-type transistor was demonstrated for the first time because the current was modulated moderately via the gate bias when using the VGAA architecture. The drain current was modulated with the SS of 88 – 95 mV/dec with the drain source voltage of 0.05 – 1.00 V. This demonstration will provide a new approach to junction design that will lead to the invention of novel transistors using the CPHJ with electron gas and unique barriers contained within the same materials.

References

[1] R. Ji *et al*., Nature Energy **7**, 1170 (2022).
[2] J. H. Sung *et al*., Nature Nanotech. **12**, 1064 (2017).
[3] I. Geijselaers *et al.*, Appl. Phys. Lett., **116**, 232103 (2020).
[4] H. Gamo *et al*., ACS Nano, **17**, 18346 (2023).

4:20 PM 1D-1.2
MOVPE Grown InGaAs/GaAs Semiconductor Quantum Dots as Gain Medium in Edge Emitting Lasers in the Telecom O-Band Michael Jetter, Philipp Noack, Nathalie Benzler and Peter Michler; University of Stuttgart, Germany

Semiconductor quantum dots (QDs) offer various unique properties that make them interesting candidates for the use as gain media in semiconductor laser diodes.
Compared to widely used quantum well laser diodes, the unique physical properties of a three-dimensional confinement within a solid-state system lead to improved thermal stability, lower threshold current densities and a fast gain recovery time in QD gain media.
Metal-organic vapor-phase epitaxy (MOVPE) is used as the method of growth for the QD structures. The self-organized QDs that are created with this technique can show a broad distribution of QD size in a single structure. This leads to a broad gain spectrum, which enables laser devices with wide tuning ranges around 1300nm.
For the use as a gain medium, we grow indium galliumarsenide (InGaAs) QDs on a gallium arsenide (GaAs)substrate. We control the growth parameters, such as material flow and growth time, to produce QDs at high area densities. We incorporate a dots-in-well structure to shift the emission into the telecom O-band and to improve charge carrier confinement. To provide sufficient gain in a broad spectrum, we especially investigate the properties of vertically stacked QD layers.
We incorporate this active region into edge-emitting laser structures, for the characterization of optical gain and absorption properties, as well as the inner losses, which are directly linked to the occurrence of defects during the growth of the active region.

4:40 PM 1D-1.3
Droplet Epitaxy of InAsP Quantum Dots on InP Nanowires for Single Photon Sources Xiaoying Huang[1], Jake Horder[2], Wei Wen Wong[1], Naiyin Wang[1], Yue Bian[1], Karin Yamamura[2], Igor Aharanovich[2], Chennupati Jagadish[1] and Hoe Tan[1]; [1]The Australian National University, Australia; [2]University of Technology Sydney, Australia

Quantum technologies have witnessed substantial advances in recent years. A key component of these systems is a high-performance quantum light source to provide single photons or entangled photon pairs. Among the different types of quantum emitters, III-V semiconductor single quantum dots have superior advantages, such as narrow optical transition lines, short radiative lifetimes, and near-unity quantum efficiency. To enhance spontaneous emission rate and indistinguishability, the quantum dot is often integrated with an optical cavity. Top-down approaches which are commonly used to create these structures generally begins with the epitaxy of quantum dots on a planar substrate, before fabricating the cavity structures such as distributed Bragg reflective grating structures, bullseye structures, or photonic crystal cavities on well-isolated quantum dot regions. However, the main disadvantage of such an approach is the time-consuming process of identifying suitable sparse quantum dot regions and the unavoidable sidewall roughness due to etching-induced damage. In comparison, bottom-up approaches offer a more efficient way of incorporating single quantum dots into high-quality optical cavities, such as in nanowires. However, one of the main challenges here is to incorporate only one quantum dot within the optical cavity.

In this work, we present a combination of droplet epitaxy with selective area epitaxy to realize the deterministic growth of single (InAsP) quantum dots in (InP) nanowire arrays. We systematically investigated the influence of TMIn deposition time and nanowire height on the density of droplets on the nanowires. Our technique allows us to deterministically grow one quantum dot at the tip of each nanowire with a uniform morphology across the entire array. By optimizing the single quantum dot growth and the nanowire cavity design, the single photon emission can be effectively coupled with the dominant mode of the nanowire to realize Purcell enhancement with a single-photon purity of g2 (0) = 0.05. Our study paves the way for the development of on-chip scalable quantum light sources.

5:00 PM 1D-1.4
Selective-Area Growth of InP/AlInP Core-Multishell Nanowires and Light-Emitting Diodes Applications Ziye Zheng[1,2], Shun Kimura[1,2], Yuki Azuma[1,2], Junichi Motohisa[1,2] and Katsuhiro Tomioka[1,2]; [1]Hokkaido University, Japan; [2]Research Center for Integrated Quantum Electronics, Japan

Light-emitting diodes (LEDs) have been developed in wide range of display and lighting technologies. The main materials currently used in the LEDs are nitride-related III-Vs in blue-green region and arsenide/phosphide-alloy III-Vs in red region. Both of those materials have difficulties in achieving

bright yellow LEDs due to the low crystal quality or indirect bandgap. In this regard, wurtzite (WZ) AlInP ternary alloy is expected to solve this challenge because the band structure can be change from indirect to direct bandgap when the crystal phase transfers from zincblende (ZB) to WZ. Recent progress in selective-area growth have demonstrated all WZ InP/AlInP core-multishell (CMS) nanowires (NWs) [1]. However, the demonstration was limited in fixed Al content, and the detailed controllability of Al content for the WZ AlInP alloy shell was unknown. In this study, we characterized the selective-area growth of WZ InP/AlInP core-shell (CS)NWs with the various Al content and demonstrated vertical LEDs using the WZ InP/AlInP CMS NWs.

A 20-nm thick SiO_2 sputtered p-InP (111)A substrates were used for the selective-area growth. Periodical hexagonal openings were formed using electron beam lithography and wet chemical etching. The opening diameter was 30 – 100 nm and pitch was 400 – 2000 nm. Vertical core InP NWs and AlInP shells were grown by low-pressure horizontal MOVPE with H_2 carrier gas. TMIn, TBP and TMAl were used as source materials, and DEZn and SiH_4 were used for p- and n-type dopants. The growth temperature for InP NWs was 660 °C with V/III = 24 and growth time was 400 sec. For AlInP shells, the growth time was 5 min at 480 - 600 °C. The Al content in vapor phase varied from 20% to 90%. As for the growth of NWs for LED application, tubular AlInP-based double heterostructure with radial pn junction was grown on the sidewalls of WZ InP core NW. The vertical NW-LEDs was fabricated by using the device process in previous report [2].

The growth results of InP/AlInP CS NWs showed the CS NWs had hexagonal structure surrounded with {-211} side facets, which were rotated with 30° against cleavage {-110} planes at 480 °C, indicating the crystal phase of the AlInP shell was continued from the WZ InP core NW to AlInP shell. While the CS NWs grown at 600 °C showed {-110} side facets were formed, indicating the ZB phase was formed. This was because the AlInP layer with ZB phase stacked on the top of WZ InP NWs and then started to grow downward along with <111>B direction. Eventually, the WZ InP core NWs were covered with the ZB-phase AlInP shell. While at low growth temperature, the ZB AlInP growth on NW top surface was suppressed and only lateral-over growth with maintaining WZ phase was dominant growth process. These differences were thought to be the competing of Al/In surface diffusion process. XRD and micro-photoluminescence spectra indicated that the Al content in solid phase grown at high temperature became higher than those in vapor phase. Further characterization of Al dependency and growth mechanism will be discussed at conference.

The NW LEDs showed moderate rectification properties with a turn-on voltage of around 0.6 V, ideality factor of around 3 and small series resistance. The EL peaks for primitive LED exhibited 1.42, 1.51 and 1.58 eV at room temperature. The main EL peaks at 1.51 eV and 1.58 eV were originated from WZ AlInP shell layers. Further optimization of the NW-LEDs for visible light emission will be discussed.

[1] F. Ishizaka *et al*., Nano Lett. **17**, 1350 (**2017**).
[2] S. Kimura *et al*., Nano tech. **33**, 305204 (**2022**).

SESSION 1D-2: Nitride Power Device/HEMT
Session Chair: Russell Dupuis
Monday Afternoon, May 13, 2024
Resort Tower, Ground Level, Bronze Room 2

4:00 PM *1D-2.1
Vertical GaN and Ga_2O_3 Power Devices Enabled by MOCVD and HVPE Chirag Gupta; University of Wisconsin-Madison, United States

Wide bandgap (WBG) semiconductors such as gallium nitride (GaN) and silicon carbide (SiC) are rapidly making inroads into the power semiconductor markets dominated by the incumbent silicon (Si). However, the performance of these WBG semiconductors are far from the ideal material limits and thus, leaves significant room for improvement. In this regard, for medium voltage (600–1700 V)/high current (>50 A) applications, with a high Baliga figure of merit (BFOM) and architectural advantages, vertical GaN offers a highly energy-efficient solution. Similarly, for high-voltage applications (>1700 V), ultrawide bandgap (UWBG) semiconductors with their high BFOM present a strong case. Gallium oxide (Ga2O3) has emerged as the UWBG material for next-generation power electronics. Together vertical GaN and vertical Ga2O3 have the potential to serve a large range of power switching applications.

In vertical GaN devices, the low channel mobility in trench MOSFETs led to the development of trench MOSFETs with a regrown channel where the channel regrowth involved the growth of a thin un-doped GaN interlayer followed by an in situ gate-dielectric deposition by MOCVD. Here, the capability of depositing an oxide and III-N material allowed pristine in-situ interface to be obtained resulting in significant improvement in channel mobility. This in situ interface enabled 3–5 times higher channel mobility in these MOSFETs compared to conventional trench MOSFETs. Here, the sidewall channel was vertical and was oriented toward the m-plane. High-performance FETs with > 1200 V have been demonstrated with low on-resistanceand normally off behavior. The first half of the talk will discuss these results.

In recent years, β-Ga2O3 has emerged as a promising candidate for the next generation of ultra-wide bandgap material. With a large bandgap (4.8 eV), high critical electric field (Ec) (8 MV/cm), and high Baliga's figure of merit, β-Ga2O3 can potentially enable power electronics that exceed high voltage performance of silicon carbide (SiC) and gallium nitride (GaN). While the use of Si still prevails in commercial applications, Si/Ga2O3 heterojunction high voltage device which may be on-chip compatible to conventional CMOS gate drivers has rarely been reported. In addition, while Si/Ga2O3 heterojunction combines materials low and high Ec, it is intriguing to investigate its breakdown mechanism. In the later half of this talk, we will discuss our recent demonstration of a Si/(001) Ga2O3 heterojunction p-n diode with a breakdown

voltage of 752 V fabricated using semiconductor grafting. The diode shows low leakage, high on-off ratio, and no C-V hysteresis. This result indicates the possibility of investigation toward gallium oxide based bipolar devices in the future.

4:30 PM 1D-2.2
From MOCVD Growth on 6-Inch Silicon Substrate to Packaging of 150 mm Wide Gate AlGaN/GaN HEMTs for Low-Voltage and High-Current Applications Tarik Moudakir[1], Yves Sama[1], Huong Ngo[1], Sri Saran Venkatachalam[1], Safa Othmani[1], Karim Bouzid[1], Mickaël Petit[2,3,4], Francis Roy[5] and Simon Gautier[1]; [1]Institut Lafayette, France; [2]SATIE, France; [3]ENS Cachan CNAM, France; [4]CNRS UMR, France; [5]Stellantis, France

III-V-based high-electron-mobility transistors (HEMTs) have become a part of modern electronics owing to their potential advantages in high power and high temperature electronics applications, especially for electric vehicles (EVs) where power switching is essential. For instance, with the emergence of autonomous vehicles, the need for a low voltage (< 48V) bus power distribution becomes increasingly evident for the vehicle traction and also for all the new power-demanding electronic functions and features appearing in the latest car generations.

For low voltage systems, the GaN transistors increase the efficiency, shrink the system size, and reduce costs, while driving significantly more current than comparable systems operating at higher voltages. To handle larger currents, transistors should be fabricated in much larger sizes, with extra wide gates up to 150 mm. This calls for MOCVD growth, processing and characterization specific challenges in order to reach the ~1cm^2 area functional devices that are required.

One of the main difficulties in growing GaN-on-silicon is the stress that develops during the growth and the cooling down. That is mostly due to the difference in lattice parameters and thermal expansion coefficients discrepancy between III-N materials and silicon. As a result, the wafer surface uniformity becomes challenging to achieve, especially for growth on large area wafers (6-inch) with extended surface, considering the structural defects that may appear and thus hinder large area device fabrication.

In this work, we report the growth and the fabrication of normally-on, large size AlGaN/GaN HEMTs. High quality and highly homogeneous crack-free AlGaN/GaN structures were grown by metalorganic vapor phase epitaxy (MOCVD) on 6-inch silicon (111) substrates. HEMTs with gate widths ranging from 30 mm up to 150 mm were fabricated, including processing, packaging by an innovative technology and final components electrical characterization. Device packaging based on die embedment in a PCB-like substrate was used to realize the components before characterization.

HR-XRD, SIMS and TEM of HEMT structures will be presented. Devices clean room processing will be described, including the particular actions taken to fabricate the extremely wide gates on the HEMTs (cm^2 sized chips). For HEMTs with a channel length of 9 µm and a width of 150 mm, the saturation current density I_{DS} of 0.4 A/mm with a minimum R_{on} of 8 mΩ were obtained. A high extinction coefficient (I_{DSon}/I_{DSOff}) of 10^{-6} and a low drain leakage current density of 10^{-7} A/mm have been achieved on square-centimeter sized chips.

4:50 PM 1D-2.3
Epitaxy of III-V Nitrides with Strain Relief Layers Analysis—TNL EpiGrow Simulator Praveen K. Saxena, P Srivastava and Anshika Srivastava; Tech Next Lab, India

To sustain the worldwide high demand of electrical energy, GaN is a strongly emerging material grown on SiC for RF frequency or on Si for power electronic device applications. However, GaN cost-effective hetero-epitaxial growth suffers with high defect densities. The technology improvements require accurate prediction with an understanding of their formation. The qualitative and quantitative extraction of types of defects is very difficult to accomplish from an experimental point of view [1-2].
TNL-EpiGrow™ simulator provides cost effective solution to replicate the epitaxial growth in a similar manner as real time reactor [3-4]. TNL-Chemical kinetics utility package provides facility to simulate and optimize the gas and surface phase chemical reactions to help a user work efficiently with large systems of chemical reactions. The adsorption, hopping and desorption mechanism rates are computed using in-house developed kinetic Monte Carlo (kMC) algorithms with capabilities to reproduce the real MOCVD reactor based epitaxial growth experiments[3-4].
In present work authors report the growth morphology of buffer layers of AlN on Si (111) substrate via MOCVD reactor equivalent to an AIXTRON CRIUS® close-coupled-shower head (CCS) architecture [3-4]. The growth process steps include epitaxy of (i) AlN, (ii) varying Al composition in $Al_xGa_{1-x}N$ buffer layers. The basic aim of present work is to understand the formation of line dislocations layer by layer. The AlN lattice parameter (a) is taken 3.1258A as compared to Si (111) 3.84 A. The lattice mismatch causes the tensile strain. At the Si/AlN interface the strain will be high. It reduces as growth proceeds for upper AlN layers. Due to high strain, the probability of formation of line dislocation at interfacial AlN layers is high as compared to upper AlN monolayers. The density of line dislocations depends upon thickness of AlN layers. Successively, epitaxial buffer layers of $Al_xGa_{1-x}N$ with x=0.8, 0.5 and 0.2 are deposited. The lattice parameters of ternary compound increases with increase of Ga content in $Al_xGa_{1-x}N$ as compared to AlN and generate the compressible strain. The thickness of various $Al_xGa_{1-x}N$ buffer layers are optimized to achieve overall minimum strain within $Si/AlN/Al_{0.8}Ga_{0.2}N/Al_{0.5}Ga_{0.5}N/Al_{0.2}Ga_{0.8}N$ structure, further used for GaN epitaxy. The thickness of each buffer layer is decided by proper optimization of partial pressures (**Table I**) of various input gases and chemical kinetics to achieve high quality GaN film with minimum dislocation defects. **Table II** depicts the dislocation data and lattice parameters of deposited

materials. It is found that dislocation density increases with the increase of Ga content (0 - 50%). However, the decrease in dislocation density is observed with the further increase of Ga content beyond 50% (**Table II)**. The dislocation densities data is also justified from the roughness curve where a sudden rise is visible for $Al_{0.8}Ga_{0.2}N$ growth which finally comes down for Ga rich layers. The island-based growth observed and justifies the experimental Stranski–Krastanov (S-K) growth mode.

Table I: input Partial Pressure of Gases

Gases	**AlN**	**$Al_{0.8}Ga_{0.2}N$**	**$Al_{0.5}Ga_{0.5}N$**	**$Al_{0.2}Ga_{0.8}N$**
TMAl	100sccm	97 sccm	94 sccm	80 sccm
TMGa	3 sccm	6 sccm	20 sccm	
NH_3	1 slm	1 slm	1 slm	1 slm
H_2	1 slm	1 slm	1 slm	1 slm

Table II: Extracted Output Parameters

Parameters	**AlN**	**$Al_{0.8}Ga_{0.2}N$**	**$Al_{0.5}Ga_{0.5}N$**	**$Al_{0.2}Ga_{0.8}N$**
Dislocation Density (/cm^2)	$2.5X10^{11}$	$5.65x10^{11}$	$3.03x10^{12}$	$2.625x10^{12}$
Lattice parameter (°A) **a**	3.8332	3.8277	3.8452	3.8861
b	3.8419	3.8489	3.8866	3.8856
c	7.6801	7.6948	7.7127	7.7208

ICM VPE XXI

2024 Las Vegas, NV

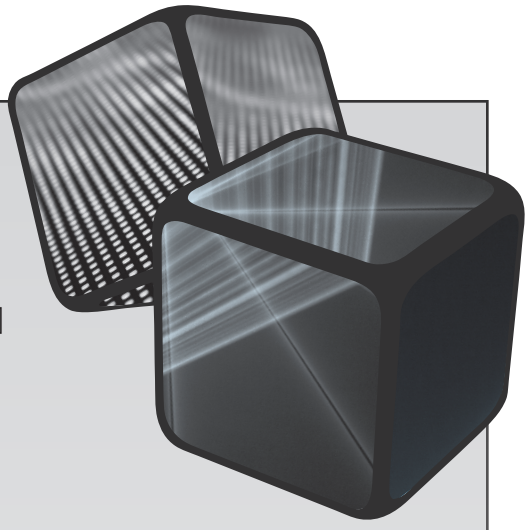

TUESDAY

Oral Presentations

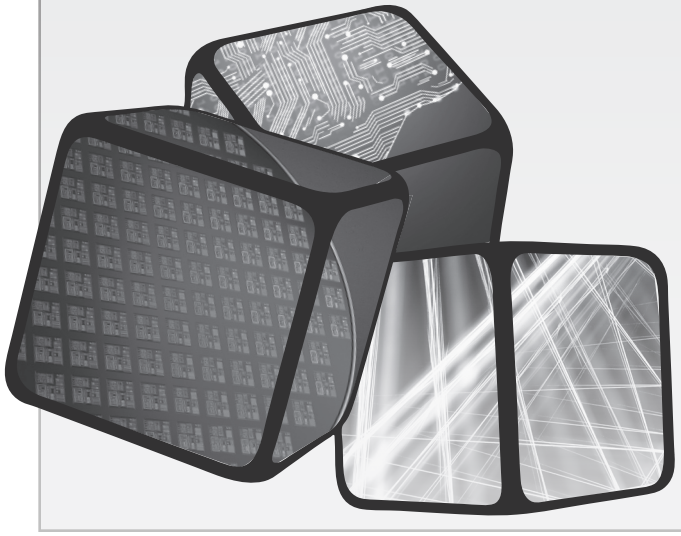

21st International Conference on Metal Organic Vapor Phase Epitaxy

SESSION 2A: Plenary Session II
Session Chairs: Xiuling Li and Nelson Tansu
Tuesday Morning, May 14, 2024
Resort Tower, Ground Level, Silver Room

8:15 AM OPENING REMARKS

8:30 AM *2A.1
Strained-Layer MOCVD Growth—A Paradigm Shift in Epitaxy James J. Coleman; University of Illinois at Urbana-Champaign, United States

Any advancing technology can be outlined by significant paradigm shifts associated with overcoming real, perceived, or poorly understood limits. The nearly sixty-year history of MOCVD growth of compound semiconductors is no exception and includes such examples as the development of purified alkyl sources, effective and safe handling of hazardous materials, high quality heterostructure interfaces, indium compound vapor epitaxy, and, of course, the growth of III-V nitride wide gap materials. In this presentation, we describe the early development of one more of these paradigm shifts - III-V strained-layer MOCVD growth. We will start from the canonical rule that is violated by strained-layer growth, discuss early suggestions of potential advantages and attempts to succeed, how practical structures were eventually grown, the proof of commercial viability, the critical application that drove the development, and some positive unexpected advantages.

9:15 AM *2A.2
MOVPE of Devices for Thermophotovoltaics and Laser Power Conversion Kevin L. Schulte[1], Ryan France[1], Daniel J. Friedman[1], John F. Geisz[1], Eric J. Tervo[2] and Myles Steiner[1]; [1]National Renewable Energy Laboratory, United States; [2]University of Wisconsin–Madison, United States

Emerging applications such as thermal energy grid storage (TEGS), waste heat recovery, small modular nuclear reactors, and portable power generation require high efficiency thermophotovoltaic converters (TPV) that collect photons at longer wavelengths than more standard devices designed for solar photovoltaic conversion. These technologies are critical to industrial decarbonization, and to the transition of our energy grid from one dominated by carbon sources to one dominated by renewable sources. Interest is also emerging in the optical transmission of power across significant distances in free space or via wired connections using lasers. Both applications require devices with high crystalline quality that are finely tuned to a specific wavelength or wavelength range, making the materials of the III-V system, integrated using metamorphic epitaxy via metalorganic vapor phase epitaxy (MOVPE), a compelling solution to realize these device needs. In this talk, I will present recent results on the development of MOVPE-grown devices for TPV and laser power conversion (LPC) applications and discuss how III-V materials can be tailored to achieve high performance for specific applications.
First, I will discuss strategies for making high-performance metamorphic materials, which enable us to tune the bandgap of our devices across a wide range while maintaining a low defect density. These strategies were developed for solar photovoltaics but can be adapted in devices for lower bandgap applications. Then, I will present tandem devices that are optimized for TEGS applications targeting high temperature emitters above 2000 °C. To maintain high system efficiency, these TEGS devices require strong rear reflectors to reject sub-bandgap photons back to the emitter where they can be reabsorbed, preserving their energy. We developed two devices, optimized for slightly different temperatures with high-reflectance Au back contacts. One device employs a GaAs (1.4 eV) junction and a metamorphic GaInAs (1.2 eV) junction while the other employs two metamorphic junctions, one AlGaInAs (1.2 eV) and one GaInAs (1.0 eV). In the latter device, both junctions are matched to the lattice constant of a single graded buffer, which is removed to eliminate a potential source of free carrier absorption, which is highly detrimental to this application. The GaAs/GaInAs device reached a maximum TPV efficiency of 41.1% with a 2,400 °C emitter, while the AlGaInAs/GaInAs device reached a maximum TPV efficiency of 39.3% for a 2,127 °C emitter. We have also developed GaInAs devices grown lattice matched to InP with a bandgap of 0.74 eV that are optimized for somewhat lower temperatures. These devices reach a maximum TPV efficiency of 38.8%% at an emitter temperature of 1,850 °C.
Lower temperature applications require even lower bandgaps. For these we developed GaInAs devices graded past the InP lattice constant to bandgaps below 0.6 eV, grown on both GaAs and InP and tuned for applications such as waste heat recovery and longer wavelength LPC applications. The GaAs-based device, which requires advanced grading techniques to bridge the lattice constant difference from GaAs past InP, has slightly higher defect density but offers similar power output to the InP-based device under high concentration. The InP-based cell is estimated to yield 1.09 W/cm^2 at 1100 °C vs. 0.92 W/cm^2 for the GaAs-based cell. The TPVefficiency of the GaAs cell is significantly lower due decreased reflectance related to elevated sub-bandgap absorption, but high reflectance is less critical for waste heat recovery. As LPCs, we estimate peak efficiencies of 36.8% and 32.5% for irradiation from an idealized 2.0 µm source. The development of these devices on GaAs has significant impacts for the scalability of these devices.

10:00 AM BREAK

SESSION 2B-1: Heteroepitaxy of Mismatched III/Vs on Si
Session Chair: Jean Decobert
Tuesday Morning, May 14, 2024
Resort Tower, Ground Level, Bronze Room 1

10:30 AM *2B-1.1
Electrically Injected InGaAs/GaAs Nano-Ridge Laser Fully Processed in a 300 mm CMOS Pilot Line Bernardette Kunert; Interuniversity Microelectronics Centre, Belgium

Silicon photonics enables the miniaturization and large-scale production of optical systems for a variety of emerging applications. However, the lack of affordable coherent light sources is a major challenge for the widespread adoption of silicon photonics, especially in high-volume, low-cost applications such as chip-to-chip optical interconnects.

Nano-ridge engineering is a unique approach for the monolithic integration of highly scalable light sources on Si substrates based on III-V compound materials. Applying selective area growth, III-V material is deposited inside narrow oxide trenches, which were fabricated onto 300 mm Si substrates, hereby ensuring effective trapping of relaxation defects. The continuous growth out of the trench pattern leads to the formation of a III-V nano-ridge with an engineered shape, increased material volume and high crystal quality. While optically pumped laser operation has been previously demonstrated by integrating an InGaAs/GaAs heterostructure to GaAs nano-ridges, the problem of achieving efficient electrical current injection has still been unsolved until now.

In this presentation, I will discuss an electrically injected nano-ridge laser that has been entirely manufactured within imec's 300 mm CMOS pilot line [www.researchsquare.com/article/rs-3187756/v1]. A novel nano-ridge contact approach has been developed, combining laser and detector devices on each nano-ridge, enabling a wafer-scale electrical read-out.

We believe that the exhibition of hundreds of III-V nano-ridge laser devices on a single 300 mm Si wafer represents a big step towards the low-cost integration of light sources in Silicon photonics.

11:00 AM 2B-1.2
Microstructural Characterization of InP Films on SOI (001) Substrates Grown by Selective Lateral Metal-Organic Vapor-Phase Epitaxy Hiroya Homma, Hiroki Sugiyama, Tatsurou Hiraki, Toru Segawa and Shinji Matsuo; NTT Corporation, Japan

Monolithic integration of Si-waveguide-coupled III-V laser diodes (LDs) by direct growth on Si platform is promising for cost reduction and enables better use of large-scale wafers, compared to heterogeneous integration. However, it is generally difficult to grow high-quality III-V materials on Si due to the large mismatches of lattice constants and thermal expansion coefficients between Si and III-V materials. Lateral aspect ratio trapping (LART) method in which III-V films are grown in lateral oxide trenches created on Si-on-insulator (SOI) wafers has been developed to overcome this [1]. In this paper, we report the microstructural characterization of InP films on (001) SOI wafers grown by MOVPE utilizing this method. The obtained InP films were large enough for LD fabrications in which threading dislocations (TDs) in the Si/III-V interface region were well-confined. However, the films tended to contain other types of defects such as stacking faults (SFs) and rotational twin boundaries (RTBs) as described in [1]. In addition, we found anti-phase boundaries (APBs) formation due to the V-groove Si seeds in this method. The mechanisms underlying the generation of these defects are discussed.

Samples were grown by a vertical reactor using TMIn, TEGa, TBAs, TBP, and PH_3 as precursors. SOI wafers were fabricated as follows. After processing the Si layer into islands and covering the entire layer with SiO_2 film on SOI wafer, lateral oxide trenches were formed by opening windows in the top SiO_2 layer and undercutting the encapsulated Si layer by anisotropic etching. Si {111} seed surfaces were exposed at the end of the trenches. After removal of the natural oxide film on the Si seed surface by dilute hydrofluoric acid treatment, the samples were annealed in hydrogen at about 800 °C. Following GaAs/InP growth at about 400 °C, InP films were grown laterally at about 570 °C.

The obtained InP films had a large area of around $4 \times 50\ \mu m^2$ with straight growth front shapes and their sizes were good enough to use as templates for LD fabrications [2]. Cross-sectional (CS) and plane-view (PV) transmission electron microscopy (TEM) revealed the confinement of TDs in the region near the Si/III-V interface thanks to the LART effect. Further structural characterization revealed other types of defects contained in typical InP films. The first is a planar defect that propagates parallel to the {111} plane from the Si/III-V interface to the growth front region. These are presumably SFs caused by the coalescence of microcrystals formed in the early growth stage. This finding indicates that controlling the initial growth condition is important to suppress SF formation.

The second type of defect parallel to the {111} plane is RTB. X-TEM clarified that some InP films contain rotational twin domains. Twining tends to occur on both the Si {111} facet and the InP {111} growth front facet during lateral growth which results in the mixture of InP domains mentioned above and the formation of kinks at growth the front. Controlling the growth front facet orientation can suppress the twining.

The third is APB which propagates parallel to the [001] direction and also appears as a kink at the growth front region. CS-annular-bright-field scanning TEM directly revealed the anti-phase arrangement of InP atoms along the [001] direction across the boundary. In the LART method, initial Si seed surfaces sometimes form a V-groove consisting of (111) and (11-1) facets. In such cases, the coalescence of InP microcrystals grown from both facets should form APBs. The initial Si facet shape is thus critical to avoid APB formation.

In summary, microstructural defects in InP films grown by the LART method were investigated. Properly controlling the initial microcrystal coalescence, growth front facets, and

initial Si seed shape is essential to suppress the generations of these defects.
[1] Z. Yan *et al*., *Light Sci. Appl.* **10**, 200 (2021).
[2] T. Fujii *et al*., *Optica* **7**, 838-846 (2020).

11:20 AM 2B-1.3
MOVPE Growth of Cubic GaN on GaP/Si (001) Templates
Peter Ludewig[1], Antje Ruiz Perez[2], Vitalii Lider[1], Andreas Beyer[1], Wolfgang Stolz[2], Sangam Chatterjee[3] and Kerstin Volz[1]; [1]Philipps-Universität Marburg, Germany; [2]NAsP III/V GmbH, Germany; [3]Justus-Liebig-Universität Giessen, Germany

Hexagonal GaN is currently the dominating technology for most LED applications. However, hexagonal InGaN/GaN QWs exhibit electric fields along the c-axis. These electric fields reduce the optical efficiency due to the quantum confined stark effect (QCSE). The QCSE increases with both, wider wells and higher In fractions, and hence, the optical efficiency is significantly reduced for higher wavelength of the visible green and amber[1]
Since the electric field in InGaN/GaN QWs is an intrinsic property other approaches are needed to further increase optical efficiency of green and amber LEDs. One approach is the use of cubic GaN, which does not have internal electric fields. Cubic GaN was already successfully grown by MOVPE in the 1990th[2]. However, there has not been much focus on cubic GaN in the past due to the success of the hexagonal GaN. The interest recently increased again because of the continuing limitations of the green and amber hexagonal InGaN/GaN LEDs[1].
One main challenge for the growth of cubic GaN is the lack of a suitable substrate. GaAs[2], 3C-SiC[2], [3] and patterned Silicon[4] have been used in the past, which all have high lattice mismatch to cubic GaN. Si substrates would be beneficial as they are cheap and available in large diameters, however, Si is non-polar and, hence, anti-phase domains (APD) form during growth.
Our approach is the use of a thin GaP interlayer (<50nm) on Si with an APD free surface[5]. This layer can be deposited homogenously on 300mm (001) Si substrates and small pieces of such a wafer can be used as templates for the subsequent growth of cubic GaN. The c-GaN is grown in a two-step process in an Aix-200 GFR system using TEGa and UDMHy as precursors. First, a low temperature nucleation layer is deposited at 600°C or below to create a smooth c-GaN film on the GaP/Si template. The sample is then heated to temperatures above 750°C for the bulk growth. HR-XRD and STEM measurements indicate pure c-GaN for the nucleation layer and high c-GaN fractions for the HT-Bulk layers. This is supported by photoluminescence measurements that show a strong peak at 3.2eV (c-GaN) and a much weaker peak at 3.4eV (h-GaN). However, we also find high defect densities within the c-GaN and roughening of the surface, which shows the need for further improvements of the growth parameters.

[1] D. J. Binks et al., "Cubic GaN and InGaN/GaN quantum wells," *Applied Physics Reviews*, vol. 9, no. 4. American Institute of Physics Inc., Dec. 01, 2022. doi: 10.1063/5.0097558.
[2] H. Okumura *et al.*, "Growth and characterization of cubic GaN," *J Cryst Growth*, vol. 178, no. 1–2, pp. 113–133, 1997, doi: 10.1016/S0022-0248(97)00084-5.
[3] A. Philippe *et al.*, "Optical properties of cubic GaN grown on SiC/Si substrates," *Materials Science and Engineering: B*, vol. 59, no. 1–3, pp. 168–172, May 1999, doi: 10.1016/S0921-5107(98)00413-9.
[4] C. J. M. Stark et al., "Green cubic GaInN/GaN light-emitting diode on microstructured silicon (100)," *Appl Phys Lett*, vol. 103, no. 23, Dec. 2013, doi: 10.1063/1.4841555.
[5] K. Volz *et al.*, "GaP-nucleation on exact Si (0 0 1) substrates for III/V device integration," *J Cryst Growth*, vol. 315, no. 1, pp. 37–47, 2011, doi: 10.1016/j.jcrysgro.2010.10.036.

11:40 AM 2B-1.4
Lasing Characteristics of GaInAsP SCH-MQW Laser Diodes Grown on Hydrophilic Bonded InP-Silicon Substrate Ryosuke Yada, Liang Zhao and Kazuhiko Shimomura; Sophia University, Japan

Silicon photonics is one of the key technology for the high-speed, high-capacity optical communication systems to integrate the passive, active optical devices and electronic circuits on the silicon platform. For the integration of laser diodes, we have grown the laser structures by MOVPE on the directly bonded InP-Silicon substrate, and successfully obtained the lasing operation. However, the threshold current was higher than the same structure grown on InP substrate. In this report, we have investigated the lasing characteristics of GaInAsP SCH-MQW laser diodes grown on hydrophilic bonded InP-Silicon substrate. The relation between voids parameters and threshold current of LDs were obtained. The threshold current almost equivalent to that of the LD grown on InP substrate was obtained.
First, we show the fabrication process of laser diodes on silicon substrate. Thin film InP about 1-2 um thickness was obtained from the chemically etched GaInAs/InP/GaInAs layers grown by low pressure MOVPE on InP substrate. Thin film InP and Silicon substrate were directly bonded by hydrophilic bonding methods. The bonded wafer was annealed at 400 degree-C, 1 hour under nitrogen flow. On this InP-Si substrate, GaInAsP SCH-MQW laser structures were grown by MOVPE. The growth temperature was 650 degree-C and the pressure was 8kPa. Tertiarybutylarsine (tBA), tertiarybutylphosphine (tBP), triethylgallium (TEG), and trimethylindium (TMI) were used as precursors with ditertiarybutylsilane (DTBSi) and diethylzinc (DEZn) as the n- and p-type dopants, respectively. The active layers consisted of five 18 nm Ga0.32In0.68As0.81P0.19 well layers with a band gap wavelength of 1.4 um, separated by 10 nm Ga0.22In0.78As0.48P0.52 barrier layers with a band gap wavelength of 1.2 um. The SCH layer, 100 nm thick, had the same composition as the barrier layer. After the MOVPE growth, AuZn and AuAl were evaporated to the p-side and n-side, respectively.
During the hydrophilic bonding process, voids were appeared at the interface between InP and Silicon. The existence of

voids influences the scattering loss of light transmission and efficiency of injection carriers to the active layers, and these voids degrade the threshold current of LDs. To investigate the relation between voids and threshold current of LD, we have observed the voids size and density before and after MOVPE growth of laser structure. The diameter and height of void was measured by profile microscope Keyence VF-7510. These dimensions were measured at about 15 points in the wafer, and average void size was obtained. The density and occupied area of voids were measured by Nomarski microscope. The typical values of voids after MOVPE growth were 30-100 um of diameter, 0.5-2.0 nm of height, 2000-4000 /cm2 of density, and occupied area was 5-20 %.
The lasing characteristics were measured by I-L tester ALT-7103B of Asahi Data Systems. The laser diodes were edge emitted, slab waveguide LD, manually cleaved from the wafer. The typical size was 300um cavity length and 100um width. The injection current was pulsed condition where pulse width of 0.5usec and repetition rate of 1msec.
We have evaluated the relation between voids parameters such as diameter, height, density, occupied area and threshold current of SCH-MQW LDs. In these parameters, the occupied area of voids was one of the key parameter to reduce the threshold current of LDs on Silicon substrate. Furthermore, we have compared the lasing characteristics of SCH-MQW LDs on InP substrate. The SCH-MQW layers were grown at the same time on hydrophilic bonded InP/Si and InP substrate. Comparable threshold current density of 1.03kA/cm2 at 20 degree-C was obtained in the SCH-MQW LD on silicon substrate when the occupied area of voids was less than 5%.

12:00 PM 2B-1.5
Defect Filtering at the Heterogeneous Epitaixal III-V on Silicon Through Templated Liquid Phase growth Hyun Uk Chae, Zezhi Wu, Juan Sanchez Vazquez and Rehan Kapadia; USC, United States

Integrating III-V semiconductors on silicon has been a long desire to realize the advanced electronics and photonics application for the future ‘extended’ Moore’s Law regime. An epitaxial transfer has been developed to integrate the III-V layer onto silicon, limited by the costive epitaxial wafer and alignment issue. Direct growth is, an alternative method to realize heterogeneous integration, which is necessary to use lattice-matching buffer layers. This imposes a significant growth challenge: thick lattice-matching buffer layers for each material must be grown with nanometer spacing, a significant challenge considering. As such, enabling high-quality growth without using lattice matching layers would provide a clear path toward direct growth of III-V on silicon. Here, we propose a defect-filtering growth technique to enable high-quality III-V growth by combining conventional growth with templated liquid phase growth to ensure the quality and uniformity of the grown material. This approach enables the growth and manufacturing of crystalline materials on silicon without requiring a nearly lattice-matched substrate, potentially impacting a wide range of fields, including electronics, photonics, and energy devices.

SESSION 2B-2: *In Situ* Monitoring/MOVPE Equipment
Session Chair: Andrew Allerman
Tuesday Morning, May 14, 2024
Resort Tower, Ground Level, Bronze Room 2

10:30 AM 2B-2.1
Growth and Calibration of GaAs-Based VCSEL Structures—Enabled by *In Situ* and *Ex Situ* Optical Metrology Andre Maaßdorf[1], Johannes K. Zettler[2], Kolja Haberland[2] and Markus Weyers[1]; [1]Ferdinand-Braun-Institute (FBH), Germany; [2]LayTec AG, Germany

The demand for vertical cavity surface emitting lasers (VCSELs) has been increasing in recent years, mainly driven by the consumer industry. In contrast to edge emitting lasers, the very narrow cavity allowing for only one longitudinal mode, which defines the wavelength of the light emitted, requires precise control of layer thicknesses in the cavity and the surrounding DBRs in the sub-percentage range. On the other hand, growth rate accuracy using state of the art MOVPE machinery is typically considered to be in the ±1% range, according to our experience. In an MOVPE production campaign without any in-situ metrology available, run-to-run adjustments would then have to be applied in order to improve the total yield.
In this work, however, we utilize in-situ and ex-situ optical metrology as much as possible to allow for better growth rate control, combined with transfer matrix based full-structure white light reflectance (WLR) simulations [1]. This is accompanied by growth rate uniformity improvements across 4” GaAs:Si wafers using a combined white light reflectance and photoluminescence mapping station. In-situ metrology provides measurement of multiple wavelength reflectance, emissivity corrected temperature and wafer curvature. by
We will demonstrate how to achieve a better “first-attempt” accuracy when growing top-emitting 795 nm VCSEL structures, where n-DBR, cavity and p-DBR are grown in sequence, by implementing the following scheme: We first grow the targeted VCSEL layer sequence with the number of DBR periods strongly reduced in the p- and n-DBR layer stacks. Then we measure and simulate the room temperature WLR spectrum using a non-linear optimization scheme for fitting. The simulated WLR spectrum is used to define adjustments required in order to tune the full recipe, now with complete DBR period counts, to meet the targeted specification window.
This full growth process is guided by the in-situ metrology system, which is able to perform a VCSEL analysis whenever a DBR period has been finished. With the knowledge of the stop band center wavelength target at growth temperature, or preferably using a reference or golden run dataset, we can spot deviations already during the 1st half of the n-DBR growth. Those deviations can be counteracted for each individual wafer by adjusting process parameters during the n-DBR growth for the subsequent layers of the VCSEL structure. This way cavity resonance and p-DBR stopband wavelengths will shift accordingly, so that the VCSEL as a whole will still have a good alignment between n-DBR, cavity and p-DBR and will

also have the cavity resonance wavelength inside the targeted window.
We will demonstrate this scheme which has been successfully applied many times using datasets that have been collected during several VCSEL growth processes.

[1] J. Puhan, B. Lipovsek, A. Burmen, and I. Fajfar, "An Accurate Representation of Incoherent Layers Within One-Dimensional Thin-Film Multilayer Structures With Equivalent Propagation Matrices," *IEEE Photonics J.*, vol. 9, no. 5, pp. 1–12, Oct. 2017, doi: 10.1109/JPHOT.2017.2728535.

10:50 AM 2B-2.2
Reaction Activation of Ammonia in Nitrides MOVPE Analyzed by Time-of-Flight Mass Spectrometry with Isotope Tracking Shugo Nitta, Daisuke Yahara, Ryo Furukawa, Yoshio Honda and Hiroshi Amano; Nagoya University, Japan

Ammonia (NH_3) is a crucial material for the human beings to cultivate grain and to grow new generation light source. In essence, NH_3 is the only nitrogen source for the vapor phase epitaxial growth of nitride semiconductors, so that it is used in the metalorganic vapor phase epitaxy (MOVPE), the halide vapor phase epitaxy (HVPE), ammonothermal, etc. Its practical decomposition ratio to H_2 and N_2 under equilibrium conditions at 400 ºC and 1 atm is 99.1 % [1]. Due to the slow reaction rate, the practical decomposition ratio under GaN growth conditions is typically at around 1000 ºC and high flow velocity in an MOVPE or HVPE system is distinguished only a few % [2]. To realize new functional electronic and optical devices using nitride semiconductors, the MOVPE growth of high-purity GaN, high-Al-composition AlGaN, high-In-composition InGaN, AlInN, or quaternary AlGaInN requires more advanced crystal growth technologies than conventional materials, and a more detailed and deeper understanding of the crystal growth process is important. Therefore, a more accurate understanding of the gas-phase reactions of raw materials that serve as precursors for surface reactions is required. Additionally, gaining such understanding eventually improves its numerical simulations of growth mechanisms.
First-principles calculations have been used to clarify gas-phase reactions. However, there are only a few examples of experimental observations reported. Although mass spectrometry is effective for analyzing intermolecular reactions, conventional techniques are practically impossible for inorganic materials, in which the number of elements detected is relatively limited owing to elements with the same molecular weight. We have realized the gas-phase reaction analysis of trimethylgallium (TMGa) and NH_3 by high-mass-resolution time-of-flight mass spectrometer (TOF-MS) with a multiturn flight path method, and we have elucidated the reaction process under conditions similar to actual MOVPE growth. In our previous study, the in situ monitoring of GaN growth conditions by TOF-MS showed NH_3 decomposition and the catalytic effect of stainless steel on the NH_3 decomposition [3]. The decomposition rate was also enhanced by TMGa supply even at a V/III ratio higher than 1000. In addition, the isotope deuterium (D) tracking technique revealed that the H–D exchange between NH_3 and D_2 molecules was occurred even at a lower temperature that NH_3 was undecomposed, indicating that NH_3 was activated to react. In this study, we focused on the practical NH_3 activation temperature under GaN growth conditions and discussed how the existence of TMGa and Ga reactants (e.g., metallic Ga, low-temperature-deposited Ga–N compounds (LT compounds), and crystalline GaN) affects the NH_3 reaction. A simple quartz reactor (I.D., 26 mm) with a 30 cm heating zone was utilized to analyze the NH_3 (or ND_3 as an alternative) reaction with D_2 (or H_2) and decomposition by TOF-MS. NH_3 was supplied using D_2 as the carrier gas. The temperature dependence of NH_3 intensity detected by TOF-MS showed that the decrease in NH_3 intensity and the increase in ND_3 intensity resulted from the H–D exchange reaction. The NH_3 reaction temperature was affected by reactor conditions in the presence of TMGa supply, Ga metal, LT compounds, and GaN on sapphire templates. The reaction temperature decreased in the presence of the Ga reactants, which proves that NH_3 reactivity is catalytically activated. However, it was clearly identified that TMGa supply decreased the NH_3 activation temperature further than the other conditions. On the other hand, trimethylindium supply and its decomposed products showed no catalytic effect on the NH_3 reaction.
This work was supported by MEXT as "Program for Promoting Researches on the Supercomputer Fugaku".
Reference:
[1] S.F. Yin *et al.*, Appl. Catal. A:General, **277**, 1 (2004).
[2] S.S. Liu *et al*., J. Electrochem. Soc. **125**, 1161 (1978).
[3] Z. Ye *et al.*, J. Cryst. growth **516**, 63 (2019).

11:10 AM 2B-2.3
***In Situ* Synchrotron X-Ray Characterization of Group III Nitrides During Metal-Organic Vapor Phase Epitaxy** Guangxu Ju[1], Dongwei Xu[2], Carol Thompson[3], Matt J. Highland[4], Jeffrey A. Eastman[4], Weronika Walkosz[5], Peter Zapol[4], Bo Shen[1] and Gregory B. Stephenson[4]; [1]Peking University, China; [2]Huazhong University of Science and Technology, China; [3]Northern Illinois University, United States; [4]Argonne National Laboratory, United States; [5]Lake Forest College, United States

Ever since the successful demonstration of a monolithic white light-emitting diode (LED) based on GaN and related materials, there has been growing interest in improving device performance by achieving highly efficient light emission. This has prompted extensive investigations into the atomic-scale growth mechanisms, encompassing aspects such as structural defects, surface dynamics, step morphology, island size distributions, domain structures, and their evolution during growth. To address these questions, we have developed a novel instrument designed for *in-situ* time-resolved observation of epitaxial film growth in Group III nitrides using organo-metallic vapor phase epitaxy (OMVPE) [1]. Our system leverages the latest advancements in synchrotron x-ray techniques, particularly the use of coherent x-ray beams [2].

This advancement enables us to study the spatial arrangement of defects and distortions within crystalline films, including atomic-scale surface features, by analyzing the time evolution of complex diffraction patterns [3].
Our recent *in-situ* investigations into GaN homoepitaxy under step-flow conditions have yielded valuable insights. Microbeam surface x-ray scattering not only allows us to unambiguously distinguish between attachment kinetics at A and B steps but also to monitor changes in terrace fractions under varying growth conditions [4]. Understanding the kinetics of atom incorporation on these terraces and steps on vicinal surfaces is crucial for epitaxial growth during introduction of alloying elements like indium or aluminum. These alloys play a pivotal role in active layers of devices such as micro-LEDs, UV-LEDs, and laser diodes.
Through the analysis of surface scattering [5] and an extension of the classic Burton-Cabrera-Frank (BCF) theory [6], we have obtained direct information on step attachment rate constants. In this presentation, I will delve into our recent experiments aimed at elucidating how the alternating dynamics of GaN (0001) steps influence the incorporation of indium during $Ga_{1-x}In_xN$ growth via OMVPE. These studies significantly enhance our fundamental understanding of the growth process and pave the way for the development of improved synthesis methods for nitride materials.
[1] Guangxu Ju et al., An instrument for *in-situ* coherent X-ray studies of metal-organic vapor phase epitaxy of III-nitrides. Rev. Sci. Instrum. 88, 035113 (2017).
[2] Guangxu Ju et al., Characterization of the X-ray coherence properties of an undulator beamline at the Advanced Photon Source. J. Synchrotron Rad. 25, 1036–1047 (2018).
[3] Guangxu Ju et al. Coherent X-ray spectroscopy reveals the persistence of island arrangements during layer-by-layer growth. Nat. Phys. 15, 589–594 (2019).
[4] Guangxu Ju et al., *In-situ* microbeam surface X-ray scattering reveals alternating step kinetics during crystal growth, Nature Communications, 12(1): 0-1721 (2021).
[5] Guangxu Ju et al., Crystal truncation rods from miscut surfaces with alternating terminations, Physical Review B, 103: 125402-1-125402-14 (2021).
[6] Guangxu Ju et al., Burton-Cabrera-Frank theory for surfaces with alternating step types, Physical Review B, 105(5): 054312-1-054312-20 (2022).

11:30 AM 2B-2.4
***In Situ* Spectroscopic Ellipsometry for Layer-Controlled Metalorganic Chemical Vapor Deposition Growth of MoS_2**
Thomas V. Mc Knight[1,1], Andrew R. Graves[1], Elizabeth Houser[2], Frank Peiris[2] and Joan Redwing[1,1]; [1]The Pennsylvania State University, United States; [2]Kenyon College, United States

The ability to monitor the growth rate of transition metal dichalcogenide (TMD) monolayer and few-layer films in-situ is an area of great interest to achieve tight control of layer number and to gain insight into the fundamental mechanisms of film growth. Optical characterization techniques such as laser reflectivity are widely used for real time measurements of growth rate during thin film deposition by metalorganic chemical vapor deposition (MOCVD) but cannot be readily extended to the growth of 2D materials which require sensitivity in the sub-monolayer regime. Spectroscopic ellipsometry (SE), on the other hand, is widely used to measure the dielectric function and thickness of thin films and is a powerful in-situ technique for atomic layer deposition providing information on film thickness per cycle and insight into the initial mechanisms of nucleation.
In this study, we investigate the use of SE as an in-situ technique to monitor the growth of MoS_2 monolayer and few-layer films by MOCVD on c-plane sapphire substrates. The studies were carried out in a vertical cold wall MOCVD reactor equipped with a J.A. Woollam M2000XI ellipsometer with a spectral range of 210 – 1687 nm integrated using purged optical ports on the reactor. Molybdenum hexacarbonyl ($Mo(CO)_6$) and hydrogen sulfide (H_2S) were used as precursors with H_2 as the carrier gas. Initial studies were carried out by keeping growth parameters constant at 100 Torr reactor pressure, 1050°C substrate temperature, $Mo(CO)_6$ flow rate of 8.6×10^{-3} sccm, S/Mo ratio of ~46700, and varying growth time (5 – 40 min) to develop a series of samples with varying surface coverage. After each growth, SE was performed as a function of temperature during cooldown to room temperature under H_2S. Atomic force microscopy (AFM) and field emission scanning electron microscopy (FE-SEM) were used to measure the film coalescence and quantify monolayer and bilayer surface coverage. An optical model of the layer structure was developed assuming an interfacial layer between the film and substrate and using an effective medium approximation to consider partial film coverage where the effective medium is a variable combination of void and the MoS_2 film. The models were first used to fit the room temperature data to extract the dielectric function of MoS_2, which compared favorably to prior literature reports. The optical model was then used to predict the variation in the ellipsometric parameters (Ψ and Δ) as a function of surface coverage demonstrating sensitivity in the sub-monolayer regime down to ~40% coverage. Additional studies were undergone to determine the temperature dependence of the dielectric function in order to refine the models to accurately measure film coverage at growth temperature. The features of the ellipsometric curves soften at elevated temperatures compared to room temperature measurements, though marked differences are observed when comparing samples of varying coverage, expounding the potential for SE to discern sub-monolayer coverages at growth temperatures. The refined optical models were then applied to monitor MoS_2 film growth in-situ, demonstrating the effectiveness of SE to allow precise measurement and control of film thickness and properties in real time through layer-by-layer tailoring of film deposition conditions. The ability to directly assess the instantaneous film growth rate throughout the deposition process gives invaluable insight into the fundamental nucleation and lateral growth mechanisms at work and their underlying relationship with film deposition parameters.

11:50 AM 2B-2.5
Equipment, Safety, Environment and Production Issues Including Low-Cost MOVPE Hephzi-bah K. Agyeman[1,2,3]; [1]Ghana Atomic Energy Commission, Ghana; [2]University of Ghana, Ghana; [3]School of Nuclear and Allied Sciences, Ghana

The metal-organic vapor phase epitaxy (MOVPE) growth technique is known to be developed over its 50-year history. The hand in hand development of MOVPE ensures safe practices. MOVPE growth technique is used for the growth of compound semiconductor films and devices structures. The growth proceeds via dissociative adsorptions of source molecules on the substrate surface. These surface reactions are accompanied by chemical and structural changes, which give rise to changes in the surface dielectric constant. This research work gives an overview of key concepts of equipment, safety, environmental and production of low cost MOVPE. Furthermore, a historic overview of the basic fundamental aspect of MOVPE such kinetics, thermodynamics and growth chemistry will be compared with other growth techniques. Moreover, the fabrication of other semiconductor materials compounds which is used in MOVPE will also be highlighted. Precursors provide the key to the success of MOVPE in providing a very-high-purity source of the components of the compound semiconductor in a convenient form that can be delivered. GaN and GaAs growth will be highlighted upon. It is confirmed that this growth method is quite effective for the improvement. However, some emphasizes will be focus on advance equipment and other chemical sources which are used in the growth technique and some properties of growth materials, impurities and dopants.
.

12:10 PM 2B-2.6
Real-Time Monitoring of Homo- and Heteroepitaxial Process for MOVPE-grown β-Ga_2O_3 Films Ta-Shun Chou[1], Saud Bin Anooz[1], Jana Rehm[1], Arub Akhtar[1], Deshabrato Mukherjee[2], Peter Petrik[2], Zbigniew Galazka[1], Marcello Binetti[3], Christian Camus[3] and Andreas Popp[1]; [1]Leibniz Institute for Crystal Growth, Germany; [2]Institute for Technical Physics and Materials Science, Hungary; [3]LayTec AG, Germany

Beta-gallium oxide (β-Ga_2O_3) is a promising ultra-wide bandgap (~4.8 eV) semiconductor material with theoretical breakdown field strength[1] of up to 8 MV/cm. It has various applications, such as high-breakdown voltage devices and solar-blind photodetectors. High-quality β-Ga_2O_3 layers (both homo and heteroepitaxial) with precise thickness and doping concentration control are crucial to the mentioned applications. In-situ observations during the growth process play an essential role in understanding the interfacial reaction and the growth mechanism of the oxide semiconductors and allow control of the quality and consistency of the growth process.

In this contribution, we report using commercial multiwavelength reflectometer (EpiTT 2017, LayTec) to in-situ monitor the growth of β-Ga_2O_3 in the MOVPE process. By innovatively implementing the autocorrelation function for homoepitaxy and the transfer matrix method (TMM) for heteroepitaxy, we successfully enhance the interpretability of the collected reflectance transient and characterize the growing film in terms of the growth rate, refractive index, and surface morphology (and roughness) without significant hardware upgrade. We demonstrate the developed techniques with applications to both homoepitaxial (on (100) and (010) orientation)[2] and heteroepitaxial[3] (on sapphire c-plane) grown β-Ga_2O_3 films. The method we developed are crucial steps paving the way to industrial mass production of β-Ga_2O_3 epiwafer.

Reference
[1] M. Higashiwaki et al., Recent progress in Ga_2O_3 power devices, Semicond. Sci. Technol. 31 (2016) 34001.
[2] T.-S. Chou et al., Homoepitaxial growth rate measurement and surface morphology monitoring of MOVPE-grown Si-doped (100) β-Ga_2O_3 thin films using in-situ reflectance spectroscopy, J. Cryst. Growth. 603 (2023) 127003.
[3] T.-S. Chou et al., In-situ spectral reflectance investigation of hetero-epitaxially grown β-Ga_2O_3 thin films on c-plane Al_2O_3 via MOVPE process, Appl. Surf. Sci. 652 (2024) 159370.

SESSION 2C-1: Etching/Passivation in Nitrides
Session Chair: Motoaki Iwaya
Tuesday Afternoon, May 14, 2024
Resort Tower, Ground Level, Bronze Room 1

2:00 PM *2C-1.1
XeF_2—A new MOCVD Source for Removal of Surface Si Contamination and *In Situ* Etching of GaN for Epitaxial Regrowth Andrew A. Allerman, Andrew T. Binder, Andrew M. Armstrong, Luke Yates, Jeff Steinfeldt, Hoang M. Vuong and Robert J. Kaplar; Sandia National Laboratories, United States

Epitaxial regrowth is being developed for fabricating advanced power and RF devices in III-Nitride semiconductor materials. For example, epitaxial regrowth of p-GaN on a lightly doped, thick (> 100 um) n-GaN drift layer grown by MOCVD or HVPE would enable MPS diodes and JFETs with breakdown voltages exceeding 10 kV. The development of regrown PN junctions has been frustrated by the presence of Si contamination at the regrowth surface from atmospheric sources and residual crystalline damage from *ex-situ* etch or CMP processes which results in excessive leakage current. Additionally, Si functions as an effective micro-mask, on air-exposed GaN surfaces resulting in rough surfaces following *in-situ* etching using common bromine and chlorine -based precursors. *Ex-situ* processes such as Ozone oxidation followed by HF can remove surface Si contamination. However, the surface is still exposed to the atmosphere prior to loading the MOCVD system, risking re-contamination by an unknow quantity of Si. *Ex-situ* Si removal processes thus

appear challenging to implement in high yield, commercial production unless re-contamination of Si can be prevented.

We present the novel use of XeF_2 for *in-situ* removal of surface Si contamination and subsequent etching of GaN in the MOCVD chamber. While XeF_2 is ubiquitous in the processing of Si devices, we are not aware of the source being used in MOCVD growth systems. Unlike chlorine (TBCl and CCl_4) and bromine (CBr_4) -based precursors we have studied; we obtained a smooth surface following *in-situ* fluorine etching of air-exposed GaN.

We also report that *in-situ* fluorine etching of ICP etched n-GaN Schottky barrier diodes (SBDs) formed by shadow mask evaporation results in reverse leakage currents more than 3 orders of magnitude lower than those formed on n-GaN layers that have only experienced ICP etching. Additionally, *in-situ* fluorine treated, ICP etched SBDs show reverse leakage currents equal to those of SBDs formed on as-grown n-GaN layers. This suggests that the *in-situ* fluorine etching is effective at removing the residual damage from the ICP etch process.

Next, this *in-situ* fluorine etch lowered the peak density of surface Si from an unusually high level of 1-2 x 10^{19} cm^{-3} to the detection level (2-4 x 10^{15} cm^{-3}) of the SIMS measurement prior to the regrowth of uid-GaN. Finally, PN diodes with a regrown p-GaN anode on a blanket etched n-GaN drift layer following *in-situ* fluorine etching exhibit reverse leakage current of ~ 1 x 10^{-8} A/cm^2 to -1000V, matching reverse leakage current measured in continuously grown PN diodes of similar structure. Optimization of the XeF_2 process is expected to reduce the ideality factor from 2.0 to the 1.5-1.6 typically measured in our continuously grown PN diodes. The similar reverse and forward current characteristics of these *in*-situ XeF_2 etched and regrown PN diodes and continuously grown PN diodes indicates that a device quality PN junction can be formed by epitaxial regrowth on *ex-situ* etched GaN. The use of *in-situ* XeF_2 etching for the first time overcomes two critical obstacles preventing the formation of more advanced PN junction devices such as MPS diodes and JFETs in GaN by epitaxial regrowth and demonstrates the utility of XeF_2 as a precursor for MOCVD processes.

2:30 PM 2C-1.2
***In Situ* Metal Organic Chemical Vapor Deposition of Boron Nitride Dielectric for AlGaN/GaN High Electron Mobility Transistors** Michael Snure, Eric Blanton and Kyle Liddy; Air Force Research Laboratory, United States

For two-dimensional materials and devices, boron nitride is “the” dielectric passivation layer due to its excellent dielectric properties, fully compensated atomically flat surface, weak van der Waals (vdW) bonding between layers, high surface optical phonon energy, and excellent thermal and chemical stability. Gallium Nitride high electron mobility transitions (HEMTs), which have become a dominate technology for high frequency and power devices, can suffer from current collapse, threshold voltage instability, high gate leakage, and high temperature instability linked to the conventional Schottky-gated. Metal-insulator-semiconductor (MIS) HEMTs can solve some of these problems, but conventional insulators, like SiNx and Al2O3, can suffer from poor interfacial quality and high interface trap densities limiting these improvements. BN offers many advantages for AlGaN/GaN HEMTs, which are extremely sensitive to surface states. Here we present work on in situ metal organic chemical vapor deposition (MOCVD) of thin BN layers on GaN and AlGaN/GaN as a potential gate dielectric and passivation layer. To achieve high quality BN/GaN interfaces we balance the high temperature requirements for growing BN with GaN decomposition and intermixing between the BN, GaN and AlGaN layers. Using a combination of structural, chemical, and surface characterization techniques we have optimized the BN on GaN growth conditions, which was applied to the growth of BN on AlGaN/GaN structures necessary for HEMTs. Using optimized growth conditions ultra-thin (~2nm) and smooth sp2 bonded BN has been grown in situ on GaN and AlGaN/GaN structures with no damage to the bulk or surface properties. BN/GaN MIS diode and MIS capacitor structures were fabricated, which show improvement over conventional Schottky GaN diodes. AlGaN/GaN two-dimensional electron gas (2DEG) structures capped with in situ BN achieved mobilities of nearly 2000 cm2/Vs and sheet electron concentrations of > 1.1 x 1013 cm-2, which are in line with uncapped AlGaN/GaN 2DEG structures. BN/AlGaN/GaN MIS capacitors and HEMTs were fabricated to investigate interfaces and transistors performance. This work demonstrates 2D BN as a potential dielectric and passivation layer for AlGaN/GaN HEMTs.

2:50 PM 2C-1.3
MOCVD Growth of Ge_3N_4 as a Passivation Layer and Dielectric for III-Nitride Semiconductor Devices Vineeta R. Muthuraj, Shuji Nakamura, Umesh K. Mishra, Steven P. DenBaars and Stacia Keller; University of California, Santa Barbara, United States

III-nitride semiconductor electronic devices, often grown by metalorganic chemical vapor deposition (MOCVD), are used for a variety of high-power and high-frequency applications due to the excellent electrical properties of the GaN materials system. On the c-plane orientation, the epitaxial growth of tensile strained AlGaN layers on top of GaN results in a 2-dimensional electron gas (2DEG) at the AlGaN/GaN interface because of spontaneous and piezoelectric polarization discontinuities between GaN and AlGaN. The current understanding is that the electrons forming the 2DEG are supplied from states on the AlGaN surface. In order to maintain high performance and stability in devices, the AlGaN surface must be passivated, as it is also prone to oxidation. Typically, Si_3N_4 layers are deposited on top of the III- nitride epitaxial layer structures, often in-situ in the MOCVD growth chamber. However, deposits of Si_3N_4 inside the MOCVD chamber are often difficult to remove due to the high thermal stability of Si_3N_4 resulting in particle formation and yield losses. An alternative to Si_3N_4 as a passivation material is Ge_3N_4. Ge_3N_4 is stable to oxidation and has similar dielectric

properties to Si_3N_4, with a bandgap of 4.7 eV and a dielectric constant of 9.5. In contrast to Si_3N_4, it starts decomposing at temperatures around 600 °C. Thus, Ge_3N_4 reactor deposits can be thermally etched, preventing a memory effect and making Ge_3N_4 growth compatible with multiple processes. These properties make Ge_3N_4 an attractive option for III-nitride surface passivation.

In this work, MOCVD growth experiments were performed to map the growth parameter space of Ge_3N_4. Ge_3N_4 layers were grown by MOCVD on co-loaded (001) silicon and (0001) sapphire substrates with nitrogen as the carrier gas. Isobutylgermane (IBGe) was used as the germanium precursor and ammonia (NH_3) as the nitrogen precursor. The thicknesses and refractive indices of the Ge_3N_4 layers grown on silicon were measured using ellipsometry. The relative electrical conductivities of the layers were evaluated on the co-loaded sapphire substrate samples.

The growth rate of Ge_3N_4 increased with decreasing the growth pressure from 60 to 20 kPa, indicating the presence of pre-reactions at elevated pressures. For this reason, most experiments were performed at 20 kPa. The Ge_3N_4 growth rate showed a maximum at 500 °C and significantly declined at temperatures above 550 °C where the films also became conductive. At 600 °C, the layer severely degraded and metal droplets formed, marking the upper temperature limit for growth of Ge_3N_4 layers. When performing experiments at 500 °C, the growth rate slightly increased from 0.022 Å/s to 0.025 Å/s when the NH_3 flow was increased from 130 to 270 mmol/min, most likely due to a increased concenetration of active nitrogen. The Ge_3N_4 films were found to be insulating over a wide range of growth parameters. Atomic Force Microscopy imaging revealed continuous films. Analysis on the effects of growth conditions on refractive index, surface roughness, and other film properties will be presented. In addition, the use of Ge_3N_4 as a dielectric for MISFETs will be discussed.

This work was funded in part by King Abdulaziz City for Science and Technology and the Solid State Lighting and Energy Electronics Center.

3:10 PM 2C-1.4

Enhancement of AlN Schottky Barrier Diodes Performance Through Oxygen-Rich Rapid Thermal Annealing Haicheng Cao[1], Xiao Tang[1], Biplab Sarkar[2], Ying Wu[1], Xiaohang Li[1] and Tingang Liu[1]; [1]King Abdullah University of Science and Technology, Saudi Arabia; [2]Indian Institute of Technology, Roorkee, India

Aluminum Nitride (AlN), with its ultrawide bandgap, high breakdown field strength, superior thermal conductivity, and outstanding stability, emerges as a prime candidate for power electronics. However, the performance of AlN SBDs has traditionally been hindered by interface states, point defects, and threading dislocations, which lead to reverse leakage current and limit device efficiency. Our research addresses this challenge by employing oxygen-rich rapid thermal annealing (O_2 RTA), a technique that significantly reduces leakage current and improves overall device performance without increasing specific on-resistance (Ron).

In this study, the AlN lateral SBDs were fabricated on a sapphire substrate using MOCVD. The structure consisted of an undoped AlN layer, an undoped AlN regrowth layer, and a Si-doped AlN layer. Standard photolithography and lift-off techniques were used for device fabrication. The ohmic contacts were formed by sputter-depositing a stack of TiAlTiAu metals on the n-AlN surface, followed by an RTA process with 950ºC and 60s in N_2. Three samples were prepared for comparison: the reference sample (Ref), the second sample (S1) underwent multiple rounds of O_2 RTA pretreatment followed by BOE wet etching, and the third sample (S2) underwent multiple rounds of O_2 RTA pretreatment only. Afterward, the Ni/Au was deposited as Schottky contact metal by E-beam evaporator.

The J-V characteristics of AlN SBDs were improved after O_2 RTA pretreatment. The treated samples showed reduced leakage current and maintained a low Ron, resulting in outstanding rectifying characteristics with an I_{on}/I_{off} ratio at ± 4V of up to ~10^7. The reduction in leakage current was attributed to the increase in the Schottky barrier height (φ) of the metal-semiconductor (M-S) junction. The elevation of φ was attributed to the formation of a thin AlOx layer at the interface and the reduction of donor-like defects near the surface. XPS characterization confirmed the enhanced passivation and oxygen diffusion near the surface. The oxygen diffusion into the AlN during O_2 RTA pretreatment led to the passivation of defects, resulting in reduced interface state density and decreased carrier concentration. The C-V curves analysis supported these findings. The treated samples also exhibited improved performance at elevated temperatures, with a reduced ideality factor, increased rectification ratio, and enhanced barrier height. The devices showed breakdown voltage over kV at a larger electrode distance. In the benchmark, the AlN SBDs on sapphire with O_2 RTA pretreatment demonstrated significant progress in advancing ultrawide bandgap power diodes for high-voltage electronic applications, surpassing the performance of recently reported AlN SBDs on different substrates.

In conclusion, oxygen-rich RTA pretreatment is demonstrated herein to be an effective method to suppress leakage current, enhances Schottky contact performance, and maintains Ron of AlN SBDs. The treated devices exhibit outstanding performance with rectification ratio of ~10^7, ideality factor of 2.04, barrier height of 1.84eV, and the highest breakdown voltages at kV level. The notable performance primarily results from the reduced defect-assisted tunneling paths after pretreatment, as confirmed by XPS and C-V analysis. This work presents a promising avenue for enhancing AlN-based SBDs, making them highly attractive for power electronic applications.

3:30 PM BREAK

SESSION 2C-2: Nitride HEMT/N-Polar Growth
Session Chair: Chirag Gupta
Tuesday Afternoon, May 14, 2024
Resort Tower, Ground Level, Bronze Room 2

2:00 PM 2C-2.1
A Demonstration of Two-Step Fe-Doped Semi-Insulating N-Polar GaN Buffer Layer for High-Frequency Devices
Swarnav Mukhopadhyay, Ruixin Bai, Surjava Sanyal, Guangying Wang, Chirag Gupta and Shubhra Pasayat; University of Wisconsin–Madison, United States

N-polar GaN high electron mobility transistors (HEMTs) can potentially outperform Ga-polar GaN HEMTs at W-band frequency of operation owing to inherent material advantages owing to the reversed polarization field direction [1,2]. The N-polar GaN deposited using MOCVD technique is known to contain unintentional n-type impurities such as O and Si which cause large buffer leakage, RF losses, and lower breakdown voltage, thus limiting the RF power output [2-4]. Obtaining a semi-insulating layer in N-polar GaN is more challenging than the Ga-polar GaN due to enhanced O incorporation in N-polar GaN [4,5]. For the compensation of the unintentional dopants in GaN, iron (Fe) dopants are preferred, however, their slow incorporation in GaN makes it non-trivial to obtain semi-insulating properties in N-polar GaN [6]. In this study, a two-step Fe-doping approach is taken to mitigate the slow incorporation issues of the Fe dopants to obtain a semi-insulating behavior. Finally, an N-polar GaN HEMT was deposited on top of the semi-insulating buffer layer which shows a 2D electron gas (2DEG) density of 1.1×10^{13}/cm^2 with mobility of 1240 cm^2/V.s. It showed a buffer leakage of 10 µA/mm and 100 µA/mm at 600 V and 1200 V, respectively, with 10 µm spacing between ohmic electrodes.
The Fe-doped semi-insulating N-polar GaN epitaxial layers were deposited using the MOCVD technique on a 4° miscut sapphire substrate. Trimethylgallium (TMGa) and ammonia (NH_3) were used as group III and group V precursors. Ferrocene (Cp_2Fe) was used as a source of Fe dopants for obtaining semi-insulating behavior. First, a thin N-polar GaN nucleation layer was deposited. Next, a 15-50 nm unintentionally doped (UID)-GaN coalescence (U_0) layer was deposited using an NH_3 flow of 78 mmol/min. Following the coalescence layer, a 60-120 nm heavily Fe-doped GaN layer (U_1) using a Cp_2Fe flow rate of 66-100 nmol/min was deposited. After that, the Cp_2Fe flow rate was decreased to 45 nmol/min for the deposition of a low Fe-doped 1.23 µm of N-polar GaN layer (U_2). Finally, a UID N-polar GaN layer of 50 nm thickness was grown with an increased NH_3 flow to reduce the memory effect of the Fe dopant. A reference UID N-polar GaN sample was prepared without any Fe-doping for the comparison of background carrier concentration. The background carrier concentration of the epitaxial layers was measured using Hall and SIMS measurements. The material quality and surface roughness were measured using XRD and AFM.
The background carrier concentration (n_b) of the UID N-polar GaN sample was 9.6×10^{17}/cm^3. The introduction of Fe dopants after 50 nm of U_0 layer with a high-Cp_2Fe flow rate of 66 nmol/min in U_1 (60 nm) decreased the n_b to 4.8×10^{16}/cm^3. Decreasing the U_0 layer thickness from 50 nm to 15 nm with the same high Cp_2Fe flow rate in U_1 (60 nm), reduced the background carrier concentration from 4.8×10^{16}/cm^3 to 3×10^{16} /cm^3. Finally, increasing the high-Cp_2Fe flow rate in U_1 from 66 to 100 nmol/min with an increased thickness from 60 nm to 120 nm fully compensated the background impurities, providing a semi-insulating N-polar GaN buffer. The surface roughness was measured to be 1.35 nm for 10×10 µm^2 AFM scan and the dislocation density was determined to be 10^9/cm^2, which is comparatively low for N-polar GaN films [2]. Thus, this approach is robust and reliable for obtaining a semi-insulating N-polar GaN buffer layer for high-frequency devices.
We acknowledge funding support from the Office of Naval Research (Dr. P. Maki)
References: *[1] B. Romanczyk et al., IEEE TED. 65, no. 1 (Jan. 2018): 45–50. [2] S. Keller et al 2014 SST. 29 113001. [3] C Mauder et al., 2021 SST. 36 075008. [4] N. A. Fichtenbaum, et al., J. Cryst. Growth 310, no. 6 (Mar. 15, 2008): 1124–31. [5] T. Tanikawa et al., PSS. (b) 254, no. 8, 2017: 1600751. [6] S. Heikman et al., J. Cryst. Growth 248 (2003) 513–517.*

2:20 PM 2C-2.2
N-polar (000-1) AlGaN/AlN Heterostructures on Sapphire Grown by MOVPE Itsuki Furuhashi, Markus Pristovsek and Xu Yang; Nagoya University, Japan

N-polar high electron mobility transistors (HEMT) offer intrinsic advantages like high thermal conductivity of the AlN buffer layer and the highest polarization contrast without a top barrier for direct contacting the channel. A first N-polar GaN/AlGaN/AlN HEMT has been recently realized by Molecular Beam Epitaxy (MBE) by Cornell University [1] using bulk AlN substrates. The latter were used because the N-polar AlN growth on sapphire is very challenging and only recently N-polar AlGaN/AlN heterostructure on sapphire was reported by MOVPE by Yamaguchi University [2].
Therefore, we optimized the growth of smooth N-polar AlN on 4°A vicinal sapphire substrate using trimethylgallium (TMGa), trimethylaluminum (TMAl), and NH3 in a 3x2" EpiQuest showerhead reactor. The heater was set to 1280°C throughout the growth (maximum temperature) corresponding to ~1255°C susceptor temperature. The carrier gas was 10 kPa hydrogen. We first started with a nitridation for about 2.5 minutes with 16% ammonia in the gas phase. Then ammonia was reduced to the growth flow. There was no nucleation layer, we directly started AlN growth at a growth rate of about 400 nm/h. The polarity of the AlN and GaN layers was checked by etching and the valence band in X-ray photo emission.
We found the V/III ratio to be the most important parameter which was varied between 1.3 and 40 (assuming TMAl monomers). For our MOVPE, only a V/III ratio of 1.75±0.1 resulted in smooth surfaces with roughness below 0.3 nm. The X-ray rocking curves were also the narrowest for these conditions with 100-300 arcsec in 0002 and 1500-200 arcsec

in 10-12. Higher V/III ratios first resulted in hillocks and even higher in valleys, while lower V/III ratios resulted in holes. For the growth of AlGaN on AlN, we investigated the effect of V/III ratio and temperature. Too high temperatures lead to low Ga incorporation despite N-polar GaN being more stable than Ga-polar GaN. Thus, a growth temperature of ~1050°C (susceptor) was chosen for the V/III ratio variation. Too low V/III ratio results in low Ga content and higher than 200 V/III ratio forms islands.
Growing GaN directly on N-polar leads to a strong step-bunching at 1050°C which decreased when decreasing the growth temperature. The smoothest GaN was obtained at 800±50°C. Even lower temperatures result in dots, probably from decorating dislocations. GaN layers on AlN were coherently strained up to at least 10 nm according to reciprocal space mapping. Variable temperature Hall measurements confirmed a 2D electron gas with more than $10^{13}cm^{-2}$ carriers but extremely low mobilities. Using triethylgallium instead reduced the resistivity but more improvement is needed. Further SIMS measurements are under way to identify whether C in GaN is the problem or rather the AlN layer itself has too much compensating defects directly at the interface.
[1] E. Kim et al., Appl. Phys. Lett. 122 (2023) 092104
[2] T. Ito et al., Phys Status Solidi B 257 (2020) 1900589

2:40 PM 2C-2.3
Nitrogen-Polar GaN Epilayers of Higher Crystal Quality, Obtained with Epitaxial Lateral Overgrowth of Microscale-Patterned 3D-Templates Pietro Pampili, Vitaly Z. Zubialevich and Peter Parbrook; Tyndall National Institute, Ireland

Nitrogen-polar III-nitride materials have gained a great deal of interest, especially for their application in the field of high-frequency electronics, due to the disruptive approach in transistor scaling that they enable [1]. Optoelectronic devices could also greatly benefit from the change of orientation of the internal polarization fields [2], if epilayers of suitable crystal quality were available.
However, despite the technological interest and intensive study over the last two decades, N-polar GaN epilayers grown on foreign substrates such as sapphire or SiC, are still of significantly worse crystal quality than their Ga-polar counterparts, with X-ray rocking curve Full Widths at Half Maxima (FWHM) at best of around 400 arcsec for symmetric, and 600 arcsec for skew-symmetric reflections (see e.g. [1] and references therein). While this might be sufficient for present electronic devices, improved heteroepitaxy would be greatly beneficial for next generation N-polar electronic devices, and imperative for any possible future optoelectronic applications.
In a previous work [3], we have shown, for the first time, that Epitaxial Lateral Overgrowth (ELO) can be successfully applied to N-polar GaN for threading dislocation reduction. Compared to standard metal-polar growth, N-polar ELO has the further advantage that the initial microscale pattering necessary for an efficient bending and annihilation of the existing threading dislocations can be obtained with a very cost-effective technique, based on selective wet-etch in hydroxide solutions.
In the present study, we have optimized our technique to reduce even further the threading dislocation concentration, with FWHM well below 250 arcsec for both symmetric and skew-symmetric reflections. The starting N-polar GaN material is grown on a vicinal sapphire substrate using the approach already reported in [4], and then patterned with a regular hexagonal array of SiN circular caps, having nearest neighbours oriented along the <1-100> directions of GaN. In a subsequent wet-etch step in a KOH solution, microscale pyramids with sidewalls oriented along {1-10-1} planes are formed at the locations defined by the SiN caps. The caps are then removed, and the so-obtained 3D-template forced to coalesce back into a 2D layer of improved crystal quality.
A crucial feature of our technique is that it allows restoration of smooth surface morphology upon coalescence of the pyramids and subsequent growth. For planar epilayers, smooth surfaces are usually obtained with the use of vicinal substrates having offcut angles as large as 4° [5,6], but in the case of N-polar ELO this solution proved to be insufficient. Being the slowest growing plane, the (000-1) facets on top of the pyramids tend to expand in a perfectly on-axis orientation losing the beneficial effect of the vicinal substrate. The use of growth conditions that delay the expansion of the pyramids' tops make it possible to keep surface supersaturation on the (000-1) facets, at any stage of the regrowth phase, below the critical level that causes the onset random nucleation of hexagonal islands, which are typical of non-optimized N-polar growth.
Using this approach, we have been able to demonstrate epilayers that have the same smooth surface morphology as the starting layers and, at the same time, to the best of our knowledge, the best crystal quality ever reported for N-polar GaN on sapphire.

[1] M. H. Wong and U. K. Mishra, chapter 9 in III-Nitride Electronic Devices, 102. Elsevier, pp. 329–395, 2019
[2] S. Keller *et al.*, Semicond Sci Technol 29:113001, 2014
[3] P. Pampili *et al.*, arXiv preprint arXiv:2402.09385, 2024 (under review)
[4] M. Pristovsek, I. Furuhashi, P. Pampili, Crystals 13(7), 1072, 2023
[5] A. Zauner *et al.*, J Cryst Growth 210:435–443, 2000
[6] S. Keller *et al.*, J. Appl. Phys., 102, no. 8, p. 083546, 2007

3:00 PM 2C-2.4
Multi-Step *In Situ* Porosification Method for Obtaining Strain-Relaxed N-Polar InGaN Pseudo-Substrate Swarnav Mukhopadhyay, Surjava Sanyal, Guangying Wang, Shuwen Xie, Chirag Gupta and Shubhra Pasayat; University of Wisconsin–Madison, United States

N-polar III-nitride-based devices have shown very high potential for both high-frequency electronics and optoelectronic applications [1,2]. To lower the effective mass of charge carriers [3,4], strain engineering can be utilized by introducing a strain-relaxed buffer layer below the active

region through porosification techniques [4,5]. The porosification in Ga-polar and N-polar GaN buffer layers can be achieved through either electrochemical etching or thermal decomposition techniques [4-7]. However, electrochemical etching involves intricate processing steps and etching of heavily n-type doped GaN buffer layers, which isn't ideal for the HEMT process due to potential microwave losses. *P. Chan et al.* have shown that using the thermal decomposition technique 85% relaxed $In_{0.04}Ga_{0.96}N$ buffer layer can be obtained [6]. However, the thermal decomposition process used by them relies on the V-pit-assisted porosification of the InGaN layer. Although, the same technique can't be used for N-polar InGaN films without degrading the morphology, due to the absence of V-pits and presence of hillocks [4]. In this study, a multi-step in-situ porosification technique is used to porosify N-polar InGaN and obtain 40% relaxation with an average Indium content of 10.4% along with a reduction of hillock density.

A 62.5 nm thick N-polar hybrid InGaN/InGaN/GaN superlattice (SL) layer was deposited on the N-polar GaN template on a 4° miscut sapphire substrate using the MOCVD technique at 820 °C temperature and 666 mbar pressure. The SL consisted of 2.7 nm of $In_{0.15}Ga_{0.85}N$/7 nm of $In_{0.08}Ga_{0.92}N$/2.8 nm of GaN with a period of 5. The deposition of the InGaN/InGaN/GaN SL layer was performed using trimethylindium (TMIn), triethylgallium (TEGa), and ammonia (NH_3) precursors in a mixture of N_2 and H_2 carrier gases. After that, the reactor temperature was increased to 1020 °C for the in-situ porosification of the N-polar InGaN/InGaN/GaN SL layer for 8-10 mins under N_2 ambient. Next, a thin 35 nm GaN layer was deposited on top of the in-situ porous layer to coalesce this porous layer created at 1020 °C temperature. Then, an $In_{0.13}Ga_{0.87}N$ (2.8 nm)/$In_{0.09}Ga_{0.91}N$ (5.2 nm) SL of total 80 nm thickness was deposited on top of the GaN coalescence layer at 850 °C. Another in-situ porosification and GaN coalescence process was performed on the InGaN/InGaN SL layer. Finally, 160 nm of $In_{0.13}Ga_{0.87}N$/$In_{0.09}Ga_{0.91}N$ SL was deposited on top of the GaN coalescence layer to obtain a strain-relaxed pseudo-substrate. A reference sample was prepared without the initial 62.5 nm InGaN/InGaN/GaN SL layer for the comparison of the relaxation. The relaxation and morphology of InGaN/InGaN SL were measured using XRD and AFM measurement techniques.

The InGaN/InGaN SL layer with the high-composition porous InGaN/InGaN/GaN SL layer underneath showed a relaxation of 40% as opposed to 8.5% for the reference sample without this layer. The surface roughness of the 40% relaxed sample was <2 nm for a 5×5 μm^2 AFM scan, indicating a good morphology. This method resulted in a 50% reduction in hillock density in the strain-relaxed InGaN buffer layer compared to the initial InGaN/InGaN/GaN SL layer. Thus, this method is useful for obtaining a strain-relaxed N-polar InGaN buffer layer without degrading the material quality which is beneficial for both electronics and optoelectronic devices.

We acknowledge funding support from the Office of Naval Research (Dr. P. Maki)

Reference: *[1] B. Romanczyk et al., IEEE TED. 65, no. 1 (Jan. 2018): 45–50, [2] Y. Li et al. IEEE Access, vol. 10, pp. 95565-95570, 2022, [3] W Li et al. SST. 35 (2020) 075007 (6pp), [4] S.S Pasayat et al. J. Elec. Mat. Vol. 49, No. 6, 2020, [5] S.S Pasayat et al. APL. 116, 111101 (2020), [6] P. Chan et al. APL 119, no. 13 (Sept. 28, 2021): 131106. [7] H. Collins et al. APL 119, no. 4 (Jul. 26, 2021): 042105.*

3:20 PM 2C-2.5

Interlayer-Free GaN Epitaxial Polarity Inversion by Metalorganic Vapor Phase Epitaxy Kazuhisa Ikeda, Masahiro Uemukai, Tomoyuki Tanikawa and Ryuji Katayama; Osaka University, Japan

Optical parametric down conversion (OPDC) devices are expected to be applied as quantum light sources for quantum information processing. A transverse quasi-phase-matched (QPM) polarity inverted GaN bilayer channel waveguide device is one of candidates for efficient wavelength conversion. We have demonstrated epitaxial polarity inversion from N-polar −c-GaN to Ga-polar +c-GaN by introducing a thin AlN interlayer and subsequent oxidation annealing [1]. However, the use of AlN interlayer may result in reduced crystalline quality and wavelength conversion efficiency due to mismatches in lattice constants and refractive indices between GaN and AlN. In this study, we attempted to fabricate a +c/−c GaN epitaxial polarity inversion without an AlN intermediate layer by metalorganic vapor phase epitaxy (MOVPE).

After nitridation the c-plane sapphire substrate surface, the 145-nm-thick −c-GaN film was grown by MOVPE. The −c-GaN film was annealed in an oxygen atmosphere at 900°C for 10–30 min. A 2-μm-thick GaN film was regrown by MOVPE method via a low-temperature GaN buffer layer. In-situ reflectance monitoring was used to investigate transients in growth mode and surface morphology. When oxidation duration was 30 min, the regrowth started in three-dimensional growth mode and then changed to two-dimensional growth mode, and the surface became smooth at a thickness of ~1 μm. By reducing the oxidation duration from 30 min to 10 min, the two-dimensional growth was more promoted. Anisotropic etching was performed using a KOH aqueous solution (60 °C, 3 mol/L) to confirm the polarity of the regrown GaN layer. The smooth surface morphology remained after the KOH treatment, indicating that the regrown film had Ga polarity. In conclusion, we have succeeded in the growth of the GaN polarity inverted structure with a flat surface without an AlN intermediate layer.

[1] K. Ikeda et al., ICNS-14, GR5-5 （2023）.

3:40 PM BREAK

SESSION 2D: Rump Session: When III-V Meets Silicon
Session Chair: Kei May Lau
Tuesday Afternoon, May 14, 2024
6:30 PM – 8:30 PM
Resort Tower, Ground Level, Silver Room

James Coleman, University of Illinois Urbana-Champaign, United States

Bernardette Kunert, Imec, Belgium

Shinji Matsuo, NTT Device Technology Laboratories, Japan

Hoe Tan, The Australian National University, Australia

Qiang Li, Cardiff University, United Kingdom

Bei Shi, University of California, Santa Barbara, United States

Jean Decobert, III/V Laboratory, France

Kai Cheng, Enkris Semiconductor, China

ICM VPE XXI

2024 Las Vegas, NV

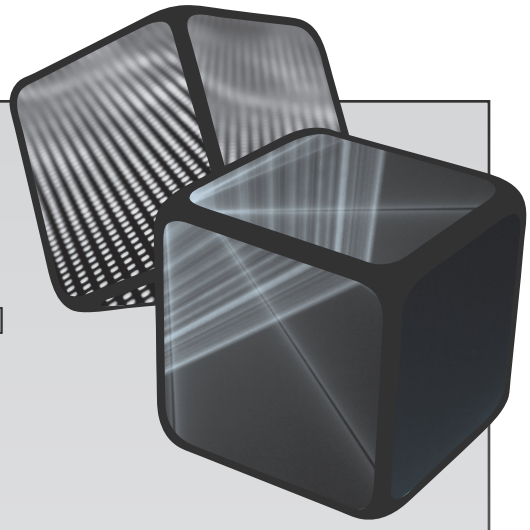

TUESDAY

Poster Presentations

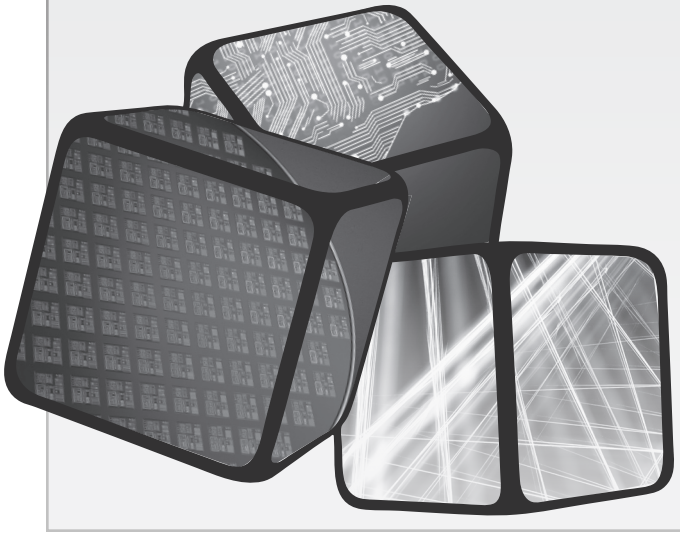

SESSION PS-1: Poster Session I
Tuesday Afternoon, May 14, 2024
4:00PM - 6:00PM
Resort Tower, Ground Level, Gold Room

PS-1.1
Investigating GaSb Growth Processes by Simulation
Hajrudin Husejni, Martin Dauelsberg, Merim Mukinovic, Bernd Schineller and Michael Heuken; Aixtron, Germany

Antimonide-based compound semiconductors play an important role in optoelectronic devices. GaSb-based materials prove valuable for mid-infrared light emitters, detectors as well as long-wavelength optoelectronic devices such as thermophotovoltaics and lasers. However, the growth mechanisms of these materials are currently only poorly understood and important physio-chemical constants are missing. The work presented is based on simulating gas phase transport phenomena using computational fluid dynamics (CFD). This modeling approach involves computing fluid dynamics, heat transfer, and species mass transfer, encompassing gas-phase chemistry and surface kinetics [1]. The study addresses multicomponent diffusion of growth-limiting chemical species in the reacting gas mixture. However, due to the coupling of diffusive fluxes and species concentrations, solving these equations incurs a high numerical cost. Therefore, we employed a simplified 2D model with a focus on adaptability to the Planetary Reactor®. This research is integral to enhancing our understanding of the chemical processes governing semiconductor growth, with potential implications for advancements in reactor design and operating conditions. The main objective of this research is to reveal the main gas phase and surface reaction pathways leading to the growth of GaSb. Trimethylgallium (TMGa), triethylgallium (TEGa), and trimethylantimony (TMSb) are the precursors under investigation. To prevent any additional phase formation, we maintain a relatively low V/III ratio: 1.29 for the TMGa/TMSb model and 1.5 for TEGa/TMSb. The temperature range is limited to 500-625°C, aligning with the constraints imposed by GaSb properties. A reduced reaction mechanism, considering homogenous and heterogenous reactions in the gas phase and at the growth surface, is incorporated into the model. The modified TMGa/TMSb model aligns with simulation results from previous studies, e.g., by M. K. Rathi et al. [2], confirming the model's robustness. Depending on the temperature and reactor geometry, the gas phase's source species undergo complete or partial decomposition. For the TMGa/TMSb model used in the horizontal tube reactor, the simulated growth rate demonstrates a linear dependence on the TMGa mole fraction at 625°C due to slower decomposition of TMGa relative to TMSb, while it is independent of the TMSb mole fraction. Conversely, the TEGa/TMSb model exhibits a sublinear dependence on group V precursor mole fraction and a slightly linear dependence on the TEGa mole fraction. Specific growth regimes associated with the TMGa/TMSb chemistry are identified, with mass transport regime dominating at higher temperatures, above 596°C, while below this temperature, surface kinetics govern the growth process. In the context of the Planetary Reactor®, the transition temperature is slightly shifted towards 620°C for the operating growth conditions. In the TEGa/TMSb model, a slight linear increase in growth rate with temperature is reported. The growth rate demonstrates either (sub)linear dependence on the molar flow rate or remains independent of it in other cases, contingent upon the growth temperature. The main reaction pathway that leads to the GaSb growth for the TEGa/TMSb model is identified. The alignment of our simulation model with observed growth trends serves as a foundation for process improvement and offers benchmarks for GaSb growth in industrial MOCVD reactors.

[1] M. Dauelsberg, L. Kadinski, Yu.N. Makarov, T. Bergunde, G. Strauch, M. Weyers, Journal of Crystal of Growth 208 (2000) 85–92
[2] M.K. Rathi, Brian E. Hawkins, Thomas F. Kuech, Journal of Crystal Growth 296 (2006) 117–128

PS-1.3
Growth of Wurtzite InP Nanofins by Selective-Area MOVPE Yuki Azuma, Ziye Zheng, Junichi Motohisa and Katsuhiro Tomioka; Graduate School of Information Science and Technology, and Research Center for Integrated Quantum Electronics (RCIQE), Japan

Crystal phase transition can stabilize metastable crystal phase as a single crystal in host materials. For example, the crystal phase transition of III-Vs changes zinc-blende (ZB) into wurtzite (WZ). These crystal phase transition materials have the advantage for optical devices applications because their bandgap changes from indirect to direct optical transition. Among the crystal phase transition materials, WZ phosphide-related (P-related) III-V alloys are expected as a new candidate light-emitting diode (LED) materials because these materials would have direct bandgap for all alloy composition [1]. Crystal phase transition nanowires were reported such as InP [2], GaP [3], InP/AlInP [4], and GaAs/SiGe [5]. Toward large-area growth for crystal phase transition materials, the disc-shaped WZ InP growth was reported [6]. However, detailed growth mechanism of planar WZ P-related III-V compound semiconductors in the selective-area growth was not fully clarified. Here, we characterized growth behavior of WZ InP fin structures by selective-area MOVPE toward the large area growth of WZ InP.
In experiment, 20 nm-thick SiO_2 sputtered InP(111)A substrates were used for the selective-area growth. For mask openings, periodical openings were formed using lithography and wet etching. Two kinds of shape were designed as mask openings. One was hexagonal openings surrounded with four short {-211} and two long {-211} sides. Another was octagonal openings surrounded with six short {-211} and two long {-110} sides. Then, InP was grown by low-pressure horizontal MOVPE with H_2 carrier gas. The source materials were trimethylindium (TMIn) and tertiarybutylphosphine (TBP). The partial pressure of TMIn and TBP were 2.7×10^{-6}

and 6.2×10^{-5} atm. The growth temperature was 660°C. Growth time for the InP was varied from 10 – 45 min. Next, two step growth was introduced for the InP growth to investigate the growth morphologies toward epitaxial lateral-overgrowth (ELO). After the growth of InP fins, InP was grown continuously for 15 min. at 600°C with same V/III partial pressure ratio.
Growth results showed InP nanofins were grown on both two kinds of opening patterns. The morphologies were hexagonal nanofins surrounded with {-211} vertical facets and octagonal nanofins surrounded with {-110} and {-211} vertical facets. Transmission electron microscopy (TEM) indicated both of InP nanofins had WZ structure. As for the growth behavior of the InP nanofins, the average height of InP nanofins was obviously different with opening shapes. The average height of hexagonal InP nanofins on the opening with {-211} long sides was 1.2 µm and those of octagonal InP nanofins was 0.6 µm. This difference in the fin height was assumed to be the difference in surface diffusion length of In adatoms on fin sidewalls. The In adatom diffusion length on {-211} facets was longer than that on {-110}. Growth time dependence indicated that the average height for both InP nanofins had saturation height and lateral growth was enhanced when the average height reached to saturation height. The InP fins eventually coalesced due to the lateral growth when the growth time was long. PL mapping image exhibited the InP nanofins showed single peak at 1.45 eV which was originated form WZ InP bandgap. The coalesced fins showed broad peak at around 1.34 eV, indicating the crystal structure of the coalescence part was ZB phase. Detailed growth results of WZ InP films using two step growth will be discussed further in this conference.

References:
[1] A. De *et al.*, Phys. Rev. B, **81**, 155210 (2010).
[2] Y. Kitauchi *et al.*, Nano Lett., **10**, 1699 (2010).
[3] S. Assali *et al.*, Nano Lett., **13**, 1559 (2013).
[4] F. Ishizaka *et al.*, Nano Lett., **17**, 1350 (2017).
[5] E. M. T. Fadaly *et al.*, Nature, **580**, 205 (2020).
[6] P. Staudinger *et al.*, Nanotechnology, **32**, 075605 (2021).

PS-1.4
Low Temperature Regrown Ohmic Contacts by MOVPE for Improved Performance of InAlGaN/GaN HEMTs
Cedric Lacam[1], Chrales Pitaval[2], Nadia El Bondry[1] and Sebastien Aroulanda[1]; [1]Thales, France; [2]Nokia, France

In this work, we report on GaN:Si ohmic contacts regrown by metal-organic vapour phase epitaxy (MOVPE) to improve the performance of InAlGaN/GaN high electron mobility transistors (HEMTs).
GaN-based HEMTs are widely used for high-voltage RF applications, thanks to their remarkable properties such as a high carrier density and mobility bi-dimensional electron gas (2DEG), and a high breakdown voltage. To achieve high power added efficiency (PAE) and power output (P_{out}), it is necessary to increase the maximum output current density by reducing parasitic resistances. This can be achieved by reducing the access resistances, i.e. the sheet resistance of the HEMT structure, and the source-drain distance, which will reduce the contact resistances (R_c).
The standard manufacturing process for ohmic contacts involves deposition and annealing of a metal stack. However, fabrication of small size components is difficult as the latter operation has to be carried out at high temperature, which can lead to alloying of the metals. In order to reduce parasitic resistances, ohmic contact regrowth is the most advantageous technique as it allows lower R_c values to be obtained with reduced source-drain dimensions since no annealing is required.
In this work, we study the selective MOVPE of silicon-doped gallium nitride ohmic contacts on InAlGaN/GaN HEMT structures. First, an InAlGaN/GaN HEMT structure is grown on a 100 mm S.I SiC substrate by MOVPE. The low sheet resistivity of these quaternary barriers ensures low access resistance. A dielectric layer is then deposited on the HEMT structure and patterned using a photolithography process and a dry etch step. A recess step of the exposed HEMT structure will therefore define the regrown regions. Finally, the patterned wafer is re-introduced into the MOVPE reactor for the selective growth epitaxy.
The main challenge is to grow a heavily doped GaN layer at a relatively low temperature, of the order of 850 °C. This low temperature is set by the quaternary barrier layer, to prevent the indium from desorbing from the barrier, which could degrade the characteristics of the heterojunction. The impact of growth rate, reactor pressure and disilane flow was studied and the growth conditions were optimised to achieve fully selective epitaxy while obtaining a doping level of 1.10^{20} cm^{-3}. Values of $R_c < 0.1$ ohm.mm were obtained, which is 5 times lower than the standard annealed ohmic contact. These low R_c values, combined with small source-drain dimensions, have a significant impact on the performance of HEMT devices. An improvement in PAE and P_{out} was measured compared, demonstrating the great interest in this technique.

PS-1.5
Large Area III-Nitride Device Structures on h-BN—Growth, Exfoliation and Transfer to Different Substrates
William Brand[1], Tim Vogt[1], Fikadu Alema[1], Andrei Osinsky[1], Vitali Soukhoveev[1], Michael Snure[2] and Nicholas Glavin[2]; [1]Agnitron Technology, United States; [2]AFRL, United States

Like its extensively researched counterpart, graphene, hexagonal boron nitride (h-BN) has emerged as a compelling two-dimensional material with a myriad of potential applications. The structural attributes of h-BN closely resemble those of graphene, characterized by a hexagonal bonding configuration with robust in-plane bonds and weaker van der Waals forces acting on out-of-plane atoms. This similarity allows for the routine exfoliation of a few monolayers of h-BN from substrate materials, akin to the process observed with graphene. The exfoliation of films grown on h-BN facilitates the heterogeneous integration of devices, particularly those based on wide bandgap and ultra-wideband gap semiconductors, with circuits or devices on Silicon or other compound semiconductors. Leveraging these unique physical and electrical properties of h-BN, it has become a favored material for growth templates for III-nitride materials on sapphire substrates. However, a limitation in h-

BN/III-nitride processes lies in the scarcity of manufacturable substrates at volume. At Agnitron, we have addressed this challenge by developing manufacturable growth processes for h-BN templates alongside various III-nitride films, serving as templates/starting materials for device fabrication.
In this work, we present the latest advancements in our growth and template transfer processes. Collaborating with the Air Force Research Laboratory, we have successfully transitioned their development process to production on sapphire substrates as large as 100mm. We consistently produce h-BN, AlN/h-BN, and GaN/h-BN templates, utilized as starting materials for HEMT, optical (LED/detector), and piezoelectric (oscillator/filter) devices on wafers as large as 100mm. Few monolayer h-BN films typically measure around 2nm (+/-10%) in thickness across a 100mm wafer. GaN templates grown on h-BN exhibit a thickness non-uniformity of ~3% across 100mm for 2µm thick films, while AlN templates display non-uniformities of +/-5%. Moreover, we have developed a production-ready film exfoliation process capable of lifting full-wafer films as large as 100mm in diameter and transferring them to other materials for processing or application. These films can be transferred to a substrate of choice for device processing, or fully processed devices/die can be individually transferred as per application requirements. Partially processed devices can also be transferred to other substrates for subsequent wafer-scale processing. Characterization of h-BN films include AFM, Raman, and X-ray reflectivity (XRR), with RMS roughness typically measuring between 0.1-0.2 nm for films near 2nm in thickness, as measured by XRR. Growth conditions are optimized to induce a self-limiting growth mode, ensuring precise control over film thickness and morphology. Growth conditions for the III-nitride template materials adhere to typical growth processes using TMAl and TMGa precursors. The characterization of these films involves AFM, XRD, and electrical conductivity measurements were completed. Within this study, we will discuss the growth, film transfer, and device characterization of h-BN template-grown films on c-plane sapphire.

PS-1.6
Compensative Nitrogen Doping of β-Ga_2O_3 by MOVPE
William Brand, Fikadu Alema and Andrei Osinsky; Agnitron Technology, United States

β-Ga_2O_3 has emerged as a central focus in semiconductor research for its potential applications in power electronics owing to its substantial bandgap of approximately 4.9 eV, an estimated high breakdown field of around 8 MV/cm, and the availability of high-quality melt-grown β-Ga_2O_3 substrates. A notable challenge associated with current native Ga_2O_3 substrates is the accumulation of interfacial silicon, which can serve as a parasitic channel detrimental to lateral power device performance. The implementation of HF etching prior to epitaxial growth has been demonstrated to substantially diminish interfacial silicon by at least an order of magnitude. An alternative approach to addressing this issue involves the utilization of compensatory/deep acceptor dopants near the interface to counteract these "killer defects." Historically, magnesium and iron have been employed to establish semi-insulating layers; however, their usage is encumbered by diffusion and surface migration challenges.
This work presents recent advancements in compensatory nitrogen doping of β-Ga2O3 using nitrous oxide, nitric oxide, and ammonia. The process parameters, including pressure, temperature, and molar flow rate of the nitrogen precursors, employed to achieve nitrogen concentrations ranging from 10^{16} to 10^{20}, will be discussed. Nitrogen doping using these precursors has exhibited consistency and reproducibility. At nitrogen concentrations of 4 to $8x10^{18}$ cm^{-3} films displayed bulk resistances of 1.9 to 76 MΩ. When employing ammonia and nitrous oxide as nitrogen sources, hydrogen is also introduced into the film. The impact of hydrogen incorporation within the films and strategies to mitigate its presence through process adjustments will be examined. A comparative analysis between nitrogen doping and the use of iron and magnesium as compensatory doping agents will be conducted. Notably, nitrous oxide and nitric oxide serve not only as nitrogen sources but also facilitate the oxidation of metal-organic gallium sources. Nitrous oxide can function independently as the primary oxidizing agent, while nitric oxide can be paired with oxygen to enhance the film growth rate. Crystal quality and surface morphology of nitrogen-doped films were evaluated via XRD and AFM. When inspecting the rocking curves for (020) and (111) reflections, little to no differences were found between unintentionally doped films (UID) and films with [N] = 4-8 x 10^{18} cm^{-3}. Further exploration into nitrogen doping and its efficacy is imperative for the ongoing advancement of gallium oxide power device development.

PS-1.7
The In Incorporation Corresponding to TMA Flow in MOVPE Growth of AlGaInN
Yuto Yamada, Takeru Kumabe, Hirotaka Watanabe, Maki Kushimoto, Shugo Nitta, Yoshio Honda and Hiroshi Amano; Nagoya University, Japan

Quaternary AlGaInN has attracted much attention for its applications in various optical and electronic devices, such as barrier layers of high-electron-mobility transistors (HEMT) and cladding layers of laser diodes. [1, 2] AlGaInN enables a flexible modulation of physical properties due to its two degrees of freedom in alloy composition. For example, the possibility of polarization engineering may be expanded by increasing the polarization charge density to keep the lattice mismatch small. Additionally, by applying AlGaInN to polarization doping, one can realize both high and low carrier densities, which ternary alloys cannot achieve. To achieve such an application, precise composition control in Metal Organic Vapor Phase Epitaxy (MOVPE) growth is important. It has been reported that the the amount of In incorporated increases with the Al composition [3, 4], but how and why it increases has not been investigated, which is a drawback toward realizing strict composition control such as polarization doping. Therefore, in this study, we focused on the change in the amount of In incorporated with TMA flow toward a strict composition control of quaternary alloys. Ternary and quaternary alloys were grown on *c*-plane 2-inch sapphire substrates by MOVPE. Trimethylgallium (TMG), TMA, trimethylindium (TMI), and ammonia (NH_3) were used

as precursors. The growth was initiated with a GaN nucleation layer, followed by 2.3-µm-thick unintentionally doped GaN and up to 100-nm-thick ternary or quaternary alloys (AlGaN, InGaN, AlGaInN). During the AlGaInN crystal growth, the TMA flow ratio [TMA/(TMA+TMG+TMI)] and growth temperature were respectively varied at 10-50 % and 775-845 °C (temperatures at which the In composition of InGaN is < 10 %). The growth pressure was 470 hPa. The flow of TMG, TMI, and NH_3 were constant. Additionally, the carrier gas was N_2 to facilitate In incorporation. The Al and In compositions in ternary alloys were determined by X-ray diffraction reciprocal space mapping (XRD-RSM). Because the composition of the quaternary alloy cannot be uniquely determined by XRD-RSM, it was determined by energy dispersive X-ray spectroscopy (EDX) and Rutherford backscattering spectrometry.
For AlGaInN, the In composition decreased with increasing growth temperature, and the Al and In compositions increased with TMA flow ratio. Furthermore, at 775 °C (temperature at which the In composition of InGaN is 4 %), the In composition also tended to increase significantly with Al composition, but at 815 °C and 845 °C (temperatures at which the In composition of InGaN is up to 1 %), the In composition did not increase significantly. EDX showed the following results. At 775 °C , at the TMA flow of 10.4 µmol/min, the Al composition (*x*) was 21.6 % and the In composition (*y*) was 4.69 %. At this temperature, at the TMA flow of 51.8 µmol/min, *x* was 49.6 % and *y* was 9.31 %. At 815 °C, at the TMA flow of 10.4 µmol/min, *x* was 16.9 % and *y* was 2.44 %. At this temperature, at the TMA flow of 51.8 µmol/min, *x* was 44.1 % and *y* was 3.11 %. In addition, the non-strained *a*-lattice constant of 775 °C samples calculated by using Vegard's law was close to that of GaN; thus, In incorporation due to TMA flow might be affected by the lattice constant of the underlying layer.
In conclusion, it was found that the In incorporation corresponding to TMA flow was temperature-dependent. At low growth temperature, the change in In composition is significant and should be taken into account. This is considered an important guideline for the MOVPE growth of AlGaInN and will help elucidate growth mechanisms.

This work was supported by JSPS KAKENHI Grant Numbers 23H01866.

References
[1] R. Wang *et al*., IEEE Electron Device Lett. **32**, 9, 1215 (2011).
[2] M. Miyoshi *et al*., Phys. Status Solidi A **217**, 1900597 (2020).
[3] B. Reuters *et al*., J. Electron. Mater. **42**, 5, 826 (2013).
[4] V. Perez-Solorzano *et al*., J. Cryst. Growth **272**, 386 (2004).

PS-1.8
Dependence of Thermal Transport on Compositional Grading in MOCVD-Grown AlGaN Layers for Polarization-Enhanced Doping Mihee Ji, LeighAnn Larkin, Gregory Garrett, Anand Sampath and Michael Wraback; DEVCOM Army Research Laboratory, United States

The optimal performance of high-power UWBG-based devices will require efficient removal of large thermal fluxes away from active regions of the device. Over almost the entire composition range, AlGaN possesses a thermal conductivity κ an order of magnitude lower than both AlN and GaN [1]. Despite its low κ, AlGaN could serve a beneficial thermal purpose in III-N-based devices as a "phonon bridge", a thin layer with intermediate vibrational properties inserted between two materials that have little overlap in their phonon modes. Such a phonon bridge was theoretically demonstrated to increase thermal conduction by up to 200 %, and, as a mass graded interlayer, up to 300 % [2]. AlGaN is also a highly polar material that can be doped *p*-type by employing polarization enhanced doping using a compositionally graded layer [3, 4]. As such, it is important to understand the relationship between thermal and electrical transport properties in compositionally graded $Al_xGa_{1-x}N$ layers.
In this study, the experimental $Al_xGa_{1-x}N$ epitaxial layers (samples A-C) were grown on AlN/sapphire templates by metalorganic chemical vapor deposition (MOCVD). Trimethylgallium ($Ga(CH_3)_3$, TMGa), trimethylaluminum ($Al(CH_3)_3$, TMAl), and ammonia (NH_3) were used as the precursors for Ga, Al, and N, respectively, and H_2 was used as the carrier gas. The growth temperature of 1120 °C and pressure of 40 Torr were identical for three samples. In preparation for the epitaxial growth, ex-situ standard solvent and acid cleaning procedures and in-situ high-temperature thermal cleaning procedures were performed. The layer structures of samples A, B, and C are a 96-nm-thick unintentionally doped $Al_xGa_{1-x}N$:ud layer (x~0.42), a ~155-nm-thick linearly graded unintentionally doped $Al_xGa_{1-x}N$:ud layer (x~1 to 0.41), and a ~165-nm-thick unintentionally doped $Al_xGa_{1-x}N$:ud layer (x~0.69), respectively. Atomic-force microscopy (AFM), optical microscopy, and X-ray diffraction (XRD) were carried out to examine surface morphology and crystalline quality of the three samples. The Al mole fractions in the $Al_xGa_{1-x}N$ epitaxial layers and their thicknesses were validated by XRD measurement. The AFM measurement showed a smooth surface and a well-developed step-flow morphology for the three samples. The $Al_xGa_{1-x}N$ samples were coated with 100 nm of Al and then characterized thermally with Time-domain Thermoreflectance (TDTR). The thermal conductivity was measured to be 9 ± 1 W/mK, 10 ± 1 W/mK, and 8 ±1 W/mK for sample A, sample B, and sample C, respectively. The observation that the thermal conductivity of the graded AlGaN layer (sample B) is ~ 20 percent higher than that of sample C, which has a similar thickness and Al composition midway between the endpoints of the grade, implies that this phonon bridge approach may be promising for the realization of high κ AlGaN devices.
Detailed structural, material, thermal, and electronic properties of $Al_xGa_{1-x}N$ layers as a function of graded layer thickness will be compared to control samples of fixed composition

along the grade and similar thickness to identify an optimum grade for both thermal and electronic transport.

References

[1] W. Liu and A. Baladin, "Thermal conduction in AlGaN alloys and thin films", *Journal of Applied Physics* 97, 073710 (2005).
[2] Pamela M. Norris, LeighAnn S. Larkin, Nam Q. Le, Carlos A. Polanco, Justin L. Smoyer, Jingjie Zhang, "Chapter Six - Progress in measuring, modeling, and manipulating thermal boundary conductance," *Advances in Heat Transfer* 53, pp. 327-404 (2021).
[3] Z. Zhang, M. Kushimoto, M. Horita, N. Sugiyama, L.J. Schowalter, C. Sasaoka, and H. Amano, "Space charge profile study of AlGaN-based p-type distributed polarization doped claddings without impurity doping for UV-C laser diodes", *Applied Physics Letters* 117, 152104 (2020).
[4] J. Simon, V. Protasenko, C. Lian, H. Xing, and D. Jena, "Polarization-induced hole doping in wide-band-gap uniaxial semiconductor heterostructures", *Science* 327 pp. 60-64 (2010).

PS-1.9

MOVPE Growth of Nitrides for MOVPE-MBE Hybrid Structures—New Approaches, Challenges and Possibilities

Damian Pucicki[1,2], Wojciech Olszewski[1,3], Paulina Ciechanowicz[1,3], Adrianna Piejko[1,2] and Detlef Hommel[1,4]; [1]Lukasiewicz Research Network - PORT Polish Center for Technology Development, Poland; [2]Wroclaw University of Science and Technology, Poland; [3]University of Wroclaw, Poland; [4]Polish Academy of Sciences, Poland

The synthesis of high-quality templates is a one of the critical step in the fabrication of nitride-based devices. Although expensive native GaN or AlN substrates are recently being used, next to Si, Ge, and ZnO, still the most popular foreign substrates like sapphire or SiC are the main choice for the commercial devices. The progress in design of the devices has led to significant modification of epitaxial growth and often to the usage of vertically oriented structures such as micropillars or nanowires. Thus, more often hybrid approach, combining MOVPE and MBE techniques, is consider in order to capitalize on the strengths of both methods to achieve enhanced material properties and breakthrough the device limitation. Although, in the most cases, MOVPE-grown GaN or AlN on sapphire templates are being used for further MBE growth, in the case of novel device constructions the material and physics limitations require MOVPE overgrowth on the MBE-grown structures. Such solution requires taking into account several differences in both mentioned techniques and disadvantages of wafer transferring between the systems. Our study encompasses novel approaches, challenges encountered, and the diverse possibilities arising from this synergistic hybridization of epitaxial growth methods.
The first aspect of hybridization need to be solved is transparency of the sapphire wafers. While in MOVPE reactors heating of the wafers is supported by heat transport by direct contact of the wafer and graphite susceptor in the MBE chamber only absorption of the heater radiation is the heating mechanism. Thus, the transparent wafers must be back-side sputtered by Ti layer. Such sputtering is mostly proceeded after the MOVPE growth of the GaN/sapphire template, directly before the wafer is transferred into the MBE system. In such a case, necessary wafer cleaning leds to defect formations at the MOVPE/MBE interface. More challenging is when the MBE-grown structure must be overgrown in MOVPE reactor. The growth temperature of ~1100°C and ammonia ambient transform titanium coverage into the TiN layer. That change influence the reflectivity-based true temperature measurement during MOVPE growth, what must be recalibrated in order to ensure optimum growth conditions. We propose sputtering of the Ti layer on the epiready sapphire wafer, before the MOVPE growth of the templates. Such approach ensure high temperature annealing and cleaning of the already back-side Ti-covered and cleaned wafers in MOVPE reactor and thus reduce influence of the wafer processing on the successively grown epilayers. In the next MBE growth, the TiN layer is then absorbing layer in spite of the pure Ti, what also must be recalibrated.
The next challenge is wafer transfer between the MOVPE and MBE systems. In the case of the MOVPE to MBE transfer, we propose an additional MOVPE-grown sacrificial layer which is easy to remove in MBE conditions. The removing of sacrificial layer was proved by in situ XPS investigation. On the other hand, the high temperature initial step of MOVPE growth is sufficient for desorption more than 20 nm of GaN layer grown in MBE chamber and is the main mechanism refreshing the surface after the wafer is transferred from MBE to MOVPE reactor.
Finally, the MOVPE templates with a modified top layer can significantly influence the MBE growth of the micropillars. For our investigation of the MBE growth of the GaN micropillars we have grown a standard MOVPE sapphire/GaN templates as well as templates with GaNAs top layers with arsenic content up to 7%.We have demonstrated that size/diameter and surface density of the MBE-grown As-induced micropillars strongly depends on the arsenic content in the MOVPE-grown top layer of the template.
All our MOVPE experiment has been done in a 3×2 flip top close coupled showerhead (FT CCS) AIXTRON reactor and in a multi chamber Scienta Omicron GmbH system with two MBE and one analytical chambers.

PS-1.10

Wavelength Extended-InGaAs(P) Photodetector Monolithically Growth on InP with Cutoff Wavelength Toward 3.2 µm

Phuc Dinh Nguyen[1,2], Suho Park[1], Jiyeon Jeon[1], Jungwon Yoon[3], Minkyeong Kim[3], Byong Sun Chun[1] and Sang Jun Lee[1,2]; [1]Korea Research Institute of Standards and Science, Korea (the Republic of); [2]Korea National University of Science and Technology, Korea (the Republic of); [3]Irspectra Co., Ltd, Korea (the Republic of)

Composition-graded InAsP metamorphic buffers are a great platform to manipulate the lattice constant of InP substrate, providing a flexible lattice constant to access the InAs operation wavelength while utilizing the advantage of InP processing technology. Compared to cation mixed InAlAs, InAsP metamorphic buffer offers better lattice mismatched quality, owing to the lack of random nucleation effect caused by anisotropic III-group mobility. However, due to the

complication in structure design as well as the degradation of crystal quality, previous reports mainly focus on the low Arsenic composition (As < 70 %) regime.
In this work, InAsP metamorphic buffer has been successfully grown, exhibiting the As composition of up to 95%. Based on that, a series of wavelength-extended $In_xGa_{1-x}As_{1-y}P_y$ photodetector is presented. Devices were pseudomorphically grown on InP substrate using metal organic vapor phase epitaxy (MOVPE). From spectral response measurement analysis, our devices displayed a tunable cut-off wavelength of up to 3.2 µm. Structural characterization by reciprocal space mapping shows that the devices exhibit high crystal quality with the degree of relaxation approaching unity. The performance of the wavelength-extended InGaAs photodetectors were systematically analyzed as a function of In composition. This study can provide useful information for future detection device development of imaging devices.

PS-1.11
Metamorphic Graded GaAsP on GaAs by MOVPE for Photocathodes Anthony Mazur[1], Adam Masters[2], Benjamin Belfore[2], Sylvain Marsillac[2], Seth M. Hubbard[1] and Stephen Polly[1]; [1]Rochester Institute of Technology, United States; [2]Old Dominion University, United States

Semiconductor photocathodes, benefiting from high quantum efficiency (QE) and carrier lifetimes, can act as high intensity electron spin polarization (ESP) sources. Such devices are used in electron accelerators to probe nuclear structures and make precision tests of the standard model. A notable example is the electron-ion collider (EIC), a future project which plans to take advantage of ESP sources to probe the binding forces of nuclei.

GaAs is an attractive commercially viable material for semiconductor photocathode production, but is limited by a maximum ESP of 50% due to degeneracy of states in the valence band. Introducing a compressive strain lifts this degeneracy allowing an increase in ESP to as much as 100%. One method to achieve this uses a strained GaAs / GaAsP quantum well (QW) super lattice structure. However, for compressive GaAs growth, the matrix lattice must be tensile to the GaAs substrate. To grow such a device, it is necessary to develop a metamorphic graded (MMG) buffer to bridge the lattice mismatch between GaAs and GaAsP, allowing strained growth of the QWs without disruption from excessive lattice defects. In addition, epitaxial growth allows the inclusion of a distributed Bragg reflector (DBR) and Fabry-Perot (FP) cavity to increase the optical path length in the QWs to further improve quantum efficiency.

This work presents details on growth iterations and characterization of a MMG from GaAs to $GaAs_{0.65}P_{0.35}$ grown epitaxially in an Aixtron close-coupled showerhead 3x2" MOVPE research reactor for use in an epitaxial photocathode device. A wide range of parameters were investigated, including substrate offcut, MMG thickness per growth step, MMG compositional change per growth step, growth temperature, growth rate, and V/III ratio. Growth was monitored in-situ via a LayTec EpiCurveTT system, providing emissivity corrected surface temperature, growth rate, and substrate curvature measurements used to extract strain at growth temperature. From ex-situ high-resolution x-ray diffraction (HRXRD), reciprocal space maps of the (224) reflection, the Langmuir incorporation coefficient of phosphorous, as well as strain and relaxation of individual layers, were extracted for a given growth condition.

From this work, we observed growth on (100) on-axis surfaces without intentional offcuts provided the best template for this tensile MMG realization, especially for subsequent multi quantum well growths to limit threading dislocations. Growth at high temperature (730 °C) with 14 MMG steps of 500 nm, a 500 nm $GaAs_{0.625}P_{0.375}$ overshoot layer, a 2000 nm $GaAs_{0.65}P_{0.35}$ fallback layer, using a 2.5% compositional delta of phosphorus and a growth rate of ~10 µm/hr, demonstrated a MMG with 100% relaxation and a final composition of $GaAs_{0.633}P_{0.367}$. Additionally, a DBR was developed using $GaAs_{0.65}P_{0.35}$ and $Al_{0.70}In_{0.30}P$ corresponding to a peak wavelength of 780 nm to target the emission wavelength of the excitation laser. The final MMG and DBR were incorporated to a device growth in which a QE of 2.9% and an ESP of 82% was observed.

PS-1.12
Structural and Electronic Properties of Low-T MOCVD Grown (Al)InGaP Structures for Multi-Junction Solar Cells Marco Calicchio, Elisabetta Achilli, Nicola Armani, Marina Cornelli, Paolo Marzatico, Emanuele Malvisi, Filippo Annoni and Gianluca Timò; RSE Spa, Italy

In this work we exploit the possibility of growing (Al)InGaP-based structures al low temperatures (≈ 550 °C) with the final aim of realizing devices with a more sustainable pathway. CPV provides the largest solar-to-energy efficiency with the downside of high cost of materials and processes. This aspect makes large scale terrestrial applications difficult and demands for a further enhancement in the performance/cost ratio. In particular, this approach would allow to combine III-V and IV group semiconductors in the same growth camber on the one side, and to gain a better quality avoiding cross contamination on the other. Specifically, the employment of a lower T prevents contamination by decreasing the diffusion mean free path of chemical species in the material. As far as CPV application is concerned, the gradual introduction of Al in the III-V layer opens the possibility to improve performances by increasing the band gap of the top cell. However, the major challenge in this field lies in the possible creation of defects due to the high reactivity of aluminum towards oxygen. Quaternary $Al_yIn_xGa_{1-x-y}P$ structures were grown by a MOCVD AIX2800 reactor applying 50 mbar of total pressure onto (100) GaAs wafers 2° off towards [110] crystallographic direction. Metal-organic precursors, employed during MOCVD growth of (Al)InGaP structures, were trimethylindium (TMI), trimethylgallium (TMGa), trimethylaluminum (TMAl) and pure phosphine (PH_3). Preparatory depositions have been carried out concerning the reduction of the background doping and for the calibration of the epitaxial structure (composition and thickness of the layers). For this purpose, *in-situ* growth rate determination,

high resolution X-Ray diffraction (HR-XRD) and scanning electron microscope (SEM) cross section and have been carried out.
A further optimization involved doping conditions to obtain *p*-doped layers (by means of DEZn) and *n*-doped layers (by means of DETe): electrochemical capacitance-voltage measurements (ECV) profiles revealed doping homogeneity along the growth direction and demonstrate contamination reduction in the structure. Eventually, the increase in bandgap was investigated thanks to photoluminescence (PL) analysis. Results obtained demonstrate good quality of the structures grown and open new routes towards a monolithic integration of III-V and IV compounds in view of sustainable multi-junction solar cells in the same growth chamber.

PS-1.13
Material Quality and Device Efficiency Engineering for III-Nitride Red LEDs Mikhail Rudinsky[1], Daria Zimina[2] and Kirill A. Bulashevich[1]; [1]Semiconductor Technology Research D.O.O. Beograd, Serbia; [2]STR US, Inc., United States

Quantum efficiency and emission spectrum of red InGaN-based light-emitting diodes (LEDs) depend on the complex interplay of multiple factors. Along with the structure design by itself, performance of InGaN-based LED is sensitive to the stress evolution, crystalline quality, and composition profile. Research aimed at improving the performance of these LED structures requires careful account and deep understanding of all of these factors. In this regard, here we analyze a LED structure described in [1] with two-step modeling, paying special attention to the above listed factors. First, STREEM-InGaN [2] is used to self-consistently simulate the MOCVD growth process, taking into account time-resolved In segregation and incorporation into the growing structure along with strain and crystal quality evolution. At the second step, these results are used to simulate band diagram, carrier transport, and light emission using SiLENSe software [2]. The applied computer modeling approach allows one to consistently follow up the effect of the growth recipe on composition and threading dislocation density (TDD) profiles in LED structure and, eventually, on the operation of the device.

The hybrid multiple quantum well (MQW) structure considered here has the following key elements: thick GaN buffer followed by 15×GaN/$In_{0.08}$GaN superlattice (SL), blue single quantum well (SQW), red InGaN double quantum wells (DQWs), and AlGaN strain compensating barriers, as well as AlN interlayer (IL). To study comparative contribution of the individual components into the LED performance, the structure has been considered as is and with modifications.

Unsteady computations of In and Al content, as well as TDD show that in the original structure design generations of new TDs accompanied by partial stress relaxation occurs during the growth of the blue QW. However, if the blue QW is removed from the structure, generation of new TDs intensifies and moves to the first red QW. Another interesting result of kinetic growth simulations is pertaining In content distribution: indium accumulation on the surface during the growth of the first red QW results in In incorporation into the immediately following AlN IL. Device simulations show that In incorporation results in decrease of the energy gap and polarization charge. Moreover, poor hole injection and very low EQE is expected for pure AlN IL, which is consistent with the simulations predicting perceptible In content.

Superlattice and AlGaN barrier are also considered in terms of their effect on stress and TDD. Simulation results are then used as input data for the modeling of LED structure operation to study the effect of all the factors considered above on the IQE and emission wavelength.

Finally, additional attention is paid to the effect of v-pits on TDs behavior during growth of the structure. It is quantitatively shown that increase of V-pit density may significantly hinder nucleation of new TDs.

[1] D. Iida *et al.*, *Appl. Phys. Lett.*, **116**, 162101 (2020); D. Iida, *presented at IWN-2022* (2022).
[2] *https://str-soft.com*

PS-1.15
Extended Short-Wavelength Infrared InGaAs Microspectrometer Using a Linear Variable Optical Filter Byong Sun Chun[1], Jiyeon Jeon[1], Suho Park[1], Yeongho Kim[2], Phuc Dinh Nguyen[1], Hyeon-June Kim[3] and Sang Jun Lee[1]; [1]Korea Research Institute of Standards and Science, Korea (the Republic of); [2]Chonnam National University, Korea (the Republic of); [3]Seoul Nation University of Science and Technology, Korea (the Republic of)

A miniaturized extended short-wavelength infrared (e-SWIR) InGaAs microspectrometer is fabricated and characterized. We have demonstrated an e-SWIR microspectrometer by monolithic integration of a 256 x1 InGaAs linear array detector with a wedge-shaped Si/SiO_2 Febry-Perot (F–P) linear variable optical filter (LVOF). The step-graded metamorphic layers of $InAs_yP_{1-y}$ enabled the growth of the p+ -$InAs_{0.63}P_{0.37}$/n-$In_{0.83}Ga_{0.17}As$ heterostructure with a 90% cutoff wavelength of 2.6 mm through a high degree of strain relaxation of 96%. The wedge-shaped LVOF fabricated on a sapphire substrate exhibits bandpass filter characteristics, whose transmission peak wavelength increases linearly with the optical thickness of the SiO_2 cavity. Similarly, the single-chip microspectrometer consisting of the wedge-shaped LVOF integrated with the 256 x 1 InGaAs detector pixel array yielded a wavelength-tunable bandpass filtering response in the spectral range of 1.6–2.6 mm. The temperature-dependent dark current characteristics of the microspectrometer indicate that at temperatures of 180–300 K, the dominant dark current mechanism is the generation-recombi-nation dark current via Shockley-Read-Hall recombination in the depletion region, whereas the diffusion dark current is suppressed by the high potential barriers at the p+ -InAsP/n-InGaAs heterointerface. At 300 K, the microspectrometer exhibits a responsivity of 0.34 AW^{-1} and a noise voltage of 76 nV $Hz^{-1/2}$, corresponding to a specific detectivity of 6.3 x 10^8 cm $Hz^{1/2}$ W^{-1}. We expect these single-chip SWIR micro spectrometers to be well-suited for applications in portable, wearable, or unmanned systems

for in-line and real-time monitoring because of their compactness, robustness, and high spectral selectivity.

PS-1.16
The Study of Structural, Mechanical and Electronic Properties of Cubic 3d-Transition Metal Nitrides Using Density Functional Theory Bhila O. Mnisi; University of South Africa, South Africa

Transition metal nitrides have gained attention globally due to their exceptional physical and mechanical properties. Despite their excellent properties, further research needs to be conducted to completely understand the structural, mechanical, electronic and optical properties. In this paper, ab initio density functional theory (DFT) calculations are performed to investigate the structural, mechanical, and electronic properties of transition metal nitrides XN (X = Sc, Ti, and V). The results are benchmarked with the available theoretical and experimental data. It is found that all the transition metal XN nitrides in the NaCl phase have negative heats of formation and are therefore thermodynamically stable. The elastic constants (C_{ij}) indicate good mechanical stability for ScN and TiN, while VN is mechanically unstable due to the negative C_{11} elastic constant. The electronic properties analysis show a metallic character in TiN and VN compounds, whereas ScN exhibits semiconducting behavior. The electron charge density analysis shows charge transfer from X to N due to their electronegativity. These XN (X = Sc, Ti) nitrides are recommended as possible alternative for high-temperature structural applications such as coating due to their extraordinary characteristics.

PS-1.17
Heat-Reliant Carrier Transport in GaN Nanowire Wrap-Gate Transistor Yeojin Choi, Mallem S. Reddy, Yuna Lee and Sungjin An; Kumoh National Institute of Technology, Korea (the Republic of)

Understanding the carrier transport pathways in nanowires is essential for developing next-generation nanoscale devices. Here, we investigate the effect of temperature on the characteristics of top-down-fabricated GaN nanowire wrap-gate transistors (WGTs). Up to 240 K, the anticipated conductance of this transistor is nearly constant; beyond that, it increases as the temperature rises. When the temperature rises at gate voltages below the threshold (Vgs < Vth), this is accurate. When the temperature rises and the gate voltage is Vth < Vgs < VFB, there are sharp oscillations. Once the gate bias is increased to Vgs > VFB, the conductance gradually drops with temperature. These observations may be explained by processes related to impurity and phonon scattering that take place on the surface or core of GaN nanowires.

PS-1.18
Growth and Characterization of n-type β-Ga_2O_3 Films on Sapphire Substrates by APMOVPE Shun Ukita, Takeyoshi Tajiri and Kazuo Uchida; The University of Electro-Communications, Japan

β-phase gallium oxide (β-Ga_2O_3) has garnered significant attention due to its ultra-wide bandgap energy, coupled with outstanding electrical and optical properties. These attributes make it promising for applications such as high-power electron devices and deep ultraviolet (DUV) optical devices. The growth of β-Ga_2O_3 has been extensively explored, achieving single bulk crystal production through the melt growth method[1]. The properties of thin films have also been investigated using heteroepitaxy and homoepitaxy growth methods, including metal organic vapor phase epitaxy (MOVPE)[2].
Among its notable properties, transparency up to DUV[3] and high n-type conductivity[4] make it suitable for a transparent conductive layer (TCL) in DUV LEDs. Our previous work on ZnO TCL for AlGaN UV LEDs confirmed ZnO's effectiveness for current injection but revealed unavoidable light absorption[5]. In pursuit of this application, we employed n-type β-Ga_2O_3 as a TCL for AlGaN UV LEDs, studying its growth on sapphire substrates and characterizing its properties. Heteroepitaxial growth on sapphire substrates was chosen due to its crystal structure similarity to AlGaN UV LEDs. While most β-Ga_2O_3 growth has employed MOVPE at low pressure to suppress parasitic reactions in gas phases, there are limited reports on β-Ga_2O_3 growth using atmospheric pressure MOVPE (APMOVPE)[6]. APMOVPE offers versatility as it eliminates the need for pressure control during growth, making it a simple and cost-effective system. In this work, we grew n-type β-Ga_2O_3 films on sapphire substrates using APMOVPE and reported their electrical and optical properties.
For β-Ga_2O_3 growth, we used APMOVPE system featuring a horizontal two-flow homemade chamber. Trimethylgallium (TMGa) and O_2 gas served as Ga and O precursors, respectively. Tetraethoxysilane (TEOS) was employed for Si doping to achieve n-type conductivity. N_2 gas served as the carrier gas for all precursors. The growth rate of undoped films was investigated for different growth temperatures from their cross-sectional scanning electron microscope observation. The rate increased with heater temperature, reaching over 6 nm/min at 450°C, but began to decrease monotonically above 500°C. Below 450°C, the growth rate could be limited by the kinetics of the decomposition reaction. Conversely, above 500°C, the rate could be constrained due to parasitic reactions in the gas phases. The doping of Si to approximately 1 μm-thick β-Ga_2O_3 on (0001) c-plane sapphire substrates were carried out by changing TEOS/(TMGa + TEOS) molar ratio, with a range of 500 to 700°C for the heater temperature.
For evaluation of the deposited films, X-ray diffraction (XRD) measurements, optical transmission spectroscopy, atomic force microscopy (AFM), and Hall measurements at room temperature were conducted. In the XRD spectra of 2θ-ω scan, a diffraction peak was detected near 2θ = 18.9°, indicating that β-phase Ga_2O_3 was formed and oriented in the (-2 0 1) plane. The optical transmittance decreased rapidly below 280 nm, which is attributed to the bandgap of Ga_2O_3. AFM results showed that the RMS value was minimized at a TEOS/(TMGa + TEOS) ratio of 5%. This suggests that Si atoms act as a surfactant, leading to smoother surfaces. Hall measurements confirmed n-type conductivity in samples with TEOS/(TMGa + TEOS) ≥ 5% and growth temperatures above 600°C. This

suggests that TEOS decomposes at high temperature, allowing Si atoms to be activated as dopant. These results validate the successful growth of n-type β-Ga_2O_3 films on sapphire substrates using our APMOVPE method.

References:
[1]. M. Higashiwaki, AAPPS Bull. **32**, 3 (2022).
[2]. A. F. M. Anhar Uddin Bhuiyan *et al.,* J. Appl. Phys. **133** 211103 (2023).
[3]. M. Orita *et al.,* Appl. Phys. Lett. **77**, 4166–4168 (2000).
[4]. Marko J. Tadjer *et al.,* ECS J. Solid State Sci. Technol. **8** Q3187 (2019).
[5]. S. Ukita *et al.,* AIP Advances **13**, 095324 (2023).
[6]. V. Gottchalch *et al.,* Phys. Status Solidi A **206**, 2 (2009).

PS-1.19

Wafer Scale Deposition of Large Domain Size WS_2 Flake by MOCVD with GN2 Carrier Gas Kuan Ning Huang[1], Cheng Huang Kuo[2], Chao Hsin Chien[1] and Edward Yi Chang[1,1]; [1]National Yang Ming Chiao-Tung University, Taiwan; [2]National Yang Ming Chiao Tung University, Taiwan

It's well know that thin two-dimensional (2D) materials have great potential to be post silicon channels of logic devices. Especially, tungsten disulfide (WS_2) as a good candidate to be the channel material [1-2]. It was found that WS_2 have the small effective masses in both the n and p branches make WS_2 ideal for the high-performance CMOS logic applications. It have been demonstrated for the growth of WS_2, such as chemical vapor deposition(CVD)[3], metal–organic chemical vapor deposition (MOCVD)[4-5], ALD[6]. Generally, MOCVD offers superior scalability for various wafer size and good uniformity. C-face (0001) sapphire has been used for 2D material growth owing to its crystalline nature. In this study, we investigate the effects of varying sulfur concentrations of the buffer layer and change the carrier gas during lateral growth to prepare the large domain size of WS_2 flake.

The WS_2 samples used in this study were all grown on C-face (0001) 6-inch sapphire substrates in a MOCVD system. Details of the growth procedures could be found elsewhere [7]. During the growth, tungsten hexacarbonyl [$W(CO)_6$] and di-tert-butyl sulfide (DTBS), were used as the source materials of W and S, respectively. N_2 serving as the carrier gas. Prior to growth, the substrate was heated up to 1050ºC to remove surface contaminations in H_2 ambient. Temperature was then reduced to around 860ºC to pre-run DTBS under the N_2 ambient in 15mins as the buffer layer. The DTBS flow is 30 sccm. We then raised the temperature to 915ºC to grow WS_2 flakes. During the lateral growth of WS_2 flakes, we kept $W(CO)_6$ flow and DTBS flow at 55 and 30 sccm in 16hrs, respectively. All of the samples were then evaluated by atomic force microscope (AFM), photoluminescence spectroscopy (PL) and Raman spectroscopy. PL and Raman spectroscopy measurement were performed with 532 nm excitation wavelength.

Firstly, the impact of changing the sulfur concentration by adjusting DTBS flow rate of the buffer layer was investigated regarding domain size of WS2 flake. AFM result shows that the domain size of WS2 flake was 250, 500, and 600 nm for buffer layer DTBS flow 30 sccm, 150 sccm, and 300 sccm, respectively. The result shows a significant improve in the domain size with increase the buffer layer DTBS flow. Raman spectra shows the characteristic fingerprint of the relative shift between the two main peaks (E_{2g} and A_{1g}), which measures 66.2 cm^{-1}. The PL emission is around 2.0 eV.

Assael Cohen et. al have been demonstrated that use a small amount of water(H_2O) vapor is introduced during the growth WS_2 by using the Growth-Etch MOCVD (GE-MOCVD)[8]. H2O was shown to etch and re-evaporate WS_2 and remove the carbon impurity from MO source. It is found that a significant domain size increase and improve quality is achieved. In this study, we replace the carrier gas from PN_2(99.9999) to GN_2(99.995). We assume that there is a small amount of H2O in GN_2. After growth, AFM result shows that the domain size of WS2 flake was 3 μm under the GN_2 carrier gas condition. The domain size was increased 5 times, compared with convention condition. Raman spectra shows the characteristic fingerprint of the relative shift between the two main peaks (E_{2g} and A_{1g}), which measures 63.8 cm^{-1}. The PL emission is around 2.0 eV.

In conclusion, we demonstrate the WS_2 samples were all grown on C-face 6-inch sapphire substrates in a MOCVD system. Under the GN_2 carrier gas ambient, domain size of WS_2 flake was 3 μm. Compared with convention condition, the domain size was increased 5 times. Such an observation can be attributed to the etch and re-evaporate growth mechanism for the GN_2 with small amount H_2O.

Reference
1. Adv. Mater. 27, 5230–5234 (2015).
2. Nat. Commun. 12, 693 (2021).
3. RSC Adv. 9, 29628–29635 (2019).
4. Nanoscale Adv. 4, 4391–4401 (2022).
5. ACS Appl. Mater. Interfaces 13(42), 50497–50504 (2021).
6. Mater. Res. Express 2, 035006 (2015).
7. Appl. Phys. Lett. 123, 183101 (2023)
8. ACS Nano 2021, 15, 1, 526–538

PS-1.20

Engineering Thermal Diffusion for High-Performance, High-Density Phase Change Memory Based on van der Waals Heterostructure Layered with MoS_2 Jun Young Choi, Ho Jin Lee, Seok Hee Hong, Seung Woo Park, Dong Hyun Kim and Tae Geun Kim; Korea University, Korea (the Republic of)

Phase change memory (PCM, PCRAM, PRAM) uses joule heat generated by the nano-heater (bottom electrode) to store data by resistance differences depending on the phase change. Among the various structures of this memory, phase change heterostructure (PCH) based on van der Waals heterostructure with a confinement material (CM) layer, a transition metal dichalcogenide (TMDC) material, is a highly utilized structure because it shows excellent characteristics compared to other structures. However, the layered TMDC materials have an inverse relationship with each other in terms of bonding strength, which measures thermal stability, and conductivity, which measures the power consumption of the structure. These inversely proportional characteristics greatly affect the electrical properties of PCH, resulting in a trade-off between low-power driving and high-durability driving. In addition, the biggest problem with PCM (including PCH) is thermal

crosstalk. When implemented as an array, the isotropic thermal diffusion of the joule heat generated during driving causes thermal interference to the neighboring devices, degrading the excellent performance of a single device. In this study, we fabricated PCH based on [MoS_2/Sb_2Te_3]n to solve the above problems through anisotropic thermal diffusion. Since phase change materials generally have a positive Seebeck coefficient, this structure is a layered structure in which MoS_2 (3-5 layers) with a negative Seebeck coefficient is sequentially layered with a phase change material (Sb_2Te_3) so that a difference in the Seebeck coefficient occurs at the interface of each material. In addition, the difference in potential at the interface is formed by the difference in the work function of each material according to the MoS_2 layer, and the carrier filtering effect caused by this difference improves the mobility of carriers in the device, thereby improving the conductivity. The device structure of this study confirms that thermal diffusion is possible from isotropic to anisotropic within the device by the difference in the Seebeck coefficient of each material and the carrier confinement by carrier filtering. At the same time, the thermoelectric effect and mobility enhancement increase the efficiency of the joule heat generated by the nano-heater. As a result, we propose a new type of PCH that exhibits low-power driving and fast switching characteristics while exhibiting high durability by solving the problem of low conductivity of the CM layer with high thermal stability and suggest the possibility of ultra-high-density arrays without thermal crosstalk through anisotropic thermal diffusion.

PS-1.21
MOCVD Growth of $MoS_{2x}Te_{2(1-x)}$ / MoS_2 van der Waals Heterojunctions for Ultra Thin Photovoltaic Applications
Dong Hyun Seo[1,2], Guen Hyung Oh[1,2], Jong Min Song[1,2] and TaeWan Kim[1,2]; [1]Jeonbuk National University, Korea (the Republic of); [2]2D Epi, Inc, Korea (the Republic of)

Van der Waals Heterojunctions based on two-dimensional (2D) transition-metal dichalcogenides (TMD) materials have become prominent in the field of optoelectronic devices, drawing considerable attention for applications in light-emitting devices, photodetectors, solar cells, and beyond. We transferred thin films consisting of compositionally graded ternary $MoS_{2x}Te_{2(1-x)}$ alloys onto molybdenum disulfide (MoS_2) grown by metal-organic chemical vapor deposition, serving as p- and n-type layers. This process resulted in the formation of a van der Waals vertical heterostructure. We investigated the photovoltaic characteristics of the fabricated $MoS_{2x}Te_{2(1-x)}$ / MoS_2 heterojunctions, focusing on the influence of tellurium (Te) incorporation. Notably, the power conversion efficiency (PCE) exhibited a remarkable increase, showing an enhancement of approximately six orders of magnitude with an increasing Te concentration. A particularly noteworthy achievement was a photoresponsivity as high as ~ 6.4 A/W. These results underscore the potential for significantly improving ultra-thin solar energy conversion in heterojunctions based on 2D TMDs.

PS-1.22
Wafer-Scale MOCVD Growth of MoS_2 Semiconductor Using Organic Chalcogen Precursor—Tailoring Electrical Properties
Jong Min Song[1,2], Guen Hyung Oh[1,2], Dong Hyun Seo[1,2], Ji Won Heo[1,2], Jin Hoo Seong[1] and TaeWan Kim[1,2]; [1]Jeonbuk National University, Korea (the Republic of); [2]2D Epi, Inc, Korea (the Republic of)

The synthesis of large-area, high-quality molybdenum disulfide (MoS_2) films grown by metal-organic chemcial vapor deposition (MOCVD) is attracting considerable attention owing to their widespread application in industrial optoelectronics, nanoelectronics, and flexible devices. Despite this interest, the precisely controlling the growth of a MoS_2 films remains a challenge, specifically in terms of atomic layer number, growth rate, and modulation of electrical properties. In this study, we achieve the wafer-scale growth of a few-atomic-layer MoS_2 thin films on SiO_2/Si wafer, using diethyl sulfide (DES) and Molybdenumhexacarbonyl (MHC) precursors. Exploring organic chalcogen precursors is directed towards identifying a safer alternative to the highly hazardous chalcogen hydrides. The characteristics of MoS2 films are determined by Raman spectroscopy, Photoluminescence, and X-ray Photoelectron Spectroscopy. We investigate the impact of growth conditions, including the DES/MHC ratio, ambient gas ratio, and growth pressure, on the optical and electrical properties of MoS2 films.

PS-1.23
Characterization of MOVPE Grown n-GaN for Re-Al-X-Au Based Ohmic Contacts—Effect of Barrier Layer (X = Re, Mo, Ni, Ti & Pd)
Amit P. Shah, Bhagyashree A. Chalke, A A. Rahman and Arnab Bhattacharya; Tata Institute of Fundamental Research, India

We report the effect of the barrier layer metal for the ohmic contacts on MOVPE grown n-GaN using Re-Al-X-Au (X = Re, Mo, Ni, Ti and Pd) on the electrical and microstructural characteristics. The Si-doped n-type GaN epilayers of 2 µm thickness were grown by metal-organic vapor phase epitaxy (MOVPE). Trimethyl gallium (TMGa) and ammonia (NH_3) were used for the growth of thhe epilayer, while silane (SiH_4) was used for n-type doping. The n-GaN samples had an electron density of around 6 x 10^{18} cm^{-3} and mobility of around 180 cm^2/Vs. Several samples of (Re-Al-X-Au : 30-100-60-100 nm) with different barrier layer metal X (Re, Ni, Mo, Ti and Pd) were prepared and annealed at 700°C temperature. The specific contact resistivity (ρ_c) was estimated using C-TLM measurements while AFM, GI-XRD and SEM equipped with EDS were used to analyze the chemical composition and microstructures of the contacts.
From C-TLM measurements of total resistance as a function of gap spacing on samples having barrier layers Re, Mo, Ni, Ti and Pd; ρ_c values were obtained. The annealing temperature was 700°C, chosen from our earlier results on Re-Al-Ni-Au contacts where we had observed the lowest specific contact resistivity [1]. The ρ_c values obtained for Ni is <10^{-7} Ω-cm^2, while for Re and Mo, the values are ~ 10^{-6} Ω-cm^2 and for Ti and Pd, the values are ~ 10^{-7} Ω-cm^2.
AFM images (40 µm x 40 µm) of the surface morphology of

Re-Al-X-Au ohmic contacts for all the barrier layers (Re, Mo, Ni, Ti and Pd) respectively were obtained for all samples annealed at 700ºC. We observed a smooth surface morphology for the barrier layers, Re and Mo; while Ti-based sample showed numerous small islands of sub-micron dimensions. The Ni-based sample showed larger sized islands of size around 2-3 μm (Al-Ni agglomerates as reported in [2]). However, the Pd-based sample showed individual islands of 1-2 μm size, accumulating in groups of islands of the size about 10 μm. The average surface RMS roughness for Re, Mo, Ni, Ti and Pd samples were 44, 60, 130, 73 and 211 nm respectively. All the samples showed sharp edge acuity.
Elemental scans (scan area of 36 μm x 27 μm) for Ga, Re, Al, (X = Re, Mo, Ni, Ti or Pd) and Au using the energy dispersive spectroscopy (EDS) measurements were carried out on all the samples to observe the distribution of various elements within the annealed contact metal stacks.
Grazing incidence x-ray diffraction (GI-XRD) characterization on different barrier layers showed various orientations of different metal alloys like Al-Au, Al-Re, Re-Ga, Re-N which are common for all samples. Apart from these, various orientations of Al-Re, Al-Mo, Al-Ni, Al-Ti and Al-Pd (Al alloys of Re, Mo, Ni, Ti and Pd) were observed.
Our study shows that nickel provides the best diffusion barrier for Re-based ohmic contacts on n:GaN.
References:
[1] A. P. Shah, B. A. Chalke, V. J. Mhatre and A. Bhattacharya, *J. Appl. Phys.* 132, 075701, (2022).
[2] A. P. Shah, B. A. Chalke, J. B. Parmar, M. B. Ghag and A. Bhattacharya, Accepted for publication in *"Applied Research"* (2024).

ICM VPE XXI

2024 Las Vegas, NV

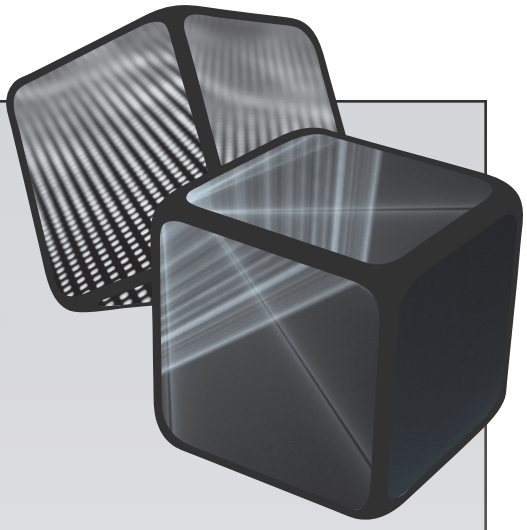

WEDNESDAY

Oral Presentations

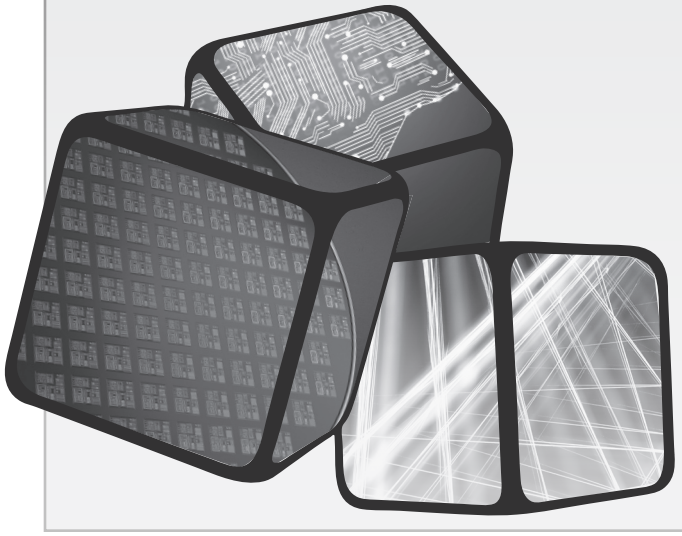

21st International Conference on Metal Organic Vapor Phase Epitaxy

SESSION 3A-1: III/V Epitaxy for Devices
Session Chair: Qiang Li
Wednesday Morning, May 15, 2024
Resort Tower, Ground Level, Bronze Room 1

8:20 AM 3A-1.1
Emerging Technology for Future VCSELs Wlodek Strupinski[1], Walery Kolkowski[1], Iwona Pasternak[1], Tomasz Czyszanowski[2], Marcin Gebski[2], Weronika Glowadzka[2], Patrycja Spiewak[2], Michal Wasiak[2], Marcus Miller[3], Philipp Gerlach[3], Roland Jäger[3], Pieter Verhulst[4], Guillaume Courtois[5], Alexandre Amoult[6], K.Ben Saddik[6] and Guilhem Almuneau[6]; [1]VIGO Photonics SA, Poland; [2]Lodz University of Technology, Poland; [3]PMDindustrial GMBH, Germany; [4]Xenomatix, Belgium; [5]Umicore, Belgium; [6]LAAS-CRNS, France

The global VCSEL (vertical-cavity surface-emitting laser) market is developing dynamically, with laser production projected to triple in the next five years. One of the driving forces behind this growth is VCSEL's wide application in the photonics industry, including short-distance communication systems, LIDARs, time-of-flight sensors, autonomous vehicles, robots, and drones. In this work, we present the epitaxial growth by MOVPE of VCSEL epi-structures grown on GaAs for various applications and a novel VCSEL epi-structure using germanium (Ge) substrates instead of traditional gallium arsenide. The critical challenge in this development is to achieve high crystal quality of grown GaAs/AlGaAs layers on Ge substrates while taking advantage of a better crystallographic lattice sameness between Ge and AlGaAs, which reduces misfit defects density and increases the quantum efficiency of the device. Germanium, offering higher yield and fewer production losses due to higher uniformity at larger-size wafers, is promised to lower the environmental impact compared to more expensive GaAs substrate. With the demand for VCSELs growing and technical requirements becoming more rigorous, there is a need to scale to larger wafer diameters and demonstrate a path for integration with CMOS technology.
These epitaxial technological efforts, with particular attention paid to the growth mechanism of nucleation layer bridging Ge substrate with GaAs/AlGaAs epi-stack, were supported by several characterization methods to be used as X-ray diffraction and topography, depth high-resolution SIMS, electron microscopy (SEM/TEM), atomic force microscopy, Nomarsky optical microscopy, PL mapping, ECV, Hall, optical spectroscopy, reflectance, epi-wafer bowing measurements. The aim was to discover differences and critical parameters of VCSEL structure grown on Ge substrates versus GaAs at the material characterization level and to develop and produce VCSELs ready for use in the demonstrators. The VCSEL/Ge device epi-technology developed at VIGO Photonics is industrial-oriented for mass production on up to 6-or 8-inch Ge wafers, offering different architecture configurations in relation to the specifications of the targeted applications.
The goal is to meet the demand of the constantly growing photonics market by providing a novel solution that will increase production yield, reduce defectivity, and introduce reduced environmental impact. Moreover, the project findings can be developed into usable tools bringing innovative change across various end-user industries (e.g., automotive, smartphone, 3D sensing technologies, and others).

8:40 AM 3A-1.2
VECSEL Active Regions for High Output Power at Wavelength Around 750 nm Michael Jetter, Rebecca Rühle, Marius Grossmann, Sergej Vollmer and Peter Michler; University of Stuttgart, Germany

Vertical external-cavity surface-emitting lasers (VECSELs) in the deep-redwavelength range between 700 nm and 800 nm have recently received much attention due to various applications such as in photodynamic therapy, atom cooling, quantum technologies and spectroscopy. A VECSEL is suitable for such applications, mainly due to the high output power in a fundamental transverse mode and its external cavity, which allows incorporation of additional elements such as etalons for single-frequency emission or birefringent filters for wavelength tuning. Emission in the 700–800 nm range can be achieved with AlGaAs quantum wells (QWs) which can be readily grown on GaAs substrates. Another alternative is the aluminum-free InGaAsP QW that can be grown lattice-matched to GaAs.
Both alternatives have either from the operational or the growth point of view some drawbacks. The Al containing active regions suffer from increased oxidation at shorter wavelengths and an overall reduced lifetime. In the quaternary InGaAsP system instead a process parameter range is present where InxGa1−xAsyP1−y mixtures decompose into InAs and GaP-rich regions.
In this contribution we present the metal–organic vapor-phase epitaxy (MOVPE) growth of AlGaAs and InGaAsP active regions for optically pumped VECSEL. Especially with the InGaAsP quantum wells different active regions were deposited and the performance of the lasers were evaluated. In both material systems Watt-level output power could be achieved.

9:00 AM 3A-1.3
InP Plasmonic DBR for the New Class of Vertical Cavity Lasers Mikolaj Badura[1], Mikolaj Janczak[2], Tomasz Czyszanowski[2], Adriana Lozinska[1], Damian Radziewicz[1], Wojciech Dawidowski[1], Monika Mikulicz[1], Michal Rygala[1], Marcin Motyka[1] and Beata Sciana[1]; [1]Wroclaw University of Science and Technology, Poland; [2]Lodz University of Technology, Poland

Mid-infrared optoelectronic devices, crucial for diverse applications like thermal imaging, free space communication, LIDAR systems, and gas detection, heavily rely on interband cascade and quantum cascade active regions within the 4 to 10

μm wavelength range. Among the various configurations, surface emission and detection are favored for their advantages, including low beam divergence, near-Gaussian beam distribution, and ease of integration.
A critical component in these configurations is the distributed Bragg reflector (DBR), traditionally facing challenges in materials like AlGaAs and AlGaSb, marked by lattice mismatch and electrical conductivity issues. As a response to these challenges, we present a novel design for highly reflective mid-infrared DBRs, leveraging a monolithic InP structure with doping modulation.
Our proposed design stands out for its lattice-mismatch-free nature and inherent electrical conductivity. The absence of interfaces eliminates Schottky junctions, allowing for precise control over layer thicknesses with varying doping concentrations. This innovative approach not only simplifies the growth process but also eradicates critical thickness limitations, ensuring the structural integrity of the device.
Taking into account classical material systems, like AlGaAs and AlGaSb, matching lattice constants and high refractive index contrast make them suitable for near and mid-infrared applications. Despite their efficacy, extensive research explores alternative materials, such as InP, aiming to achieve lattice matching with other systems. However, even for lattice-matched materials, mid-infrared devices pose additional challenges, with the required total DBR thickness exceeding the critical thickness of the stack, leading to defects and mechanical instability.
To overcome these challenges, usage of the features of semiconductors in the mid-infrared range, where variations in the refractive index, induced by free carriers' collective oscillations, known as plasmons, become prominent. Our design exploits this variation in the complex refractive index, achieved by modulating free electron concentration. Unlike conventional DBRs, our approach is not constrained by lattice-match requirements, providing both electrical conductivity and lattice-mismatch-free characteristics.
In conclusion, our proposed design for mid-infrared DBRs using a monolithic InP structure with doping modulation not only addresses existing challenges but also opens new possibilities for the advancement of optoelectronic devices in the mid-infrared spectrum. The innovative use of semiconductor properties introduces a versatile solution, promising enhanced performance and reliability in various applications.

Acknowledgement
This work was co-financed by: the Polish National Science Centre under the project OPUS-17 No. 2019/33/B/ST7/02591; the Polish National Centre for Research and Development grant No. TECHMATSTRATEG1/347510/15/NCBR/2018 “SENSE″; the Polish National Agency for Academic Exchange under the contract BPN/BSK/2023/1/00040 and Wroclaw University of Science and Technology subsidy.

9:20 AM 3A-1.4
Accelerated Raw-Material Utilization-Efficiency of GaAs Using Vertical Flow Type, Single-Chamber Hydride Vapor Phase Epitaxy Ryuji Oshima[1], Guanxi Piao[2], Yasushi Shoji[1], Kikuo Makita[1], Akinori Ubukata[2], Shuichi Koseki[2] and Takeyoshi Sugaya[1]; [1]National Institute of Advanced Industrial Science and Technology, Japan; [2]Taiyo Nippon Sanso, Japan

III-V multijunction solar cells have demonstrated potential for exceptionally high conversion efficiency. These technologies can open new applications, such as use in mobility and transportation systems in addition to the applications already in use today. However, one obstacle for implementing such solar cells is their high manufacturing cost. As hydride vapor-phase epitaxy (HVPE) is a high-speed growth technique using less expensive group III precursors, such as GaCl, InCl, and $AlCl_3$, it would be a possible pathway to lower the cost of III–V devices. We previously developed 2-inch, a vertical flow-type, atmospheric pressure HVPE with triple growth chambers [1] and demonstrated GaAs solar cells grown at 200 mm/h with 24.0% in conversion efficiency [2]. However, a GaCl utilization efficiency was calculated to be as low as 46%. In order to further reduce growth costs, both scalability and raw material utilization efficiency need to be improved. For this reason, we have recently been developing a vertical HVPE system that can mount one 6” wafer. This HVPE is equipped with a run/vent switching parts within the reactor, allowing for heteroepitaxy using a single growth chamber. Furthermore, in order to supply uniform gas to the growth surface, we introduced both a showerhead and high-speed substrate rotation of up to 1000 rpm. When GaAs was grown on 6” GaAs(001) under atmospheric pressure at 660 °C with a GaCl partial pressure of 6.6×10^{-3} atm and V/III ratio = 3, the growth rate was significantly increased from 45 mm/h for 60 rpm to 200 mm/h for 500 rpm. This was because the boundary layer becomes thinner due to high-speed rotation. As a result, we improved a GaCl utilization efficiency to larger than 80% for 500 rpm from that of 18% for 60 rpm. This is a groundbreaking achievement for the mass production of low-cost III-V solar cells. [1] R. Oshima et al., Jpn. J. Appl. Phys. 57, 08RD06 (2018). [2] R. Oshima et al., Crystals, 13, 370 (2023).

9:40 AM 3A-1.5
III-V Metamorphic Buffer Layers on Ge Substrates—MOVPE Growth and Structural Investigation Elisabetta Achilli[1], Nicola Armani[1], Marco Calicchio[1], Giovanni Abagnale[1], Erminio Greco[2], Roberta Campesato[2], Fabio Pezzoli[3], Jacopo Pedrini[3] and Gianluca Timò[1]; [1]Ricerca sul Sistema Energetico RSE, Italy; [2]CESI S.p.A., Italy; [3]L-NESS and Università degli Studi di Milano-Bicocca, Italy

The increase in population density in big cities has boosted the efforts aimed at meeting the subsequent growth in energy demand. Amongst the different technologies, PV has attracted much attention for the power and inexhaustibility of its source but represents a major challenge because of the lack of available space on the roofs and the cost of land in metropolitan areas. The purpose of this work lies in the

investigation of materials for solar cell buffers to be integrated in a highly performant and ultra-light versatile modules. In particular, the attention is focused on III-V based layers with variable composition grown on Ge substates. With respect to traditional InGaP/InGaAs/Ge cells, in the *bottom cell*, Ge is replaced by a III-V alloy so that Ge substrate can be removed and reused. This path would lead to the double advantage of allowing substrate recicling and obtaining lighter devices. Preliminary research was carried out by growing and investigating III-V based samples deposited in a MOCVD reactor. Buffers were obtained upon varying parameters concerning both content and growth conditions. Specifically, we explored the sample characteristics by modifying: *(i)* composition to obtain a graded metamorphic layer; *(ii)* the material type as nucleation layer (AlGaAs or InGaP); *(iii)* doping level (by adding tellurium); *(iv)* substrate crystallographic orientation and *(v)* deposition parameters. A comprehensive study was carried out to investigate physic-chemical, morphological and electro-optical properties. HRXRD provided information about the crystallographic properties, composition and thickness while RSMs allowed to study tilt and stress. From a chemical point of view, µ-Raman addressed alloying and homogeneity. Furthermore, thanks to AFM, it was possible to obtain insights about roughness and defects (dislocations). Eventually, we studied electro-optical properties by photoluminescence and reflectivity. Using an AlGaAs nucleation film, we deposited a double layer of InGaAs with increasing In content along the growth direction. This gave rise to a high-quality metamorphic domain. Doping, necessary for a future realization of high-efficiency PV devices, was evaluated by introducing tellurium in the compound semiconductor and demonstrated that Te neither affects the structural parameters nor degrade the materials quality. To reduce defects in metamorphic epitaxial layers, we should consider growth surfaces, since different crystallographic orientations result in different symmetry and energy properties which, in turn, can affect the early stages of layers deposition and the final device properties. In this regard, the increase in Ge substrate miscut up to 9 ° was found to affect both the surface morphology and the order-disorder ratio of the InGaP layers grown on top of the nucleation layer. In addition, a tilt of the alloy with respect to the substrate was highlighted. Another important aspect to investigate is the nucleation layer on Ge substrate which might change the atomic steps on the surface of epitaxial layer. In the following step of this research, the attention was shifted to an alternative to AlGaAs nucleation layer: InGaP alloy. Its direct deposition on Ge is challenging because different growth parameters of InGaP nucleation layer might affect the surface morphology and its roughness (*e.g.* temperature bake before growth for depleting the reactor of volatile contaminants, sufficient overpressure of phosphine from the start of the process to avoid the effects of desorbed species). In this case, an In-rich layer with a *ca.* 46.5% degree of relaxation was obtained. Eventually, simulations were carried out to estimate materials critical thicknesses with the final aim of an optimized graded buffer domain with In molar fractions up to 15%. These findings represent an important outcome for III-V compound semiconductor properties and pave the way towards a sustainable and successful solution for BIPV.

10:00 AM BREAK

SESSION 3A-2: hBN and Related Epitaxy
Session Chairs: Hongxing Jiang and Jingyu Lin
Wednesday Morning, May 15, 2024
Resort Tower, Ground Level, Bronze Room 2

8:20 AM 3A-2.1
High-Quality, Wafer-Scale Epitaxial Boron Nitride as a Platform for Applications in Optoelectronics Aleksandra K. Dabrowska, Mateusz Tokarczyk, Johannes Binder, Jakub Iwanski, Rafal Bozek, Grzegorz Kowalski, Roman Stepniewski and Andrzej Wysmolek; University of Warsaw, Poland

Boron nitride (BN) in its sp^2-hybridized structure belongs to the group of so-called two-dimensional materials. It is also a member of the III-nitrides family, which comprises classical compounds that underpin today's optoelectronics. The most important properties of BN are its layered structure, wide bandgap (about 6 eV), and resistance to harsh environmental conditions [1] making it a very desirable material in modern optoelectronics, especially in the deep ultraviolet (DUV) range [2]. Today's devices are fabricated on micrometer-sized flakes, which are suitable for prototyping purposes, but the repeatability and scalability of such a solution in mass production are questionable.

Our research group has worked intensively on the development of the growth of sp^2-BN by Metal Organic Vapor Phase Epitaxy (MOVPE) on two-inch sapphire wafers. It allowed us to obtain valuable information about the growth mechanisms [3] paving the way for the fabrication of high-quality epitaxial layers with very good optical and structural properties [4,5].

In this communication, I will discuss the influence of the substrate and pre-growth procedures on the quality of the resulting material. I will show that a two-stage growth mode [4] and the use of different substrate c-plane off-cut angles [5] are crucial for improving the growth quality at the beginning of the process, which in turn determines the quality of the entire layer. Improving the nucleation on the substrate has made it possible to obtain an exceptionally smooth, uniform layer with a lattice constant of 3.35 Å, close to the literature value expected for hexagonal boron nitride and an E_{2g} line in Raman spectra with half-width below 20 cm^{-1}, which is an excellent value for BN grown by MOVPE [4,5]. Correlations between initial growth conditions (temperature, carrier gas, etc.), sapphire substrate off-cut angle, and preparation before the growth will be discussed.

The high quality of our hBN has enabled its utilization e.g. as a substrate for monolayer $MoSe_2$ growth [6] and for structures

that visualize hydrogen generation [7]. The scalability, reproducibility, financial viability, speed, and ease of MOVPE-based large-area BN production will make it a promising candidate for different applications in the future.

This work was supported by the National Science Centre, Poland, under decisions 2019/33/B/ST5/02766 and 2020/39/D/ST7/02811 and by Excellence Initiative Research University, under decision BOB-IDUB-622-639/2023.
[1] E. Naclerio and P.R. Kidambi, *Adv. Mater*. **35**, 2207374 (2023)
[2] SB. Song et al., *Nat Commun* **12**, 7134 (2021)
[3] K. Pakula et al., arXiv: 1906.05319 (2019)
[4] A.K. Dabrowska et al., *2D Mater*. **8** 015017 (2021)
[5] M. Tokarczyk et al., *2D Mater.* **10** 025010 (2023)
[6] K. Ludwiczak et al., *ACS Appl. Mater. Interfaces* **13** 47904–11 (2021)
[7] J. Binder et al., *Nano Lett.* **23**, 4, 1267–1272 (2023)

8:40 AM 3A-2.2
Epitaxial Growth of hBAlN Alloys—Tuning the Crystal Structure and Optical Properties Jakub Iwanski[1], Mateusz Tokarczyk[1], Aleksandra K. Dabrowska[1], Krzysztof Korona[1], Guillaume Cassabois[2], Bernard Gil[2], Johannes Binder[1] and Andrzej Wysmolek[1]; [1]University of Warsaw, Poland, Poland; [2]Université de Montpellier, France

The potential for effective sterilization using deep ultraviolet light (DUV, 200-280 nm, 4.4-6.2 eV) serves as a compelling incentive for advancing semiconductor light sources within this spectral range. However, the current semiconductor technology predominantly relies on AlGaN-based structures, resulting in a limited efficiency for DUV light sources (typically only a few percent) [1]. A promising solution for this problem would be the utilization of high-quality hexagonal boron nitride (hBN) [2], [3], exhibiting a bandgap energy similar to AlN (~6 eV). Despite its indirect bandgap, this two-dimensional (2D) layered material demonstrates efficient photoluminescence, surpassing AlN by two orders of magnitude [4]. The advantage of alloying of high-quality hBN with other elements - such as aluminum - offers the potential to tune bandgap properties, including transition from indirect to direct bandgap for certain compositions [5], [6]. This would result in creating an effective DUV emitter with a hexagonal, sp^2-bonded crystal structure. However, very limited knowledge regarding the epitaxial growth of $hB_{1-x}Al_xN$ hinders the attainment of the material with desired properties, emphasizing the crucial need for systematic exploration in this field. It is primary important to understand the procedures for effective growth of sp^2-bonded $hB_{1-x}Al_xN$ alloys, especially considering the current reliance on AlGaN-based technology.

Within this research, we grew a series of hBAlN samples on sapphire substrates using an Aixtron CCS 3x2" MOVPE system. During the growth process NH_3, TEB, and TMAl were used as nitrogen, boron, and aluminum precursors, respectively. Various growth parameters, including temperature, precursor flows, and growth protocols, were investigated. Two specific growth regimes were explored: continuous flow growth (CFG) and flow modulation epitaxy (FME), with different precursor injection schemes. All samples maintained a layered, sp^2-bonded crystal structure.

The hBAlN layers obtained underwent in-depth characterization, including X-Ray Diffraction, Scanning Electron Microscopy, UV-Vis, Photoluminescence, and Fourier-transform infrared spectroscopies. This detailed analysis enabled us to establish correlations between the material properties and growth conditions. In the presentation, we will show that the CFG growth protocol should not be applied for such alloy since it leads to the creation of misoriented flakes in random directions. In contrary, FME provides flat, two-dimensional morphology. We show that changing the sequence of precursor injection allows to control the growth rate, the migration of Al on the surface and to limit parasitic reactions. The injection sequence appears to be very important for obtaining a high-quality crystal structure and elimination of AlN clustering. Most importantly, by adjusting growth conditions we were able to tune the bandgap energy of the hBAlN alloys as well as its indirect/direct character. The obtained results allow to discuss challenges and opportunities of MOVPE growth of hBAlN and its applications.

[1] H. Amano *et al.*, *J Phys D Appl Phys*, vol. 53, no. 50, p. 503001, Sep. 2020, doi: 10.1088/1361-6463/ABA64C.
[2] A. K. Dabrowska *et al.*, *2d Mater*, vol. 8, no. 1, 2020, doi: 10.1088/2053-1583/abbd1f.
[3] M. Tokarczyk *et al.*, *2d Mater*, vol. 10, no. 2, 2023, doi: 10.1088/2053-1583/acb44a.
[4] A. Maity, *et al.*, vol. 76, no. November 2020, 2021, doi: 10.1016/j.pquantelec.2020.100302.
[5] Q. Zhang *et al.*, *Appl Surf Sci*, vol. 575, p. 151641, 2022, doi: 10.1016/j.apsusc.2021.151641.
[6] J. Iwanski *et al.*, May 2023, [Online]. Available: http://arxiv.org/abs/2305.15810

9:00 AM 3A-2.3
MOVPE van der Waals Epitaxial Growth of Hexagonal Boron Nitride and its Applications Suresh Sundaram[1,2,3], Phuong Vuong[2], Vishnu Ottapilakal[2], May Tran Thi[2], Rajat Gujrati[2], Ashutosh Srivastava[2], Tarik Moudakir[4], Simon Gautier[4], Paul L. Voss[1,2], Jean Paul Salvestrini[1,2,3] and Abdallah Ougazzaden[1,2]; [1]Georgia Institute of Technology, France; [2]CNRS, France; [3]GT Europe, France; [4]Institut Lafayette, France

Wafer-scale growth of high quality two dimensional (2D) materials with possible integration with existing III-nitrides and other conventional devices have recently attracted lots of interest [1, 2]. Especially, h-BN, a 2D wide bandgap nitride semiconductor has several advantages, one of them being that it can be grown in the same MOVPE reactor as other III-nitrides, leading to facile integration avoiding contamination and reproduciblity issues. Here we report, exploration of this h-BN 2D material system by MOVPE van der Waals eptaxial growth and successful demonstration of its integration with other III-nitride devices [3]. Especially, characteristics of the light emitting diodes grown on h-BN/sapphire which can be

peeled off from the sapphire susbtrates, preserving the phyical properties and vertically integrated among other color LEDs for realization of full color micro-LEDs display will be discussed [4]. Finally, controllable growth of this 2D materials on dielectric patterned substrates leading to selective area growth of III-nitride based device arrays will be presented [5]. This growth experiment on dielectric patterned sapphire gives a very important insight on the evolution of h-BN which will be discussed as a path forward to solve the critical issues in free standing/indivually addressable, thin and flexible devices.

References:

1. X. Li, S. Sundaram, Y. El Gmili, T. Ayari, R. Puybaret, G. Patriarche, P. L. Voss, J. P. Salvestrini, A. Ougazzaden, Cryst. Growth Des. 2016, 16, 3409.
2. T. Ayari, S. Sundaram, X. Li, Y. El Gmili, P. L. Voss, J. P. Salvestrini, A. Ougazzaden, Appl. Phys. Lett. 2016, 108, 171106.
3. P.Vuong, T. Moudakir, R. Gujrati, et. al., *Adv. Mater. Technol.,* 2023, 2300600, 1–7.
4. J. Shin, H. Kim, S. Sundaram, et. al., *Nature*, 2023, 614, 81.
5. R. Gujrati, A. Srivastava, P. Vuong, et. al., *Adv. Mater. Technol.,* 2023, 2300147, 1–10.

9:20 AM 3A-2.4
Selective Epitaxial Growth of High-Quality hBN on Epigraphene Patterns Using MOVPE Vishnu Ottapilakkal[1], Abhishek Juyal[1], Suresh Sundaram[1,2,3], Phuong Vuong[1,2], Adama Mballo[1], Lin Beck[3], Grant H Nunn[3], Annick Loiseau[4], Frederic Fossard[4], Jean-Sebastien Merot[4], David Chapron[5], Thomas H Kauffmann[5], Jean Paul Salvestrini[1,3,2], Paul L. Voss[1,3], Walter A. de Heer[3], Claire Berger[1,3] and Abdallah Ougazzaden[2,3]; [1]IRL Georgia Tech - CNRS, France; [2]Georgia Tech Europe, France; [3]Georgia Institute of Technology, United States; [4]Lab. d'Etude des Microstructures, ONERA-CNRS, Universite Paris Saclay, France; [5]Lab. Materiaux Optiques, Photonique et Systèmes, Universite de Lorraine & CentraleSupelec, France

Hexagonal boron nitride (hBN) is effective in protecting the electronic properties of graphene from environmental effects by serving as a passivation layer[1]. Unlike the widely used mechanical transfer method for BN on graphene, metal-organic vapor phase epitaxy (MOVPE) enables the direct growth of epitaxially aligned hBN on epigraphene with complete coverage and scalability to large substrate with excellent interface quality.[2] However, the presence of surface contaminants and step edges can cause nucleation of crumpled BN, which may in turn cause inhomogenity in the electrical properties of epigraphene based devices.[2] To address this issue, a potential solution is to avoid the areas with crumbled BN during device fabrication. In this context, we use a selectively area growth approach with MOVPE to grow high-quality hBN over epigraphene patterns.
Here, we demonstrate high-quality hBN growth on epigraphene by a two-step approach. Epigraphene was first selectively etched to keep only graphene structures of the desired/needed device geometry before hBN was grown on the whole sample. This two-step method is a reverse approach compared to the conventional patterning of hBN/graphene heterostructures after BN deposition (or transfer)[1]. We show that micron-size epigraphene patterns facilitate the lateral growth[2] of a uniform and smooth hBN layer over graphene while reducing particle formation that is essentially confined to the bare SiC (i.e. graphene-etched) areas.
Specifically, We demonstrate selective growth of a continuous hBN film down to about 20 hBN monolayers (6nm) on epigraphene, with a smooth, pleated morphology. In contrast, on the graphene-free areas, BN shows a granular morphology. The Raman spectrum of the heterostructure reveals a prominent graphene 2D peak, indicating the presence of high-quality epigraphene after hBN deposition. Furthermore, the absence of a graphene D peak in the spectrum indicates that the epigraphene quality was preserved under the hBN growth conditions. Cross-sectional TEM measurements performed on the heterostructure show layered hBN on epigraphene patterns and randomly oriented BN on SiC substrate.
Our study confirms that this MOVPE process is promising for fabricating epitaxially aligned and single-crystalline 2D heterostructures. This method can enable efficient device isolation with the selection of optimal devices and industrial scalability. It opens new possibilities for the fabrication and integration of novel van der Waals heterostructures for the next generation of nano-electronics devices.

[1] Dean, C.R. *et al*., *Nat. Nano* **5**, 722–726 (2010).
[2] Gigliotti, J. *et al.*, *ACS Nano* **14**, 12962 12971(2020).
[3] Ottapilakkal, V. *et al.*, *J Cryst Growth* **603**, 127030 (2023).

9:40 AM 3A-2.5
Advancing GaN-Based LEDs—Scalable Growth and Fabrication on Hexagonal Boron Nitride Templates on 6-inch Sapphire Substrates Phuong Vuong[1,2], Tarik Moudakir[3], Rajat Gujrati[1], Ashutosh Srivastava[1,2], Vishnu Ottapilakkal[1], Simon Gautier[3], Paul L. Voss[1,4], Suresh Sundaram[1,2,4], Jean Paul Salvestrini[1,2,4] and Abdallah Ougazzaden[1,4]; [1]CNRS, Georgia Tech – CNRS IRL 2958, France; [2]Georgia Tech-Europe, France; [3]Institut Lafayette, France; [4]Georgia Institute of Technology, School of Electrical and Computer Engineering, United States

The van der Waals (vdW) epitaxy of three-dimensional (3D) materials on two-dimensional (2D) layers has progressed rapidly over the last decade, attracting tremendous attention, especially for III-Nitrides, where new pathways have been opened for optoelectronic/electronic nitride devices and their applications such as GaN-based LEDs. However, the scaling up of this LED fabrication is challenging due to spontaneous delamination of the epilayer which happens at the size of 6-inch and hinders the commercialization of this technology. Here, the growth of hexagonal boron nitride (h-BN) and vdW epitaxy of blue multi-quantum well (MQW) GaN-based LED heterostructures on 6-inch sapphire substrates using metal-organic chemical vapour deposition (MOCVD) is demonstrated. We identified and resolved the main challenges lead to delamination, resulting in functional GaN-based LEDs with zero delamination throughout the growth, fabrication, and

transfer processes by controlling the spatial uniformity of the growth temperature, optimizing the slope of temperature variations during the growth and cooling process, and managing the surface temperature during switching of gas flows. The GaN-based LED devices were then fabricated and we reported the current-voltage (I-V) characterization and bright blue illumination with an electroluminescence peak at 437 nm. Additionally, we demonstrated the lift-off of these LEDs and their transfer to a flexible copper carrier. With these results, the fabrication of GaN based LEDs on h-BN/sapphire becomes more appealing for commercialization and especially the study to avoid the delamination developed in this paper can be applicable to larger substrates, 8-inch, 10-inch, 12-inch and beyond to respond to the scale up of the sapphire substrates production.

10:00 AM BREAK

SESSION 3B-1: Epitaxy for Photovoltaics
Session Chair: Hoe Tan
Wednesday Morning, May 15, 2024
Resort Tower, Ground Level, Bronze Room 1

10:30 AM 3B-1.1
GaInAs/GaAsP Strain-Balanced Superlattices for High Efficiency Solar Cells Ryan France and Myles Steiner; National Renewable Energy Laboratory, United States

Strain-balanced GaInAs/GaAsP superlattices can extend the absorption range of solar cells beyond GaAs without the introduction of dislocations. The extra absorption is beneficial for single-junction devices, and also enables a more optimal bandgap combination in dual- and triple-junction devices. However, the superlattice must be several microns thick for complete absorption of long-wavelength photons. Careful growth control is needed in order to: 1) maintain strain-balancing over several microns of growth 2) limit strain-induced step-bunching and composition modulation and 3) limit unintentional interfacial compounds. In situ wafer curvature is used to maintain strain-balancing, but strain-induced thickness and composition modulations can lead to decomposition even in a strain-balanced structure, as determined by TEM. By using growth conditions that limit surface adatom mobility, we demonstrate high-quality optically-thick superlattices over 4 μm thick. Without dislocations or material degradation, high quality superlattice solar cells are created with open-circuit voltages only 0.3 V below their effective bandgap. Incorporating these superlattice solar cells into multijunction devices enables very high efficiency 2- and 3-junction devices with 32.9% and 39.5% efficiency, respectively.

10:50 AM 3B-1.2
Development of Ultra-Fast Grown GaAs Rear-Heterojunctions for Low Cost Tandem Solar Cells
Christoph Klein, Robin Lang, Jonas Schön, Jens Ohlmann, Frank Dimroth and David Lackner; Fraunhofer Institute for Solar Energy Systems ISE, Germany

The energy conversion efficiency of single-junction silicon photovoltaics is fundamentally limited to 29.4% (AM1.5g). To overcome this limit, especially for applications with limited area (e.g. vehicle integrated photovoltaics), multi-junction technology is a promising candidate. III-V solar cells have a proven track history of high efficiency up to 39.5% at one sun (AM1.5g) achieved with a quantum well enhanced triple-junction device and long-term stability even under harsh environmental conditions as they cover most of today's satellite missions. For widespread terrestrial application of III-V photovoltaics, the main challenge is cost-reduction. Thus, we suggest a thin film AlGaAs/GaAs dual-junction with a mirror below the bottom junction which has a realistic efficiency potential above 33%. The cost of such a III-V cell is roughly evenly spread over the cost for a) the wafer, b) the MOVPE process and c) the solar cell fabrication (backend processing). The wafer cost can be reduced by lift-off processes and subsequent wafer re-use which has been already demonstrated. Regarding backend processing we have recently demonstrated a low-cost processing chain based on printing and electro-plating, thus completely omitting photo-lithography. Regarding a significant reduction of the epitaxy cost, we minimize the thickness of the III-V stack by limiting the device to two junctions and reduce the physical absorber thickness of the bottom subcell with the help of the backside mirror. To further reduce process cost we employ ultra-high growth rates.
This work focuses on the epitaxy development of the bottom GaAs subcell in a close coupled showerhead reactor (CRIUS). It is known, that increasing the growth rates also increases the As anti-site density. By employing only n-type GaAs as absorber we can minimize the impact of the anti-site defect and achieve minority carrier lifetimes that are more than one order of magnitude higher than in comparable p-type material. We show the impact of the V/III ratio on the anti-site density by DLTS measurements. At a low V/III ratio of 5 the anti-site density is below 8×10^{14} $cm^{-3}$and we find a maximum of the minority carrier lifetime of 240 ns for a doping concentration of 2×10^{16} cm^{-3} for double hetero structures. This is a sufficient lifetime to achieve open circuit voltages above 1.05 V under AM1.5g for fully processed GaAs solar cells on substrate according to a simple model, significantly exceeding previous publications for ultra-high growth rate material. The solar cells are currently in processing and experimental results will be ready to be presented at the conference.

11:10 AM 3B-1.3
MOVPE Growth of InGaAs/GaAsP Quantum Wells for Improved Photovoltaic Efficiency Stephen Polly, Brandon Bogner, Anastasiia Fedorenko and Seth M. Hubbard; Rochester Institute of Technology, United States

Photovoltaics (PV) made from III-V materials offer the highest power conversion efficiency of any PV technology, with the best performing devices made from several sub-junctions with decreasing bandgaps to split the solar spectrum for efficient collection. Tailoring sub-junction bandgaps to optimal values, based on the detailed balance, typically requires the use of lattice-mismatched materials requiring thick metamorphic grades. As the number of junctions increases, development and associated losses of the required tunnel junctions becomes more difficult, and overall device performance may become more susceptible to radiation damage as current matching becomes increasingly multivariate. Quantum wells (QW) can modify the effective bandgap of e.g. GaAs, allowing sub-bandgap photon collection normally lost to transmission, enabling a better detailed balance match in a simpler, nominally lattice matched, two-junction device. Historically, the introduction of low bandgap QWs have demonstrated some increase in short circuit current density at the expense of open circuit voltage, often causing an overall loss in power conversion efficiency. In this work we present the results of a series of growth experiments to develop high quality InGaAs/GaAsP strain balanced quantum wells for improved efficiency dual-junction photovoltaics.

Initial work with a small number of compressively strained $In_{0.1}Ga_{0.9}As$ quantum wells incorporated into GaInP/GaAs heterojunction solar cells indicated using GaAs barriers of approximately 4 nm minimized losses in Voc to less than 10 mV, while allowing sufficient increase in current density to exhibit a 0.3% absolute increase in AM1.5G efficiency. In this result, only three QWs were used to maintain the total InGaAs volume below its critical thickness to avoid defect formation. Increasing the number of QWs was necessary to increase absorption and current collection, which required strain balancing with a tensile film for growth of many repeat units without the onset of relaxation and defect formation. GaAsP was chosen as the strain balancing material, using 34% phosphorus to allow adequate strain balancing of the 9 nm InGaAs wells.

Here, we examine the growth mechanisms necessary to realize high quality multiple quantum wells made from compressively strained InGaAs balanced with tensile strained GaAsP on GaAs. This system is highly sensitive to substrate orientation offcut, growth temperature, and individual layer stress. Non-optimized growth conditions caused significant step bunching, which caused a significant buildup of surface morphology and complete collapse of high resolution x-ray diffraction superlattice peaks. PV devices with these films suffered significant loss in Voc, and in turn, efficiency. While on-axis substrates minimized this effect, offcut substrates are necessary for control of GaInP junction bandgap through CuPt ordering, necessitating a growth regime on samples with an offcut. The gas switching sequence between individual QW layers, as well as lowering the growth temperature and the phosphorus content, was investigated to improve growth conditions with verification by HRXRD and TEM.

Using improved growth conditions, highly uniform MQW structures with as many as 50 wells were grown and incorporated into a GaAs PV cell. To further increase the optical path length in the QWs when inserted into a photovoltaic cell, a GaAs lattice-matched carbon doped AlGaAs/AlGaAs DBR was developed to reflect unabsorbed sub-gap photons back incorporating these QWs. Combined, these structures enabled sub-bandgap current collection of more than 40 $\mu A/cm^2$/QW under AM0, while minimizing Voc loss to only 15 mV as compared to a control device without QWs. Inserted into a two-junction GaInP/GaAs solar cell enabled demonstration of a two-junction device with 27.5% efficiency under AM0, or 30.3% under AM1.5G, representing absolute efficiency improvements over control devices of 3.6%, or 1.8%, respectively.

11:30 AM 3B-1.4
Dual-Use Laser and Solar Photovoltaics Enabled by Lattice-Mismatched Epitaxy Ryan France[1], Darin Meeker[1,2], Kaitlyn VanSant[1], Sarah Collins[1] and John F. Geisz[1]; [1]National Renewable Energy Laboratory, United States; [2]Colorado School of Mines, United States

Satellite-to-satellite laser power beaming is currently being investigated as a way to supplement solar power generation. For this application, novel photovoltaic devices are needed that convert both incident laser and solar spectra. 1070 nm fiber lasers can achieve very high powers, and so are a natural wavelength choice for power beaming. Metamorphic InGaAs, which we have previously optimized for inverted metamorphic multijunction devices, can be bandgap-tuned to this laser wavelength, resulting in high laser conversion efficiency by minimizing thermalization loss. Here, we present three device structures that utilize lattice-mismatched InGaAs for laser conversion, but also are part of a device structure that converts the solar spectrum. First, a single junction lattice-mismatched InGaAs can convert both solar and laser as long as there are no absorbing layers present and the emitter sheet resistance is low. Second, a two-junction device employing two independently lattice-mismatched subcells, one of which is optically thin, interconnected with a metamorphic tunnel junction. Third, a three-junction inverted metamorphic multijunction device that utilizes the metamorphic buffer to spread current from the laser to a middle terminal. Trade-offs between solar and laser conversion efficiency will be discussed, and initial experimental results will be presented.

11:50 AM 3B-1.5
Demonstration of Photovoltaics on Acoustically Spalled Surface by MOVPE Seth M. Hubbard[1], Elijah Sacchitella[1], Stephen Polly[1], Pablo Coll[2] and Mariana Bertoni[3]; [1]Rochester Institute of Technology, United States; [2]Crystal Sonic, Inc, United States; [3]Arizona State University, United States

III-V solar cells, both single and multi-junction, exhibit exceptional conversion efficiencies, particularly for growing space power market. Their high-power density and radiation resistance makes them extremely desirable for space-related uses, yet their cost, still exceeding $100/W, can hamper widespread adoption in future large mega constellations (e.g. StarLink) not to mention terrestrial applications (e.g. power on UAV). The primary cost contributor is the substrate, accounting for over 50% of total cost. One cost reduction method being explored by our team is acoustically controlled spalling to remove and reuse the substrate. Current spalling methods induce a crack that propagates along the natural crystallographic planes of the GaAs substrate resulting in a rough surface that may need further chemical and mechanical polishing before regrowth. An alternative spalling process using sonic lift-off to control crack propagation uses ultrasonic waves, effectively reducing the magnitude of the surface facets that arise from traditional spalling techniques.

This study demonstrates the progress in the application of sonic lift-off technology for substrate reuse in GaAs based photovoltaics. GaAs solar cells were grown at RIT on both 50 and 75mm (100) GaAs substrates, with a 2° offcut towards the <100> plane, using our 3x2" Aixtron close coupled shower head metalorganic vapor phase epitaxy (MOVPE) system. Acoustic spalling was then performed by ASU. We have conducted device performance at various states of this process using both ex-situ and in-situ methods to reduce surface roughness. In our study, the surface of a spalled substrate (substrate with thin film removed by spalling) had residual surface roughness in the range of 1 um. This was reduced to the 200-300 nm range using a five minute etch in a mixture of H_2SO_4:H_2O_2: H_2O. The spalled thin films with devices were mounted to silicon wafers as handles using a nonconductive epoxy.

In our initial study, four devices were studied, a control device directly grown on an epi-ready substrate (control), a thin film device spalled from an epi-ready substrate (1st film), a device grown on a substrate that had been spalled once (1st substrate) and a thin film device grown on the substrate that had been spalled and then removed using spalling (2nd film). Devices were processed using standard III-V processing methodology, device size varied from 0.25x0.25 cm^2 to 1x1 cm^2, measurements were taken under calibrated AM1.5g illumination. Encouraging results were seen for the control, 1st film and 1st substrate devices, with average results from these wafers showing almost identical solar cell metrics (J_{sc}=26.2 mA/cm2, V_{oc}=1001 mV, fill factor =84%, efficiency=22%). In addition, the device yield across the control and 1st film were comparable, while the standard deviation in Voc increased for the 1st substrate (from 5mV to 20 mV), indicative of a correlation between roughness and dark current. On the other hand, the 2nd film had significant degradation in average values with loss in carrier collection (J_{sc}=11 mA/cm2) and increased dark current (V_{oc}=700 mV). This was likely due to a poor spalling process on the initially rougher 1st spall substrate. More details of the analysis of these devices including quantum efficiency, electroluminescence and further electrical characterization will be presented during our talk.

We are currently investigating growth conditions that can improve this roughness as well as spalling parameters that produce a more consistent film and device metrics. Conditions under investigation using GaAs/AlGaAs SEM test structures to monitor the evolution of growth include doping with CCl_4, DETe, or Si_2H_6, as well as altering standard growth temperature and V/III ratio. Results comparing in situ telemetry with realized structures will be presented as well as full device characterization.

12:10 PM 3B-1.6
Wafer-Bonded Four- and Six-Junction Solar Cells for Micro-CPV Applications David Lackner, Patrick Schygulla, Oliver Höhn, Malte Klitzke, Jonas Schön, Eduard Oliva, Michael Schachtner, Alexander Wekkeli, Gerald Siefer, Henning Helmers and Frank Dimroth; Fraunhofer Institute for Solar Energy Systems ISE, Germany

Concentrator photovoltaics (CPV) is the PV technology with the highest conversion efficiency, a proven track record of stable operation in the field and a significantly lower carbon footprint than silicon photovoltaics. The Micro-CPV technology approache promises a significant cost reduction by reducing the size of the solar cells to less than 1 square mm, thereby enabling the elimination of dedicated heat spreader elements and the use of standard circuit board technology, while implementing parallelized high throughput processes for module assembly. The terrestrial market is predominantly cost driven, thus the main development focus has shifted to cost reduction in the recent years. Still, since most of the system costs are area proportional, increasing solar cell conversion efficiency provides a large lever for cost reduction. A wafer-bonded MOVPE-grown III-V four-junction cell made of $Ga_{0.51}In_{0.49}P/Al_{0.03}Ga_{0.97}As//Ga_{0.15}In_{0.85}As_{0.65}P_{0.35}/Ga_{0.47}In_{0.53}As$ operated under 665-fold concentration (AM1.5d) and has recently been demonstrated with a conversion efficiency of 47.6%. This is currently the highest solar cell efficiency achieved.
In this work, current developments to overcome the limitations of the current champion device will be presented. In a first step, the series resistance is improved by 20% by optimizing the sheet resistance of the topmost GaInP subcell without compromising in deterioration of the high external quantum efficiency. Finally, thermalization losses are reduced by increasing the number of junctions to six and redistributing the bandgaps to ideally suit the AM1.5d spectrum. Detailed potential analyses confirm that the latter device concept has a realistic efficiency potential of 50% conversion efficiency for a 1000-fold concentration. First electro-optical

characterization results of this device will be presented at the conference.

SESSION 3B-2: TMDC and Other Layered Materials and Characterization
Session Chair: Andrew Graves
Wednesday Morning, May 15, 2024
Resort Tower, Ground Level, Bronze Room 2

10:30 AM 3B-2.1
MOCVD of 2D-TMDC—Nucleation, Lateral Growth and Vertical Heterostructures Songyao Tang[1], Yibing Wang[1], Yingfang Ding[1], Hleb Fiadziushkin[1], Amir Ghiami[1], Andrei Vescan[1], Holger Kalisch[1] and Michael Heuken[2,1]; [1]RWTH Aachen University, Germany; [2]Aixtron SE, Germany

2D transition metal dichalcogenides (TMDC) are extensively explored by the scientific community as potential building blocks for (opto-)electronic components. 2D devices such as field-effect transistors (FET) based on MoS_2 or WSe_2 have shown promising performance and are even considered for integration into Si CMOS technology. Meeting all requirements of commercialization, metal-organic chemical vapor deposition (MOCVD) has been widely accepted as a scalable and controllable technique to realize multi-wafer fabrication of 2D TMDC with excellent quality, homogeneity and reproducibility. Nevertheless, the detailed mechanisms of 2D-MOCVD are not fully understood, and systematic efforts need to be devoted to study the impact of different growth parameters in detail.
In this work, we report on the latest progress using MOCVD for the fabrication of TMDC monolayers and the direct synthesis of their 2D-2D heterostructures. A commercial AIXTRON CCS reactor (7 × 2" setup) with advanced ARGUS and LayTec spectroscopic in-situ monitoring systems is employed as the experimental platform.
Tungsten/molybdenum hexacarbonyl (WCO/MCO), di-tert-butyl sulfide (DTBS) and di-iso-propyl selenide (DiPSe) are used as precursors with H_2 as carrier gas. 2" c-plane sapphire with a nominal 0.2° off-cut towards m-plane is chosen as substrate. A 30 min sapphire desorption in H_2 (150 hPa, 1050 °C) is carried out before each deposition.
Temperature, as one of the most powerful MOCVD parameters, influences not only the critical nucleus size, but also the diffusion length of adatoms on the substrate surface. For different TMDC from the $(Mo,W)(S,Se)_2$ family, the nucleation temperature is correspondingly adjusted in a range from 460 to 750 °C, in order to achieve a uniform distribution of the seeded TMDC nuclei on the wafer. In addition to temperature, other factors like substrate morphology (quality) and the chemical termination of the substrate surface are also found to play a vital role. For instance, by injecting DiPSe prior to WCO, the coverage and uniformity of WSe_2 nuclei on the Se-passivated sapphire surface are improved in comparison to nucleating on the pristine H_2-desorbed Al-rich sapphire surface.
Usually, during the following lateral growth step, closing a monolayer without premature bilayer formation is rather challenging. Bilayer nucleation inevitably sets on when size of monolayer domains already formed exceeds the metal adatom migration length (of the order of tens of nm) on top of these domains. Nevertheless, by smart MOCVD recipe design, for example by carefully tuning the parameters (incl. temperature) for the lateral-growth stage and ramping down the flux of the growth-limiting metal species, coherent monolayers with sparse bilayer coverage (< 20%) can be achieved.
Based on the individual MOCVD recipes for TMDC monolayers, pioneering studies about the directly successive growth of 2D-2D heterostructures are presented. It is found that the growth of the second material is highly influenced by the first material underneath. Generally, a larger growth rate can be observed. Compared to the individual monolayers, the heterostructures show unique optical and structural properties, which is possibly caused by interlayer coupling. Preliminary electrical characterization results of FET built on 2D-2D heterostructures are also included in this work. Furthermore, 2D-2D heterostructures prepared by mechanical transfer and stacking are characterized and compared with the ones directly fabricated by MOCVD, which reveals the impact of the interface on the optical properties of these two processes of 2D-2D heterostructure formation.

10:50 AM 3B-2.2
Synthesis of Two-Dimensional Gallium Sulfide with Ultraviolet Emission by MOCVD Oliver Massmeyer[1], Robin Günkel[1], Jürgen Belz[1], Philip Klement[2], Badrosadat Ojaghi Dogahe[1], Johannes Glowatzki[1], Sangam Chatterjee[2] and Kerstin Volz[1]; [1]Philipps-University Marburg, Germany; [2]Justus Liebig University, Germany

Two-dimensional (2D) materials are gaining great attention due to their extraordinary thickness-dependent properties. The layered III-VI semiconductors such as GaS and GaSe show a unique band structure. Furthermore, 2D GaS and GaSe have a bandgap in the UV region, which makes them candidates for several LED and detector concepts. Moreover, the composition tuning of multilayer GaS_xSe_{1-x} alloys allows for establishing bandgaps between 2.0 and 2.5 eV.
Hence, group III-chalcogenides are promising materials for next-generation optoelectronic applications, as they even reach these properties with comparably little use of material. Typical preparation routine for 2D materials, however, is the mechanical exfoliation, which is no suitable technique when applications are aimed for. Hence, we establish metal organic chemical vapor deposition (MOCVD) to find suitable growth routines for 2D materials using a well-accepted growth technique. We investigate the MOCVD growth of GaS on sapphire (0001) substrates using well-established metal-organic precursors. The samples are characterized by means of Atomic Force Microscopy (AFM), Scanning Electron Microscopy (SEM), Raman spectroscopy, and Transmission Electron Microscopy (TEM) as well as several optical spectroscopy techniques.
Due to prereactions of the di-*tert*-butyl-sulphide (DTBS) and tri-*tert*-butyl-gallium (TTBGa) precursors on the surface, a

pulsed growth scheme is applied, offering the precursors intermittently. This results in the formation of 2D, closed films instead of 3D structures containing liquid Ga on the surface. This is enabled by a specific interface reconstruction between the sapphire and the GaS. Photoluminescence shows a room - temperature emission at 3.3 eV, underlining the potential of the 2D III-VI structures.
The presentation will summarize our current understanding of the MOCVD growth of group III-chalcogenides by systematic variation of different growth parameters such as temperature, chalcogen/group III gas phase ratio and deposition sequences and correlate the findings to optoelectronic properties of the layers.

11:10 AM 3B-2.3
MOCVD Growth of Two-Dimensional, High-Mobility InSe
Robin Günkel[1], Milan Solanki[1], Markus Stein[2], Daniel Anders[2], Nils Langlotz[1], Jürgen Belz[1], Sangam Chatterjee[2] and Kerstin Volz[1]; [1]Philipps-University Marburg, Germany; [2]Justus-Liebig-University Giessen, Germany

To keep up with Moore's Law [1], transistors must shrink in size while maintaining exceptional performance. On the one hand, there is a fundamental limitation for 3D semiconductor-based transistor gates, as their size is limited to a few nanometers due to the rapid performance degradation with decreasing thickness of the semiconductor volume, mainly due to increased surface scattering effects [2]. On the other hand, 2D materials have become a fascinating field of research, since the Nobel Prize in Physics was awarded in 2010 for the discovery of graphene [3]. Indeed, some of these thin 2D materials are semiconductors with high field effect mobilities and could replace common 3D semiconductors as gate materials with enhanced miniaturization [2].
Nonetheless, the new transistor materials must not only have proper inherent characteristics, but also has the synthesis and processing to be cost-effective, reliable, and scalable. This has been achieved for decades using metal organic chemical vapor deposition (MOCVD) as growth method.
Especially, group III chalcogenides, like indium selenide (InSe) or gallium sulfide (GaS) can be grown with metal organic precursors established in the III-V laser industry that decompose at low temperatures and are free of oxygen. In this study we focus on layered InSe, known to feature a high field effect mobility [4]. Its application for logic devices has been demonstrated [5]. One main challenge of InSe growth is its rich phase diagram leading to undesirable phases of In_xSe_y [6]. Sensitive adjustment of the provided ratio of di-iso-propyl selenium (DiPSe) and tri-methyl indium (TMIn) allows us to grow single phase InSe homogeneously on 2" c-plane sapphire as verified by Raman spectroscopy. The number of layers grown depends on the growth time. We show by atomic force microscopy (AFM) that the growth initiates from small nuclei, which grow together to form a coalesced single layer film. After the first layer is closed, the growth behavior changes. This change is attributed to a different environment for precursor decomposition on the surface, underlining the importance of surface chemistry. The second layer contains InSe triangles up to 2 µm in size.
Terahertz time-domain spectroscopy studies of the MOCVD-grown InSe indicate a high mobility of charge carriers in the range of 1000 $cm^2/(Vs)$ as expected in the literature [3].
The presentation will summarize our current understanding of 2D InSe growth and its properties and discuss some improvements, including generating heterostructures of InSe and other van-der-Waals materials.
References:
[1] Moore, Gordon E. "Cramming more components onto integrated circuits, Reprinted from Electronics, volume 38, number 8, April 19, 1965, pp. 114 ff." *IEEE solid-state circuits society newsletter* 11.3 (2006): 33-35. https://doi.org/10.1109/N-SSC.2006.4785860
[2] Su, Sheng-Kai, et al. "Layered semiconducting 2D materials for future transistor applications." *Small Structures* 2.5 (2021): 2000103. https://doi.org/10.1002/sstr.202000103
[3] Novoselov, Kostya S., et al. "Electric field effect in atomically thin carbon films." *science* 306.5696 (2004): 666-669. https://doi.org/10.1126/science.1102896
[4] Arora, Himani, and Artur Erbe. "Recent progress in contact, mobility, and encapsulation engineering of InSe and GaSe." *InfoMat* 3.6 (2021): 662-693. https://doi.org/10.1002/inf2.12160
[5] Feng, Wei, et al. "Back gated multilayer InSe transistors with enhanced carrier mobilities via the suppression of carrier scattering from a dielectric interface." *Advanced materials* 26.38 (2014): 6587-6593. https://doi.org/10.1002/adma.201402427
[6] Okamoto, H. "In-Se (indium-selenium)." *Journal of phase equilibria* 19.4 (1998): 400-400. https://doi.org/10.1361/105497198770342175

11:30 AM 3B-2.4
***In Situ* and *Ex Situ* Characterization of 2D WS_2 Epilayers on Sapphire Grown in a Commercial MOVPE Reactor**
James Gupta, Jean-Félix Milette, Victoria Howard, Katelyn Warren, François Drouin, Mathias Roman, Jeremy Leung, Sebastian Schaefer, Aidan Karmali and Marouane Meziane; University of Ottawa, Canada

2-dimensional transition-metal dichalcogenides (TMDs) are interesting for numerous optoelectronic technologies because of their visible-wavelength direct-bandgaps, defect-related single-photon emission, and unusual “valleytronic” properties which have exciting potential applications in quantum information. To date, most studies of these materials have used mechanically-exfoliated films having lateral sizes of a few 10’s of micrometers. Despite the novelty of the observed physical properties, the small sizes of these films have severely limited the technological deployment. Recently a few groups have demonstrated high-quality, wafer-scale growth of 2D-TMDs by MOVPE, which provides a critically-necessary path towards the advancement of technology-readiness-level and eventual commercialization.

In this work we describe the growth and characterization of 2D WS_2 films grown on C-plane sapphire substrates in a commercial, multi-wafer Aixtron CCS 3X2 system recently commissioned at the University of Ottawa, Canada. The

system is currently capable of growing a variety of 2D materials including graphene, hexagonal boron nitride and several TMDs (WS_2, MoS_2, WSe_2, and $MoSe_2$). For WS_2 the growth uses tungsten hexacarbonyl and d-tert-butyl-sulfide precursors ($W(CO)_6$ and DTBS, respectively) with H_2 and N_2 carrier gases and a reactor pressure of 50mbar.

In-situ optical reflectance measurements were made at wavelengths of 405nm, 633nm and 950nm using a Laytec EpiTT system. The reflectance transients were used to study the initial stages of high-temperature (1050-1200°C) sapphire annealing under a H_2 ambient and the nucleation and growth of WS_2 films at temperatures between 500 and 800°C. The reflectance measurements show clear differences in the early-stage nucleation kinetics at different temperatures, which were further studied using *ex-situ* atomic force microscopy (AFM) measurements of sub-monolayer WS_2 depositions. The measurements show that at low temperatures nucleation at sapphire substrate step edges is dominant, while at higher temperatures the nucleation occurs on flat sapphire terraces. Following approaches developed elsewhere, multi-step nucleation-coalescence-growth processes were used to obtain high-quality closed monolayer films.

Ex-situ spectroscopic reflectance measurements over the range 350-1100nm were made using an Ocean Insights fiber-coupled dual-spectrometer and a custom, Python-based software analysis suite. The analysis uses a genetic algorithm fitting approach to determine the optical properties of the full-monolayer WS_2 films using a 5-peak Forouhi-Bloomer model for the complex refractive index and a transfer-matrix method to calculate the reflectance of the film/substrate stack. The model accurately captures the observed critical points in the room-temperature reflectance spectra, including the direct-bandgap peak near 620nm.

Room-temperature photoluminescence (PL) measurements were used to characterize the WS_2 film uniformity across full 50mm wafers using a custom Labview-based mapping system using a 520nm illumination laser through a 50X microscope objective with a Princeton Instruments SP-2750 spectrograph and PyLoN:400 CCD camera. The measurements indicate very high uniformity of the PL peak emission across the epitaxial wafers, providing a clear indication of the suitability of the films for further device development.

11:50 AM 3B-2.5
Characterizing Intrinsic Defects in 2D materials via Transport Through Atomically Thin Membranes Piran Kidambi; Vanderbilt University, United States

2D materials present potential for disruptive advances in electronics, energy, and separation technologies. Although bottom-up synthesis of 2D materials via CVD and MOCVD have emerged as the most widely used synthesis methods, these methods typically incorporate intrinsic defects at the sub-nanometer to nanometer scale. Characterizing such intrinsic defects over large areas remains prohibitively expense via conventional microscopy/imaging methods. Here, we present a facile and statistically robust new approach to characterize intrinsic defects in 2D materials over centimeter scale areas by forming atomically thin membranes and measuring through plane transport via complementary transport measurements that utilize several distinctly different driving forces. Our approach allow for quantification of defects in 2D materials allowing quality benchmarks necessary to advance these materials towards practical applications.

References
Naclerio and Kidambi Adv. Mat. 2023
Kidambi et al. Science 2021
Cheng et al. submitted
Chaturvedi et al. submitted
Naclerio et al. submitted

12:10 PM 3B-2.6
Quantum Defects in Layered Materials Sanjay Behura; San Diego State University, United States

Creating spin defect-based quantum emitters hosted on the surface of the material in contrast to the defects buried within the bulk of the material is promising for quantum information science and technology. Atom-thin 2D quantum materials are truly surfaces and they have unique chemical structures and novel electronic and optical properties. Hexagonal boron nitride (h-BN), a 2D wideband gap material hosts optically active defects within their energy bandgap that emit single photons of light while displaying spin-optical quantum properties at room temperature. However, currently, the search is largely focused on probabilistic sources of quantum light found in exfoliated monolayer h-BN crystals with atomic and molecular defects created via thermal or ion or electron or nuclear irradiations. These approaches not only cause lattice distortions but also creates large density of defects causing ineffective single photon emission with poor brightness. Ability to create and control h-BN spin defects directly on integrated photonic substrates will be transformative as the defects hosted on atomically thin materials offer the ability to expose their chemical and electronic structure to controls by proximity effects. In this talk, I will first discuss the quantum many-body physics of spin defects in h-BN including the development of Hamiltonian model followed by surface chemical design principles to synthesize and characterize h-BN crystals directly on various photonic substrates.

ICM VPE XXI

2024 Las Vegas, NV

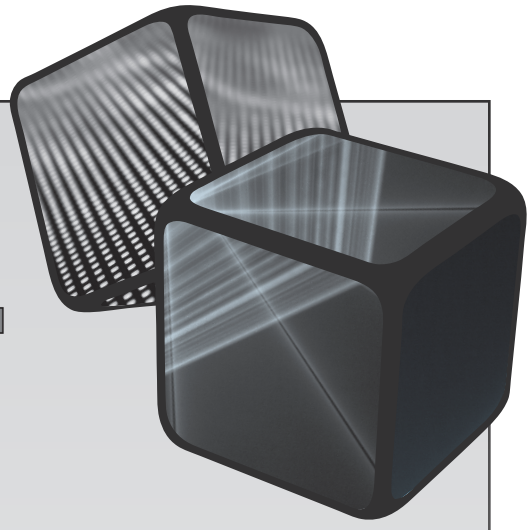

THURSDAY

Oral Presentations

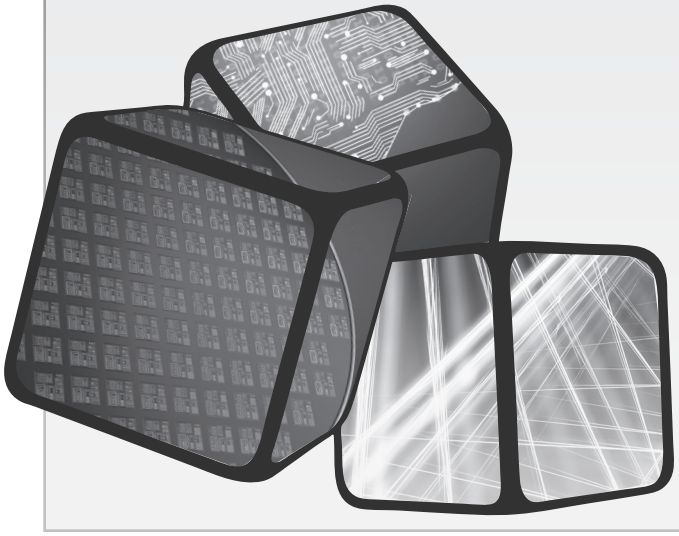

21st International Conference on Metal Organic Vapor Phase Epitaxy

SESSION 4A: Plenary Session III
Session Chairs: Russell Dupuis and Luke Mawst
Thursday Morning, May 16, 2024
Resort Tower, Ground Level, Silver Room

8:15 AM OPENING REMARKS

8:30 AM *4A.1
Recent Developments in Long Wavelength III-N Emitters for Mini-Displays and Electronic Materials Using MOVPE
Shubhra S. Pasayat; University of Wisconsin–Madison, United States

In this talk the presenter will be talking about the innovative techniques used to achieve state of the art long wavelength (580-630 nm) micro-LEDs for mini display applications using porous nitrides and complex oxides realized using MOVPE. She will also present the developments made in MOVPE of III-N electronics for RF electronics for next generation of wireless communication applications.

9:15 AM *4A.2
Machine Learning Modeling of Epitaxy and Nanostructures Evolution Francesco Montalenti; University of Milano-Bicocca, Italy

From the point of view of a computational researcher running atomistic simulations, deposition reactors are terribly slow. Growth of a thin film or of a peculiar set of nanostructures occurs on “human” time scales: several minutes if not hours. With this respect, MOVPE does better than MBE, but still works in the quoted temporal range. Molecular Dynamics (MD) simulations, i.e. the most natural atomistic approach, can hardly reach the microsecond time scale, meaning that an acceleration of the deposition rate of several orders of magnitude with respect to the experimental one must be forced when trying to provide a fully MD-based modeling of growth. Unfortunately, this artificially causes significant out-of-equilibrium conditions.

Unsurprisingly then, the need for modeling long temporal evolution has pushed the theoretical community to develop alternative methods. If one is willing to keep an atomic-scale description of the process a popular approach is surely Kinetic Monte Carlo (see [1] for an early application to growth), proposed also in an advanced, on the fly version [2]. Accelerated MD has been also exploited [3]. However, these approaches lose effectiveness at high temperatures and struggle in tackling large enough systems.

More recently, attempts to insert realistic physics in continuum approaches have been presented, allowing one to match experimental conditions. Despite yielding only an average description of the system behavior, continuum models can tackle several realistic aspects of growth such as preferential exposure of crystalline facets, strain relaxation, and out of equilibrium morphologies [4]. Examples of all such complexity will be given by analyzing our results on several diverse systems such as films, pillars, islands, and nanowires.

While working at the continuum level allows for a significant reduction of the computational costs, there is still the need of further speeding up simulations, particularly when use of finite element methods is required at every timestep. This is why in the last three years we started to work on new ways to exploit Machine Learning (ML), with the ultimate goal of providing a new class of simulation tools for epitaxy.

As a first example, we shall show that a convenient convolutional, recurrent neural network (NN) approach [5] can tackle the problem of predicting structural evolution by surface diffusion, after being trained on a phase-field generated dataset. While showing good accuracy, the ML approach guarantees very significant speed ups.

Furthermore, we used convolutional NN to deep-learn the elastic chemical potential at the surface of a stressed film. This allowed us to accurately investigate Stranski-Krastanow island formation at a fraction of the computational cost required by the FEM-based numerical solution [6].

While in the above described applications attention was limited to two (or 1+1) dimensional problems, extension of the formalism to full 3D is rather straightforward, as we shall briefly illustrate by showing a recent application of the same methodology to spinodal decomposition.

Exciting perspectives, also in terms of extending machine-learning approaches beyond deterministic models, are finally discussed. By handling fluctuations, such “generative, adversarial” models [7] could allow for the acceleration of KMC approaches and/or provide a natural framework to add proper noise to deterministic continuum models.

References
[1] S. Clarke and D.D. Vvedensky, Phys. Rev. Lett. 58, 2235 (1987).
[2] G. Henkelman and H. Jónsson, J. Chem. Phys. 115, 9657 (2001).
[3] A.F. Voter, F. Montalenti, and T.C. Germann, Annu. Rev. Mat. Res. 32, 321 (2002).
[4] M. Albani et al., Sci. Rep. 11, 18825 (2021).
[5] D. Lanzoni et al., Phys. Rev. Mat. 6, 103801 (2022).
[6] L. Martin-Encinar et al., “Deep learning of surface elastic chemical potential in strained films: from statics to dynamics” (submitted, 2024).
[7] D. Lanzoni, O. Pierre-Louis, and F. Montalenti, J. Chem. Phys. 159, 144109 (2023).

10:00 AM BREAK

SESSION 4B-1: Epitaxy of As/P/Sb/Bi Alloys for Devices
Session Chair: Kerstin Volz
Thursday Morning, May 16, 2024
Resort Tower, Ground Level, Bronze Room 1

10:30 AM 4B-1.1
MOVPE Growth of InAs/GaSb Type-II Superlattices on InAs Substrates for IR Detectors Ranging from 4-12µm
Richard Brown[1], Chen Liu[1,2], Ka Ming Wong[1], J. Iwan Davies[2] and Qiang Li[1]; [1]Cardiff University, United Kingdom; [2]IQE plc., United Kingdom

Mid-wave and long-wave infrared devices play an important role in cutting edge applications including gas detection, biomedical sensing, thermal imaging and Light Detection and Ranging (LIDAR). Antimony (Sb) based type-II superlattice (T2SL) materials are a strong candidate for next generation infrared technologies due to advantageous manufacturability and flexible band engineering, when compared to the classically used mercury cadmium telluride. Traditionally, T2SLs are predominately developed via MBE on lattice-matched GaSb substrates. This work however, focuses on transferring the growth from MBE to MOVPE, in order to reduce cost and increase the commercial viability of the T2SL for the wide range of IR applications available.

The InAs/GaSb T2SL was grown in an Aixtron CCS-FT reactor and the precursors used were TMIn, TBAs, TEGa and TESb. The range of optimal growth parameters is very narrow for the InAs/GaSb T2SL which makes the growth difficult. The optimal growth temperature was found to be 520°C which gave a good surface roughness of 0.13nm. However, increasing or decreasing the growth temperature by 10°C would increase the surface roughness to over 2nm. The V/III gas ratio of GaSb was also very sensitive; a change of 0.1 would result in large surface defects appearing. InAs/GaSb T2SL growth is also particularly challenging since it is not naturally lattice-matched to any substrate, which necessitates the use of strain balancing layers. In the case of MBE this is overcome using InSb strain balancing layers to lattice-match to GaSb substrates. Unfortunately, the melting point of InSb is 530°C making its growth incredibly challenging for the higher temperatures required from MOVPE. This work gets around this problem by utilising growth interruption stages to create GaAs-like interfaces allowing the InAs/GaSb T2SL to be lattice-matched to InAs substrates. These GaAs-like interfaces were created by introducing growth interruption time between the layers with TBAs flowing and utilising the As for Sb exchange that occurs in GaSb to introduce some As into the GaSb. The TBAs flow rate and time could be used to control the thickness of these interfaces and were tuned to lattice-match to the InAs substrates. The lattice match was verified using XRD and the 1st satellite peak FWHM was 50 arcsecs indicating a high-quality interface. By adjusting the InAs layer thicknesses within the T2SL, the peak wavelengths of the InAs/GaSb T2SLs can be tailored from 4 up to 12 µm, all still matched to InAs substrates. Photoluminescence measurement was performed across the wavelength range at 77K and showed a low FWHM of 20 meV at the 9 µm wavelength. Since the different wavelengths of T2SL are all lattice-matched to each other, it is possible to grow multiple wavelengths of T2SL in a single structure. This allows for barrier-based diodes which have superior dark current performance compared to a more basic PIN detector. The stacking of multiple T2SLs detecting at different wavelengths also allows for more complex dual and multi-wavelength detectors that can span a large wavelength range with a single detector.

10:50 AM 4B-1.2
High-Accuracy *In Situ* Thickness Measurements During MOVPE of AlGaInAs-Based Laser Structures on InP and Silicon (InPoSi)-Substrates—Enabling High-Accuracy Plasma-Etch End-Pointing and Improved *Ex Situ* PL Line-Shape Analysis
Jean Decobert[1], Nicolas Vaissiere[1], Claire Besançon[1], Delphine Neel[1], Daniel Micha[1], Vladyslav Vakarin[1], Nasim Rezaei-Hartmann[2], Marcello Binetti[2], Anthony Martinez[2], Adrian Adrian[2] and Thomas Zettler[2]; [1]III-V Lab, France; [2]LayTec AG, Germany

State-of-the-art in situ metrology during MOVPE gives access to layer-by-layer thickness measurements with very high accuracy on a very wide range of III-V materials. During plasma-etching of the same vertical structures, however, achieving such real-time thickness accuracy is much more challenging. Therefore, in this study we demonstrate, how high-accuracy in-situ layer thickness measurements during MOVPE can enable high-accuracy thickness control also in subsequent plasma etching. AlGaInAs-based laser structures grown on InP and on InPoSi (a thin InP seed layer bonded onto Silicon) are one example where this precision is required to allow strict control of the stack conformity and reproducibility. In this work, the laser structure was grown with an Aixtron CCS 6x2" reactor equipped with an EpicurveTT operating at 950, 633 and 405 nm. The use of different wavelengths is a necessary condition for the thickness measurements (a few nm up to several µm) of layers having different ternary and quaternary material compositions. A real-time thickness accuracy of up to ±0.5nm is achieved thanks to the following optimized conditions during MOVPE:
- The wafer temperature is accurately measured by emissivity corrected pyrometry;
- High precision nk(T) optical data, referenced to ex-situ XRD measurements, are available at epitaxial growth temperature;
- The absolute reflectance scale can be in situ auto-calibrated on the epi-ready substrate surface, just before the growth process starts;
- All interfaces are time correlated with the gas switching sequences.
- The in-situ measured growth-rates are correctly transformed into high-temperature layer thicknesses and layer thickness shrinking during down-cool due to thermal expansion is corrected. This is even more relevant on InPoSi where additional effects come from the different Si and InP coefficients of thermal expansion (CTE).
Once the layer stack is grown by MOVPE, the laser ridge fabrication requires precise etching steps. In this work, we

carried out $Cl_2/H_2/Ar$ plasma etching in an Oxford PlasmaLab 100 ICP-RIE 180 equipped with a LayTec TRIton metrology at 365, 405 and 670 nm. The Fabry-Perot oscillation (FPO) reflectance signatures acquired during MOVPE and ICP-RIE, at 633 and 670 nm respectively (and with inverted time scale for one of the reflectance signal), turned out to be very similiar. However, real-time extraction of thicknesses during plasma etching at a precision comparable to that obtained by epitaxy is extremely challenging, because the current state-of art in plasma etching can be described as follows:
(a) wafer surface temperature T_{wafer}^{etch} is not better known than ± 20K, therefore:
(b) the nk(T) material parameters in the typical range of T_{wafer}^{etch} are not precisely known;
(c) the reflectance scale is relative but not absolute, because differently to MOVPE real-time calibration to substrate reflectance level is not feasible;
(d) the precise assignment of interface signatures in the reflectance data during etching is a challenge.
As a consequence, in plasma-etching real-time thickness measurements, and therefore end-pointing, are made critically random. In this study we will demonstrate, how high-accuracy in-situ measurements during MOCVD (growth rates, high-temperature nk(T)) – after forwarding them to the plasma-etching system - can provide solutions for each of these obstacles (a) to (d).
In this paper we will concentrate on the MOVPE aspects of this methodology: how to achieve maximum in-situ thickness accuracy during growth of complex, InP based laser structures, how to determine layer thickness uniformity for assigning the correct thicknesses to the wafer segments where the measurement test-pads in the masks will be located for later in-situ plasma-etch monitoring and how to derive nk(T) data that correctly span the temperature range between MOVPE temperatures, plasma etching temperatures, device operation temperatures and room-temperature.

11:10 AM 4B-1.3
Recent Advances in W-Type Structures Employing Highly Mismatched Alloys Thilo Hepp[1], Robin Günkel[1], Oliver Massmeyer[1], Sangam Chatterjee[2] and Kerstin Volz[1]; [1]Philipps-Universität Marburg, Germany; [2]Justus-Liebig-Universität Giessen, Germany

Mid-infrared laser devices on GaAs (001) substrates grown by MOVPE are an eagerly awaited dream for industry. However, efficient and stable laser devices emitting beyond 1.3 µm and 1.55 µm on GaAs substrates remain to be demonstrated. One proposed approach are W-type structures, which combine two materials to achieve a significantly reduced emission wavelength compared to the individual materials. One material confines the electrons while the other material confines the holes. Depending on the materials chosen, this features very flexible design possibilities. However, it has not been possible to demonstrate laser operation at 1.55 µm and beyond using this approach. Ga(N,As) and Ga(As,Bi) are promising candidates for W-type structures in the infrared region due to the significant conduction and valance band shifts caused by the incorporation of dilute amounts of nitrogen (N) and bismuth (Bi), respectively. Furthermore, it is possible to stain-engineer these structures since N incorporation induces tensile strain while Bi incorporation induces compressive strain in GaAs. [1]
In a recent publication we demonstrated the growth of W-type structures using Ga(N,As) and Ga(As,Bi) as active materials. Interface formation between these highly mismatched alloys is the critical step during growth. Strong adjustments are required to enable the growth of high-quality samples. In particular, Bi segregation has to be considered in this delicate growth process, including a wetting step with trimethyl bismuth (TMBi) and a desorption step to remove segregated Bi. However, the optical properties deteriorate especially with increasing N fractions in Ga(N,As). [2]
In this talk we investigate the two crucial interfaces in detail and correlate the optical properties with the growth conditions. For this purpose, dedicated type-II structures are grown in which one Ga(N,As) quantum well is intentionally missing in order to study the interfaces individually. Optical characterization using photoluminescence (PL) spectroscopy shows quite significant differences in peak intensity and position of the peak we correspond to the type-II transition. The differences in the PL spectra, their causes and possible solutions will be correlated with other characterization methods, such as X-ray diffraction or atomic force microscopy, and discussed during the talk.
References:
[1] C. A. Broderick et al., Sci. Rep. 7, 46371 (2017)
[2] T. Hepp el al., Cryst Growth Des. 21, 11, 6307-6313 (2021)

11:30 AM 4B-1.4
Multiwafer As/P Based MOCVD Technology for Low-Cost, Large-Scale and High-Quality Epitaxy Ilio Miccoli, Hassan Larhrib, Gintautas Simkus, Adam Boyd, Michael Heuken, Thomas Korst and Jared Holzwarth; Aixtron SE, Germany

MOCVD is today the preferred technology for the large-scale epitaxial growth of As/P based semiconductor compounds which we find in a multitude of optoelectronic devices, such as AlGaAs based VCSEL for surface sensing, red micro-LEDs for displaying and InGaAsP/AlInGaAs lasers for datacom. We have lately developed a new fully cassette-to-cassette wafer automated MOCVD Reactor for large scale production of As/P based materials with in-situ Chlorine-based clean process. Groundbreaking production technology developments based on the Planetary Reactor® configuration will be thus introduced. Reactor geometry and related inlet geometry for both 6 and 8 inch wafer size has been redesigned with the introduction of a novel 4-fold injector, which proves to be the key component to enable the epitaxial growth up 200 mm with comparable in-wafer uniformities and precursor efficiencies to those achieved on smaller substrates. In this presentation, we focus on three case scenarios, extremely appealing for the current expanding market, namely VCSEL on 200 mm Ge substrates, AlInGaP based Micro LED on 200 mm GaAs substrates and for the very first time quaternary InGaAsP/AlInGaAs lasers on 150 mm InP substrates.

Uniformity, tunability and reproducibility results will be thus presented to corroborate reactor flexibility in meeting industry requirements for next device generation.
Driven by the commercialization of 850-940 nm VCSEL-based 3D sensors in smartphones, there has already been a transition from 75 mm to 150 mm GaAs substrates in 2015-2017 to meet the high demand for this class of lasers. However, the next big step to 200 mm substrates would be not possible due to inherent wafer deformation triggered by slightly larger AlAs lattice constant with respect to GaAs. Among possible alternatives that could even allow scaling to 300 mm, germanium is a very good candidate. 940 nm emitting VCSELs have previously been demonstrated on 150 mm Ge substrates [1]. In this work, we demonstrate the feasibility of further scaling up to 200 mm Ge without suffering from the well-known Ge auto doping effects, thanks to in-situ clean capabilities while improving overall bow by up to 10x with respect to GaAs for the same VCSEL structure.
Photonic devices with even longer wavelength up to 1550nm, such as lasers and detectors in fiber optic telecommunications have been established for decades but are becoming increasingly important, forming the backbone of the datacom and AI revolution we are currently witnessing. These lasers are mostly deposited on 75mm InP substrates but transition to 150 mm wafers would be crucial to meet the current market demand since it may take advantage of already available backend-of-the-line from the VCSEL market, provided that comparable uniformity specifications can be meet. Hereby, we thus focus on two prototypical structures for Telecommunication, i.e. a 500 nm thick layer 1100nm InGaAsP bulk and a strained 1540 nm AlInGaAs multi-quantum-well, and prove that wavelength uniformity <1 nm standard deviation (std) can be easily achieved on 150 mm InP wafers without drawbacks in terms of thickness uniformity across the wafer surface and any drift in a multiple run campaign.
Last, we consider the Micro LED case, which has even more strict requirements for uniformity and defectivity. In this regard, we demonstrate that cassette automation in combination with in-situ clean allows to reduce particle adders from 0.5 to 0.05/cm2 while composition uniformity for a full red micro LED on 200 mm GaAs can be optimized down <0.2 nm std.
Current results represent a leap in technology enabling best in class wavelength uniformity, 10x reduced defectivity, and enables an easy-to-use production tool capable of lowering the cost per wafer by 30%, beyond enabling new applications and use cases for the industry.

[1]Johnson, Andrew J. et al. “High performance 940nm VCSELs on large area germanium substrates: the ideal substrate for volume manufacture.” (2021)

11:50 AM 4B-1.5
Growth Optimizations for the Realization of InGaAs-Based Quantum Cascade Laser Structures on Metamorphic Buffer Layers Shining Xu, Jeremy Kirch, Dan Botez and Luke Mawst; University of Wisconsin-Madison, United States

Previously, we have demonstrated InP-based quantum cascade lasers (QCLs) on non-native substrates, such as GaAs and Si, emitting in mid-infrared wavelength range (~ 5 and 8 μm). The device results showed the unique and robust properties of QCLs: high tolerance to threading dislocation density (TDD) and substrate roughness. The above achievements pave the way to realize QCLs on a “virtual substrate” with a customized lattice constant. Therefore, a variety of novel laser device structures with expanded compositional design space could be employed to extend current QCL’s emission wavelength and performance. However, there are many technical challenges in growing the complex full-laser structure on a virtual substrate, which remain to be solved, such as establishing appropriate growth conditions for both the strained-superlattice active region and the doped low-index cladding layers to form the optical waveguide.

Here, we establish the MOVPE growth conditions for realizing a quantum cascade laser employing an InGaAs/AlInAs SL active region and thick $Al_{0.86}In_{0.14}As$ cladding layers on a $In_{0.15}Ga_{0.85}As$ metamorphic buffer layer (MBL). First, MBLs with either compositionally step-graded, superlattice graded structures, or two-step direct growth are characterized by XRD and AFM. All three MBLs exhibit relatively low surface roughness (RMS < 2 nm over 10 x 10 μm^2 area) while broad XRD satellite peaks indicate that the buffer layers are not optimized and have a high density of threading dislocations. Also, different degrees of relaxation and surface morphology are observed among the types of MBL. Then, 1 μm-thick strained and lattice-matched superlattices to mimic the QCL active region were grown on the MBLs. The surface becomes rougher (RMS ~ 5 nm), although well-defined XRD superlattice satellite peaks were observed. Hazy surface and hillocks were initially observed after growing the Al-containing materials, especially for the AlInAs cladding layers. It was suspected that the presence of high dislocation density combined with local shear strain/stress and low Al surface mobility could be the potential reasons. Improved surface was found after adjusting the indium composition in the cladding layers to closely match with the underlying MBL’s lattice. After increasing the growth temperature from 605 C to 700 C, pyramid-like hillocks were found to become flat-terrace islands and no intensity reduction was observed during the 1 μm-thick AlInAs cladding growth from in-situ reflectance.

To successfully realize the QCL on virtual substrate, another important factor in the epitaxial growth is the doping of the active and cladding layers. Previously, from the study of InP-based QCLs on GaAs and Si, we have observed lower threshold current and higher series resistance compared with devices on native InP substrate, which was suspected to be

related to reduced silicon incorporation in the defect layers. Doping calibration consisting of bulk InGaAs and AlInAs layers on $In_{0.15}Ga_{0.85}As$ buffers indicate the carrier concentration in the InGaAs layers maintains a linear relationship with silane flow despite the high TDDs, while the doping is not linear with silane flow rate for the AlInAs layers. The doping concentration for AlInAs layers is saturated around cm^{-3} for the given indium composition and growth condition, and the sample surface would become hazy with higher silane flow. This value is comparable with most InAlAs buffer layers latticed-matched to InP in prior studies. Moreover, the AlInAs layers exhibit higher resistivity compared to the InGaAs layers with similar sheet concentration level due to their low electron mobility. Given these efforts on growth optimization, we believe QCLs on virtual substrate can be realized in near future.

12:10 PM 4B-1.6
InP-Based Mid-Wave Infrared (MWIR) Optoelectronic—Strain Engineering Design of Ga-Free InAs(Sb)/InAsPSb Multiple Quantum Wells Light-Emitting Diodes Phuc Dinh Nguyen[1,2,3], Minkyeong Kim[3], Changsug Lee[4], Dongwan Kim[1], Suho Park[1], Byong Sun Chun[1], Hyeon-June Kim[5] and Sang Jun Lee[1,2]; [1]Korea Research Institute of Standards and Science, Korea (the Republic of); [2]Korea National University of Science and Technology, Korea (the Republic of); [3]Irspectra Co., Ltd, Korea (the Republic of); [4]Korea Spectral Products, Korea (the Republic of); [5]Seoul Nation University of Science and Technology, Korea (the Republic of)

Mid-Wave infrared (MWIR, 2 – 5 μm) electromagnetic has many applications including environmental monitoring, spectroscopy, and free space communication. In this wavelength regime, substrate choice is dominated by "6.1 Å" substrates such as GaSb or InAs. Devices grown on InP substrate would receive many advantages due to its superior thermal conductivity, and mature processing technology. However, those devices only exhibit operation wavelengths of up to 1.7 μm due to the low lattice constant (a_c = 5.87 Å). Consequently, our motivation is to implement this operation wavelength to InP-based devices, taking advantage of InP-based technology. Because of that, high lattice mismatch (~ 3%) problem needed to be solved.
In this work, Ga-free InAs(Sb)/InAsPSb multiple quantum wells (MQWs) platforms were realized, achieving intense room temperature electroluminescence from 2.4 μm to 3.3 μm. Devices were monolithically grown on InP substrates using metal-organic vapor phase epitaxy (MOVPE) on InP (001) substrate. InAsP metamorphic virtual substrate scheme has been firstly adopted to reduce the lattice mismatch. By adjusting the lattice constant to a desired value while confining threading dislocation at the bottom layer through controlled strain-relaxation process, a large amount of strain has been relieved. The active layer consists of type I InAs(Sb)/InAsPSb strain-compensated multiple quantum wells (MQWs). Composition and strain of InAsPSb quaternary compound were engineered for two purposes: compensating the compressive strain of InAs(Sb) quantum well while maintaining a high degree of carrier confinement. As suggested by theoretical modeling, InAs(Sb)/InAsPSb MQWs exhibit large band offsets (Conduction band: 90 – 120 meV, Valence band: 190 – 250 meV), allowing carriers to be welled confined within the quantum wells. Crystallographic analysis by X-ray diffraction and transmission electron microscopy reveals a high degree of crystal quality (R ~ 96 – 98%), low surface roughness (R_q < 1 nm), and a low degree of dislocation (< 5×10^{-2} μm^{-2}).

SESSION 4B-2: DUV LED
Session Chair: Maki Kushimoto
Thursday Morning, May 16, 2024
Resort Tower, Ground Level, Bronze Room 2

10:30 AM *4B-2.1
Epitaxial Growth of AlGaN on Face-to-Face Annealed AlN Template and Deep UV-C LED Fablication Hideto Miyake, Ryota Akaike, Kenjiro Uesugi and Takao Nakamura; Mie University, Japan

To fabricate deep-ultraviolet(DUV)-LEDs with high efficiency, the crystallinity of AlGaN must be improved, and is significantly influenced by that of the underlying AlN template. The face-to-face annealed sputter-deposited AlN templates (FFA Sp-AlN) on sapphire have achieved screw- and edge-dislocation densities (TDDs) of 10^4 cm^{-2} and 10^7 cm^{-2}. Reduction of TDDs in FFA Sp-AlN and surface flattening of $Al_xGa_{1-x}N$ grown on the FFA Sp-AlN play important roles to achieve a high external quantum efficiency (EQE). After the MOVPE homoepitaxial growth of AlN, the FFA Sp-AlN exhibits ideally smooth surface morphology. The EQE of the UV-C LED fabricated on FFA Sp-AlN increased with the TDD reduction of the FFA Sp-AlN. Maximum EQE of 8.0% and output power of 6.6 mW at a 20-mA input were achieved with the peak emission wavelength of 263 nm. We also fabricated 230 nm and 236 nm LEDs on the FFA Sp-AlN templates.

11:00 AM *4B-2.2
Metalorganic Vapor Phase Epitaxy of AlGaN Based UVC LEDs Tim Wernicke; Technische Universität Berlin, Germany

Metalorganic vapor phase epitaxy is today the prevailing method to grow AlGaN-based UV-LEDs whereas the "near UVC" and "far UVC" wavelength regions are ideally suited for disinfection as they can effectively inactivate viruses, bacteria, and fungi by a physical mechanism. Near UVC LEDs, e.g. emitting at 265 nm, exhibit already today a high external quantum efficiency, wall plug efficiency and long lifetime and are very interesting for the disinfection of water, air and surfaces. Far UVC LEDs emitting at wavelengths < 240 nm allow for skin-safe disinfection as light at such short wavelength in activates microorganisms but does not penetrate the upper layers of the skin. This allows to , e.g. for fighting multi-resistant pathogens in hospitals. However, their

efficiency and lifetime are inferior to that of near UVC LEDs. In this paper MOVPE-growth and analysis of near and far UVC LEDs will be discussed. Here we will use a new method to break down the measured external quantum efficiency (EQE) into carrier injection efficiency (CIE), radiative recombination efficiency (RRE) and light extraction efficiency (LEE) and show how emission wavelength, heterostructure, growth condition and mounting affect these quantities.

MOVPE-growth of UVC-LEDs requires AlGaN heterostructures with high aluminum content impacting the point defect incorporation as well as n- and p-type doping which is especially challenging for far UVC LEDs. We will discuss the status of n- and p- doping in AlGaN and compare p-doping by Mg to novel distributed polarization doping.

In near UVC LEDs threading dislocations limit the radiative recombination efficiency. However, also the compressive strain due to growth on AlN buffer layers can lead to additional defect formation and lower emission output powers for longer wavelengths. High temperature annealing of AlN/sapphire substrates has led to a strong reduction in threading dislocation density, but these substrates also exhibit a smaller in-plane lattice constant compared to AlN substrates or MOVPE-grown AlN. Therefore both threading dislocation and in-plane lattice constant must be considered for the ideal substrate.

The stability of LEDs is also very important and limits the performance, especially for LEDs emitting at 233 nm. We have demonstrated >10.000 h of lifetime for 265 nm LEDs and even though lifetimes of 233 nm LEDs are still short < 100 h are increasing with improving technology. However, we found in many cases an anticorrelation of lifetime and emission output power showing that that “performance” is more complex than initially anticipated but also allowing conclusions on the physical mechanism of LED-degradation.

11:30 AM 4B-2.3
Increasing the Efficiency of 219-222 nm AlGaN Far-UVC LEDs with Graded Al Content AlGaN Polarization Doping Layers Hideki Hirayama[1], Harshitha Rangaraju[1], Yuki Nakamura[1,2], Sachie Fujikawa[2,1], M.Ajmal Khan[1], Hiroyuki Yaguci[2] and Yasushi Iwaisako[3]; [1]RIKEN, Japan; [2]Saitama University, Japan; [3]Nippon Tungsten, Japan

Human harmless virus inactivation using far-UVC light-emitting diodes (LEDs) is attracting much attention, because of considerable market increase of disinfection application fields in human working space. In order to cut off the harmful part of the spectral range longer than 240 nm, it is desirable to develop shorter peak wavelength LEDs, i.e., LEDs with peak wavelengths between 220-225 nm. The major problem of such a short wavelength far-UVC LED is that the efficiency is too small for practical applications. In this study, we improved the external quantum efficiency (EQE) of 219-222 nm LEDs up to 0.01% level by optimizing each layer of AlGaN LED and introducing Al graded AlGaN polarization doping (PD) p-side layers. Several AlGaN quantum well (QW) LEDs with wavelengths between 219-222 nm were grown on c-plane sapphire/AlN templates by MOCVD. In this study, we attempted to realize shorter peak wavelength (near 220 nm) as well as increasing their efficiency, by shifting the optical absorption edge to shorter wavelength using a higher Al composition of n-AlGaN buffer layer. The emission peak wavelengths of the LEDs were shifted to 224.4 nm, 223.8 nm, and 221.5 nm by changing the Al composition of the n-AlGaN layer to 89%, 90%, and 91%, respectively. We also optimized the QW and p-type layers including electron blocking layer (EBL) aiming to obtain high internal quantum efficiency (IQE) and electron injection efficiency (EIE). Also we introduced undoped Al graded AlGaN PD layer with Al content linearly changed from 96% to 40% just above the undoped AlN EBL. As a result, we demonstrated the EQE of 0.01% and 0.005% for the 222 nm and 220 nm LEDs, respectively. The shortest wavelength of the LEDs was 219 nm. Obtained EQE shows relatively high value among the reported values for wavelengths shorter than 225 nm. We hope that the safety against human body of fabricated 220-222 nm LEDs would be high, since the harmful wavelength longer than 240 nm is almost cut off.

11:50 AM 4B-2.4
225 nm Band AlGaN Far-UVC LED on c-Sapphire with EQE of 0.022% M.Ajmal Khan[1,2,3], Taiga Kirihara[1,2], Mitsuhiro Muta[3], Oogami Hiroyuki[3], Kouhei Fujimoto[2], Yukio Kashima[1], Hiroyuki Yaguchi[2], Yasushi Iwaisako[3] and Hideki Hirayama[1]; [1]RIKEN, Japan; [2]Saitama University, Japan; [3]Nippon Tungsten Co., Ltd, Japan

The increasing resistance of bacteria (MERSA) to antibiotics is major challenge facing by mankind [1,2]. According to UNO report, around 700,000 patients worldwide die every year from an infection with multidrug resistant organisms (MROs) [1]. Fungi such as Candida auris become more widespread throughout the U.S. and deaths related to severe fungal infections are rising in USA [3]. Also, the expected risk of bringing a new type of bacteria and viruses from outer space by astronauts also exists. We can safely inactive such new type of germs including SARS-CoV2 in the space station by using 225nm Far-UVC LEDs. However, the emission beyond 230 nm needs some additional filter system to remove the extra shoulder of Far-UVC spectra, which is not safe for human applications and such additional filter increases the complexity of the Far-UVC module as well as the cost of UV devices. In our Lab, we are developing a short-wavelength Far-UVC LEDs with a peak wavelength shorter than 225 nm on low-cost c-Sapphire to cut off the longer-wavelength spectrum part (> 230nm), which is harmful to the human body. To achieve a short wavelength of 225 nm efficient LED, it is necessary to balance the transparency and electron conductivity of the n-AlGaN buffer layer. In this study, we investigated the Al composition optimization of the n-AlGaN layer, which is essential for achieving high efficiency in 225 nm Far-UVC LEDs. Finally, a 225 nm AlGaN-based Far-UVC LED structures on a c-Sapphire/AlN template using MOCVD (SR4000) reactor was attempted. The Al composition of Si-doped n-AlGaN layer varied from 84% to

90% and as a result the absorption edge wavelength was successfully shifted from around 229 nm to 224 nm. It has been already reported that the resistivity of Si-doped AlGaN rapidly increases with the Al composition of over 80〜85% [4]. Considering this fact, we decided that 87% or even higher Al content in the n-AlGaN is required for 225 nm Far-UVC LED. The electroluminescence (EL) and external quantum efficiency (EQE) of 225 nm Far-UVCLED by varying Al composition of the n-AlGaN layer was evaluated. It was found that EL intensity was dramatically increased by increasing the Al composition of n-AlGaN from 84 to 90%. This could be attributed to the reduction of absorption by n-AlGaN layer after increasing Al composition. Eventually a record EQE of 0.022% and light power of 0.05 mW on wafer at 225 nm emission under pulse operation at RT was achieved.

References

[1]. Political declaration on antimicrobial resistance, United Nations General Assembly, 71st session, Sept 22, 2016, Agenda item 127,A/71/L.2.
[2]. O'Neill, J., Review On Antimicrobial Resistance (London, Grande-Bretagne & Wellcome Trust (London. Antimicrobial resistance: tackling a crisis for the health and wealth of nations: December 2014. (Review On Antimicrobial Resistance, 2014). https:// wellcomeco llect ion. org/ works/ rdpck 35v.
[3]. accessed in Dec 2023: https://www.wsj.com/articles/fungi-drugs-doctors-research-104b50a6]
[4]. R.Collazo et al., Phys. Status Solidi C **8**, 2031 (2011).

12:10 PM 4B-2.5

Thermal Investigation of AlGaN UVB LED on c-Sapphire Having External-Quantum Efficiency of 10% M.Ajmal Khan[1], Javier Gonzalez Rojas[2], Pablo Fredes[2], Ernesto Gramsch[2], Yukio Kashima[1], Hiroyuki Yaguchi[3], Yasushi Iwaisako[4] and Hideki Hirayama[1]; [1]RIKEN, Japan; [2]University of Santiago, Chile; [3]Saitama University, Japan; [4]Nippon Tungsten Co., Ltd, Japan

The external-quantum efficiency (EQE) of remarkably improved AlGaN-based ultraviolet-B light-emitting diodes (UVB LEDs) is still restricted to a world record value of 10% on wafer with a relatively high thermal heat emissivity using highly transparent as well as Al-graded p-AlGaN hole-source layer (HSL) and p-AlGaN contact-layer and using reflective Ni /Al p-electrode [1,2]. Such thermal effect may degrade the life-span of the UVB LED devices for various real-world applications [3,4]. As we know that the UVB and UVC LED light sources can replace the toxic chemicals and pesticides in the farming industry because both the UVC and the UVB are based on green AlGaN materials, which can widely be used to inactivate infections of viruses, bacteria, and fungal/spore in wide range of animals, social animals, plants and vegetables. Especially, a narrow-band (NB) UVB light sources centred on 310 nm can be deployed for: cancer immunotherapy; the treatment of vulgaris, psoriasis, and atopic dermatitis; and plant growth with enriched phytochemicals. In addition, emitters centred around the slightly shorter wavelength of 294 nm can be used to prevent plant diseases, attack the tomato mosaic virus, and produce vitamin D_3 in the human body [1-2]. However, the highly efficient UVB LEDs are confronted with high junction temperature. To remove such problematic thermal heat from the UVB LED, first we need to know the scenario of junction temperature. Therefore, in this work an experimental temperature of the bare chip on p-contact surface side of UVB LED are investigated. This study also shows the empirical thermal scenario on the p-contact of the 304 nm-band UVB LED and proposes a methodology to estimate the temperature values of the active region (T_J) in the semiconductors heterostructure. Thermal management of UVB LEDs by enhancing heat transfer in both vertical and lateral directions is a key design parameter at both the package and system levels. A 304nm-band AlGaN UVB LED on wafer with EQE of 10% and maximum light power of 42 mW is analyzed for its junction temperature, using thermal camera FLIR C5TM from a distance of approx. 10 cm. The thickness and area of the LED are known. The temperature of the bare chip around the p-AlGaN contact-layer at various levels of current drive with an increment of 20 mA from 0 to 120 mA is investigated. It was found that the temperature of UVB LED increases linearly with increasing of input current drive and quite high thermal emissivity of heat approximately ~ 64 °C under 120 mA is observed. The estimation of the thermal impedance can be computed using the previously known data of the thermal properties of the material components of each layer in LED heterostructure [2,3]. The thickness and area of the LED are known. By using the surface area of 100 × 100 μm^2 (p-contact region) the junction temperatures of 80 °C is estimated using the known temperature of 64 °C around the p-contact region of UVB LED.

It is of no surprise that these low-cost UVB devices on c-Sapphire are overshadowed by their blue cousins. But still the performance of UVB LEDs is restricted by low light extraction efficiency (LEE) of 14%, by low IQE of 57% and by low hole injection toward the MQWs [1,2]. Recently, a simultaneous effect of an optimized hole type nano-patterned sapphire substrate (nanoPSS) and photonic crystal (PhC) in p-AlGaN contact layer for flip-chip AlGaN-based UVB LED has been investigated and the theoretical light extraction was remarkably enhanced up to 150%. More than 21% of EQE is expected using such approaches of better thermal management system and better optical model of nanoPSS and PhC in the AlGaN UVB LEDs.

References

1). Khan et al. Sci Rep **12,** 2591 (2022).
2). Khan et al. Phys. Status Solidi A, 2300581 (2024).
3). Fredes et al. Microelectron. Reliab. **98**, 24–30, (2019).
4). Shatalov et al. Appl. Phys. Lett. **86**, 20, 1–3 (2005).

SESSION 4C-1: Ga_2O_3 Epitaxy and Characterization
Session Chair: Hongping Zhao
Thursday Afternoon, May 16, 2024
Resort Tower, Ground Level, Bronze Room 1

2:00 PM 4C-1.1
Highly Uniform β-Ga_2O_3 Epitaxial Growth on Sapphire and Native Substrates by MOCVD Aadil Waseem[1], Clifford McAleese[2], Omar Salwan[3], Andrew Pakes[2] and Xiuling Li[1]; [1]The University of Texas at Austin, United States; [2]Aixtron, United Kingdom; [3]Aixtron Inc, United States

Monoclinic β-phase gallium oxide (β-Ga_2O_3) is a wide bandgap oxide semiconductor with an estimated breakdown field of ~8 MV/cm. It has high transparency in the visible and UV wavelength regions. It is an emerging semiconducting material for a wide range of applications in the realm of power semiconductor devices, deep ultraviolet (UV) solar-blind photodetectors, and high-temperature gas sensors. With its remarkable ultrawide bandgap of ~ 4.9 eV and an impressive Baliga figure-of-merit of 3400, β-Ga_2O_3 exhibits substantial promise for harnessing high-power electronic devices and UV photodetector technologies. In contrast to third-generation wide bandgap semiconductors like GaN and SiC, the unique advantage of β-Ga_2O_3 lies in its capacity for single crystal growth of native substrate via conventional techniques, including the floating zone (FZ) process and the Czochralski process. Using the newly commissioned Aixtron CCS MOCVD reactor at the University of Texas at Austin, we have demonstrated heterogeneous epitaxy of β-Ga_2O_3 on sapphire substrates, which are still much cheaper than the native substrates, and the homoepitaxy of β-Ga_2O_3 on (010) native substrates.
It is well known that the considerable lattice mismatch between β-Ga_2O_3 and sapphire, owing to their disparate crystal systems, has resulted in the formation of multiple types of β-Ga_2O_3 crystal grains on sapphire substrates during the nucleation stage, giving rise to a high density of dislocations [1,2]. In this work, we first explore the precise tuning of growth parameters to achieve the state-of-the-art crystal quality of β-Ga_2O_3 thin films on on-axis and 6° off-angled c-plane sapphire substrates. Our exploration extended to the nuanced influence of substrate anneal temperature, nucleation temperature, growth temperature, and reactor pressure on the crystalline perfection of β-Ga_2O_3 epitaxial films. The specific emphasis was on the effect of growth parameters on the diffusion of Ga adatoms and the attainment of step-flow growth.
For growth on sapphire substrate, XRD scans for the (-201) reflection indicate that the phase pure β-Ga_2O_3 films of 0.6 µm thick exhibit state-of-the-art FWHMs values of 2,834 for on-axis and 1,755 arcsec on sapphire substrates that are on-axis and 6° offcut toward <1-100> direction, respectively. Over a 2-inch wafer, a thickness uniformity of less than 1% has been demonstrated. SIMS of the layers grew under suitable conditions using TMGa show carbon (C) levels around or below the detection limit of $1x10^{17}$ cm^{-3} and Si levels at the low 10^{15} cm^{-3}. Note that N2 instead of the more popular argon carrier gas was used, and the films grown using N_2 carrier gas showed no detectable nitrogen incorporation. Offcut sapphire substrate exhibited enhanced crystal quality because the atomic steps on the surface of such off-angle substrates serve as preferential bonding sites for adatoms, facilitating step flow growth and improving film quality.
For growth on (010) Fe-doped native substrate, XRD indicates that the lattice matched films were obtained. A room temperature Hall mobility of 134 cm^2/Vs at a carrier concentration of $3.2x10^{16}$ cm^{-3} has been achieved. In the case of Si-doped layer, a room temperature Hall mobility of 148 cm^2/Vs has been achieved at a carrier concentration of 1.26 x 10^{17} cm^{-3}, with growth rate of 2.6 µm/hr.
In summary, we have achieved highly uniform and high quality β-Ga_2O_3 epitaxial growth on sapphire and native substrates by a Aixtron CCS MOCVD. Detailed growth parameter space mapping and their effect on the film quality will be presented.
References
[1] R.-H. Horng, D.-S. Wuu, P.-L. Liu, A. Sood, F.-G. Tarntair, Y.-H. Chen, S.J. Pratap, C.-L. Hsiao, Mater. Today Adv. 16 (2022) 100320.
[2] T.C. Ma, X.H. Chen, Y. Kuang, L. Li, J. Li, F. Kremer, F.-F. Ren, S.L. Gu, R. Zhang, Y.D. Zheng, H.H. Tan, C. Jagadish, J.D. Ye, Appl. Phys. Lett. 115 (2019) 182101.

2:20 PM 4C-1.2
Electrical, Micro-Structural and Thermal Properties of Epitaxial Ga_2O_3:Si Grown by MOCVD on GaN/Sapphire and Bulk Ga_2O_3 Substrates Emma Rocco[1], Michael Liao[2], Daniel Pennachio[3], James S. Lundh[1], Hannah Masten[1], Marko Tadjer[3], Michael Mastro[3] and Jennifer Hite[4]; [1]NRC Postdoctoral Associate residing at the U.S. Naval Research Laboratory, United States; [2]Apex Microdevices, United States; [3]U.S. Naval Research Laboratory, United States; [4]University of Florida, United States

Towards extending the performance of high-power, high-frequency electronics and solar-blind photodetectors, Ga_2O_3 materials are likely to be employed in the next generation of devices. Among its advantageous material properties, the β-phase of Ga_2O_3 possesses an ultra-wide band gap energy of 4.8 eV, as well as a critical electric field estimated to be 8 MV/cm. As a result, the Baliga figure of merit for β-Ga_2O_3 is higher than that of GaN and SiC. Technological developments are needed to address fundamental challenges in order to realize the full potential of β-Ga_2O_3 devices. The low thermal conductivity (11-17 W/m-K) and lack of efficient p-type dopants in β-Ga_2O_3 has thus far limited the attainable device structures and geometries.

The formation of an n-Ga_2O_3/p-GaN heterojunction may be advantageous to overcome the difficulties of p-type doping and thermal conductivity in Ga_2O_3. Towards this goal, we report here, for the first time, epitaxial growth of Ga_2O_3:Si films by metal organic chemical vapor deposition (MOCVD) on Ga- and N-polar GaN/sapphire, as well as comparison to growth on bulk β-Ga_2O_3 substrates. Ga- and N-polar GaN templates were grown by MOCVD using a Veeco D180

reactor dedicated to III-nitride materials. All β-Ga_2O_3 films were deposited in an Agnitron Agilis 500 oxide MOCVD using triethylgallium (TEGa) and O_2 precursors. By varying the Ga_2O_3 n-type dopant precursor, silane (SiH_4), molar flow rate we report controllability of the carrier concentration in a range from 3.4 x 10^{18} cm^{-3} to 3.6 x 10^{20} cm^{-3} for Ga_2O_3:Si films grown on bulk (010) β-Ga_2O_3 substrates. Prior to transitioning to the growth of Ga_2O_3:Si on GaN, first unintentionally doped (UID) Ga_2O_3 films were grown by MOCVD on both Ga- and N-polar GaN/sapphire templates. The resulting UID Ga_2O_3/GaN structures were interrogated with x-ray diffraction (XRD). The Ga_2O_3 films grown on Ga-polar or N-polar GaN GaN exhibits a 6-fold in-plane rotation of the {-201} grains. For the Ga_2O_3 film grown on N-polar GaN an additional 6-fold rotation is observed. Finally, Si-doped Ga_2O_3 films were grown on Ga- and N-polar GaN templates. We will present the electrical properties of the Ga_2O_3:Si films on Ga- and N-polar GaN with comparison to that grown on the bulk Ga_2O_3 substrates, as determined by Hall effect and Lehighton measurements. An assessment of the microstructure and morphology of these films will be shown by XRD and AFM, and we will discuss the influence of the microstructure on the electrical performance. Toward assessing the thermal performance of structures containing Ga_2O_3:Si, thermoreflectance measurements will be reported for Ga_2O_3 structures grown on GaN/sapphire and compared to Ga_2O_3 on bulk (010) β-Ga_2O_3 substrates.

2:40 PM 4C-1.3
Recent Advances in Uniform Growth and Doping of β-Ga_2O_3 Using MOVPE William Brand, Fikadu Alema and Andrei Osinsky; Agnitron Technology, United States

β-Ga_2O_3 has become a focal point of semiconductor research for application in power electronics due to its large bandgap of ~ 4.9 eV, estimated high breakdown field of ~ 8 MV/cm, and availability of melt grown high-quality β-Ga_2O_3 substrates. The growth of high-quality epitaxial β-Ga_2O_3 films with low dislocation density and background impurities on top of native substrates is critical to realize high-performance power electronic devices. Among the available epitaxial techniques, metal organic vapor phase epitaxy (MOVPE) has proven suitable for producing high-quality epitaxial β-Ga_2O_3 films at a fast growth rate with controllable doping. High-purity homoepitaxial β-Ga_2O_3 films with low-temperature (LT) electron mobility ranging between 10,000 cm^2/Vs and >23,000 cm^2/Vs, and residual acceptor concentrations extracted from charge neutrality fitting as low as 2×10^{13} cm^{-3} have been demonstrated. This high LT e-mobility obtained from MOVPE β-Ga_2O_3 is >8x and >4x higher than the best values reported by MBE and by HVPE, respectively, and is ~2-3x higher than the state-of-the-art LT mobility values of the best SiC and GaN bulk films [1, 2].

In this work, we will present recent advancements in Ga_2O_3 growth, employing an innovative close injection showerhead (CIS) design. Achieving uniform thickness and doping across wafer diameters of 2 inches and beyond has been successfully realized using both Trimethylgallium (TMGa) and Triethylgallium (TEGa) through a wide range of process conditions. With the introduction of this novel showerhead design, we have attained growth rates of up to 20 µm/hr with TMGa, while maintaining thickness non-uniformity of <1%. Process conditions such as growth temperature, chamber pressure, and precursor molar flow for the growth of β-Ga_2O_3 will be discussed. Comparisons between TMGa and TEGa growth techniques and film characteristics will also be accessed. A systematic study of RMS roughness on films up to 5 µm display values of <1nm, making them suitable for kV class vertical power device fabrication. Miscut substrates have shown RMS roughness <0.6 nm for layers >5 µm. Carrier concentrations from 1E14 to 3E20 were achieved using various dopants and growth conditions. We will compare the use of Silane, Disilane, and Germane for uniform film doping. The effect of carbon concentration on room temperature (RT) and LT mobility as well as methods to manage its incorporation will be discussed. The underlying purity of both precursors will also be examined, specifically pertaining to background silicon concentrations of unintentionally doped (UID) layers.

[1] G. Seryogin, Appl Phys. Lett. 117, 262101 (2020).
[2] F. Alema, Compound Semiconductor Mag. 28, 16 (2022).

3:00 PM 4C-1.4
Photoluminescence Mapping of Defects in β-Ga_2O_3 Epilayers Matthew D. McCluskey[1,2], Jesse Huso[2], Cassandra Remple[1], John McCloy[1], Arkka Bhattacharyya[3] and Sriram Krishnamoorthy[3]; [1]Washington State University, United States; [2]Klar Scientific, United States; [3]University of California, United States

Monoclinic gallium oxide (β-Ga_2O_3) is an ultrawide bandgap semiconductor with potential applications in power electronics. Photoluminescence (PL) spectroscopy is an important method to characterize dopants and defects in this material. Common features in the PL spectrum include the intrinsic UV band, blue and green bands that involve donor-acceptor pairs, and red emission due to Cr^{3+} impurities. Subtle changes in the spectra, revealed by peak fitting, can reveal defects and inhomogeneities with high sensitivity.

PL mapping with excitation wavelengths ranging from 266 to 532 nm reveals the spatial distribution of these features with submicron resolution. Homoepitaxial layers grown by metalorganic chemical vapor deposition (MOCVD) show defects that are observed via the shifts in the PL band, likely due to the strain field around a dislocation core. Damage due to high-intensity, sub-bandgap laser pulses results in a drop in the intensity of the UV band. A ring or “halo” around the damaged region is observed under 532 nm excitation. This visible PL emission may be due to a color center, such as oxygen interstitial, that was created by the damage process.

3:20 PM *4C-1.5
β-Gallium Oxide Metal Organic Vapor Phase Epitaxy for Lateral and Vertical Power Devices Sriram Krishnamoorthy; University of California, Santa Barbara, United States

This work focuses on growth, doping, epitaxial stack engineering, and characterization of β-Ga_2O_3 thin films and heterostructures for lateral devices and thick epitaxial drift layers for vertical power devices. β-Ga_2O_3 is an emerging ultra-wide bandgap (UWBG) semiconductor material that offers projected size, weight, and power (SWaP) performance advantage over the incumbent power semiconductors for solid-state power switching applications due to its high breakdown field strength (~ 8 MV/cm). We demonstrate a large growth window for this material, including electronic grade material quality at a growth temperature of 600°C , which also enables low resistance regrown Ohmic contacts and growth on composite substrates for thermal management. We demonstrate a hybrid low temperature - high temperature (LT-HT) buffer/channel stack growth using MOVPE with record carrier mobility values (range of 196–85 cm^2/V s) over four orders of doping range ($2\times10^{16} – 1\times10^{20}$ cm^{-3}). The improvement in transport properties was achieved mainly by realizing pristine doped channels, eliminating undesired parasitic conduction paths, and minimizing carrier compensation. In this work, we will also discuss growth of thick epitaxial drift layers for vertical high voltage devices with high growth rates, low background carrier concentration and record drift layer mobility. We will also highlight growth of modulation-doped Aluminum Gallium Oxide/ Gallium Oxide heterostructures with the first demonstration of pure 2DEG grown by MOCVD. We also highlight advances in high field strength in-situ MOCVD dielectrics. Rapid advances in the material growth and device demonstrations show pathways for achieving epitaxial films with exceptional transport properties and designing next-generation medium-to-high voltage Ga_2O_3 low-loss power devices.

3:50 PM BREAK

SESSION 4C-2: Nitride LD
Session Chair: Hideto Miyake
Thursday Afternoon, May 16, 2024
Resort Tower, Ground Level, Bronze Room 2

2:00 PM *4C-2.1
Advancements in AlGaN-Based Laser Diodes on AlN Substrates Maki Kushimoto[1], Zhang Ziyi[1,2], Akira Yoshikawa[1,2], Koji Aoto[1], Yoshio Honda[1], Leo Schowalter[1], Chiaki Sasaoka[1] and Hiroshi Amano[1]; [1]Nagoya University, Japan; [2]Asahi Kasei Corporation, Japan

The AlGaN-based deep ultraviolet laser diode (LD) is anticipated for various applications such as sterilization, sensing, and laser processing, due to its compact size, high efficiency, and environmentally friendly deep ultraviolet laser light source. Our research group has been conducting device studies using single-crystal AlN substrates to achieve LDs in the UV-C wavelength range (wavelengths from 200 nm to 280 nm). Significant breakthroughs, including high-quality AlGaN thin film crystals grown on single-crystal AlN substrates and control of p-type conductivity using dispersion polarization doping, have led to the demonstration of room-temperature pulsed lasing [1].
However, the demonstrated device's threshold current density and voltage were high, at 25 kA/cm2 and 13 V, respectively. In order to attain continuous wave lasing at room temperature, we took additional measures to decrease the threshold gain by enhancing optical confinement. Simultaneously, we improved the threshold current density and reduced the driving voltage. Our investigation also delved into addressing the defects that emerged during the fabrication of the device, a previously encountered design limitation [2]. Upon meticulous analysis, we identified the defects as dislocations resulting from localized residual shear stresses during the mesa formation on a highly strained epitaxial layer. Consequently, we developed a model to assess the stress distribution at the mesa stripe's edge and demonstrated a technique to mitigate local shear stress concentration by employing a tilted mesa geometry [3]. With these modifications, the device now achieves a threshold current density of 3.0 kA/cm^2 during pulsed current operation. Furthermore, the packaged device has successfully achieved CW lasing under direct current operation with a threshold current density of 4.2 kA/cm^2 and a threshold voltage of 8.7 V [4]. This presentation provides an overview of the deep ultraviolet LD device research results in our group, discussing key technologies that played a crucial role in these achievements.

References
[1] Z. Zhang *et al.*, *Appl. Phys. Express* **12**, 124003 (2019)
[2] M. Kushimoto *et al*., *Appl. Phys. Express* **14**, 051003 (2021)
[3] M. Kushimoto *et al*., *Appl. Phys. Lett.* **121**, 222101 (2022).
[4] Z. Zhang *et al*., *Appl. Phys. Lett.* **121**, 222103 (2022).

Acknowledgement
This work was supported by JSPS KAKENHI Grant Number 21H04560.

2:30 PM 4C-2.2
Formation of Sharp Heterojunction Interface Between P-Side Waveguide Layer/P-Electron Block Layer of AlGaN-Based UV-B Laser Diodes by MOVPE Growth and Its Effect on Device Characteristics Takumu Saito[1], Ryosuke Kondo[1], Rintaro Miyake[1], Ryoya Yamada[1], Yoshinori Imoto[1], Shundai Maruyama[1], Toma Nishibayashi[1], Eri Matsubara[1], Yusuke Sasaki[1], Sho Iwayama[1], Hideto Miyake[2], Tetsuya Takeuchi[1], Satoshi Kamiyama[1] and Motoaki Iwaya[1]; [1]Meijo University, Japan; [2]Mie University, Japan

We have achieved room-temperature (RT) pulsed oscillation by growing AlGaN-based UV-B laser diodes (LDs) on the lattice-relaxed high-quality AlGaN templates using the

MOVPE method and processing the wafers. Meanwhile, the device contains heterojunction interfaces with large compositional differences, with a maximum value of 0.55 between the p-side AlGaN waveguide layer and the p-AlGaN electron blocking layer (EBL). Such a large Al composition difference makes it difficult to form a sharp heterojunction interface due to the composition pulling effect. The sharpness of the interface is reduced even in UV-C LDs with a small difference in Al composition, and it has been reported that a sharp interface is formed by lowering the growth temperature below 1000°C only in the 60-nm region adjacent to the interface with the core layer of the p-cladding layer [1]. In this study, we investigated the dependence of the sharpness of the heterojunction interface between the waveguide layer and the EBL of UV-B LDs on the crystal growth temperature of MOVPE and the device characteristics of UV-B LDs prepared under such growth conditions.

In this experiment, the structure reported in ref. 2 was used as the reference structure. The crystal growth temperature in this discussion is the susceptor surface temperature obtained using a pyrometer. In the experiment, after crystal growth of the n-AlGaN cladding layer at 1,100°C, the n-side AlGaN waveguide layer and the two-period quantum well active layer were stacked at 1,000°C. In this experiment, we continued to use wafers stacked at 1,000°C as a reference and compared two types of wafers: one in which only the EBL were stacked at low temperature, and the others in which both the p-side waveguide layer and the EBL were stacked at low temperature. After growing the EBL, the growth temperature after the p-AlGaN cladding layer was kept constant at 1000°C. The sharpness of the interface was evaluated by Z-contrast image of the cross-sectional transmission electron microscope (TEM) and EDX measurement. In addition, the fabricated wafers were processed into gain-waveguide LDs and device characteristics were compared. The effect of heterointerface sharpness was also investigated using a device simulator, SiLENSe.

As a result, we found that lowering the growth temperature of both layers was effective in forming relatively sharp interfaces. When both layers were formed at 1000°C, TEM analysis showed that a region of varying Al composition with a film thickness of ~26 nm, which we call the pulling layer, was formed, suggesting that this appeared due to the composition pulling effect. Similar to ref. 1, it was confirmed that lowering only the EBL layer growth temperature decreased the thickness of the pulling layer. However, even though the temperature was drastically lowered to 650°C, the thickness of the extraction layer was limited to ~15 nm. Meanwhile, when the growth temperatures of both layers were lowered, the thickness of the pulling layer was reduced to ~11 nm even when crystals were grown at the relatively high temperature of 850°C. Furthermore, differences in device characteristics were also observed. Comparing the intensity of spontaneous emission measured from the sapphire substrate side at the same current value under RT-pulsed driving, the integrated light intensity increased by ~1.8 times when both layers were grown at 850°C compared to the reference sample in which both layers were grown at 1000°C. These results are also confirmed to be theoretically explainable, since they are equivalent to the carrier injection efficiency increase rate obtained by simulation. The LD in which both layers were grown at the temperature of 850°C was evaluated by RT-pulse driving, and was confirmed to oscillate at a threshold current density of about 16 kA cm^{-2} at a wavelength of 305 nm.

2:50 PM 4C-2.3

Growth and Analysis of Ultraviolet Laser Diodes of High AlN-Mole-Fraction AlGaN Heterostructure on Non-Planar GaN Substrates with Topography Induced Crack Suppression via Anisotropic Strain Relaxation Yuto Ando[1], Zhiyu Xu[1], Theeradetch Detchprohm[1], Preston Young[2] and Russell Dupuis[1]; [1]Georgia Institute of Technology, United States; [2]Photodigm Inc., United States

We have investigated and developed crack-suppression techniques for the epitaxial growth of heterostructures containing thick strained lattice-mismatched layers and applied this technology to the growth of $Al_xGa_{1-x}N$ layers having a relatively high AlN-mole-fraction grown on *c*-plane GaN substrates. This technology employs 3D surface topographic features with a geometry suitable for the growth of ultraviolet laser diodes [1][2]. In this non-planar growth (NPG) scheme, microns-tall mesa stripes with various widths of tens to hundreds of microns were implemented on GaN substrates. Subsequently, metalorganic chemical vapor deposition (MOCVD) was used to grow InGaN/AlGaN-based heterostructures for UV-A laser diodes (LDs)[3]. This NPG approach facilitates anisotropic in-plane strain mitigation allowing the tensile in the mesa stripes to be partially relaxed along the direction parallel to the stripe while the strain along the direction perpendicular to the stripe is gradually diminished toward the stripe edge. Using this approach, cracking of thick high-AlN-mole-fraction AlGaN layers can be effectively reduced on the mesa stripes for narrower stripe widths or taller mesa heights [1][2]. For example, derived from X-ray reciprocal space mapping of the (1-105) and (-1-124) reflexes of 1.5mm thick AlGaN short-period superlattice layers with an average AlN-mole-fraction of 0.18, grown on 100mm-wide NPG mesas, the strain relaxation was found to be ~53% and ~93% for directions parallel and perpendicular to the stripes, respectively. As a result, UV-A LDs can be grown with high AlN-mole-fraction AlGaN cladding layers much thicker than the critical layer thickness reported for the growth of the same AlGaN layers on a planar GaN surface. A demonstration of UV-A LD NPG epitaxy with an $In_{0.02}Ga_{0.98}N/Al_{0.07}Ga_{0.93}N$ quantum-well active region and $Al_{0.09}Ga_{0.91}N$ waveguide layers sandwiched between 600nm thick $Al_{0.16}Ga_{0.84}N$ cladding layers was successfully carried out on patterned GaN substrates having ~6mm tall mesa stripes parallel to the *m*-axis of GaN. The strain relaxion in the full LD device structure was observed to be ~20% and ~90% for direction parallel and perpendicular to the 100 mm wide mesa stripes, respectively. The wafers were fabricated into cleaved-facet Fabry-Perot LDs with various ridge widths, e.g., 6, 12, and 20 mm for cavity lengths of 500, 750, and 1000 mm. Laser operation at 300K was confirmed with uniform emission peak wavelength around 372+/-2nm under pulsed conditions, e.g., 100 ns pulses at a 0.01%duty cycle. LD

threshold current densities were 9-16A/cm^2 for LDs having a 1000 mm cavity length. More detailed results will be presented.
[1] F. Mehnke *et al.*, J. Appl. Phys. **131**, 073103 (2022)., [2] Y. Ando *et al.*, J. Cryst. Growth **607**, 127100 (2023)., [3] Y. Ando *et al.*, Appl. Phys. Lett. **123**, 130401 (2023).

3:10 PM 4C-2.4
InGaN Laser Diodes with Higher Optical Gain Enabled by a Strain Relaxed Template with Reduced Threading Dislocation Density Hsun-Ming Chang, Vincent Rienzi, Norleakvisoth Lim, Michael Gordon, Steven P. DenBaars and Shuji Nakamura; UC Santa Barbara, United States

In this work, we experimentally demonstrate electrically driven c-plane InGaN blue edge emitting laser diodes (EELDs) with higher optical gain on a strain relaxed template (SRT) with reduced threading dislocation density (TDD). Moreover, a lower threshold of EELDs on the SRT than those on freestanding GaN substrate is achieved for devices with cavity shorter than 900 µm due to the higher material gain enabled by SRT and its lower TDD compared to previous work.
Although strain relaxation technology is promising for InGaN emitters, so far most of the devices demonstrated utilizing strain relaxation methods are still limited to light-emitting diodes (LEDs), and very few have discussed about the crystalline quality, which plays a highly crucial role in LDs. Here, we successfully developed a new SRT with TDD reduced by more than 1 order of magnitude while still generating comparable relaxation degree of the InGaN film. Cathodoluminescence (CL), atomic force microscopy (AFM) and X-ray diffraction (XRD) are performed to characterize the SRT and the InGaN layers above. Compared to previous work, we successfully reduce the TDD of SRT from > 1E9 to <1E8 cm^{-2}, where an in-plane lattice constant of 3.192 Angstrom of the InGaN buffer grown above is achieved. Moreover, relaxation degree of InGaN over 50% is also successfully demonstrated by optimizing the growth, which is comparable to our previous work.
Blue LD structure is grown on the new SRT, where from the on-wafer external quantum efficiency (EQE) versus current density characteristics it exhibits higher peak EQE than previous SRT EELD samples. Furthermore, the peak EQE positioned at a lower current density, indicating a lower non-radiative recombination rate, which is also in accordance with the reduced TDD. All EELDs on the previous SRT, new SRT, and freestanding GaN substrate are fabricated and tested. EELDs on the new SRT demonstrate superior performance to previous SRT – a low threshold of 7.4 kA/cm^2 is achieved compared to the high threshold of above 40 kA/cm^2 previously. Furthermore, from amplified spontaneous emission (ASE) measurement, the internal loss also exhibits significant improvement from 30 – 35 cm^{-1} to 8 – 10 cm^{-1}. The improved LD characteristics are credited to the following: first, the reduced TDD and consequently a higher IQE, and second, the reduced mode leakage into the highly optically absorptive strain relaxed layer and therefore a lower internal loss. To compare with EELDs directly grown on freestanding GaN substrate without the SRT, the threshold current density versus cavity lengths is plotted. It is found that the threshold increased slower for EELDs on the new SRT as the cavity length decreases. Moreover, the threshold of EELDs on the new SRT outperforms that on freestanding GaN substrate at 900 µm cavity length. Various stripe length method is performed to extract the laser parameters, and the gain at threshold versus injected current density is plotted. A more than 1.5x higher material gain is demonstrated in EELDs on the new SRT, which explains the slower increase in threshold as cavity length reduces and eventually a lower threshold at 900 µm. Despite a small degree of relaxation by the new SRT in this work, a higher gain can still be realized. We attribute this to the locally unidirectional strain relaxation, which can cause symmetry breaking in valence band, and therefore a reduced density of states and higher optical gain.
In summary, this work presents a new SRT with TDD reduced by more than 1 order, and the promising properties of InGaN EELDs grown on it. With the new SRT, the characteristics of laser diodes are greatly improved compared to our previous SRT work. In addition, due to the higher material gain enabled by the strain relaxation, lower threshold is achieved for EELDs on the new SRT than those directly on freestanding GaN without the SRT as cavity length reduces to 900 µm.

3:30 PM BREAK

ICM VPE XXI

2024 Las Vegas, NV

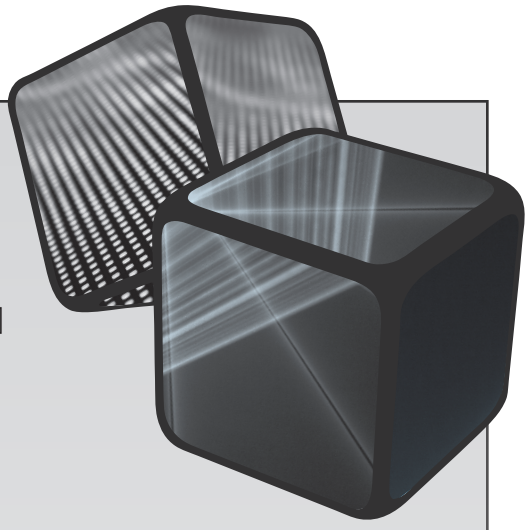

THURSDAY

Poster Presentations

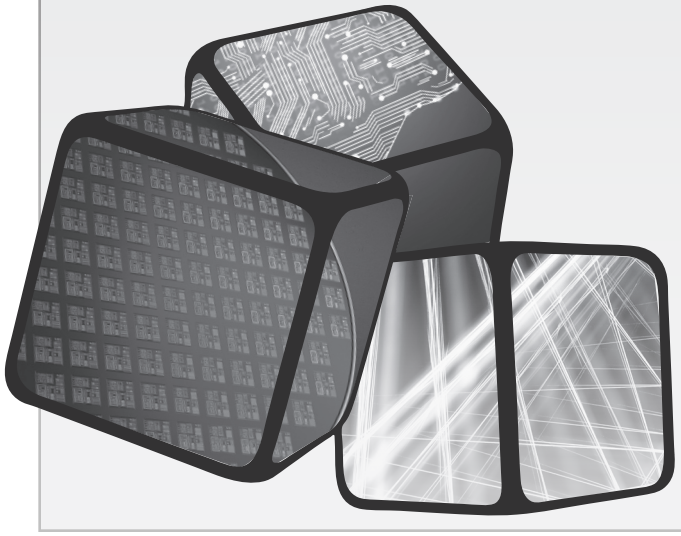

PS-2.1
Low-Temperature Growth of 2D-MoS2 Thin Films by Plasma-Enhance Atomic Layer Deposition Using New Molybdenum Precursor Ji-Hoon Ahn and Woo-Hee Kim; Hanyang University, Korea (the Republic of)

Layered two-dimensional molybdenum sulfide (MoS2) has attracted great interest for a promising candidate material for opto-electronics and photo sensors applications due to its unique characteristics such as tunable bandgap, high electron mobility and high current on/off ratio. In order to apply MoS2 to the industrial field, significant efforts have been placed in obtaining a wafer-scale uniform MoS2. Plasma-enhanced atomic layer deposition (PEALD) is a promising approach for depositing a 2D-MoS2 because of its excellent thickness control. However, the low growth temperature of PEALD makes it difficult to guarantee the quality of the MoS2 thin films. In the present study, to overcome this limitation, Cp based molybdenum precursor was used for the PEALD of MoS2 thin films. This novel precursor with high thermal stability resulted in MoS2 thin films with high crystallinity without post thermal treatment. The composition and crystallinity of MoS2 thin films depends on the PEALD process conditions were investigated by X-ray photoelectron spectroscopy and transmission electron microscopy. Furthermore, through fabricating the field-effect transistors, the potential of MoS2 for electric device component was investigated.

PS-2.2
MOVPE Growth of III/V Nanowires on β-Ga_2O_3 Substrates Mahesh Gokhale, Emroj Hossain, Bhagyashree A. Chalke, Nilesh Kulkarni, Arnab Bhattacharya and Amit P. Shah; Tata Institute of Fundamental Research, India

β-Ga_2O_3 is a conductive wide-bandgap semiconductor with a monoclinic crystal structure which can be used as a substrate for growth of semiconductor optoelectronic devices [1,2]. Lot of work has been done on the growth and optimization of planar GaN layers on β-Ga_2O_3, however, there is much less reported on the growth of nanowires on β-Ga_2O_3. Recently, we have synthesized (100)-oriented single crystal β-Ga_2O_3 using the optical float zone technique [3] and we use thin cleaved slices of these crystals as substrates for nanowire (NW) growth. We have attempted the growth of nanowires of several III-V semiconductors such as GaAs, InAs, and GaP on β-Ga_2O_3 substrates via MOVPE using the catalyst-mediated (VLS) technique. The NWs were grown using 5 nm diameter Au colloidal particles as catalyst, and the growth parameters: temperature (400 ^{0}C to 500 ^{0}C) and V/III ratio (20 to 100), varied to check the influence on NW growth. For all materials, NWs with length of ~10 μm and diameter < ~100 nm can be obtained. The NWs were characterized using GIXRD measurements and electron microscopy studies for crystal structure, and PL/Raman spectroscopic measurements for optical characterization.

1] S. Stepanov et al., *Rev. Adv. Mater. Sci*. **44** (2016) 63
2] S. Pearton et al., *Appl. Phys. Rev.* **5** (2018), 011301
3] E. Hossain et al., *ECS J. Sol. Stat. Sci. Technol.* **8** (2019) Q 3144.

PS-2.3
Heterogeneous Integration of Telecom C-Band Emitting Quantum Dots on Silicon Photonics Platform by Adhesive Bonding Michael Jetter, Ponraj Vijayan, Fiona Braun, Robert Sittig, Stephanie Bauer, Simone Luca Portalupi and Peter Michler; University of Stuttgart, Germany

Silicon photonics for telecommunications applications has garnered much attention in recent decades. The optical transparency and the large refractive index contrast of silicon in the telecommunication wavelengths allow the implementation of high-density photonic integrated circuits. The drawback of silicon photonics is that there is no native efficient light source due to the indirect band-gap nature of silicon. Integration of III-V material, which offers outstanding optical emission properties, on silicon, provides a potential solution. The direct growth of III-V materials on silicon is the most desired approach because it is economically favorable. However, it is challenging because of the large lattice mismatch between the III-V materials and silicon. An alternative approach for large-scale integration is through heterogeneous integration of III-V membrane using adhesive bonding technique. For such integration, it is crucial to have a robust bonding procedure that provides a uniform bonding layer with a desired thickness and to employ a coupling scheme that can maximize the light coupling between III-V active layer and the silicon photonic platform.
Our group has previously developed InAs QDs/InGaAs MMB/GaAs substrate structures for long-distance optical fiber applications. In this contribution, we will report on the integration of the InGaAs-based layer which embeds single telecom C-band InAs QDs usable for photonic quantum implementations on a silicon platform through adhesive bonding. We also discuss the route to fabricate InGaAs waveguides to effectively couple the QDs emission into silicon platform through evanescent coupling schemes.

PS-2.4
Integration of Telecom C-Band Emitting InAs Quantum Dots on Si Platform Based on Direct Bonding of Membrane and Epitaxial Regrowth Michael Jetter[1], Ponraj Vijayan[1], Robert Sittig[1], Marco Werner[2], Jakob Hirlinger-Alexander[3], Sergej Vollmer[1], Matthias Seibold[2], Stephanie Bauer[1], Fiona Braun[1], Simone Luca Portalupi[1] and Peter Michler[1]; [1]University of Stuttgart, Germany; [2]Twenty-One Semiconductors GmbH, Germany; [3]University of Ulm, Germany

Silicon photonics for telecommunications applications has garnered much attention in recent decades. The optical transparency and the large refractive index contrast of silicon in the telecommunication wavelengths allow the implementation of high-density photonic integrated circuits (PICs). The drawback of silicon photonics is that there is no native efficient light source due to the indirect band-gap nature of silicon. Integration of III-V material, which offers outstanding optical emission properties, on silicon, provides a potential solution. The direct growth of III-V materials on silicon is the most desired approach because it is economically favorable. However, it is challenging because of the large lattice mismatch between the III-V materials and silicon. An alternate monolithic approach for large-scale integration of III–V materials is through heterogeneous integration of thin III-V membrane using a direct bonding technique followed by an epitaxial regrowth. This integration scheme is promising because it can overcome the challenges of the conventional monolithic integration approach, such as the high-density threading dislocation and anti-phase domain.
Our group has previously developed InAs QDs/InGaAs MMB/GaAs substrate structures for long-distance optical fiber applications. In this contribution, we will report on the integration of the telecom C-band emitting InAs QDs on a silicon platform utilizing this direct bonding followed by the epitaxial regrowth method mentioned above. We demonstrate that the InAs QDs grown on GaAs/Si substrate have crystal quality and optical properties comparable to the one grown on standard GaAs substrate which paves the way for establishing high density III-V/Si PICs in the future.

PS-2.5
Transition Metal Dichalcogenide Nanowires for Highly Efficient Hydrogen Evolution Reaction Hyeonkyeong Kim and Youngdong Yoo; Ajou University, Korea (the Republic of)

Transition metal dichalcogenides (TMDs) have great potential as effective catalysts for hydrogen evolution reaction (HER). TMDs have important advantages as HER catalysts, such as near-zero Gibbs free energy of adsorbing hydrogen atoms, large surface area, and relatively low cost. However, due to the limited number of active sites and low electrical conductivity, TMDs have reported relatively low catalytic performance compared to their electrocatalytic potential. Here we report for the synthesis of dense TMD nanowires grown vertically on conductive carbon cloths through a chemical vapor deposition method. The vertically aligned TMD nanowires maximize exposure of active sites. The TMD nanowires have an excellent Tafel slope and good mechanical long-term stability in the HER. Our results present a facile strategy for fabricating vertically aligned TMD nanowires for efficient electrochemical catalysis.

PS-2.6
Designing Surface Chemistry of Colloidal Nanocrystals for Wearable Electronics Seoyeon Park and Ji-Hyuk Choi; Korea Institute of Geoscience and Mineral Resources, Korea (the Republic of)

The progressing developments in functional materials hold significant potential for addressing challenges in wearable electronics, given their outstanding electronic, optical, and mechanical properties. Among these materials, colloidal nanocrystal (NC) films, often referred to as "nano-inks," stand out as promising candidates for wearable and implantable electronic systems. Their appeal lies in their ease of processing, cost-effectiveness, and remarkable electrical conductivity. However, a challenge arises as these NCs are initially capped with bulky, electrically insulating organic ligands, hindering efficient charge transfer. Recently, the introduction of tailored surface chemistry for NC, aiming to enhance electronic coupling and passivate surface trap states through solution-based surface chemical engineering techniques, has resulted in high-mobility charge transport in nanocrystal films. In this study, a combination of structural, spectroscopic, and electronic properties supports the conclusion that our developed surface engineering process effectively adjusts the surface chemistry of the nanocrystal (NC) films to enhance charge transport. Specifically, we will delve into 1) how surface chemistry and doping can improve electronic transport in semiconducting NC films and 2) the diverse applications of various NC types as promising components for Wearable Electronics.

PS-2.7
The Effect of Graphene Quantum Dots on the Photoactive Response of Graphene Field Effect Transistor Muhammad Shehzad Sultan[1], Ernesto Espada Nazario[1], Bianca S Umpierre Ramos[1], Daniela D Negron Negron[1], Amanda M. Gracia Mercado[1], Wojciech Jadwisienczak[2], Brad Weiner[1] and Gerardo Morell[1]; [1]University of Puerto Rico - Río Piedras, United States; [2]Ohio University, United States

Graphene and highly luminescent graphene quantum dots (GQDs) have been widely used in optoelectronic devices as a photoactive material. In this study, we report the preparation of a GQDs/Graphene heterostructure to investigate the effect of GQDs on photoactive response of graphene. Using UV-vis absorption and photoluminescence (PL) spectra, the optical properties of graphene and the GQDs/Graphene heterostructure were measured and compared. Moreover, to investigate their electronic and charge transfer properties, we fabricated field-effect transistors (FET) on pristine graphene and GQDs/Graphene heterostructure thin films and investigated their photoactive electrical properties. Under illumination, both pristine and GQDs/Graphene FETs showed an increase in current and carrier mobility. The increased current and carrier mobility of GQDs/Graphene FET is due to the presence of a large number of photoexcited charge carriers. The current and carrier mobility in the GQDs/Graphene heterostructure FET were also lower than those in the pristine graphene FET. This is explained by GQDs' n-type doping effect on graphene, which reduces the accumulation of holes in the active p-channel near the insulating layer and causes charge to be transferred from the GQDs to the graphene. As a result, we discovered a charge transfer effect in the GQDs/Graphene heterostructure, which could be used in optoelectronic devices.

PS-2.8

Novel Synthesis and Tuning Optical Properties of High Quantum Yield Nitrogen Doped Graphene Quantum Dots

Muhammad Shehzad Sultan[1], Ernesto Espada Nazario[1], Bianca S Umpierre Ramos[1], Amanda M. Gracia Mercado[1], Daniela D Negron Negron[1], Wojciech Jadwisienczak[2], Brad Weiner[1] and Gerardo Morell[1]; [1]University of Puerto Rico - Río Piedras, United States; [2]Ohio University, United States

The graphene quantum dots (GQDs) have attracted the attention of researchers due to their excellent properties and potential applications in biomedicines, energy storage devices, and photovoltaics. The photoluminescence is one of the most important characteristics of GQDs. The doping of GQDs with nitrogen atoms is one of the most effective ways to tune their photoluminescence emission and increase quantum yield. In this work, high-quality nitrogen-doped graphene quantum dots (N-GQDs) were synthesized by using the pulsed laser synthesis method at various irradiation powers of the pulsed laser and changing the concentration of nitrogen doping to effectively tune the photoluminescence emission and improve the quantum yield (QY) of the as-synthesized N-GQDs. The TEM, HRTEM, XPS, XRD, Raman spectroscopy, and FTIR were carried out to observe the morphology, size distribution, crystalline structure, and to prove successful doping of GQDs with nitrogen atoms. To observe the optical properties of the as-synthesized N-GQDs, UV-vis and photoluminescence measurements were carried out. The as-synthesized NGQDs exhibit a high-quality crystalline structure of graphene. A high quantum yield was exhibited by the obtained N-GQDs as compared to the pristine GQDs. The obtained N-GQDs with oxygen-rich functional groups exhibit a strong emission. This work may be helpful to expand the scope of GQDs, especially in biomedical applications.

PS-2.9

High-Performance Self-Powered UV Photodetector Based on NGQD/Graphene Schottky Diode

Muhammad Shehzad Sultan[1], Ernesto Espada Nazario[1], Bianca S Umpierre Ramos[1], Amanda M. Gracia Mercado[1], Daniela D Negron Negron[1], Wojciech Jadwisienczak[2], Brad Weiner[1] and Gerardo Morell[1]; [1]University of Puerto Rico - Río Piedras, United States; [2]Ohio University, United States

Nitrogen-doped graphene quantum dots (GQDs) have been widely used for various optoelectronic devices as a photoactive material due to their high absorption coefficient and tunable bandgap. However, the low mobility of NGQD films results in poor charge collection and device performance. By combining NGQDs with graphene into hybrid NGQD/Graphene photodetectors, photocarriers from NGQDs are transferred to graphene, improving charge collection and transport, and drastically increasing the photoresponsivity. In this study, we report the preparation of a NGQD/Graphene heterostructure in order to investigate the effect of NGQD on the photoactive response of graphene. Using UV–vis absorption and photoluminescence (PL) spectra, the optical properties of NGQD/Graphene heterostructure were measured. Moreover, to investigate their electronic and charge transfer properties, we fabricated the photodetectors with pristine graphene quantum dots and an NGQD/Graphene heterostructure to analyze and compare their photoactive electrical properties. Under illumination, NGQD/Graphene PD showed an increase in both current and carrier mobility as compared to NGQD PD. The increased current and carrier mobility of NGQD/Graphene PD are due to the presence of a large number of photoexcited charge carriers. This is explained by NGQDs' n-type doping effect on graphene, which reduces the accumulation of holes in the active p-channel near the insulating layer and causes charge to be transferred from the NGQDs to the graphene. As a result, we discovered a charge transfer effect in the NGQD/Graphene heterostructure, which could be used in optoelectronic devices.

PS-2.10

Superparamagnetic Properties of Metal-Free Nitrogen-Doped Graphene Quantum Dots

Muhammad Shehzad Sultan[1], Ernesto Espada Nazario[1], Bianca S Umpierre Ramos[1], Amanda M. Gracia Mercado[1], Daniela D Negron Negron[1], Wojciech Jadwisienczak[2], Brad Weiner[1] and Gerardo Morell[1]; [1]University of Puerto Rico - Río Piedras, United States; [2]Ohio University, United States

Here we report the superparamagnetic behavior of metal-free nitrogen-doped graphene quantum dots (N-GQDs). The pulsed laser ablation (PLA) method was utilized to synthesize N-GQDs with an average diameter of 3.45 nm and a high doping level (N/C) of 1.4. The magnetic properties of as-synthesized N-GQDs were explored by performing magnetization *vs.* magnetic field (M-H) and magnetization vs. temperature (M-T) measurements. The M-H plots measured in a temperature range of 2 K–300 K revealed the superparamagnetic behavior of N-GQDs. The value of saturation magnetization was found to be directly correlated to the nitrogen concentration, and a saturation magnetization up to 28.7 emu/g was obtained at room temperature (300 K). The M-T measurements with zero-field-cooled (ZFC) and field-cooled (FC) conditions were employed to study the anisotropy energy barriers and blocking temperature. A variation in the blocking temperature (*TB*) from 288 K to 61 K was observed when the external magnetic field (H) was changed from 0.1 T to 0.6 T. The origin of superparamagnetism was attributed to the presence of graphitic nitrogen bonding configurations and defect states. The observed superparamagnetic properties along with the optical properties of N-GQDs, create an opportunity for developing materials for biomedical applications and data recording devices.

PS-2.11

Study on Enhanced Electron Field Emission Properties of Graphene Quantum Dots Synthesized by Pulsed LASER Ablation

Muhammad Shehzad Sultan[1], Ernesto Espada Nazario[1], Bianca S Umpierre Ramos[1], Daniela D Negron Negron[1], Amanda M. Gracia Mercado[1], Wojciech Jadwisienczak[2], Brad Weiner[1] and Gerardo Morell[1]; [1]University of Puerto Rico - Río Piedras, United States; [2]Ohio University, United States

Graphene quantum dots (GQDs) and nitrogen-doped graphene

quantum dots (N-GQDs) were synthesized by the Pulsed LASER Ablation method. The nanostructure and chemical composition of the GQDs were analyzed by means of TEM, HRTEM, Raman, XPS, and FT-IR spectra. Field emission is a quantum mechanical phenomenon where electrons tunnel from the cathode to the anode through vacuum under an applied electric field. So far, the field emission properties of two-dimensional (graphene) and one-dimensional (CNT) carbon nanostructures have been extensively studied. For the first time, to the best of our knowledge, the field emission behavior of GQDs and N-GQDs, deposited on n-Si (100) substrates, is studied. As a candidate of cold cathode, the GQDs display good field emission performance. The field emission properties of GQDs and N-GQDs were studied by measuring turn-on field (*E*) and field enhancement factor β.The results show that nitrogen doping improved the field emission properties of GQDs by reducing the turn-on field from 13.1V/μm (GQDs) to 7.9V/μm (N-GQDs) and enhancing the field enhancement factor β from 1427 (GQDs) to 2511 (N-GQDs). The field emission behavior of pristine GQDs and N-GQDs is explained in terms of change in the effective microstructure as well as a reduction in the work function, as probed by measured characterizations. The enhanced emission properties of N-GQDs are mainly attributed to the upshifting of fermi energy level and defects produced as a result of nitrogen doping. The good emission performance of the GQDs field emitters suggests promising applications in next-generation vacuum micro and nano-electronic devices.

PS-2.12
High Performance Self-Powered UV Photodetector Based on Nitrogen-Doped Graphene Quantum Dot Schottky Diode Muhammad Shehzad Sultan[1], Ernesto Espada Nazario[1], Bianca S Umpierre Ramos[1], Daniela D Negron Negron[1], Amanda M. Gracia Mercado[1], Wojciech Jadwisienczak[2], Brad Weiner[1] and Gerardo Morell[1]; [1]University of Puerto Rico - Río Piedras, United States; [2]Ohio University, United States

We report a straightforward bottom-up approach for the synthesis of high-quality nitrogen-doped graphene quantum dots (NGQDs). This approach is cost-effective, environmentally friendly, and suitable for the production of high-quality NGQDs on a large scale. The as-synthesized NGQDs have high crystalline quality with an average size of 3.26 nm, are water soluble, and show strong fluorescence. The UV-vis spectra indicate that N-doping introduces new energy levels into the electronic structure of graphene, which tune the optical properties, resulting in a photoluminescence quantum yield (PLQY) of 73%. The NGQDs show excitation wavelength-dependent fluorescence with a maximum excitation and emission at 340 and 431 nm, respectively. Using the as-synthesized NGQDs, we fabricated a high-efficiency and fast-response self-powered UV photodetector. Under the illumination of 365 nm UV light with a power density of 25 mW/cm, the NGQD photodetector shows a high photoresponsivity of 37 A/W, detectivity of 1 * 10 Jones, and external quantum efficiency (EQE) of 12.6 * 10%. This UV photoresponse is fast, with rise time of 0.29 s and fall time of 0.33 s. This work paves the way for the development of graphene-based high-performance optoelectronic devices.

PS-2.13
Monolithic Integration of InAsP Nano-Heterostructures onto Silicon for Photonic Applications Alisha Nanwani[1,1], Pawel Wyborski[2], Michael Seifner[1,1], Shima Kadkhodazadeh[1,1], Marcin Syperek[2], Pawel Holewa[1,1], Kresten Yvind[1,1], Grzegorz Sek[2] and Elizaveta Semenova[1,1]; [1]Technical University of Denmark, Denmark; [2]Wroclaw University of Science and Technology, Poland

Silicon (Si), well known for its scalability in optoelectronic applications, encounters a challenge in efficiently emitting light due to its inherent indirect bandgap nature. Overcoming this limitation is essential for progressing integrated nano- and quantum photonics. To address this demand, we focus on the monolithic integration of direct bandgap III-V nano-heterostructures to Si operating in the telecom wavelength range. Thus, such a gain medium will enable efficient light sources on the Si photonic platform for both quantum and classical applications.
In this contribution, we present the selective area epitaxy of InP/InAs(P)/InP in Si, using metalorganic vapor phase epitaxy (MOVPE). This method offers two significant advantages: a small footprint to reduce defect density and precise positioning of low-dimensional active material, providing deterministic fabrication and scalability for nanophotonic devices. The investigated structure is grown on (001)-oriented Si, covered by a thin SiN hard mask. The fabrication process involves electron beam lithography followed by wet etching of Si to create inverted pyramidal holes defined by {111} planes ranging from 20 to 50 nm in diameter. During growth, a thin InP layer is epitaxially grown on (111)-facets of Si in the etched holes[1,2]. Subsequently, an As/P exchange is performed in an arsenic-rich ambient, forming a few InAs(P) monolayers, subsequently covered with an InP cap.
Systematic investigations of the morphology and crystal properties of the grown nanostructure are conducted using scanning electron microscopy (SEM), high-resolution scanning transmission electron microscopy (HRSTEM), and EDX maps. The optical properties are examined by photoluminescence (PL) and time-resolved PL. High spatially resolved PL at room temperature reveal emission at the telecom range from nano-heterostructures. This approach promises to advance Si-based integrated photonics with efficient light sources, opening new avenues for research in this field.

PS-2.14
Comparative Study of GaN Layers Grown on Multiple Patterning Types Localized on a Single Sapphire Substrate Jan Batysta[1,2], Yoann Levy[3], Inam Mirza[3], Thibault J. Derrien[3], Nadezhda M. Bulgakova[3], Filip Dominec[1], Tomas Hubacek[1], Frantisek Hajek[1], Karla Kuldova[1], Alice Hospodkova[1] and Jiri Pangrac[1]; [1]FZU – Institute of Physics of the Czech Academy of Sciences, Czechia; [2]Czech Technical University, Czechia; [3]The Czech Academy of Sciences, Czechia

Patterned substrates have been an industry standard for applications such as blue LEDs [1]. However, still some increase of throughput in LED preparation for industry can be

of great interest.
In this work, we investigate the possibility of using laser-induced periodic surface structures (LIPSS) [2-5] on sapphire as a substrate for subsequent growth of a thick GaN layer. First, double-side polished sapphire samples were laser nanostructured using a commercial femtosecond infrared amplified laser system [3]. To obtain different surface patterning (including LIPSS), sixteen 3x3 mm^2 areas were fabricated on the surface of the wafers, each with different irradiation conditions. The laser peak fluence and/or the overlap between subsequent laser spots were the main parameters changed to generate the surface texturing.
Then, the GaN growth process was performed using a close coupled showerhead MOVPE apparatus Aixtron 3x2. We used standard low temperature nucleation process with subsequent coalescence [1] at higher process temperatures ranging from 1180 to 1250 °C with TMGa as gallium precursor and hydrogen as carrier gas.
As a result, we present photoluminescence and cathodoluminescence measurements as well as other complementary techniques to assess the quality and morphology of GaN layers grown on laser-patterned areas in contrast to pristine polished regions. Comparing differently patterned spots on the same wafer offers an efficient way to eliminate reproducibility problems.
[1] Peng, D. et al., *Journal of Crystal Growth*, **395**, 9-13 (2014)[2]
[2] Gnilitskyi, I. et al., *Scientific reports,* **7**, 8485 (2017).
[3] Alamri, S. et al., *Materials,* ***12***, 1018 (2019).
[4] Sládek, J. et al., *Applied Surface Science,* **605**, 154664 (2022)
[5] Sládek, J. et al., *Materials,* **16**, 2883 (2023).

PS-2.15
Investigation of Ga Vacancies in MOVPE-Prepared GaN Layers
Tomas Hubacek[1], Jakub Cizek[2], Frantisek Hajek[1,3], Karla Kuldova[1], Jan Batysta[1,4], Jiri Pangrac[1] and Alice Hospodkova[1]; [1]Institute of Physics, Czech Academy of Sciences, Czechia; [2]Faculty of Mathematics and Physics, Charles University, Czechia; [3]Institute of High Pressure Physics Unipress, Poland; [4]Faculty of Nuclear Sciences and Physical Engineering, Czech Technical University, Czechia

Nitride semiconductors have been widely used industrially in the last two decades, but there are still many unresolved problems and questions to be answered. For example, what is the real cause of the native n-type conductivity of undoped GaN layers, or why In-containing layers (InGaN, InAlN) need to be grown in a nitrogen atmosphere (hydrogen carrier gas suppresses In incorporation). Another area where knowledge is lacking is the formation of point defects, such as gallium (V_{Ga}) or nitrogen (V_N) vacancies and their clusters or complexes with various impurities. To study vacancies and related defects is important since they are responsible for decomposition of quantum wells, especially with higher In concentration, and they may also influence other properties of nitride heterostructures. The open questions are: why do GaN layers contain considerable concentrations of V_{Ga}, although the V_{Ga} formation energy is quite high according to theoretical predictions, or how V_{Ga} influences the electrical and optical properties (yellow band and non-radiative recombination), and how V_{Ga}-related defects formation is related to different growth conditions in metal organic vapor phase epitaxy (MOVPE). Answering these questions would help to improve the quality and lifetime of devices based on nitride semiconductors.
Positron annihilation spectroscopy (PAS) is the most suitable technique to study V_{Ga}-related defects in nitride films. It is based on the annihilation of positrons in negatively charged open volume defects (vacancies). By measuring the positron lifetime or the Doppler shift in the energy of the annihilation γ-rays, we can distinguish different vacancies, their clusters, or complexes with different open volumes. In studied samples most common V_{Ga}-related defects were complexes with oxygen and hydrogen, clustering of vacancies was observed for samples grown at higher temperature.
In our previous work [1], we investigated the influence of growth temperature, type of carrier gas and type of Ga precursor to find a link between technological conditions, GaN layer properties, and the concentration of V_{Ga}-related defects. In this work, we will continue this research. Other MOVPE growth parameters, such as growth rate or n-type doping, will be studied. Annealing in different atmospheres (N_2, H_2, NH_3 or O_2) will also be applied to study changes in point defects. PAS will be mainly used for characterization, followed by other techniques such as photo- and cathodoluminescence, SEM, etc. We will show that growth rate has no significant effect on the type and concentration of point defects, while O_2 annealing has a significant influence on V_{Ga}-related defects.

[1] A. Hospodková, et al., *Materials* 15 (2022) 6916.

PS-2.16
Improved Reliability of Phase Change Heterostructure Memory via Oxygen-Doped Sb_2Te_3/$TiTe_2$ Superlattices
Dong Hyun Kim, Jun Young Choi, Ho Jin Lee, Jin Suk Oh, Jong Min Joo, Seok Hee Hong and Tae Geun Kim; Korea University, Korea (the Republic of)

The onset of the fourth industrial revolution, with its core focus on artificial intelligence and extensive data analytics, necessitates the development of next-generation memory devices capable of swift and efficient data processing. Among the array of emerging technologies, phase change random access memory (PCRAM) devices have garnered significant attention due to their remarkable data handling capabilities and impressive durability, positioning them as a promising candidate for this technological evolution. Nonetheless, these devices encounter critical challenges concerning the structural relaxion of amorphous phase, which hinder reliability and durability of devices, poses a significant barrier to their further application. To address these challenges, extensive research is imperative for mitigating grain growth phenomena, which are well-known to exert a substantial influence on the reliability and durability of PCRAM devices. In this study, we introduce an innovative approach by incorporating oxygen into Sb_2Te_3, leading to the formation of Sb-O precipitated phases. This strategic intervention effectively curtails grain growth during the crystallization process, a critical step in the development of PCRAM technology. Subsequently, we employ a phase

change heterostructure (PCH) technology, with integration $TiTe_2$ layers, strategically engineered to restrict the expansion of crystalline islands to less than 10-nm distance. The meticulous control and manipulation of nanoscale features result in remarkable enhancements in device performance, spanning the spectrum of device reliability. This multifaceted approach holds the potential to revolutionize the field of PCRAM technology and stands as a promising avenue for future developments in this domain.

PS-2.17
Optimization of Copper Oxides for P-Type Transparent Conductors Arturo Rodríguez Gómez; Instituto de Física - Universidad Nacional Autónoma de México, Mexico

Copper oxides (Copper(I) and Copper(II) oxides) have been of interest to the academic community due to their interesting properties and applications in the area of semiconductors. One of its most striking possible uses is the manufacture of p-type transparent conductive oxides (TCOs). In copper oxide, there is a hybridization between the 2p orbitals of oxygen and the closed shell 3d10 orbitals of copper. This hybridization reduces the problem of the deep levels of acceptors in the valence band observed in other transparent oxide semiconductors such as zinc oxide or indium-tin oxide where the valence band is highly localized, and there are higher hole effective masses, lower hole mobilities, and lower hole concentrations. In this work, we present a straightforward strategy that consists of growing thin copper films by sputtering and subsequently oxidizing/aging them in a controlled manner for more than 300 h. This methodology has allowed us to obtain p-type TCOs based on copper oxides with conductivities ranging between 1.8 and 5.0 x 10^-2 S/cm and average transmittances in the visible spectrum ranging between 50 and 75%. If we improve the surface of our TCOs (smoother and flatter), we could achieve heterojunctions that are “abrupt” enough so that the diffusion length of the carriers is greater than that of the interface and thus build translucent diodes.

PS-2.18
Developing Nickel Phosphide-Based Nanomaterial as an Anode Electro-Catalyst for the Energy and Environmental Remediation Application Dejen K. Demssie; National Taiwan University of Science and Technology, Taiwan

Environmental pollution coupled with energy crises becomes one of the biggest problems we are facing today throughout the world. Urea waste is one of environmental pollutant and a simple renewable energy source. Urea decomposition results ammonia to the soil which affects ground water and results soil acidity which in turn reduces soil fertility for agricultural purposes (reduced crop productivity) and also releases NOx compounds to the atmosphere resulting acid rain. As a result, rural communities, in particular, suffered a lot from healthy problems. To address such a problem, electrochemical decomposition of urea in to electricity without emission of environmental pollutant is investigated. However, urea electro-oxidation reaction is a sluggish kinetics due to 6e-transfer process. Therefore, it requires a highly active anode electro-catalyst nanomaterial with high conversion performance. The purpose of this paper is to develop nickel phosphide-based nanomaterial as an anode electro-catalyst to convert urea into electricity without the release of environmental pollutants. A number of nickel phosphide-based materials were synthesized and characterized using XRD, FESEM, FTIR, UV-VIS, TGA, and EDX. The physical characterization shows nanospherical nickel phosphide with a particle size of 2.4 nm, molecular interaction, and multifaceted crystal phase. After physical characterization, the electro-catalytic performance of the proposed material was tested using a cyclic voltammeter. Among synthesized materials, PdNiP@PEDOT:PSS/rGO shows outstanding urea conversion performance with a low onset potential of 0.32 V vs SCE to deliver a maximum current density of 149 mAcm-2 . This is due to the higher electrochemically active surface area of 3.28 cm-2 , high kinetics, and durability of the as-synthesized material. Therefore, the developed nanomaterial is a promising candidate as an anode electro-catalyst material for the conversion of urea waste into electricity to minimize energy crises and environmental problems.

PS-2.19
Chemical Vapor Deposition of CuI on Sapphire Stefan J. Merker, Valeria Zittel, Gabriele Benndorf, Marius Grundmann and Harald Krautscheid; Universität Leipzig, Germany

Copper(I)-iodide in its thermodynamically stable zincblende phase (γ-CuI) is a promising wide-bandgap material ($E_G \approx 3.1$ eV). Due to its large exciton binding energy ($E^B_X \approx 62$ meV), intrinsic p-type conductivity with a hole mobility of up to 43 cm^2/Vs in bulk crystals and its high thermoelectric figure of merit, it is a material for transparent optoelectronic and thermoelectric applications.[1]
Thin layers of CuI were deposited, among others, by spin coating of a CuI precursor solution, thermal evaporation, reactive sputtering, pulsed laser deposition (PLD), laser-assisted molecular beam deposition (LAMBD) and chemical vapor deposition (CVD) techniques. The epitaxial growth of CuI by chemical vapor deposition has been little studied so far.[2]

We investigated the formation of CuI on sapphire by chemical vapor deposition. The growth experiments have been performed in a horizontal cold-wall MOCVD reactor (AIX 200, Aixtron Corp.) equipped with a carbon susceptor. For the use of $[Cu(sec\text{-}Bu\text{-}Me\text{-}amd)]_2$ as Copper(I)-precursor[3], we modified the CVD system in order to heat the bubbler, valves and piping above the melting point of the precursor (up to 105 °C). As source of iodine ethyl iodide or *tert*-butyl iodide were used. We studied the influence of the substrate orientation, iodine precursor, growth temperature, total pressure and I/Cu-partial pressure ratio on CuI phase formation, amount of deposited material, surface morphology and optical properties. Since γ-CuI with the growth direction <111> perpendicular to the substrate surface has a strong tendency towards island growth, special attention was paid to the surface coverage. The deposited CuI was characterized by X-ray diffraction, laser scanning microscopy and photoluminescence spectroscopy.

Results on the position and amount of material deposited on the sapphire wafer depending on the deposition temperature with respect to different iodine precursors will be presented. Due to the high sublimation rate of CuI, much effort was paid in optimization of the growth temperature and pressure. This is underlined by microscopic images of the surface morphology.
Under certain growth conditions, another CuI phase with interesting optical properties was detected by XRD, which forms at higher temperatures in the transition region between γ-CuI and α-CuI.

References:
[1] M. Grundmann, F.-L. Schein, M. Lorenz, T. Böntgen, J. Lenzner, H. v. Wenckstern *Phys. Status Solidi A* **210** (2013) 1671–1703.
[2] V. Gottschalch, S. Blaurock, G. Benndorf, J. Lenzner, M. Grundmann, H. Krautscheid *Journal of Crystal Growth* **471** (2017) 21–28.
[3] Z. Li, A. Rahtu, R. G. Gordon*, Journal of The Electrochemical Society* **153** (2006) C787-C794.

PS-2.20
Mechanism of Lithium and Magnesium Oxides (Li_xO_x and Mg_xO_x) Adsorption onto Pristine Graphene—Density Functional Theory Approach Mahlatse Matloga; UNISA, South Africa

We computationally investigated the adsorption behaviour of lithium oxides (LixOx) and magnesium oxides (MgxOx) onto pristine graphene during oxygen reduction reaction (ORR) for metal air batteries operation using density functional theory (DFT). We proposed various pathways and studied different adsorption configurations in each system, comprising the O_2, Li, Mg as ORR reactants and the LiO_2, MgO_2, Li_2O_2 and Mg_2O_2 as ORR products. Mg atom weakly adsorbed onto graphene with an adsorption energy of (-0.035 eV to -0.043 eV), followed by O_2 molecule (-0.101 eV to -0.134 eV) moreover Li atom adsorbed strongly with an adsorption energy of (-0.985 eV to -1.296 eV). The ORR product MgO_2 adsorbed strongly (-1.536 eV) than other reaction products LiO_2, Li_2O_2 and Mg_2O_2 with their calculated adsorption energies (+0.768 eV, -0.535 eV and -0.879 eV) respectively onto graphene.

PS-2.21
Simulation of the Flow of a Photon in a Solar Cell Applying the Monte Carlo Method and Percolation Theory Yessica Calderon Segura and Gennadiy Burlak; UAEM, Mexico

The simulation of an optimization algorithm is presented by the Monte Carlo-Percolation Method (MMC-Percolation) and the Fermat principle, where a coherent approach was achieved through a simulated porous medium of the PBDB-T:ITIC material, which It is widely used in solar cells. The main electrical parameters of the cluster were validated in simulation by FEA in sizes from 20x20x20 nm to 100x100x100 nm, so that in a radius of 0.9 nm a Jsc was obtained Jsc = 173 A/m2, Voc = 0.92 V, ρ = 266 kΩm, σ = 3.76 uS, I = 69.2 fA, R =13.3 TΩ, P = 63.7 fW, ohmic Loss = 7.962x109 W/m3, FF = 70.5 y PCE = 11.2 %(11.1±0.1). Better results were obtained at porosity levels where the intersection due to the increase in pore radii ranges from 0.5 to 1 nm, generating a uniform channel that allows 90% reliability and adequate filtration of the light beam. Therefore, the radii of the pore that did not allow the formation of the infinite percolation cluster range from 0.1 to 0.4 nm.

PS-2.22
Contribution to High-Quality Semiconductor Manufacturing with Face-Down MOCVD Keitaro Ikejiri[1], Kenichi Eriguchi[1], Guanxi Piao[1], Junya Yoshinaga[1], Kazutada Ikenaga[1], Yoshihisa Koyama[2] and Shuichi Koseki[1]; [1]Taiyo Nippon Sanso Corporation, Japan; [2]Taiyo Nippon Sanso CSE Ltd., Japan

In semiconductor manufacturing, face-down metal-organic chemical vapor deposition (MOCVD) equipment is notable for its innovative design that offers several advantages over traditional face-up equipment. This design effectively reduces gas turbulence, which is a common issue in face-up equipment where wafers are heated from below, causing a bottom-to-top temperature gradient and resultant upward turbulence. In contrast, face-down equipment reverses this gradient, placing the wafer and heater above the flow channel. This creates top-to-bottom temperature gradient that suppresses turbulence, resulting in a more stable gas flow over the wafer and leading to a uniform, high-quality film deposition. Furthermore, this configuration reduces particle adhesion on the wafer surface. Since particles larger than 1 μm tend to move downward due to gravity, positioning the wafer above the flow channel helps minimize particle contamination.
We have developed optimal face-down MOCVD equipment for several semiconductor materials. BMC-301, FR8000-N, and FR2000-OX for GaAs/InP, GaN, and β-Ga_2O_3, respectively, will be described and their advantages for epi growth.
The face-down MOCVD equipment BMC-301 is a multiple wafer growth reactor developed for mass production of GaAs and InP, supporting wafer diameters from 2" to 6". GaAs and InP have been applied to high-speed electronic devices and laser elements in optical communications because of their high electron mobility and direct band gap. However, the presence of particles on the wafer surface of this material can increase carrier recombination and significantly reduce device efficiency. Thanks to its face-down characteristics, BMC-301 prevents particle deposition on the wafer-facing surface and deposits high-quality epitaxial films.
FR8000-N was developed as a face-down MOCVD equipment for GaN. It can grow a single wafer up to 8-inches in size for use in the R&D and mass production prototyping stages. In conventional face-up MOCVD equipment, periodic cleaning of the reactor is necessary because when the deposition thickness exceeds 10 μm, peeling of the deposition on the flow channel becomes significant and defects are formed on the epi-wafer. On the other hand, with FR8000-N, we confirmed that even after multiple GaN growth runs and deposition of a total film thickness of 10 μm or more, foreign matter did not

peel off and fall onto the epi-wafer. This result indicates that FR8000-N can reduce downtime for reactor cleaning and improve productivity.

Recently, we have developed a face-down MOCVD equipment, FR2000-OX, for crystal growth of β-Ga_2O_3 systems. β-Ga_2O_3 has a dielectric breakdown field strength (>7 MV/cm) that is even higher than that of GaN, so it is expected to be applied to next-generation power devices. We believe that MOCVD is one of the most suitable growth methods for the fabrication of drift layers, which require particularly complicated designs, because of its precise growth control. FR2000-OX is a system that supports a single 2-inch wafer for use in R&D. As a result of recent studies, growth of high-purity β-Ga_2O_3 with reduced hydrogen and carbon contamination was demonstrated based on the optimal conditions found by thermodynamic studies. It was also confirmed that a thick β-Ga_2O_3 layer could be grown at high speed while maintaining high purity.

Each of these materials requires strict growth conditions, and these face-down systems are designed to meet these requirements. We expect face-down systems to become even more important as demand for high-quality semiconductor materials increases. We will discuss the stability of the face-down MOCVD during multiple sequential growth and the effectiveness of particle reduction based on experimental data.

ICM VPE XXI

2024 Las Vegas, NV

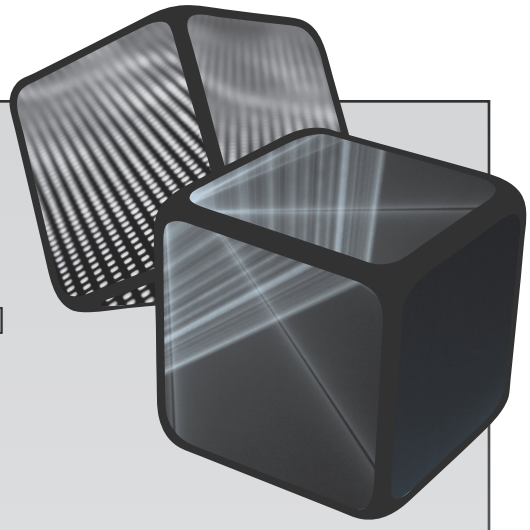

FRIDAY

Oral Presentations

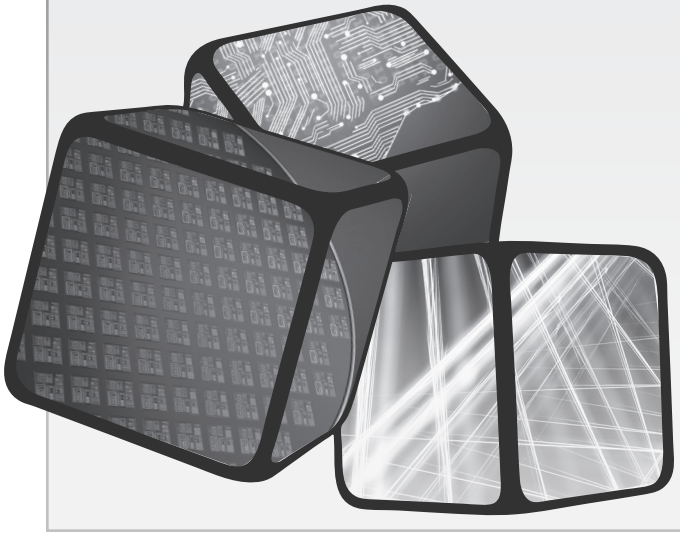

21st International Conference on Metal Organic Vapor Phase Epitaxy

SESSION 5A-1: In Containing Nitride
Session Chair: Stefano Leone
Friday Morning, May 17, 2024
Resort Tower, Ground Level, Bronze Room 1

9:00 AM 5A-1.1
Electrical Properties of InN Grown by Pressurized MOVPE Yudai Yamashita, Kazuhide Kumakura and Yoshitaka Taniyasu; NTT Basic Research Laboratories, Japan

Indium nitride (InN) suffers from high residual electron concentration, which is an obstacle to its device applications. The origins of the residual electron concentration are thought to be point defects such as nitrogen vacancies [1], impurities such as hydrogen and oxygen [2], and threading dislocations (TDs). Because InN has high nitrogen vapor pressure at the growth temperature, pressurized growth was proposed to suppress the decomposition of InN for MOVPE [3]. In this study, we performed pressurized MOVPE growth of InN and characterized the electrical properties to provide a guideline for development of the InN MOVPE growth.
In this study, a 3-μm-thick GaN template layer was grown epitaxially on a sapphire (0001) substrate, and then 500-nm-thick InN was grown by the MOVPE. The concentrations of residual impurities were investigated by secondary ion mass spectrometry (SIMS). The TD densities were estimated from XRD measurements.
In order to study the influence of the growth pressure (P), InN was grown at 600–1500 hPa. The electron concentration (n) decreased from 1.3×10^{19} to 7.6×10^{18} cm^{-3}, and the mobility (μ_e) increased from 1320 to 1570 cm^{2}V^{-1}s^{-1} with increasing P from 600 to 1500 hPa. The TD densities were 5×10^9 cm^{-2}, and the residual impurity concentrations of hydrogen and oxygen were almost unchanged regardless of the P. Among the origins of donors, it is therefore considered that the pressurized growth mainly reduced the point defects, resulting in the decrease in the residual electron concentration and increase in mobility.
Next, to remove hydrogen from the MOVPE-grown InN, we carried out post-annealing (PA) at 450 °C for 20 – 40 min in a nitrogen atmosphere under normal pressure. We confirmed that even after the PA the TD densities remained unchanged at 5×10^9 cm^{-2}. By the PA, n decreased by about 90% to 1.6×10^{18} cm^{-3}. The residual hydrogen concentration was also reduced by about 90% from 1.5×10^{21} to 2.3×10^{20} cm^{-3} by the PA. Although the absolute value is two orders of magnitude higher, it suggests that some of the hydrogen incorporated into InN also acts as donors. On the other hand, the μ_e decreased from 1570 to 1430 cm^{2}V^{-1}s^{-1} with the PA. Analysis of the relationship between μ_e and n shows that for InN with a TD density of 5×10^9 cm^{-2}, an ionized impurity scattering dominates at n of above 10^{19} cm^{-3}, while a dislocation scattering dominates at n around 10^{18} cm^{-3}. Thus, the PA-induced reduction in n changes the dominant scattering mechanism from ionized impurity to dislocation scattering, consequently reducing mobility. Further enhancements in carrier mobility of InN may be realized through the reduction of TD density.
References: [1] J. K. Sheu and G. C. Chi, *J. Phys. Condens. Matter* **14,** R657 (2002). [2] G. Pettinari *et al*., *Phys. Rev. B* **77**, 125207 (2008). [3] T. Matsuoka, *Int. J. Optomechatronics* **9**, 1–8 (2015).

9:20 AM 5A-1.2
High-Temperature Plasma-Enhanced MOCVD of InN/Al_2O_3 in Vertical Gas-Flow Configuration Hisashi Yamada, Tokio Takahashi, Takahiro Gotow, Naoto Kumagai, Tetsuji Shimizu, Tatsuro Maeda and Toshihide Ide; National Institute of Advanced Industrial Science and Technology (AIST), Japan

InN is expected to have the smallest effective mass (0.04 m_0), the highest electron mobility (14000 cm^2/Vs), and the highest saturation drift velocity (~5×10^7 cm/s) among III-nitride semiconductors [1]. Therefore, InN has attracted significant interest as a material for next-generation (6G) high-frequency devices as well as for near-infrared opt-electronic devices owing to the bandgap of ~0.7eV. Besides, by layer stacking with InGaN and GaN, it is expected to realize full-color light-emitting diodes (LEDs) and tandem-type solar cells. Furthermore, these compounds can contribute the SDGs society that meets an environmentally friendly manufacturing process without using toxic precursors, such as AsH_3 and PH_3. However, the growth of high-In-content (In>0.4) InGaN and InN by conventional metal-organic chemical vapor deposition (MOCVD) using NH_3 for nitrogen precursor is extremely difficult. High growth temperature enhances decomposition of InGaN and InN due to the etching effect under hydrogen ambient by NH_3 decomposition. Low growth temperature typically results in indium droplet mainly owing to the low decomposition efficiency of NH_3. Therefore, there is almost no growth window for high-In-content (In>0.4) InGaN and InN. To overcome these issues, we developed a microstrip-line microwave plasma source with an active nitrogen radical density of ~2×10^{14} cm^{-3} [2] and installed it into the MOCVD system. Using this technology, InN crystal growth was demonstrated on a 2-inch GaN/Al_2O_3 (0001) template using trimethylindium (TMI) and N_2 as the precursors. The InN layer displayed excellent crystalline quality of indium droplet free with a total threading dislocation density of 2.4×10^9 cm^{-2} [3]. Additionally, it delivers a strong photoluminescence (PL) spectrum with a peak energy of 0.687 eV and a full-width-at-half-maximum (FWHM) of 0.1 eV at room temperature. However, we also noted that the surface of the InN layer was rough, and some voids existed at the InN/GaN interface.
In this study, we present atomically smooth InN epitaxy, grown directly on 2-inch c-plane Al_2O_3 substrate, with modified plasma-enhanced MOCVD. The growth was conducted at the susceptor temperature from 600 to 800°C under the reactor pressure of 2 kPa using TMI and active nitrogen radicals from N_2 gas. The plasma power and nitrogen gas flow rates were 38W and 2 L/min, respectively. The ω/2θ of the XRD confirms the InN (0002) peak along with the

sapphire (0006). The thickness of InN was increased from 30 to 34 nm increasing the susceptor temperature from 600 to 750°C. At 800°C, InN thickness decreased to 30 nm, suggesting accelerated In-N decomposition during high-temperature growth. The surface grown at 750°C was an atomically smooth with roughness as low as 0.9 nm in 20 x 20 µm, confirmed by atomic force microscopy (AFM). Using high-density nitrogen radicals at a relatively high temperature of 750°C allows for atomically smooth InN epitaxy that cannot be achieved with NH_3. The Hall effect measurements confirmed the electron carrier concentration and the mobility of $4x10^{20}$ cm^{-3} and 75 cm^2/Vs, respectively. The highly *n*-type carrier concentration is likely caused by the residual impurities. The origin of carrier concentration in the InN epitaxial layer must be addressed to realize InN high electron mobility transistors (HEMT).

[1] V. M. Polyakova and F. Schwierz, Appl. Phys. Lett. **85**, 1523 (2004).
[2] J. Kim, H. Sakakita, H. Ohsaki, and M. Katsurai, Jpn. J. Appl. Phys. **54**, 01AA02 (2015).
[3] H. Sakakita, N. Kumagai, T. Shimizu, J. Kim, H. Yamada, and X.-L. Wang, Appl. Mater. Today **27**, 101489 (2022).

9:40 AM 5A-1.3
Epitaxial Growth and Characterization of AlInN/GaN Superlattices Haotian Xue, Elia Palmese, Ben Sekely, Brian Little, Fred Kish, John Muth and Jonathan J. Wierer; North Carolina State University, United States

III-nitride semiconductors have had successes in optoelectronic and electronic devices. Of the ternaries in this family, AlInN is the least explored and implemented in devices. AlInN is attractive because it can be lattice-matched to GaN, has a wider bandgap and higher electric field at breakdown, has a high refractive index contrast compared to GaN, and has high polarization fields to create 2-dimensional electron gases. However, AlInN is challenging to implement because of growth limitations that lead to poor surface morphology at thicknesses greater than 50 nm, even with the best-known growth conditions. Island growth dominates, and mounds form in alignment with the step-like surface of the underlying GaN. Pits originating from the substrate or within the AlInN grow as the layer thickness increases. Usually, AlInN thicknesses are limited to ~300nm before the surface becomes too rough or pitted to be of use. This work presents data on near-lattice-matched AlInN/GaN superlattices (SLs) with superior morphology than thick (bulk) AlInN layers [1].

The SLs and bulk AlInN are grown by metalorganic chemical vapor deposition in a Taiyo Nippon Sanso Co. reactor. The layers are grown on free-standing GaN and GaN-on-sapphire substrates. The SL samples consist of 20 or 100 pairs of ~3nm thick AlInN and ~1nm thick GaN layers (80nm or 400nm thick) at varying temperatures and pressures. The layer thicknesses are chosen to prevent defects from forming and achieve an SL consisting predominately of AlInN to retain its desirable properties. For comparison, bulk layers of AlInN are grown at the same thicknesses. All samples are grown in an N_2 ambient with a V/III ratio of $\sim 1.44\times10^4$ and are unintentionally doped. The growth temperature and pressure are constant for all layers to avoid temperature or pressure ramping and growth interruptions.

Growth conditions are explored to find optimum conditions. The $Al_{1-x}In_xN$ indium content decreases linearly (x=0.2-0.15) with increasing temperatures (775-800°C), the same behavior as bulk AlInN. The SLs grown at pressures between 20-40kPa exhibit step-like surface morphology, while at 10kPa and 50kPa they roughen. There is also a decrease in the AlInN growth rate (3.6-2.5nm/min) with increasing pressure (10-50kPa) and higher indium content at higher pressures. A pressure of 30kPa is chosen for the following growth results. The SLs suppress island growth and pit formation that occurs in bulk AlInN and exhibit superior morphology with lower roughness. The 20-period SLs and GaN-on-sapphire substrates exhibit extremely smooth surfaces with atomic force microscope (AFM) scans showing root mean square (RMS) roughness of 0.3nm and atomic steps closely resembling the underlying GaN layers. Pits caused by threading dislocations are present with a density of $\sim 1.36\times10^8$ cm^{-2}, comparable to the dislocation density of the substrates before growth. The bulk AlInN control sample shows the typical small mounds aligning to the atomic edges of the underlying GaN with an RMS~0.65 nm. Increasing to 100 periods slightly increases pit sizes, but stepped surfaces remain.

AlInN/GaN 20-period SLs grown on free-standing GaN substrates have excellent surfaces with nearly linear atomic steps, matching the step morphology of the underlying GaN. Pits are only observed in the larger 20µm×20µm AFM scans and are formed from the pits in the underlying GaN substrate. Transmission electron microscope images show a highly periodic SL with consistent composition and slight layer intermixing.
The refractive index versus wavelength of the AlInN/GaN SL shows a weighted value between those of AlInN and GaN at ~3:1, matching the thickness of each layer. Light emission from the AlInN/GaN SL grown on GaN substrates is observed in cathodoluminescence with a peak at ~317 nm from transitions in quantum states within the thin SL GaN layers.

[1] H. Xue, et al., "Growth and Characterization of AlInN/GaN Superlattices," *J. of Crystal Growth* (2024).

10:00 AM BREAK

SESSION 5A-2: Nanoscale Characterization
Session Chair: Andrew Graves
Friday Morning, May 17, 2024
Resort Tower, Ground Level, Bronze Room 2

9:00 AM 5A-2.1
µLaue Diffraction and XEOL Analysis of Nitride Materials Joël Eymery[1,2], Jean-Sébastien Micha[1,2] and Olivier Ulrich[1,2]; [1]CEA, France; [2]University Grenoble Alpes, France

The emergence of new functionalities in nitrides is strongly related to the growth and technology process controls, but also to the development of advanced characterization techniques with high spatial resolutions. Focused X-ray beams provide innovative solutions to analyze quantitatively and correlatively the strain and light emission by combining µLaue diffraction (µLaue) and X-ray excited optical luminescence (XEOL), the two signals being recorded for the same time during mappings. This work will illustrate some recent experimental and analysis breakthroughs obtained at the BM32 beamline of the European Synchrotron Radiation Facility. The new opportunities of this technique will be illustrated with nitride materials in terms of structural analysis (epitaxial relationships, strain, orientation) and light emission, and compared to other techniques (e.g., EBSD and cathodoluminescence for electron probes and photoluminescence for a laser light excitation).

The light emission of GaN µwires [1-3] and µLEDs obtained by etching GaN/InGaN Multiple Quantum Well (MQW) of commercial MOVPE UV heterostructures are studied by XEOL hyperspectral analysis, and the local strain variation and lattice rotation is obtained from µLaue analysis. A complete mapping of µLED takes benefits from the small beam size (~ 250 nm), short counting time (~1 s), and from the polychromatic diffraction Laue pattern method that can record many Bragg reflections without rocking the sample.

The XEOL data are analyzed in detail with the AI-related method of Non-negative Matrix Factorization. It is shown that the three main emissions of the samples (MQW, near band edge peaks, and defects band) can be directly retrieved in a fast and “ab initio” way. The µLaue analysis is first illustrated by a conventional method of indexation and of the refinement of the diffraction patterns (i.e., with the LaueTools program developed on the ESRF BM32 beamline), but also with a new method based on feed-forward neural network that can index in real-time the diffraction spots recorded during the synchrotron experiments [4].

The results of the combination of both methods enable the correlating of the visible emission and the crystalline structure of the materials, and therefore to improve manufacturing techniques. It will be also demonstrated that fast scans allow for obtaining a statistical description of the samples opening the way to production control and a fast and systematic screening of optoelectronic materials and microstructures. New potential applications for different MOVPE materials will be given in this communication.

References
[1] Koester R et al. M-plane core-shell InGaN/GaN multiple-quantum-well on GaN wires for electroluminescent device. Nano Lett. 2011; 11: 4839.
[2] Salomon D et al. Silane-Induced N-Polarity in Wires Probed by a Synchrotron Nanobeam. Nano Lett. 2017; 17, 946.
[3] Segura-Ruiz J et al. Spatially and time-resolved carrier dynamics in core-shell InGaN/GaN multiple-quantum wells on GaN wire. Nano Letters 2021; 21:9494.
[4] Purushottam Raj Purohit R.R.P. et al. LaueNN: Neural network based hkl recognition of Laue spots and its application to polycrystalline materials. J. Appl. Cryst. 2022; 55:737.

9:20 AM 5A-2.2
Excitons in Epitaxially Grown WS_2 on Graphene—A Nanometer-Resolved EELS and DFT Study Max Bergmann[1], Jürgen Belz[1], Oliver Massmeyer[1], Badrosadat Ojaghi Dogahe[1], Robin Günkel[1], Sergej Pasko[2], Simonas Krotkus[2], Michael Heuken[2], Stefan Wippermann[1] and Kerstin Volz[1]; [1]Philipps-University Marburg, Germany; [2]Aixtron SE, Germany

Two-dimensional (2D) transition metal dichalcogenides (TMDs) have emerged as a captivating area of research with remarkable potential, particularly in the domain of valleytronics. TMDs form a diverse class of 2D materials with semiconducting properties making them ideal for various applications like battery electrodes, solar cells and field-effect tunneling transistors. They also feature an indirect-to-direct band-gap transition in the monolayer limit, which leads to a vastly enhanced quantum efficiency and significant increase in photoluminescence illustrating their potential for optoelectronic applications.
Typical preparation routine for 2D materials, however, is the mechanical exfoliation, which is no suitable technique when applications are aimed for. Hence, we establish metal organic chemical vapor deposition (MOCVD) to find suitable growth routines for 2D materials, in particular WS_2 grown on graphene, which has potential applications for field-effect transistors. In this study we investigate the excitonic properties of the structures by monochromated electron energy loss spectroscopy (EELS) in a scanning transmission electron microscope (STEM). Understanding the effect of the dielectric environment due to changing layer numbers and multi-material heterostructures on the optical properties is crucial for tailoring device properties. Monochromated EELS provides the required spatial resolution at the nanometer scale in combination with high energy resolution in the meV range. This enables the unique optoelectronic characterization of materials at nonometer length scales and correlation with atomic-scale structural properties.
To complement the experimental results, theoretical investigations using density functional theory applying the Bethe-Salpeter equations are conducted. We find that by transitioning from mono- to bi- to multilayers of WS_2 the spectra show redshifts for both, the K-valley excitons at about 2.0 and 2.4 eV as well as excitonic features of higher energies. The latter features originate from so called band nesting of transitions between the Γ and K point. In addition to the dielectric environment caused by multilayers, we find that graphene has a strong influence on the excitonic spectrum.

This presentation will summarize and discuss the excitonic properties of MOCVD-grown WS_2 in different layer configurations and environments, as are realistically needed for future device concepts and property tuning. Finally, we show that nanometer scale electron spectroscopy supported by careful theoretical modeling can successfully link atomic structure and optical properties, such as exciton energy shifts, in non-idealized complex material systems like multilayer 2D heterostructures.

9:40 AM 5A-2.3
Nanoscale Crystallographic Orientation Mapping of Advanced Metallic Nanostructures and Thin Films
Conrado R. Afonso; Universidade Federal de São Carlos (UFSCar), Brazil

The β Ti-based alloys have attracted considerable interest as biomedical materials due to their unique characteristics such as excellent biocompatibility, low elastic modulus (E), low density, and corrosion and wear resistances in biological environment. Ti, Nb, and Zr are non-toxic and non-allergenic biocompatible metals. Mg-Fe immiscible alloys for hydrogen storage forming MgH2 and Mg2FeH6 complex hydride can be characterized by crystallographic orientation using ACOM. Characterization of nanocrystalline alloys and interfaces in this work was done in order to improve resolution for the characterization of nanoscale phases it was used TEM analysis together with associated techniques: STEM-EDS, HRTEM using a TITAN Themis TEM/STEM 300kV with Chemistem EDS detector. The distribution of phases and grain orientation maps were determined with an Automatic Crystal Orientation Mapping (ACOM) system installed in a JEOL JEM 2100F (TEM/STEM) 200kV with field emission gun (FEG). A ASTARTM NanoMegas system was used for ACOM diffraction data acquisition. Usually the step sizes (resolution) adopted in ASTAR mapping starts in 1 nm to 10 nm, and cover areas through the sample from 100 x 100 pixels (nm2) up to 700 x 700 pixels (µm2). Crystallographic mapping through ASTAR technique was able to characterize and identify submicron down to nanometric advanced metallic alloys grain size. High entropy alloys (HEA) such as the case of study of boron addition on the solidification sequence and microstructure of AlCoCrFeNi alloys were explored, and automatic crystallographic orientation (ACOM) and phase mapping using ASTAR shows Index Quality (IQ) image, phase map with IQ overlapped and orientation mapping in the beam direction with IQ for B2, BCC and FCC and orthorhombic boride Cr2B-type phases. TEM micrograph in bright field (BF) mode of C5 sample of Ti-15Nb alloy processed by SLM, showing alfa prime martensite needles (brighter) and β-Ti matrix, h) ASTAR image of inverse pole figure in x direction (IPF-X), i) virtual bright field (VBF) and j) Phases map with alfa prime martensite needles (green) and β-Ti matrix (red). Another application of nanoscale phases identification through ASTAR is the cold-rolled melt-spun Mg-Fe metallic ribbons after partial hydrogenation shows virtual bright field (VBF) image of Mg-hcp grains and hydrides at the border of the sample, virtual dark field (VDF) of a hydride spot extracted from crystallographic map, IPF-y orientation image combined with reliability and Phase map combined with Index showing distribution of phases: Mg-HCP (red), MgH2 (light blue), Mg2FeH6 (green) hydrides and MgO (yellow). The complementary characterization was carried out using other TEM accessory techniques such as scanning and transmission electron microscopy (STEM) coupled with energy-dispersive X-ray spectroscopy (EDS) and selected area diffraction (SAD), besides STEM and HR-STEM high angle annular dark field (HAADF) image using Z-contrast**.**

10:00 AM BREAK

SESSION 5A-3: IV-IV Materials and Devices
Session Chair: Francesco Montalenti
Friday Morning, May 17, 2024
Resort Tower, Ground Level, Silver Room

9:00 AM *5A-3.1
Epitaxy of Hexagonal SiGe Heterostructures Erik Bakkers; Technische Universiteit Eindhoven, Netherlands

Silicon and germanium cannot emit light efficiently due to their indirect bandgap, hampering the development of Si-based photonics. However, alloys of SiGe in the hexagonal phase are predicted to have a direct band gap [1]. In this work, we grow hexagonal SiGe as shells on wurtzite GaAs and/or GaP template wires using the crystal structure transfer method [2]. Efficient light emission from hexagonal SiGe, up to room temperature, accompanied by a short radiative life time of around a nanosecond are shown, which are the hallmarks of a direct band gap material [3]. The band gap energy is tunable in the range of 0.35 till 0.7eV opening a plethora of new applications. One of our next goals is to demonstrate lasing from hexagonal SiGe. We do have first indications of amplified spontaneous emission (ASE) in non-optimized structures, and have revealed the limiting factors for obtaining lasing, among which the crystal quality is an important factor. In this work, we study the growth kinetics as a function of the SiGe composition in order to optimize the crystal quality. We reveal a new type of defect in this new SiGe material system, which is identified as I_3 [4]. We study the formation mechanism using in-situ transmission electron Microscopy [5], and their structural and electronic properties. We find that the defects form when the growth front is roughened, which happens at higher material fluxes and/or lower growth temperatures.
Next, we focus on the growth of hexagonal SiGe heterostructures, such as quantum wells (QWs). These QWs are essential to reduce the laser threshold. We study the growth of pure Ge and $Si_{0.1}Ge_{0.9}$ QWs embedded in Si-rich barrier material in detail as a function of the growth conditions and thickness/strain. We show that the emission energy increases with decreased thickness, indicating confinement of both the electrons and the holes in the QWs. The QWs show bright emission up to room temperature with a short radiative

lifetime.

[1] C. Rodl et al., Phys.Rev.Materials 3, 034602 (2019).
[2] H.I.T. Hauge et al. ***Nano Letters*** 15, 5855 (2015).
[3] E.M.T. Fadaly *et al.*, ***Nature*** 580, 205 (2020)
[4] E.M.T. Fadaly *et al, **Nano Letters**,* 21, 3619 (2021).
[5] L. Vincent et al., ***Adv. Mater. Interfaces***, 2102340 (2022).

9:30 AM 5A-3.2
P-channel Heterojunction Field Effect Transistor Fabricated in Si-face 3C/4H-SiC Heterostructure Hiroyuki Sazawa, Shigeyuki Kuboya, Hitoshi Umezawa, Tomohisa Kato and Yasunori Tanaka; AIST, Japan

A high electron mobility transistor (HEMT) has previously been reported that utilizes a 2D electron gas at the heterointerface between 3C-SiC and C-face 4H-SiC as a channel [1]. The 2D electron gas mirrors the fixed positive charge on the 4H-SiC surface formed by spontaneous polarization in the 4H-SiC. It has been predicted that an analogous 2D hole gas could be formed if the 3C-SiC layer was grown on a Si-face 4H-SiC substrate, because of the reversed polarity of the 4H-SiC surface [2]. This would be expected to allow the development of high-performance p-channel transistors. However, to date, there has been no experimental demonstration of the formation of such a 2D hole gas. This is presumably mainly because of the difficulty in growing a high-quality 3C-SiC layer on Si-face 4H-SiC. It is well known that heteroepitaxially grown 3C-SiC layers frequently include rotational domains (mixed stacking sequences of ABC… and ACB…) regardless of the 4H-SiC surface polarity [3,4]. In a previous study, we successfully grew a single-domain 3C-SiC layer on C-face 4H-SiC by utilizing a step-controlled substrate, where steps with a height of one unit cell (1*C* steps) were formed on the substrate surface by in-situ etching prior to 3C-SiC growth [5]. Based on the speculated domain formation mechanism, this method is also expected to be effective for Si-face 4H-SiC. In the present study, we attempted to grow a high-quality single-domain 3C-SiC layer on Si-face 4H-SiC using this approach. Thermal chemical vapor deposition was used to grow a 26-nm-thick 3C-SiC layer on a Si-face step-controlled substrate to form a 3C/4H-SiC heterostructure. X-ray diffraction φscans for 3C-SiC 113 were obtained to identify the presence of rotational domains in the grown layer. Hall measurements in the temperature range from 78 to 300 K were performed using a van der Pauw structure formed on the heterostructure. Source, drain, and gate electrodes were produced on a heterostructure mesa using conventional lithography to fabricate a lateral transistor, whose *I-V* characteristics were evaluated in DC mode.
The φ-scan profile exhibited three peaks with an angular separation of 120°, establishing that the 3C-SiC layer was single-domain. In addition, the Hall coefficient was determined to be positive, indicating hole transport in the heterostructure. The sheet carrier density (N_{sh}) and Hall mobility at room temperature were 1.6×10^{13} cm^{-2} and 30 $cm^2V^{-1}s^{-1}$, respectively. The N_{sh} values were almost constant in the measured temperature range, which is typical for 2D carriers. The fabricated transistor exhibited clear current modulation and pinch-off under a gate bias voltage. This is the first demonstration of a p-channel transistor utilizing a 2D hole gas in a 3C/4H-SiC heterostructure. This work was supported by the Innovative Science and Technology Initiative for Security (Grant Number JPJ004596), ATLA, Japan.
References
[1] H. Sazawa et al. First demonstration of SiC transistor utilizing 2D electron gas in 3C/4H-SiC heterostructure. ICSCRM 2024.
[2] M. V. S. Chandrashekhar et al. Electronic properties of a SiC polytype heterojunction formed on the Si Face. Appl. Phys. Lett. 2007;90:173509-1–173509-3.
[3] H. S. Kong et al. An examination of double positioning boundaries and interface misfit in beta-SiC films on alpha-SiC substrates. J. Appl. Phys. 1988;63:2645-2650.
[4] Y. Shi et al. A comparative study of high-quality C-face and Si-face 3C-SiC(1 1 1) grown on off-oriented 4H-SiC substrates. J. Phys. D: Appl. Phys. 2019;52:345103-345110.
[5] H. Sazawa et al. High-mobility 2D electron gas in carbon-face 3C-SiC/4H-SiC heterostructure with single-domain 3C-SiC layer. Appl. Phys. Lett. 2022;120:212102-1–212102-4.

9:50 AM 5A-3.3
Heteroepitaxy of Strained Germanium Quantum Well Heterostructures on a Silicon Wafer Exhibiting the Highest Hole Mobility Maksym Myronov; The University of Warwick, United Kingdom

Mobility of free carriers in conduction (electrons) or valance (holes) bands, along with a reasonably large energy band gap, is one of the most important quality measures of any semiconductor material, determining its suitability for advanced applications in a large variety of classical electronic, optoelectronic and sensor devices, as well as for novel applications in emerging quantum electronics. Higher mobility enables faster operation of a device at lower power consumption and thus leading to reduced Joule heat dissipation, which is essential to minimize for large-scale quantum architectures as well for increasing the speed and bandwidth of electronic devices. Advantages offered by record-high mobility materials are even more important for those devices and electronics which operate at cryogenic temperatures, for example, for fast readout and advanced control of distributed registers of quantum processors. Also, carrier mobility is the critical quality of a semiconductor material for quantum devices, often playing a key role towards new discoveries.[1]
Over the last 4 decades research and development of epitaxial growth techniques like Molecular Beam Epitaxy (MBE) and Chemical Vapour Deposition (CVD) and technologies along with understanding physics of carrier scattering mechanisms in low-dimensional systems resulted in appearance of strained Si, $Si_{1-x}Ge_x$ and Ge quantum well (QW) heterostructures, epitaxially grown on standard Si(001) substrates, with very high mobility electrons or holes, at both, cryogenic and room-temperatures.
Recently, a record-high mobility of holes, reaching 4.3×10^6 $cm^2V^{-1}s^{-1}$ in an epitaxial compressively strained Ge

semiconductor 2D system, grown on a standard Si(001) wafer (cs-GoS) was reported.[2] This significant increase of the mobility by over four times, compared to the previous state of the art, allows for the first time hole devices to outperform electron ones in the group-IV semiconductor materials. A similar situation has not been reported for any other semiconductor materials system. This major breakthrough in the enhancement of hole mobility in cs-GoS was achieved due to the development of state-of-the-art epitaxial growth technology culminating in superior monocrystalline quality of this material system with a very low density of background impurities and other imperfections. This superior material system with the combination of unique properties will lead to new opportunities for innovative quantum device technologies and applications in quantum as well as in classical electronics, optoelectronics and sensors.
In addition to the record mobility, this cs-GoS material platform reveals a unique combination of properties, which are: a very large and tuneable effective g*-factor, the lowest percolation density and the smallest effective mass. [2-4] This long-sought combination of parameters in one material system is important for the research and development of low-temperature electronics with reduced Joule heating, and for quantum electronic circuits based on spin qubits.
Furthermore, this achievement reduces the gap between the highest hole mobility in gallium arsenide (GaAs) 2D system heterostructures grown on the same material substrate, i.e. GaAs, which was just recently increased from 2.3×10^6 $cm^2V^{-1}s^{-1}$ to 5.8 $cm^2V^{-1}s^{-1}$. [5,6] All other known semiconductors, including III-V, II-VI, perovskites, 2D materials, etc. show substantially lower carrier mobility than in the cs-GoS and GaAs heterostructures.

References

[1] G. Scappucci, C. Kloeffel, F. A. Zwanenburg, D. Loss, M. Myronov, et al, Nature Reviews Materials, 926 (2021).
[2] M. Myronov, et al, Small Science **3** (2023).
[3] M. Myronov, et al, Communications Materials **4**, 104 (2023).
[4] C. Morrison and M. Myronov, Appl. Phys. Lett. **111**, 192103 (2017).
[5] J. D. Watson, et al, Phys. Rev. B **85**, 165301 (2012).
[6] Y. J. Chung, et al, Physical Review Materials **6**, 034005 (2022).

10:10 AM BREAK

SESSION 5B-1: Novel Nitride Material and Other Oxides
Session Chair: Tim Wernicke
Friday Morning, May 17, 2024
Resort Tower, Ground Level, Bronze Room 1

10:30 AM *5B-1.1
MOCVD of AlScN and AlYN for Electronic Applications

Stefano Leone, Isabel Streicher, Patrik Stranak, Mario Prescher, Peter Brueckner, Philipp Doering, Sebastian Krause, Stefan Mueller, Patrick Waltereit and Lutz Kirste; Fraunhofer Institute for Applied Solid State Physics, Germany

Our society's increasing need for interconnectedness calls for reliable electrical components. Nitride semiconductors, especially Sc and Y alloyed with wurtzite-AlN, address challenges like higher data volume, frequency, and low-energy memory storage. AlScN and AlYN, non-centrosymmetric crystals with enhanced piezoelectric properties, show promise for RF filters, non-linear optics devices, high electron mobility transistors (HEMTs), and ferroelectric non-volatile memories. Valence electrons in *d* orbitals and the large ionic radius of Sc and Y contribute to their unique properties. AlScN (18% Sc) and AlYN (11% Y) achieve lattice matching with GaN. AlScN HEMTs surpass AlGaN counterparts, ensuring higher reliability. While the enhancement in these figures of merits is higher for AlScN when compared to AlN, AlYN benefits from the fact that Y is more earth-abundant, cost-effective, and more accessible to extract and purify [1].
Two main electrical components benefit from AlScN and AlYN properties: HEMTs and ferroelectric non-volatile memories like Fe-RAM. AlScN-based HEMTs surpass standard AlGaN HEMTs in current density, amplifier output power, and reliability due to lattice matching with GaN [2]. At the same time, ferroelectricity demonstrated in AlScN and AlYN, even at significantly higher temperatures compared to perovskite oxides, represents a key enabler for non-volatile memories, which are of utmost importance for energy-efficient data storage.
Fabrication involves molecular beam epitaxy (MBE) for HEMTs, while ferroelectric layers are mainly produced through sputtering or occasionally MBE. Metal-organic chemical vapor deposition (MOCVD), preferred for mass production, ensures high-quality epitaxial layers on multi-wafer systems at a low operation cost. At Fraunhofer IAF, we pioneered AlScN [3] and AlYN [1] epitaxial growth on a commercial MOCVD reactor, controlling the molar flow of low vapor pressure Sc and Y precursors. Innovative precursors heated at 100–150 °C enable depositing high-quality epitaxial layers, catering to diverse layer properties and device demands.
Typically, the MOCVD process for both materials is carried out at temperatures ranging from 1000 to 1100 °C, pressure close to 50 mbar, and a relatively high V/III ratio of 1000 and above. Colder growth conditions lead to sharper interfaces but higher impurities (O and C) incorporation. Higher temperatures promote the formation of less thermodynamically stable cubic inclusions. Relatively high growth rates of 0.07nm/s were demonstrated in the case of Scandium when using the precursors $(EtCp)_2Sc(bdma)$ or $(EtCp)_2Sc(dbt)$; similar growth rates for AlYN were achieved with $(EtCp)_2$(iPr-amd)Y. However, in the case of AlYN for HEMT heterostructures, where the purity of the layer plays a crucial role, the lower vapor pressure precursor $(MeCp)_3Y$ was preferred.

In the last years, we have established and advanced the growth of AlScN layers, demonstrating HEMT-based power amplifier with output power beyond 8 W/mm at 30 GHz [2], thanks to the capability of growing high structural quality heterostructure of GaN with 5 to 20 nm thick AlScN layer with Sc content adjustable between 1 to 30%. Recently, ferroelectricity in a 250 nm thick $AlSc_{0.15}N$ layer was proven, paving the way to MOCVD-grown ferroelectric nitride layers. In the case of AlYN, which was developed only last year, we have so far demonstrated the growth of pure wurtzite AlYN with Y content close to 30%, but above all, excellent electrical characteristics of AlYN/GaN heterostructures suitable for the upcoming fabrication of HEMT and most likely featuring also ferroelectric characteristics.

References
[1] Leone, S. et al., DOI: 10.1002/pssr.202300091.
[2] Krause, S. et al., DOI 10.1109/LED.2022.3220877.
[3] Streicher, I. et al., DOI: 10.1002/pssr.202200387.

11:00 AM 5B-1.2
MOCVD Growth of Epitaxial Ferroelectric ScAlN and Related Alloys Andrei Osinsky, William Brand, Vitali Soukhoveev and Fikadu Alema; Agnitron Technology, United States

Scandium Aluminum Nitride alloy (ScAlN) has recently gained significant attention as a barrier layer in Gallium Nitride-based High Electron Mobility Transistors (GaN HEMTs) due to its high polarization coefficients. Incorporating Sc into AlN's lattice softens its bonds, enhancing the material's piezoelectric characteristics [1]. For instance, with 18-20% Sc content, ScAlN matches GaN's lattice with ~1.5 times higher spontaneous polarization than AlN. While AlN is an excellent barrier material in AlN/GaN HEMTs, its critical thickness of around 5 nm limits its suitability to support Schottky gate contact, leading to high device leakage current due to quantum and trap-assisted tunneling. The use of lattice matched ScAlN barriers in ScAlN/GaN HEMTs allows for the increased sheet charge density at the interface without encountering critical thickness limitations. Moreover, the high polarization coefficients of ScAlN alloy make it promising for various applications, including optoelectronics, acoustoelectric devices, and ferroelectric memory.

The growth of ScAlN has been studied using magnetron sputtering, halide vapor phase epitaxy (HVPE), MBE, and MOCVD. Magnetron sputtering and HVPE have limitations when it comes to HEMTs. MBE has successfully been used to grow ScAlN/GaN HEMTs but suffers from slow growth rates, making it unsuitable for large-scale production. MOCVD offers a promising solution but has not been widely used due to the hardware challenges with the existing commercial MOCVD reactors [2]. The primary challenge in using existing commercial MOCVD reactors for ScAlN growth is the absence of Scandium (Sc) metal-organic (MO) precursors with sufficiently high vapor pressure. The Sc MO sources have significantly lower vapor pressure and require heating at elevated temperatures, which in turn demands the gas delivery components to sustain an even higher temperature to prevent precursor condensation in the delivery network.

In this work, we report on the MOCVD growth of high-quality epitaxial ScAlN alloys using a custom-built reactor. The reactor features a high-temperature Sc precursor delivery module, ensuring sufficient Sc vapor delivery without condensation. Control over Sc incorporation into the AlN lattice was achieved through source temperature, reactor pressure, substrate temperature, and ammonia flow rate. The as-grown ScAlN thin films were extensively characterized using optical transmission, XRD, EDS, RBS, AFM, and SIMS. These analyses confirmed films with Sc composition exceeding 40%, while maintaining the wurtzite crystal structure. A preliminary MOCVD-grown ScAlN/GaN HEMTs on SiC substrates revealed a 2DEG charge density of ~2x1013 cm-2 and electron mobility of 900 cm2/Vs. On a 2” wafer, ScAlN films with <1% thickness non-uniformity, >95% Sc uniformity, and <0.3 nm surface roughness was demonstrated. Finally, we will discuss the optical, doping, pyroelectric, and piezoelectric characteristics of the films, as well as the growth of other nitride alloy families, such as ScGaN and Y(Al,Ga)N grown by our reactor.

[1] S. Manna *et al.*, *Journal of Applied Physics,* vol. **122**, no. 10, (2017).
[2] S. Leone *et al.*, *physica status solidi (RRL) – Rapid Research Letters,* vol. **14**, no. 1, (2019).

11:20 AM 5B-1.3
Development of MOCVD Equipment for Nitride Semiconductors Compatible with Low Vapor Pressure Precursor Supply Yudai Shimizu, Guanxi Piao, Keitaro Ikejiri, Yuya Yamaoka, Sadahiro Yamada and Shuichi Koseki; Taiyo Nippon Sanso Corporation, Japan

Metal-organic chemical vapor deposition (MOCVD) is an important technology in the production of nitride semiconductors and is widely used in the production of electronic and light-emitting devices. In recent years, the addition of new raw materials (rare earth elements such as Sc: scandium, Eu: europium, Er: erbium, Tm: thulium, and Gd: gadolinium) to existing nitride semiconductor growth has resulted in faster electronic conduction (Sc), more stable and sharp luminescence (Eu, Er, Tm), for spintronics and magnetic devices (Gd), and other useful properties not found in conventional nitride semiconductors. Therefore, research and development in this area is starting up. Although magnetron sputtering, molecular-beam epitaxy (MBE), hydride vapor-phase epitaxy (HVPE), and ion implantation have been proposed as methods for adding rare earth elements to GaN, we believe that fabrication using MOCVD is superior in terms of mass production, precise control of structure, and crystal quality.
However, one of the main obstacles to utilizing rare earth elements in MOCVD is the inherently low vapor pressure precursors used to supply these elements. Therefore, it was difficult to apply the same conventional precursor supply

system to growth processes containing rare earth elements. Alternative precursors with higher vapor pressures are being considered to solve this problem, but it is also necessary to develop a feeding system with the versatility to flexibly accommodate materials of various vapor pressures. In this presentation, we introduce a newly developed MOCVD equipment for low vapor pressure precursor supply (SR4000-HT-LV, Taiyo Nippon Sanso) that was developed to solve this problem and its effectiveness was experimentally confirmed.

The feed piping for pressures such as TMG (trimethylgallium) and TMA (trimethylaluminum), which are conventionally used as precursors for nitride semiconductors, was heated to a maximum of about 50 °C to achieve a stable supply, but for low-vapor pressure precursors, the thermobath and piping must be kept at 130 °C or higher to achieve a sufficient supply rate. If there is even one cold spot in the path from the precursor to the piping, the supply efficiency will be greatly reduced. This is because aggregation will be easier than with conventional precursors, such as TMG. Therefore, SR4000-HT-LV is designed to efficiently feed low-vapor pressure sources by optimizing the selection of equipment and materials, piping structure, etc. so that the source and piping to the process introduction can be kept at a high temperature.

As a low-vapor pressure precursor, we used a precursor (referred to as precursor A in this paper) with a vapor pressure that is about an order of magnitude lower at 130 °C than the vapor pressure of Cp_3Sc, which has already been reported. The bottle section and supply piping were set at 130 °C and 150 °C, respectively.
GaN samples with precursor A were grown under standard undoped GaN growth conditions with an precursor A feed rate of about 0.42 µmol/min. The concentration of element A in the sample was evaluated by SIMS (secondary ion mass spectrometry). The concentration incorporated into the crystal was 1.88×10^{20} cm^{-3}. This indicates that when Cp_3Sc is supplied by SR4000-HT-LV, the supply capacity is capable of depositing AlScN films containing percent order Sc. Additionally, by baking and scraping off deposits on the susceptor cover after GaN growth with precursor A, the concentration of element A incorporated into the crystal during subsequent GaN growth was found to be below the lower limit of detection by SIMS. The above experimental results show that SR4000-HT-LV is capable of efficiently feeding low vapor pressure precursors and minimizing the effects of residual these precursors in the furnace, and that the temperature of the feeding system can be controlled at high temperatures.

11:40 AM 5B-1.4
MOCVD Growth of $MgGeN_2$ Films on GaN and Sapphire
Chenxi Hu[1], Kaitian Zhang[2], Vijay Gopal Thirupakuzi Vangipuram[2], Chris Chae[2], Jinwoo Hwang[2], Yumi Ijiri[3], Hongping Zhao[2,2] and Kathleen Kash[1]; [1]Case Western Reserve University, United States; [2]The Ohio State University, United States; [3]Oberlin College, United States

$MgGeN_2$ and $MgSiN_2$, present potentially significant opportunities for developing new semiconductor technology associated with their large band gaps. $MgGeN_2$ is characterized by a direct band gap of 4.11 eV. $MgSiN_2$ exhibits a direct band gap nearly equivalent to that of AlN, at 6.3 eV, while its indirect band gap is slightly lower, at 5.84 eV. From Vegard's law, the direct band gap for the $Mg(Ge,Si)N_2$ alloy ranges from approximately 4 to 5 eV. Hence these materials are of interest for potential applications in both power electronics and as deep ultraviolet light emitters.
Results of $MgGeN_2$ film growth by molecular beam epitaxy and by RF-plasma deposition have been reported previously. We report here on the synthesis of $MgGeN_2$, by metal organic chemical vapor deposition (MOCVD). Films were grown on GaN/c-sapphire templates as well as a-plane, c-plane, and r-plane sapphire substrates. The growth temperature of 720 °C and a wafer rotation speed of 1000 rpm were chosen to reduce magnesium evaporation. The precursors used were both Cp_2Mg, the common p-dopant precursor for AlGaN, and $MeCp_2Mg$, along with germane and ammonia, with N_2 employed as the carrier gas. Stoichiometry, measured by energy-dispersive x-ray diffraction (EDS), was achieved with a ratio of flow rates of the Mg precursor to germane set to between 7 and 13.
Growth rates of approximately 100 nm/h were estimated by fitting the EDS spectra to a given film thickness using the NIST DTSA-II software. These fits were found to be consistent with the film thicknesses measured by transmission electron microscopy. The measured film thicknesses are approximately a factor of 2.5 lower than estimates obtained using the Chapman-Enskog equation for mass-transport-limited growth, assuming 100% incorporation, and no re-evaporation, of the Mg atoms. Scanning electron microscopy images show faceted surfaces characteristic of some three-dimensional rather than planar growth. X-ray diffraction spectra have verified that the films are highly crystalline but, when grown on GaN templates, oriented and more single-crystal-like in registry with the GaN template. Film thicknesses and stoichiometries were observed to be the same, within measurement uncertainty, for samples grown simultaneously on both GaN templates and the sapphire substrates. Film roughness, measured over 5 µm x 5 µm areas by atomic force microscopy, varied with growth parameters and substrates but were typically of the order of 10 nm.
In summary, we report the growth of crystalline, stoichiometric $MgGeN_2$ by MOCVD at 720 °C, at growth rates of approximately 100 nm/h, on GaN templates and sapphire substrates. Films grown on GaN templates were found to be preferentially oriented in alignment with the substrate. Further refinements to the growth process, as well as optical characterization, are in progress at the date of this submission. This work is an important step toward exploring the Mg-IV-N_2 materials, in particular $MgGeN_2$ and $MgSiN_2$ and their alloys, for optical emitters in the deep ultraviolet, as well as for power electronics.

12:00 PM 5B-1.5
Incorporation of Phosphorus into AlN by Metalorganic Vapor Phase Epitaxy for AlPN/GaN High Electron Mobility Transistors Xu Yang, Itsuki Furuhashi and Markus Pristovsek; Nagoya University, Japan

GaN-based high electron mobility transistors (HEMTs) with AlGaN barriers have been proven to be an important device technology in high-frequency and high-power applications. To further improve, new barrier materials are under investigation, including AlInN and AlScN, which both have MOVPE growth-related problems. Thus, AlPN, a new member of the III-Nitride family lattice-matching to GaN, was first experimentally synthesized by our group recently [1]. As barrier material for HEMTs, AlPN also results in high polarization-induced carrier concentrations. However, AlPN is less challenging in terms of Ga carry-over and temperature influence and has no strain-driven lateral inhomogeneities that commonly occur in AlInN growth by MOVPE [2]. Though AlScN could provide even higher polarization, it lacks a Sc precursor with high enough vapor pressure for the standard MOVPE system [3], while both PH_3 and tertiary-butylphosphin (tBP) precursors are proven P-precursors for classical III-V MOVPE.
Since the AlPN material system is still in its infancy, our focus is first on the epitaxial growth of AlPN on GaN/sapphire templates in a showerhead MOVPE system using tBP and NH_3 as precursors. P seems to occupy both Al and N sub-lattices, depending on the NH_3 partial pressure. Low NH_3 pressures promote P incorporation into the desired N sub-lattice. With increasing P or N partial pressure, P incorporated more on the anti-site (P on Al sub-lattice) up to a point, where more P is on the Al sub-lattice than the N sub-lattice. The reaction is likely driven by the very high energy between P and N and occurs probably even in the gas phase. Consequently, an increased tBP/NH_3 ratio in the gas phase does not increase P-content in AlP_yN_{1-y} beyond a certain point, and instead, it yields $Al_{1-x}P_{x+y}N_{1-y}$ with the appearance of dot-like features on the surface and a shift of the c-lattice constant to smaller values than AlN.
We are currently doing miscibility calculation between AlP and AlN. If the formation of anti-site P formation is driven by miscibility, high growth temperatures and strain should both facilitate the incorporation of P into the N sub-lattice. However, higher temperatures increase unwanted Ga carry-over during the slow AlPN growth at extremely low V/III ratios below 10. Thus, growth temperature and V/III ratio must be optimized to minimize the P-N reaction, force the P incorporation into the N sub-lattice, and avoid the thermal degradation of the GaN channel. With the optimized growth condition (~1000°C and V/III ratio below 10), 10 nm thick AlP_yN_{1-y} layers with P-content of ~1% could be achieved, which were coherently strained to the underlying GaN with smooth surfaces. These AlP_yN_{1-y}/GaN heterostructures showed a clear two-dimensional electron gas (2DEG) in temperature-dependent Hall effect measurements and a sheet resistance comparable to that from non-optimized AlGaN/GaN HEMTs. More discussion of the growth behavior of AlPN and the electrical properties in AlPN/GaN heterostructures will be presented at the conference.
[1] M. Pristovsek et al., Appl. Phys. Express 13, 111001 (2020).
[2] M. Hiroki et al., *J. Crystal Growth* **382**, 36 (2013).
[3] S. Leone et al., *Phys. Status Solidi RRL* **14**, 1900535 (2020).
Acknowledgements: This work was partly supported JSPS KAKENHI (Grant Nos. 21K03418 and JPJSJRP 20221603). We like to thank Dr. Eberhard Richter at FBH-Berlin for GaN templates on sapphire and helpful discussion.

12:20 PM 5B-1.6
Defects Engineering for Thin Films of $SrTiO_3$, $CaTiO_3$ and Their Solid Solution Epitaxially Grown by Metal Organic Vapor Phase Epitaxy Mohamed Abdeldayem, Changming Liu, Izaz-Ali Shah, Andreas Fiedler, Detlef Klimm, Martin Albrecht and Jutta Schwarzkopf; Leibniz-Institut für Kristallzüchtung, Germany

In recent years, $SrTiO_3$ thin films have gained a lot of interest due to their potential for application in resistive switching devices and neuromorphic computing. Most commonly, oxygen deficient $SrTiO_3$ films are used in memristive applications. Hereby, the switching mechanism is based on the formation and destruction of conductive filaments from oxygen vacancies. However, analog switching behavior without a forming step is preferred for neuromorphic devices, which requires the development of an alternative switching mechanism. Sr deficient $SrTiO_3$ thin films revealed an analog switching behavior without the need of a forming step (Baki et al., 2021) and which scales with the Sr/Ti cation ratio in the films. It is assumed that the switching is based on nano-polar domains formed by Ti anti-site defects. Due to the assumption that the polarization is strongly influenced by A-cation size mismatch with Ti (Klyukin et al., 2018), incorporated lattice strain and disorder effects, we have extended the material range to $CaTiO_3$ and the corresponding solid-solution $(Sr,Ca)TiO_3$. It is the ultimate goal to explore defect engineering in off-stoichiometric perovskite thin films of $SrTiO_3$, $CaTiO_3$ and their solid solution $(Sr, Ca)TiO_3$ in order to design their functional properties for memristive devices, which require films with high structural quality and well-controlled off-stoichiometry.
In this work, we have epitaxially grown $SrTiO_3$, $CaTiO_3$, and their solid solutions $(Sr,Ca)TiO_3$ with different Ca/Sr ratios in thin film form by liquid-delivery spin metal-organic vapor phase epitaxy (MOVPE). This method uses solid metal-organic precursors solved in dry toluene with precisely adjusted concentration and brought into the gas phase by a flash evaporation. It provides the growth of perovskite oxide thin films without a significant amount of oxygen vacancies and with high structural quality as well as smooth surfaces and interfaces. Different off-stoichiometries between the Ti and the A-site cation in the films are realized taking advantage of the MOVPE, as all elements can be independently controlled by the composition of the gas phase via the adjustment of each gas flow. Stoichiometric as well as intentionally off-stoichiometric films, especially with A-site deficiency, have been grown fully strained on oxide substrates while

maintaining the perovskite structure in a single phase. By means of thermogravimetry analysis, decomposition behavior of MO precursors was studied to determine both vaporization temperature as well as substrate temperature to ensure full pyrolysis in the diffusion limited regime. By utilizing X-ray diffraction, and scanning transmission electron microscopy, phase purity of the films, strain state and defect formation could be investigated. Atomic force microscopy was used to demonstrate the smooth surfaces of the grown films. Furthermore, electrical behavior which has been determined by IV curves in a vertical MIS structure showed the potential of these materials for memrsitive devices applications.

12:40 PM 5B-1.7
Growth of GeO_2 via MOCVD—Transition from Amorphous to Polycrystalline Imteaz Rahaman, Mike Scarpulla and Kai Fu; The University of Utah, United States

Rutile Germanium Dioxide (GeO_2) has been recently theoretically identified as a new ultrawide bandgap (UWBG) semiconductor, boasting a bandgap of 4.68 eV, dopability for both n-type and p-type, ~2x higher Baliga figure of merit (BFOM) than Ga_2O_3, 2x higher thermal conductivity than Ga_2O_3, and availability of large size single crystal substrate. These outstanding material properties position rutile GeO_2 as a highly attractive UWBG semiconductor for power electronics. However, the epitaxial synthesis of this promising material into its most advantageous polymorph, ensuring controlled phase, pristine surface/interface quality, precise microstructure, and optimal functional properties, is still in its infancy. So far, initial results on the epitaxial growth of rutile GeO_2 films by the molecular beam epitaxy (MBE) and mist chemical vapor deposition (mist-CVD) have been reported. In this work, we present a comprehensive exploration of growing GeO_2 films on both C-plane and R-plane sapphires through the Metal-Organic Chemical Vapor Deposition (MOCVD) technique. Utilizing tetramethylgermane as a precursor, we have investigated the influences of different parameters on the film properties, including growth temperature, chamber pressure, Ge/O ratio, gas flow rate, and annealing temperature. Chamber pressure emerged as a crucial parameter, with initial attempts at film growth under varied temperatures and lower chamber pressure resulting in no films. Subsequent adjustments to oxygen and argon gas flow rates, as well as pressure modifications, also failed to produce films. Efforts to reduce the boundary layer thickness through changes in substrate-to-shower head distance and susceptor rotation speed were unsuccessful. By optimizing the chamber pressure and growth temperature, GeO_2 films from amorphous to polycrystalline were obtained with a clear transition by adjusting these two parameters characterized by X-ray diffraction (XRD), scanning electron microscope (SEM), energy dispersive X-ray spectroscopy (EDX), and atomic force microscopy (AFM). The polycrystalline film exhibited distinctive flower-patterned morphologies. Annealing in the MOCVD at O_2 ambient demonstrated substantial efficacy in facilitating this transition. Further investigations into the effects of Ge/O ratio and gas flow rate on the phase transition indicated a direct correlation between flow rate and crystallinity, with increased gas flow rate enhancing the prevalence of flower-patterned regions. Ongoing investigations are currently underway to expand upon these preliminary findings. These pioneering outcomes are poised to contribute to the advancement of epitaxial growth techniques for GeO_2 using MOCVD and the development of this new UWBG semiconductor.

SESSION 5B-2: Fundamental Studies/Modeling of Epitaxy
Session Chair: Shugo Nitta
Friday Morning, May 17, 2024
Resort Tower, Ground Level, Bronze Room 2

10:30 AM 5B-2.1
MOCVD/MOVPE Epitaxy Solution of Group III-V Nitride with Atomistic Prospective and Cost Effectiveness Praveen K. Saxena, P Srivastava and Anshika Srivastava; Tech Next Lab, India

Due to superior physical properties (wide bandgap, high electron saturation velocity, high breakdown field, and high chemical stability) of gallium nitride (GaN), it is extensively exploits for the present and future high-power and high-frequency devices applications. Though SiC or diamond substrates are used for GaN commercial prospects, the critical issues GaN-based devices still face incompatibility with the Si-based integrated circuits in terms of their expensive cost. Integration of GaN with Si can boost great potential for the fabrication of low-cost and multi-functional chips [1]. The commercial product exploiting GaN epitaxial layers integrated on Si through uses thick strain relief layers e.g. AlN/AlGaN/GaN need to be used due to their large mismatches (Si and GaN). However, many technical challenges are associated with the AIN growth on Si substrate e.g. the substantial discrepancy in the thermal expansion coefficient and the high lattice mismatch between the substrate [2-3].
The current work deals with the modeling and simulation of MOCVD/MOVPE growth processes pertaining to AlN buffer layer grown on Si. The work considers a commercially available MOCVD reactor geometry and models the gas flow, chemical kinetics and surface diffusion processes involved in growing films. Synergistic use of different aspects to model an entire film growth is carried out within the framework of TNL-EpiGrow simulator software. Additionally, the simulation results have been matched with previous experimental results and show good agreement between the two, indicating the relaibility of the simulations [4-7]. The TNL-EpiGrow simulator helps in better understandings of the MOCVD/MOVPE growth mechanisms at atomistic scale and to achieve the optimum growth conditions of group III-V nitrides. In turn reduce the experimentation cost. In present paper, the authors have attempted to reproduce the AlN epitaxy (using MOCVD AIXTRON 200/4 RF-S horizontal flow reactor geometry) at atomistic scale [2]. The major issue of gas phase parasitic reactions and the impact of variation in

the V/III ratio over the crystal quality of the film are given due consideration. The pulsed atomic-layer epitaxy (PALE) technique implemented in is exploited to improve the surface morphology and crystal [2-3]. The adsorption, hopping and desorption mechanism rates are computed using in-house developed kinetic Monte Carlo (kMC) algorithms with capabilities to reproduce the real deposition experiments [4-6]. In first step, thick AlN nucleation layer is grown over Si substrate at a low temperature (1080C) with simultaneous precursors flow (TMAl - 14 sccm and NH_3 - 1200 sccm) for 300 s. Whereas, IInd growth step exploits the PALE method at different temperatures (1365C, 1410C, and 1450C) to grow three AlN samples. The extraction capabilities of TNL-EpiGrow simulator make it possible to extract each deposited atom position over the lattice layer-by-layer. The growth rates ~0.06 nm/s in first step growth (simultaneous precursors flow) and ~1 nm/pulse in IInd step growth (Pale Technique) are achieved respectively. The simulated growth rates show good agreement with the experimental growth rates[2]. The roughness of each sample is extracted. The extracted dislocation densities and lattice parameters of deposited materials are compared for all three samples. It is observed that the dislocation density decrease with the increase in surface temperature. It can be explained on the basis of each atom hopping rate which increases under high temperature. The lattice parameters i.e. in-plain 'a', 'b' and 'c' of each sample are extracted. The average of lattice parameters are obtained through position vectors of all deposited atoms of total number of deposited monolayers. The thickness of deposited film is obtained through total number of monolayers multiplied by c axis values. The layer-by –layer in-plane and c-axis strain is calculated using lattice parameters.

10:50 AM 5B-2.2
Asymmetric Step Interactions in MOVPE of GaN Gregory B. Stephenson[1], Dongwei Xu[2], Carol Thompson[3], Matt J. Highland[1], Jeffrey A. Eastman[1], Weronika Walkosz[4], Peter Zapol[1], Bo Shen[5] and Guangxu Ju[5]; [1]Argonne National Laboratory, United States; [2]Huazhong University of Science & Technology, China; [3]Northern Illinois University, United States; [4]Lake Forest College, United States; [5]Peking University, China

We have been studying the dynamics of atomic steps on vicinal surfaces during MOVPE growth of GaN (0001) [1-3]. For these surfaces, the αβαβ stacking sequence of the basal planes produces half-unit-cell-height steps, the structures of which alternate between A and B types, depending upon step azimuth. We have recently carried out *in situ* surface X-ray scattering measurements showing that the surface coverage of α and β terraces is asymmetric; specifically, under the NH_3-rich MOVPE environment, there was a higher coverage of α than β, even at equilibrium (zero growth rate). This implies that the repulsion between A and B steps is asymmetric, e.g. larger for B above A than A above B. Furthermore, this asymmetry depends upon the presence of H_2 in the carrier gas. We will discuss the implications of the asymmetry for various models of step repulsion.

[1] Guangxu Ju *et al.,* In-situ microbeam surface X-ray scattering reveals alternating step kinetics during crystal growth, Nature Communications **12**, 1721 (2021).
[2] Guangxu Ju *et al.,* Burton-Cabrera-Frank theory for surfaces with alternating step types, Physical Review B **105**, 054312 (2022).
[3] Guangxu Ju *et al.,* Crystal truncation rods from miscut surfaces with alternating terminations, Physical Review B **103**, 125402 (2021).

11:10 AM 5B-2.3
Enhancing Crystal Quality of AlN on Silicon (111) Substrates Through Boron Pretreatment in MOCVD Processes Mingtao Nong[1], Xiao Tang[1], Chehao Liao[2], Haicheng Cao[1], Tingang Liu[1] and Xiaohang Li[1]; [1]King Abdullah University of Science and Technology (KAUST), Saudi Arabia; [2]National Yunlin University of Science and Technology, Taiwan

Nowadays, Aluminum Nitride (AlN), distinguished by its direct-gap semiconductor nature and a wide bandgap (Eg = 6.2 eV), holds significant promise for advancing technologies such as ultraviolet (UV) light-emitting diodes, photodetectors, acoustoelectric devices, high electron-mobility transistors, and various piezoelectric applications.[1] Due to the high cost of the native substrate, AlN is commonly grown on foreign substrates, including sapphire, SiC, and silicon (Si), etc. Compared with sapphire and SiC, Si can be a promising alternative for AlN growth owing to its cost-effectiveness, high thermal conductivity, widespread availability, large-scale production feasibility, and potential for integration with other electronics.[2] However, the large lattice mismatch of 19% and the coefficient of thermal expansion (CTE) of ~43% between AlN and Si leading to an extremely high density of misfit dislocations ($>10^{10}$ cm^{-2}) near the AlN/Si interface and cracks of AlN during cooling.[3]
The study investigated the growth AlN thin films on Si (111) by metal-organic chemical vapor deposition (MOCVD). Through the introduction of triethylboron (TEB) during trimethylaluminum (TMAl) pretreatment[4], high-quality nearly crack-free AlN films were acquired, with a thickness of 500 nm.
This research compared the growth of AlN films with (S1) and without (S2) TEB in the pretreatment. Atomic force microscopy (AFM) revealed larger grains on S1's surface post-TEB, which was beneficial to the subsequent 3D island growth of the buffer layer. Laytec reflection curves demonstrated a morphological shift from 3D to 2D growth during AlN deposition for S1. Notably, S1 exhibited a significant reduction in curvature by 20 km^{-1} during growth, corresponding to a 3.8 cm^{-1} blue shift in the Raman spectrum peak compared to S2. This shift suggested a marked decrease in surface tensile stress for S1. Optical microscopy images highlighted a stark contrast between the two samples; S1 presented a crack-free surface, whereas S2 was riddled with cracks. This difference was attributed to S1's more prominent 3D island growth, which effectively mitigated cracks by releasing more surface tensile stress during cooling and enhanced crystal quality. X-ray diffraction (XRD) analysis

supported this observation, showing significant decreases in the full width at half maximum (FWHM) values of (002) and (102) reflections for S1 (0.22° and 0.36°, respectively), both of which were the lowest recorded values for AlN films on planar silicon substrates by MOCVD.
In conclusion, the integration of TEB in the pretreatment during the MOCVD growth of AlN thin films on Si(111) substrates had proven to be a transformative step. The analysis of AFM images, Laytec reflection curves, Raman spectra, and XRD rocking curve FWHM values collectively highlighted the positive impact of TEB on the growth dynamics and structural properties of AlN films. This breakthrough not only advanced the understanding of AlN deposition processes but also paved the way for the practical realization of high-quality AlN films with significant implications for advanced electronic and optoelectronic applications.
1. Strite, S.; Morkoç, H., GaN, AlN, and InN: A review. *Journal of Vacuum Science & Technology B: Microelectronics and Nanometer Structures Processing, Measurement, and Phenomena* **1992,** *10* (4), 1237-1266.
2. Feng, Y.; Wei, H.; Yang, S.; Chen, Z.; Wang, L.; Kong, S.; Zhao, G.; Liu, X., Competitive growth mechanisms of AlN on Si (111) by MOVPE. *Sci Rep* **2014,** *4*, 6416.
3. Robin, Y.; Ding, K.; Demir, I.; McClintock, R.; Elagoz, S.; Razeghi, M., High brightness ultraviolet light-emitting diodes grown on patterned silicon substrate. *Materials Science in Semiconductor Processing* **2019,** *90*, 87-91.
4. Bao, Q.; Luo, J.; Zhao, C., Mechanism of TMAl pre-seeding in AlN epitaxy on Si (111) substrate. *Vacuum* **2014,** *101*, 184-188.

11:30 AM 5B-2.4
Process Optimization Using a Comprehensive Modeling Study of SiC Epitaxial Growth in Veeco Single-Wafer Horizontal Hot-Wall CVD Reactor Bojan Mitrovic[1,2], Drew Hanser[1], Aniruddha Bagchi[1], Tushar Gulati[1], Tae-Seok Lee[1], Boomjoon Kim[1], Ming Pan[1], Michael MacMillan[3], Roger Nilsson[3] and Johannes Kaeppeler[2]; [1]Veeco Instruments Inc., United States; [2]Veeco GmbH, Germany; [3]Veeco SiC CVD Systems AB, Sweden

Silicon carbide (SiC) has recently become a semiconductor material of choice for high temperature, high frequency, and high-power electronic devices due to its characteristics such as wide band gap, high thermal conductivity, and high breakdown electric field strength. One of the most important processes in the fabrication of SiC-based high-power devices is the homoepitaxial growth of SiC, and the most commonly used technique to grow thick, high quality epitaxial SiC layers is the chemical vapor deposition (CVD) process. Therefore, proper design of the CVD-SiC epitaxial equipment plays a critical role in meeting the material specifications and high demand for SiC based power devices.

Advanced simulation and modeling have recently become one of the most important tools used for the design and performance optimization of SiC-CVD reactors. There are several important aspects in utilizing those tools that help avoid costly hardware design iterations and sometimes time consuming and laborious experiments. Modeling and simulation can facilitate optimization of reactor chamber design parameters such as, gas injector for uniform flow distribution, reactor geometry for good deposition uniformity, heating system for optimal growth temperature uniformity, etc. It also enables better understanding of the SiC growth process and can predict optimal process parameters to obtain high growth rate, high-quality SiC epi with good deposition and doping uniformity. Reactor design and process parameters can also be optimized using simulation tools to reduce parasitic deposition in the chamber and minimize thermal stresses introduced at high growth temperatures used during the CVD-SiC growth.

In this work, a comprehensive modeling and simulation study of the SiC epitaxial growth in Veeco SiC CVD reactor is presented. Trichlorosilane (TCS) and propane (C_3H_8) precursors diluted in H_2 are used for SiC growth and N_2 and for n-type doping. This system is a single-wafer horizontal hot-wall reactor equipped with six resistive heating zones for precise wafer and wall temperature control, as well as 3 gas injection zones for accurate thickness and doping uniformity tuning, both for 150 mm and 200 mm substrates. Independent control of precursors and dopants is enabled for each injection zone.

Computational Fluid Dynamics (CFD) and SiC deposition kinetics are employed for the modeling, using commercial software such as ANSYS Fluent and CVDSim. The methodology presented in this work involves comprehensive 3D reactor modeling that includes detailed thermal analysis to provide for accurate temperature boundary conditions, detailed flow dynamics and mass transfer of the species, and it incorporates detailed chemical reaction mechanisms in the reactor chamber. A systematic study was performed to investigate the effects of operating parameters on the SiC deposition rate and uniformity as well as the doping concentration and uniformity. Those parameters include inlet C/Si ratio, inlet source gas concentration, total flow rate and distribution for each injection zone, growth temperature, wall temperature upstream of the wafer, ceiling, and side wall reactor temperatures, etc. The methodology for the optimization of process parameters for the best growth rate and doping uniformity is presented. It is shown that significant improvement in uniformities can be achieved by finding the optimal flow distribution and C/Si ratio between the injector zones. Parasitic deposition on reactor walls and its effect on SiC layers growth and doping on the wafer are also analyzed and ways to reduce it by process and temperature optimization are identified.

Finally, excellent agreement between the obtained modeling results and the experimental data it is demonstrated, so that the developed predictive model and the described methodology can be used for further process optimization, better understanding SiC growth kinetics and future optimization of CVD-SiC reactor chambers.

11:50 AM 5B-2.5
Tunable Bandgap Engineering in GaN Nanostructures Through Isoelectronic Impurity Incorporation for Enhanced Solar Photo Absorption Aadil Waseem[1], Clarence Chan[2], Xihang Wu[1], Yujie Liu[3], Yifan Shen[3], Manos Kapritsos[3] and Xiuling Li[1]; [1]The University of Texas at Austin, United States; [2]Department of Electrical and Computer Engineering, Holonyak Micro and Nanotechnology Laboratory, University of Illinois, United States; [3]Department of Electrical Engineering and Computer Science, University of Michigan, United States

The tunable energy bandgap of III-nitride semiconductors is essential for a variety of applications including solar-photocatalysis, LEDs, and lasers.This study explores the incorporation of arsenic (As) isoelectronic impurities into gallium nitride (GaN) nanostructures to enhance solar photo absorption. Solar-photocatalysis emerges as a promising strategy for sustainable synthesis of chemicals and fuels; however, it faces formidable challenges related to low photon-to-chemical conversion efficiency because of the narrow visible light response range using III-nitride semiconductors. One challenge in harnessing the full potential of III-nitride materials for visible-light-driven electrochemical processes arises from the inherent UV-region band edge emission of materials like GaN. For optimal light absorption, bandgap of GaN can be reduced by alloying it with indium (In). To achieve the bandgap of ~2 eV, around 30% of In-composition is required, inevitably leading to a lot of defects and diminished material quality.
We propose an alternative approach of incorporation of isoelectronic impurities such as Arsenic (As) into GaN nanostructures. This strategy results in a substantial downward bowing of energy bandgap even with ultra-dilute isoelectronic impurity addition (less than 1%), potentially circumventing the limitations of alloying with high In-composition. The experimental results of the samples implanted with As at various implantation temperatures (20, 550, and 1000 °C) emphasized the significance of elevated implantation temperatures, particularly at 1000 °C, in enhancing dopant activation, minimizing crystal damage, and promoting uniform doping profiles.
Photoluminescence (PL) spectroscopy taken at room temperature shows the distinctive As-related emission centered at ~ 490 nm at an implantation dose of 4 × 1013 cm-2 at 100 keV. The peak intensity varies depending on the morphology of GaN nanostructures, their doping type, as well as implantation condition. Remarkably, 50% and 100% enhancements were observed in peak intensity of 490 nm peak with respect to bandedge peak, respectively, when the implantation temperature was increased from room temperature to 550 and 1000C, underscoring the significance of elevated implantation temperatures in activating dopants and mitigating crystal damage. We also performed the first-principal calculation that indicates an energy level at ~ 2.06 eV when As is occupying the N site, and 2.0 eV when As occupies Ga- and N-sites confirming the isoelectronic nature. The room temperature emission at 490 nm with dilute isoelectronic impurity addition observed here highlights the potential of high temperature ion implantation as a viable approach to tune the optical response in III-Nitrides, providing a foundation for improving the photon-to-chemical conversion efficiency in solar photocatalysis and a variety of other optoelectronic applications.

12:10 PM 5B-2.6
Advancements in Wafer-Scale Metalorganic Chemical Vapor Deposition of Monolayer Transition Metal Dichalcogenides—Process Development, Device Performance and Impact of Reactor Design Andrew R. Graves, Thomas V. Mc Knight, Meghan Leger, Chen Chen, Nicholas Trainor and Joan Redwing; The Pennsylvania State University, United States

Wafer-scale epitaxial growth of semiconducting transition metal dichalcogenide (TMD) monolayers such as MoS_2 is of significant interest for device applications to circumvent size and process scalability limitations associated with the use of flakes exfoliated from bulk crystals. However, epitaxy is required to achieve single crystal films over large areas via coalescence of TMD domains with the same crystallographic direction.

Achieving high-quality epitaxial films at the wafer-scale is a non-trivial engineering challenge, which is unique to each MOCVD reactor design. These challenges will be discussed as they present themselves in the context of a process development study on the synthesis of epitaxial films of MoS_2 on sapphire at the two-inch wafer scale. In this study, two MOCVD reactor configurations are compared. The first utilizes a vertical stainless steel reactor chamber with the precursor gas flow from injectors oriented perpendicular to a resistively heated rotating substrate. The second utilizes a horizontal cold-wall laminar flow reactor with stacked precursor injectors oriented parallel to an inductively heated rotating substrate.

Both systems utilize ultra-high purity hydrogen as a carrier gas to deliver hydrogen disulfide (H_2S) and molybdenum hexacarbonyl ($Mo(CO)_6$) precursors to 2-inch c-plane sapphire wafer growth substrates. The impact of key growth parameters such as temperature, pressure and total gas flow were studied. In both reactor geometries, a substrate temperature between 900 °C – 1050 °C, reactor pressures ranging between 50 - 300 Torr and a chalcogen to metal ratio of >10,000:1 were found to produce the highest quality films. Although the optimum conditions were similar, each reactor required slightly different conditions to achieve the highest quality films. The design aspects of each reactor that lead to this slight difference in optimum conditions will be discussed.

The electrical properties of the MoS_2 films, as characterized by field effect transistor (FET) measurements, will also be presented. These include the on-state current, field-effect mobility, on-off ratio and sub-threshold swing values. Preliminary results demonstrate a strong correlation between the growth temperature and the microstructure of the MoS_2 monolayers which, in turn, impacts the transport properties of

the films as determined from field-effect measurements. As the growth temperature is increased from 900 °C to 1000 °C, the areal percentage of inversion domains in the MoS_2 monolayers decreases from ~50% to ~10% which corresponds to an increase in the on-state current and field effect mobility of the MoS_2 FETs. This identifies growth temperature as an important process variable, particularly for films grown for electronic devices.

These results are of interest to the broader MOCVD community as they can inform future reactor designs and help to elucidate the interplay between reactor growth conditions and the large area growth of monolayer TMD films. This understanding is critical in advancing the growth of 2D TMD films from the laboratory to the industrial scale.

12:30 PM 5B-2.7
GaN Thin Film Growth Design, Control and Optimization Through Physical Models and DeepONet Integration
Jingxi Sun, Bochao Su, Richu Jin, Chufang Wu, Shouwen Wen, Dongjun Zhang, Qianghua Liao, Jinnan Cao, Runhui Liang, Yi Duan, Changning Wei, Cong Gao, Xiaoxiao Xin, Wei Yang, Minzhi Deng and Bo Zhang; Shenzhen Polytechnic University, China

The gallium nitride (GaN) Metal-Organic Chemical Vapor Deposition (MOCVD) is a complex process with many variables, making the process very challenging to design, control and optimize for the desired materials and device properties. In this study, we leverage physical models as well as AI algorithms to uncover the hidden physical relationships among GaN MOCVD growth variables for process improvement. Specifically, we employ Deep Operator Networks （DeepONet）to tackle the intricate multi-scale process challenges inherent in GaN MOCVD reactors. DeepONet, by design, encapsulate the capability to model nonlinear dynamic systems over various scales, making them exceptionally suitable for this purpose.

Our research method involves the development and application of DeepONet that can accurately model and predict the dynamic behavior of GaN films during deposition, considering variables across different scales—from atomic interactions to macro-level materials properties. This study aims to bridge the gap between microscopic phenomena and macroscopic outcomes, enabling a more nuanced understanding of MOCVD-based novel materials synthesis.

Through integrating known differential equations directly into the network's loss function to enhance the accuracy of the models under sparse data conditions, our preliminary results has shown an approximate 30% improvement in prediction accuracy combined with a 50% reduction in the data-set size needed for training. In addition， we include feature expansions in both the trunk and branch networks of the DeepONet to better capture the complexities of the GaN growth process under varying conditions for adaptive learning.

SESSION 5B-3: Patterned Growth
Session Chair: Erik Bakkers
Friday Morning, May 17, 2024
Resort Tower, Ground Level, Silver Room

10:30 AM 5B-3.1
Development and Study of Active-Passive Butt-Joint Regrowth of AlGaInAs and GaInAsP on InP via MOVPE
Gustavo Afonso de Castro[1], Nicolas Vaissiere[1], Cosimo Calo[1], Jean-François Paret[1], Daniel Micha[1], Mokhtar Korti[1], Giancarlo Cerulo[1], Sébastien Cavalaglio[2], Franck Bassani[2], Thierry Baron[2], Frederic Pommereau[1] and Jean Decobert[1]; [1]III-V Lab, France; [2]Laboratoire des Technologies de la Microélectronique - LTM, France

The growing access and utilization of data-intensive applications such as, high-resolution video streaming and artificial intelligence results in a need to increase the data traffic supported by the current telecommunications network. One of the ways to increase performance and yield is by improving current production steps and integration technologies of Photonic Integrated Circuits (PICs), such as active-passive Butt-Joint Regrowth (BJR) realized by Metal-organic Vapor Phase Epitaxy (MOVPE). During this step, optically passive layers are selectively grown on a substrate containing protected areas of Multiple-Quantum Wells (MQWs) layers grown on a previous step. This allows for an independent optimization and design of both equally important parts of a PIC, which provides the most versatility in design. Due to this, BJR is by far the most used technique for active-passive integration in PICs, despite the necessity of extra separate epitaxial steps when compared with Selective Area Growth (SAG) or Mono-epitaxial approaches [1,2].
However, BJR done by MOVPE has some technical challenges. First, the technique introduces an interface between active and passive layers, which needs to be as optically transparent as possible to avoid optical or electrical losses. Secondly, the alignment of layers must be finely controlled so as to guarantee a good optical coupling between active and passive sections. Finally, overgrowths introduced by selective growth must be controlled and minimized to facilitate the processing steps that follow. These three aspects of BJR need to be mastered in order to increase yields and performance of PICs produced with this technology.
In this work, we have realized and studied BJR done via MOVPE from wafer preparation up until device characterization. The authors compare the current technique applied at the III-V lab, which involves physical and chemical etching steps by inductively Coupled Plasma (ICP) and HBr, with a process involving two separate selective chemical etching steps and the introduction of GaInAsP etch-stop layers. The new process is results in a less rough regrowth surface, a controllable etch depth, and at the same time in a mask under-etch that aids in limiting overgrowths resulting from selective area epitaxy in MOVPE [3, 4]. *In-situ* CBr_4

etching is also studied as a tool to limit overgrowths, decrease surface roughness and increase overall regrowth quality. These have been studied with Photoluminescence (PL) mapping and Atomic-Force Microscopy (AFM). This implementation is made possible by *in-situ* reflectometry tools from which etch and growth speeds are derived from. With the goal of providing a direct link between eEpitaxy and device performance, strain-compensated AlGaInAs MQW-based Fabry-Pérot (FP) lasers of different lengths have been produced and integrated with GaInAsP optically passive bulk guiding layers. All growths have been realized on a AIXTRON Closed Coupled Showerhead (CCS) 6x2" MOVPE reactor. The FP lasers produced have different BJR interface angles in relation to the <0-11> direction ranging from -45° to 45°, which are introduced to limit light reflections at the interface. The impact on the growth morphology of the addition of an interface angle is observed by µ-PL, Scanning-Electron Microscopy (SEM) and Focused Ion Beam (FIB) milling followed by Transmission Electron Microscopy (STEM) and Energy-Dispersive X-ray Spectroscopy (EDX). The observations made before and after BJR provide insight into the growth mechanisms and how they impact composition at the interface, and the limitation of overgrowths. Finally, sub-threshold Amplified Spontaneous Emission (ASE) analysis [5] of the lasers have been made, which permits the characterization of the intensity optical reflections at the Butt-joint interface morphology and their dependency on the interface angle.

10:50 AM 5B-3.2
Defect Reduction in GaSb Nano-Ridge Engineering on (001) Si Substrates Michiel De Maeyer[1,2], Yves Mols[1], Reynald Alcotte[1], Janusz Bogdanowicz[1], Davide Colucci[1,2], Peter Swekis[1], Robert Langer[1], Dries Van Thourhout[2] and Bernardette Kunert[1]; [1]IMEC, Belgium; [2]Ghent University, Belgium

The use of III-V materials in integrated circuits has enabled key advancements in both photonics and RF, owing to more beneficial material properties such as higher optical gain and absorption as wells as increased carrier mobility compared to silicon. A next logical step to further propel III-V device development is the monolithic integration of III-V materials directly onto Si substrates. This allows for denser and more complex device integration with existing Si-based functionalities while simultaneously reducing production costs.

Most of the III-V research is dedicated to devices based on GaAs and InP. Alternatively, antimony-containing alloys show great promise for photonic devices operating in the short-wave infrared (1-3 µm) as well as high-speed/low-power applications in advanced RF [1,2]. Here, we present the use of nano-ridge engineering (NRE) for the monolithic integration of GaSb onto Si. NRE builds on selective area growth and aspect ratio trapping of misfit defects by depositing in high-aspect ratio trench structures patterned on exactly oriented (001) Si substrates. This technique innovates however in its ability to significantly increase the defect free III-V volume via the growth out of the trench, giving rise to large nano-ridges (NR) [3].

In a previous study [4], we discovered that utilizing a GaAs seed in GaSb NRs leads to a low threading dislocation density (TDD) but high planar defect density (PDD). The application of an InAs seed however led to the opposite behaviour. In this study, we developed a GaSb seed allowing for the simultaneous reduction of both defect kinds. Optimizing the seed and trench filling growth conditions results in a TDD and PDD below $5x10^5$ cm^{-2} and 0.3 μm^{-1}, respectively. A systematic electron channelling contrast imaging (ECCI) investigation reveals an unexpected arrangement of TDs along a straight row, which seems to impact the presence of PDs. Such a periodic defect structure was never observed before in NRE and its origin requires further investigation.

Furthermore, the use of NRE allows for the shape-controlled growth of the NR out of the trench by adjusting the growth conditions. Interestingly, the used precursors play a significant role for the shape engineering, observed here for GaSb NRs grown with TMGa or TEGa. Box-shaped NRs with a wide (001) top facet were used for the first growth of heterostructures based on aluminium and indium containing Sb-alloys.

Lastly, III-V device integration based on NRs requires the deposition of doped layers, yet the determination of the doping concentration and resistivities on such 3D structures is not trivial. Here, we perform micro four-point probe measurement that allow us to extract resistivity values of intentionally doped NRs. The strength of this technique is evidenced by the ability to individually contact NRs, and thus extract values for isolated NRs with different volume and crystal quality [5].

[1] Tournié, E. et al. (2022). Mid-infrared III–V semiconductor lasers epitaxially grown on Si substrates. *Light: Science & Applications*, 11(1), 165.

[2] Chou, Y. C. et al. (2007). Manufacturable and reliable 0.1 µm AlSb/InAs HEMT MMIC technology for ultra-low power applications. *IEEE/MTT-S International Microwave Symposium*, 461-464.

[3] Kunert, B et al. (2018). How to control defect formation in monolithic III/V hetero-epitaxy on (100) Si? A critical review on current approaches. *Semiconductor Science and Technology*, 33(9), 093002.

[4] Baryshnikova, M. et al. (2020). Nano-ridge engineering of GaSb for the integration of InAs/GaSb heterostructures on 300 mm (001) Si. *Crystals*, 10(4), 330.

[5] Bogdanowicz, J. et al. (2018). Width-Dependent Sheet Resistance of Nanometer-Wide Si Fins as Measured with Micro Four-Point Probe. *physica status solidi (a)*, 215(6), 1700857.

11:10 AM 5B-3.3
AlGaN Layers Grown by MOVPE on Spatially Shaped Substrates Robert Czernecki[1], Ewa Grzanka[1], Mikolaj Grabowski[1], Frantisek Hajek[2,1], Artur Lachowski[1,3] and Michal Leszczynski[1]; [1]Institute of High Pressure Physics PAS Unipress, Poland; [2]Institute of Physics of the Czech Academy of Sciences, Czechia; [3]Faculty of Materials Science and Engineering Warsaw University of Technology, Poland

Thick, good quality AlGaN layers are an essential element of nitride lasers used as cladding layers. Due to the large lattice mismatch to the GaN substrate (2.5%), they tend to relax stress through cracking. One of the methods to reduce this stress is to prepare the substrate with spatial shapes.
This study investigates the growth of AlGaN layers on spatially shaped substrates utilizing Metalorganic Vapor Phase Epitaxy (MOVPE). These substrates are prepared by reactive ion etching (RIE) on thick GaN layers (>6µm) deposited on sapphire or on bulk GaN substrates. A series of AlGaN layers were deposited on the engineered substrates, and their morphological, structural and optical properties were analyzed using atomic force microscopy (AFM), cathodoluminescence (CL), X-ray diffraction (XRD) and scanning electron microscopy (SEM).

11:30 AM 5B-3.4
Local Epitaxial Growth of GaAs on Si(001) by Laser-Assisted MOVPE Christian Bruckmann, Jürgen Bläsing, Armin Dadgar and André Strittmatter; Otto-von-Guericke-University Magdeburg, Germany

Further advancement of integrated circuit technology heavily depends on capabilities for implementation of III/V compound semiconductors on Si substrates. Monolithic integration schemes based on heteroepitaxial growth are attractive, time-saving approaches that have been investigated for decades. Major obstacles in achieving a high crystalline quality for growth on Si are the differences in fundamental material properties, such as coefficient of thermal expansion and lattice constant, but also compliance of the epitaxy process with IC manufacturing principles. Selective area epitaxial growth enables to separate growth areas from electronic device areas. While existing approaches are scaled to full wafer growth, a local growth approach would allow an additive manufacturing process tool for fabrication of compound semiconductor layers in spatially confined target areas and to implement different optoelectronic device structures on the same chip.
To realize this approach we developed a tool for laser-assisted metalorganic vapor-phase epitaxy[1] (LA-MOVPE). Local growth is achieved by using high-power infrared laser radiation to heat a designated wafer area. The diameter of the heated area can be varied from 50 µm to over 1000 µm. Pyrolithic chemical reactions take place only above the heated area leading to epitaxial island growth.
For heteroepitaxial growth of GaAs on Si(001) we used a two-step growth approach consisting of a low-temperature nucleation layer and subsequent high-temperature buffer layer. With our current LA-MOVPE that allows for gaussian temperature profiles only, process temperatures are related to peak temperatures in the center of the heated spot. Nevertheless, crucial growth parameters of the nucleation layer (thickness, temperature) can be investigated.
With LA-MOVPE GaAs islands were grown on Si(001) wafers using this two-stage growth approach. For these initial experiments, substrates with low offcut angles were used. In order to ensure homogeneous nucleation layer conditions over the final growth island we used enlarged heated areas during the nucleation phase so that flat temperature profiles over a few hundred microns diameter are obtained. For the final growth island (corresponding to buffer growth in conventional GaAs/Si(001) epitaxy) the heated area was reduced to match the homogenous nucleation region.
X-ray ω-scans of the GaAs(004) reflection yield FWHM of 0.257 degree at optimum for an island height of 3 µm. Roughness measurements in the center of the islands exhibit RMS values down to around 4.0 nm while the qualitative dependence of the roughness value on nucleation temperatures is comparable to planar MOVPE. An optimum thickness of the nucleation layer is found at around 6 nm. Continuous growth during the heat-up stage for buffer layer growth proves essential for improved crystalline quality.
Currently, we are working on LA-MOVPE on patterned Si substrates to further improve crystalline quality.

[1]M. Trippel et al., "Laser-assisted local metal-organic vapor phase epitaxy", Rev. Sci. Instrum. 93, 113904 (2022)

11:50 AM 5B-3.5
Selective Area Growth of GaN-Based Micro-LEDs on 2D Hexagonal Boron Nitride Substrates for Enhanced Device Performance Thi May Tran[1], Suresh Sundaram[1,2,3], Phuong Vuong[1,2], Vishnu Ottapilakkal[1], Mohamed Bourras[1], Rajat Gujrati[1], Jean Paul Salvestrini[1,2,3], Paul L. Voss[1,3] and Abdallah Ougazzaden[1,3]; [1]National Center for Scientific Research, CNRS, France; [2]Georgia Tech-Europe, France; [3]Georgia Institute of Technology, United States

GaN-based micro-LED displays have attracted considerable attention due to their numerous advantages such as high luminance, ambient contrast ratio, resolution, energy efficiency, and extended lifetimes. Nevertheless, GaN-based micro-LEDs face challenges, particularly the decrease in External Quantum Efficiency (EQE) arising from conventional etching processes and the limitations associated with traditional lift-off methods. To address these issues, our study focuses on the epitaxial growth of GaN-based micro-LED heterostructures by employing the combination of Selective Area Growth (SAG) and van der Waals (vdWs) epitaxy growth techniques. This method employs a patterned dielectric mask made of dielectric silicon nitride (SiN) on sapphire substrates to define the openings for micro LED structure growth through Metalorganic Chemical Vapor Deposition (MOVPE)[1]. Additionally, we explore van der Waals (vdWs) epitaxy on hexagonal boron nitride (h-BN) as a SAG-enabling solution for GaN-based device transfer offering enhanced control, high yield, and cost-effectiveness[1,2,3]. The process starts with van der Waals epitaxy of thin 2D h-BN growth on silicon nitride (SiN) masks, featuring square,

triangular, and hexagonal patterns on sapphire substrates. Subsequently, selective area growth of Multi-Quantum Well (MQW) LED heterostructures is executed. The research findings are reinforced by high-resolution XRD measurement results, confirming the excellent quality of the LED structure on a patterned sapphire substrate. Notably, GaN micro-LEDs show selective growth within patterned areas, with no observed GaN growth on randomly oriented hexagonal boron nitride (h-BN) on silicon nitride (SiN), as observed in SEM images. GaN-based micro-LEDs show smooth surfaces and sidewalls without V-pits, indicating a high-quality selective area growth (SAG) with a low dislocation density comparable to previously reported results. Overall, our findings highlight the successful epi growth process of micro-LED heterostructures, ranging from 32 μm to 1.4 μm in size on 2" substrates, utilizing three distinct mask opening shapes: square, hexagonal, and triangular. Further, the results were compared with the successful demonstration of GaN-based micro LEDs on SiO_2 patterned sapphire substrates, these studies indicate that this method is promising and can be extended for different device architectures.

12:10 PM 5B-3.6
GaN Nanopillar Array with Tunable Surface Termination by MOCVD for Photocatalysis Aadil Waseem and Xiuling Li; The University of Texas at Austin, United States

The III-nitride material system, encompassing compounds such as GaN, InN, and AlN, exhibits exceptional properties that make it highly attractive for a wide range of applications. These include power switching, high-frequency RF, and high-power applications, owing to its high electron mobility and large breakdown field. Furthermore, the alloying of GaN with In and Al enables direct bandgap engineering across a broad spectrum, making it suitable for optoelectronics applications and photocatalysis. The lack of inversion symmetry in wurtzite III-nitrides results in distinctive polarization effects, rendering them attractive for sensing and microelectromechanical (MEMS) applications. The existing epitaxial growth techniques allow for the tuning of surface termination and facets.
Optimizing the growth of these GaN nanopillars with tunable crystallographic planes and polarity is crucial for electronic, optoelectronic, and photocatalysis applications. GaN nanostructures with multi-facets exhibit significantly different structural, physical, chemical, and electrochemical properties. Non-polar planes of GaN are essential for LEDs and photocatalysis due to their lower quantum confined stark effect (QCSE). The QCSE in GaN nanostructures grown along the polar direction results in strong piezoelectric polarization, significantly impacting their optoelectronic properties. In this presentation, we report the growth of GaN nanopillars under continuous and pulse mode using the newly commissioned Aixtron CCS MOCVD dual-mode reactor. GaN nanopillars with vertical planes (m-plane) and flat top (c-plane), as well as the nanopillars with vertical planes and pyramidal top with six semi-polar planes (r-planes) are demonstrated. Subsequently, InGaN/GaN quantum well shells are grown over core GaN nanopillars. We have synthesized the nanopillars with variable diameters of 200 nm, 500 nm, and 3 μm all with high aspect ratio. For photocatalysis, the nanostructures with non-polar planes demonstrate a photocatalysis for longer period (3,000 hrs continuously) without performance degradation.
The growth mode, continuous or pulsed, significantly influences the quality of GaN nanostructures. Continuous mode growth offers enhanced precision and uniformity in the selective area epitaxy of GaN nanostructures with vertical m-planes, making it the preferred method for optimizing the growth and properties of these nanostructures. The adoption of continuous mode growth allows for better control and optimization of the tuning of different polar facets, leading to improved morphological quality and structural uniformity of the GaN nanostructures. In contrast, pulse mode growth presents challenges due to non-uniform adatom supply, particularly on m-planes where Ga adatoms have lower mobility, resulting in non-uniform growth. Additionally, the growth rate in pulse mode can lead to 3D growth mode and potentially poor crystal quality, particularly on GaN polar surfaces. Therefore, controlling the growth rate is crucial in pulse mode growth to achieve high crystal quality and desired morphological characteristics in GaN nanostructures.

12:30 PM 5B-3.7
MOVPE Growth Control for a Uniform Array of 6-Fold and 3-Fold Symmetric Group III-Nitride Pyramid Structures Toward Scalable Single Quantum Dot Emitters Yong-Ho Song, Hwan-Seop Yeo and Yong-Hoon Cho; Korea Advanced Institute of Science and Technology, Korea (the Republic of)

A quantum dot system based on group III-nitride semiconductors is an excellent quantum platform for generating deterministic and high-purity quantum light sources operating at room temperature. Here, we present the growth control for a uniform array of single InGaN quantum dots (QDs) directly formed at the apexes of the 6-fold and 3-fold symmetric GaN pyramid array by selective area epitaxy using metal-organic chemical vapor deposition (MOCVD) [1]. Especially for the development of single-photon sources for scalable quantum technologies, controlling the site, size, and shape of QDs is essential. We fabricated site-controlled GaN micro-pyramid structures with a high degree of uniformity and 6-fold symmetry by controlling the H_2/N_2 carrier gas ratio, growth temperature, and V/III ratio to achieve self-limited width at the GaN pyramid apex via a self-limited growth mechanism [2], showing single-photon emission from the apex QD with suppressed background side QW emission and maintained high hexagonal QD symmetry over the large area of the wafer. Next, we successfully form the 3-fold symmetric group III-nitride QDs at the apex of a triangular pyramid at the self-limited growth regime [3]. Controlling the in-plane symmetry of QDs is important for generating polarization-entangled photon pairs via the biexciton–exciton cascade process. We found relatively low optical polarization anisotropy and small fine structure splitting for the 3-fold symmetric QD. Our approach for controlling the QD symmetry provides a new perspective on such QDs, as polarization-entangled photon pairs. We could also obtain

high purity of single photons by using a self-limited growth technique, nanoscale luminescence quenching, and polarization-controlled quasi-resonant excitation.

References:

[1] "Highly uniform array of hexagonally symmetric micro-pyramid structures for scalable and single quantum dot emitters", Y. H. Song, H. S. Yeo, C. Y. Sung, B. S. Kim, S. Ahn, and Y. H. Cho*, **Advanced Materials Interfaces** 10 2202085 (2023).
[2] "Strong and robust polarization anisotropy of site- and size-controlled single InGaN/GaN quantum wires", H. S. Yeo, K. Lee, Y. C. Sim, S. H. Park, and Y. H. Cho*, **Scientific Reports** 10, 15371 (2020).
[3] "Control of the 3 Fold Symmetric Shape of Group III-Nitride Quantum Dots: Suppression of Fine-Structure Splitting", H. S. Yeo, K. Lee, J. H, Cho, S. H. Park, and Y. H. Cho*, **Nano Letters** 20, 8461 (2020).